

AD 738177

Special Technical Report 39

PATTERN MEASUREMENT AND MODELING OF FULL-SCALE VHF ANTENNAS IN A THAILAND TROPICAL FOREST

By: G. E. BARKER W. A. HALL

Prepared for:

U.S. ARMY ELECTRONICS COMMAND
BUILDING 2504, CHARLES WOOD AREA
FORT MONMOUTH, NEW JERSEY 07703

CONTRACT DAAB07-70-C-0220
Order No. 5384-PM-63-91



This document has been approved for public release and sale; its distribution is unlimited.

Sponsored by

ADVANCED RESEARCH PROJECTS AGENCY
ARPA ORDER 371
AND
U.S. ARMY ELECTRONICS COMMAND

Reproduced by
NATIONAL TECHNICAL
INFORMATION SERVICE
Springfield, Va. 22151



STANFORD RESEARCH INSTITUTE
Menlo Park, California 94025 • U.S.A.

R187

**BEST
AVAILABLE COPY**

ACCESSION for	
CFSTI	WHITE SECTION <input checked="" type="checkbox"/>
DDC	BUFF SECTION <input type="checkbox"/>
UNANNOUNCED	<input type="checkbox"/>
AUTHORIZATION	
BY	
DISTRIBUTION/AVAILABILITY CODES	
DATE	STAFF, REG/NO SPECIAL
A	

NOTICES

Disclaimers

The findings in this report are not to be construed as an official Department of the Army position, unless so designated by other authorized documents.

The citation of trade names and names of manufacturers in this report is not to be construed as official Government indorsement or approval of commercial products or services referenced herein.

Disposition

Destroy this report when it is no longer needed. Do not return it to the originator.

DOCUMENT CONTROL DATA - R & D

(Security classification of title, body of abstract and indexing annotation must be entered when the overall report is classified)

1. ORIGINATING ACTIVITY (Corporate author) Stanford Research Institute 333 Ravenswood Avenue Menlo Park, California		2a. REPORT SECURITY CLASSIFICATION UNCLASSIFIED	
		2b. GROUP N/A	
3. REPORT TITLE PATTERN MEASUREMENT AND MODELING OF FULL-SCALE VHF ANTENNAS IN A THAILAND FOREST			
4. DESCRIPTIVE NOTES (Type of report and inclusive dates) Special Technical Report 39			
5. AUTHOR(S) (First name, middle initial, last name) G. E. Barker and W. A. Hall			
6. REPORT DATE December 1971		7a. TOTAL NO. OF PAGES 228	7b. NO. OF REFS 21
8a. CONTRACT OR GRANT NO. DAAB07-70-C-0220		8a. ORIGINATOR'S REPORT NUMBER(S) Special Technical Report 39	
8b. PROJECT NO. Order No. 5384-PM-63-91		8b. OTHER REPORT NO(S) (Any other numbers that may be assigned this report)	
10. DISTRIBUTION STATEMENT This document has been approved for public release and sale, its distribution is unlimited.			
11. SUPPLEMENTARY NOTES		12. SPONSORING MILITARY ACTIVITY U.S. Army Electronics Command Fort Monmouth, New Jersey	
13. ABSTRACT Measurements of the radiation patterns of full-scale simple VHF antennas (half-wavelength dipoles) were performed while the antennas were situated in a second-growth tropical forest in Thailand. These measurements were performed by towing a special-purpose transmitter with an aircraft in orbits around the measurement antennas. The measurement data indicated significant variations in the received signal strength as a function of azimuth angle while the transmitter was towed in orbits at constant elevation angles. These data were processed statistically using a digital computer to provide contour plots of the median signal strength as a function of azimuth and elevation angle. In addition to the contour plots of the radiation patterns for the two polarizations, estimators of the standard deviations of the signal strength, and a comparison of the relative gains of the average signal strength at the measured pattern maxima are provided. Vertically polarized signals received by the measurement antennas exhibited only slightly stronger perturbations than horizontally polarized signals, thus it is assumed that the forest was fairly isotropic as compared to previous measurements in a eucalyptus grove in California which resulted in larger signal reduction and			

13. Abstract (Concluded)

pattern perturbations for the vertically polarized component in comparison with the horizontally polarized component.

Horizontal dipoles typically exhibited about 6 dB more gain than vertical dipoles when a comparison of relative maximum response was made without regard to the polarization of the incident signal. The maximum response of a horizontal dipole to E_θ (vertical polarization) exceeded that of a vertical dipole by only about 3 dB, whereas for E_ϕ (horizontal polarization) the difference increased to 17.5 dB for antennas in both clearing and forest. The ratio of maximum response for each polarization (E_θ/E_ϕ) on a given measurement frequency for similar antennas in the clearing was about -5 dB for the horizontal dipoles whereas for the vertical dipoles a ratio of +12 dB was more typical. This ratio was observed to increase by about 3 dB for both vertical and horizontal dipoles when the antennas were measured in the forest.

A mathematical model previously developed to predict the radiation patterns of HF dipole antennas immersed in a forest was tested at VHF for antennas in the Thailand forest. This model provided contour plots of the predicted radiation patterns, which were plotted on the contour plots of the measured radiation patterns. The measured median patterns resemble the calculated patterns quite well in some cases (especially in the main lobes); however, it was concluded that the model can be used to provide only a rough estimate of the average directivity pattern (above about 15 degrees elevation) of the main lobes of dipoles placed in forest environments.

These measurements show that calculation of the performance of VHF communication systems employing dipole antennas located in forests must include not only average pattern factor changes (as predicted by the model) but also the rapid fluctuations (caused by scatter from the vegetation) which are superimposed on the average variation. Thus far we have only empirical data on these rapid fluctuations. Further study of modeling these rapid fluctuations--especially their statistical nature--is recommended.

14

KEY WORDS

LINK A

LINK B

LINK C

ROLE

WT

ROLE

WT

ROLE

WT

Antenna directivity patterns

Simple VHF antennas

Xeledop (acronym)

Tropical forest

Antenna radiation patterns

Dipole antennas

Antenna pattern measurements

SEACORE

Southeast Asia

Thailand

Jungle

Antenna impedance

VHF

Antenna gain

Antenna pattern models



STANFORD RESEARCH INSTITUTE
Menlo Park, California 94025 · U.S.A.

Special Technical Report 39

December 1971

PATTERN MEASUREMENT AND MODELING OF FULL-SCALE VHF ANTENNAS IN A THAILAND TROPICAL FOREST

By: G. E. BARKER W. A. HALL

Prepared for:

U.S. ARMY ELECTRONICS COMMAND
BUILDING 2504, CHARLES WOOD AREA
FORT MONMOUTH, NEW JERSEY 07703

CONTRACT DAAB07-70-C-0220
Order No. 5384-PM-63-91

SRI Project 8663

This document has been approved for public release and sale; its distribution is unlimited.

Approved by:

R. F. DALY, *Director*
Telecommunications Department

E. J. MOORE, *Executive Director*
Engineering Systems Division

Sponsored by

ADVANCED RESEARCH PROJECTS AGENCY
ARPA ORDER 371
AND
U.S. ARMY ELECTRONICS COMMAND

ABSTRACT

Measurements of the radiation patterns of full-scale simple VHF antennas (half-wavelength dipoles) were performed while the antennas were situated in a second-growth tropical forest in Thailand. These measurements were performed by towing a special-purpose transmitter with an aircraft in orbits around the measurement antennas.

The measurement data indicated significant variations in the received signal strength as a function of azimuth angle while the transmitter was towed in orbits at constant elevation angles. These data were processed statistically using a digital computer to provide contour plots of the median signal strength as a function of azimuth and elevation angle. In addition to the contour plots of the radiation patterns for the two polarizations, estimators of the standard deviations of the signal strength, and a comparison of the relative gains of the average signal strength at the measured pattern maxima are provided.

Vertically polarized signals received by the measurement antennas exhibited only slightly stronger perturbations than horizontally polarized signals, thus it is assumed that the forest was fairly isotropic as compared to previous measurements in a eucalyptus grove in California which resulted in larger signal reduction and pattern perturbations for the vertically polarized component in comparison with the horizontally polarized component.

Horizontal dipoles typically exhibited about 6 dB more gain than vertical dipoles when a comparison of relative maximum response was made without regard to the polarization of the incident signal. The maximum response of a horizontal dipole to E_{θ} (vertical polarization) exceeded

that of a vertical dipole by only about 3 dB, whereas for E_{ϕ} (horizontal polarization) the difference increased to 17.5 dB for antennas in both clearing and forest. The ratio of maximum response for each polarization (E_{θ}/E_{ϕ}) on a given measurement frequency for similar antennas in the clearing was about -5 dB for the horizontal dipoles whereas for the vertical dipoles a ratio of +12 dB was more typical. This ratio was observed to increase by about 3 dB for both vertical and horizontal dipoles when the antennas were measured in the forest.

A mathematical model previously developed to predict the radiation patterns of HF dipole antennas immersed in a forest was tested at VHF for antennas in the Thailand forest. This model provided contour plots of the predicted radiation patterns, which were plotted on the contour plots of the measured radiation patterns. The measured median patterns resemble the calculated patterns quite well in some cases (especially in the main lobes); however, it was concluded that the model can be used to provide only a rough estimate of the average directivity pattern (above about 15 degrees elevation) of the main lobes of dipoles placed in forest environments.

These measurements show that calculations of the performance of VHF communication systems employing dipole antennas located in forests must include not only average pattern factor changes (as predicted by the model) but also the rapid fluctuations (caused by scatter from the vegetation) which are superimposed on the average variations. Thus far we have only empirical data on these rapid fluctuations. Further study of modeling these rapid fluctuations--especially their statistical nature--is recommended.

PREFACE

The work described in this report was performed with the support, and using the facilities, of the Military Research and Development Center (MRDC) in Bangkok, Thailand. The MRDC is a joint Thai-U.S. organization established to conduct research and development work in the tropical environment. The overall direction of the U.S. portion of the MRDC has been assigned to the Advanced Research Projects Agency (ARPA) of the U.S. Department of Defense who, in 1962, asked the U.S. Army Electronics Command (USAECOM) and Stanford Research Institute (SRI) to establish an electronics laboratory in Thailand to facilitate the study of radio communications in the tropics and related subjects. The MRDC-Electronics Laboratory (MRDC-EL) began operation in 1963 [under Contract DA-36-039 AMC-00040(E)] and since that time the ARPA has actively monitored and directed the efforts of USAECOM and SRI. In Bangkok, this function is carried out by the ARPA Research and Development Center (RDC-T). The cooperation of the Thai Ministry of Defense and the Thailand and CONUS representatives of the ARPA and USAECOM made possible the work presented in this report. The preparation and printing of this report was supported by USAECOM under Contract DAAB07-70-C-0220.

CONTENTS

ABSTRACT.	iii
PREFACE	v
LIST OF ILLUSTRATIONS	ix
LIST OF TABLES.	xv
ACKNOWLEDGMENTS	xxi
I INTRODUCTION	1
II DESCRIPTIONS OF THE MEASURED ANTENNAS.	5
A. Horizontal Unbalanced Dipole Antennas	5
B. Vertical Sleeve Dipole Antennas	7
C. Horizontal and Vertical Balanced Dipole Antennas. .	7
D. Horizontal and Vertical Folded Dipole Antennas. . .	11
III DESCRIPTION OF THE MEASUREMENT SITE.	13
IV PATTERN-MEASUREMENT EQUIPMENT.	21
A. The VHF Xeledop	21
B. Aircraft Tracking and Guidance.	22
C. Receiving and Recording	23
V DATA PROCESSING.	27
VI STATISTICAL ESTIMATIONS FROM THE PATTERN DATA.	33
A. Comparison of Mean and Median Amplitudes.	46
B. Pattern Contour Plots	49
C. Estimated Standard Deviations of the Amplitude About the Median.	53
D. Effect of Variation of Slant Range.	53

E. Relative Gains.	60
F. Comments on Absolute Gains.	64
VII IMPEDANCE MEASUREMENTS	67
VIII COMPUTER-MODELING OF THE VHF ANTENNA RADIATION PATTERNS	69
A. Description of the Model.	69
B. Antenna Radiation Patterns.	70
IX DISCUSSION OF RESULTS.	73
A. Measured Antenna Radiation Patterns	73
B. Relative Gain Results	77
C. Measured Antenna Feed-Point Impedance	78
D. Comparison of Measured and Calculated Patterns. . .	79
X SUMMARY AND RECOMMENDATIONS.	81
Appendix A--CONTOUR PLOTS OF THE ESTIMATED MEDIAN AMPLITUDES AND TABLES OF STANDARD DEVIATIONS FOR ANTENNA SET 1	85
Appendix B--CONTOUR PLOTS OF THE ESTIMATED MEDIAN AMPLITUDES AND TABLES OF STANDARD DEVIATIONS FOR ANTENNA SET 2	135
Appendix C--EXAMPLE APPLICATIONS OF THE VHF ANTENNA PATTERN DATA.	181
REFERENCES.	193
DISTRIBUTION LIST	197

DD Form 1473

ILLUSTRATIONS

Figure 1	Map of Thailand Showing Antenna Pattern Measurement Site	2
Figure 2	Horizontal Unbalanced Dipole Antenna	6
Figure 3	Vertical Sleeve Dipole Antenna	8
Figure 4	Typical Vertical Sleeve Dipole Installation.	9
Figure 5	Photograph of Horizontal Balanced Dipole Installation.	10
Figure 6	Aerial Photograph of Antenna Measurement Site.	14
Figure 7	Site Map for Antenna Set 1	15
Figure 8	Site Map for Antenna Set 2	16
Figure 9	Electrical Constants of Foliage Measured at Ban Mun Chit.	18
Figure 10	Ground Constants Measured in Forest at Ban Mun Chit	19
Figure 11	VHF Xeledop and Stabilizing Hardware	22
Figure 12	Block Diagram of VHF Receiving and Recording System	24
Figure 13	Flow Chart of Major Steps in VHF Antenna Pattern Data Processing.	28
Figure 14	A Contour Plot as a Map of a Hemisphere.	51
Figure 15	Contour Plot of the Mean Response of the Horizontal Unbalanced Dipole in the Forest-- E_{θ} at 75 MHz	55
Figure 16	Contour Plot of the Mean Response of the Horizontal Unbalanced Dipole in the Forest-- E_{ϕ} at 75 MHz	57
Figure 17	Comparison of E_{ϕ} Response for the 100 MHz Unbalanced Dipole Antenna in the Forest at 3-, 4-, and 6-Mile Slant Ranges at 15 Degrees Elevation	59

Figure 18	Idealized Lossy Dielectric Slab Model.	70
Figure A-1	Contour Plot of the Median Response of the Horizontal Unbalanced Dipole in the Clearing-- E_{θ} at 50 MHz	89
Figure A-2	Contour Plot of the Median Response of the Horizontal Unbalanced Dipole in the Clearing-- E_{ϕ} at 50 MHz	91
Figure A-3	Contour Plot of the Median Response of the Horizontal Unbalanced Dipole in the Forest-- E_{θ} at 50 MHz	93
Figure A-4	Contour Plot of the Median Response of the Horizontal Unbalanced Dipole in the Forest-- E_{ϕ} at 50 MHz	95
Figure A-5	Contour Plot of the Median Response of the Vertical Sleeve Dipole in the Clearing-- E_{θ} at 50 MHz	97
Figure A-6	Contour Plot of the Median Response of the Vertical Sleeve Dipole in the Clearing-- E_{ϕ} at 50 MHz	99
Figure A-7	Contour Plot of the Median Response of the Vertical Sleeve Dipole in the Forest-- E_{θ} at 50 MHz	101
Figure A-8	Contour Plot of the Median Response of the Horizontal Unbalanced Dipole in the Clearing-- E_{θ} at 75 MHz	103
Figure A-9	Contour Plot of the Median Response of the Horizontal Unbalanced Dipole in the Clearing-- E_{ϕ} at 75 MHz	105
Figure A-10	Contour Plot of the Median Response of the Horizontal Unbalanced Dipole in the Forest-- E_{θ} at 75 MHz	107
Figure A-11	Contour Plot of the Median Response of the Horizontal Unbalanced Dipole in the Forest-- E_{ϕ} at 75 MHz	109
Figure A-12	Contour Plot of the Median Response of the Vertical Sleeve Dipole in the Clearing-- E_{θ} at 75 MHz	111

Figure A-13	Contour Plot of the Median Response of the Vertical Sleeve Dipole in the Clearing-- E_{ϕ} at 75 MHz	113
Figure A-14	Contour Plot of the Median Response of the Vertical Sleeve Dipole in the Forest-- E_{θ} at 75 MHz	115
Figure A-15	Contour Plot of the Median Response of the Vertical Sleeve Dipole in the Forest-- E_{ϕ} at 75 MHz	117
Figure A-16	Contour Plot of the Median Response of the Horizontal Unbalanced Dipole in the Clearing-- E_{θ} at 100 MHz.	119
Figure A-17	Contour Plot of the Median Response of the Horizontal Unbalanced Dipole in the Clearing-- E_{ϕ} at 100 MHz.	121
Figure A-18	Contour Plot of the Median Response of the Horizontal Unbalanced Dipole in the Forest-- E_{θ} at 100 MHz.	123
Figure A-19	Contour Plot of the Median Response of the Horizontal Unbalanced Dipole in the Forest-- E_{ϕ} at 100 MHz.	125
Figure A-20	Contour Plot of the Median Response of the Vertical Sleeve Dipole in the Clearing-- E_{θ} at 100 MHz.	127
Figure A-21	Contour Plot of the Median Response of the Vertical Sleeve Dipole in the Clearing-- E_{ϕ} at 100 MHz.	129
Figure A-22	Contour Plot of the Median Response of the Vertical Sleeve Dipole in the Forest-- E_{θ} at 100 MHz.	131
Figure A-23	Contour Plot of the Median Response of the Vertical Sleeve Dipole in the Forest-- E_{ϕ} at 100 MHz.	133
Figure B-1	Contour Plot of the Median Response of the Horizontal Unbalanced Dipole in the Clearing-- E_{θ} at 50 MHz	139

Figure B-2	Contour Plot of the Median Response of the Horizontal Unbalanced Dipole in the Clearing-- E_{ϕ} at 50 MHz	141
Figure B-3	Contour Plot of the Median Response of the Horizontal Folded Dipole in the Forest-- E_{θ} at 50 MHz	143
Figure B-4	Contour Plot of the Median Response of the Horizontal Folded Dipole in the Forest-- E_{ϕ} at 50 MHz	145
Figure B-5	Contour Plot of the Median Response of the Vertical Sleeve Dipole in the Clearing-- E_{θ} at 50 MHz	147
Figure B-6	Contour Plot of the Median Response of the Vertical Sleeve Dipole in the Clearing-- E_{ϕ} at 50 MHz	149
Figure B-7	Contour Plot of the Median Response of the Vertical Folded Dipole in the Forest-- E_{θ} at 50 MHz	151
Figure B-8	Contour Plot of the Median Response of the Vertical Folded Dipole in the Forest-- E_{ϕ} at 50 MHz	153
Figure B-9	Contour Plot of the Median Response of the Horizontal Unbalanced Dipole in the Forest-- E_{θ} at 75 MHz	155
Figure B-10	Contour Plot of the Median Response of the Horizontal Unbalanced Dipole in the Forest-- E_{ϕ} at 75 MHz	157
Figure B-11	Contour Plot of the Median Response of the Horizontal Dipole with Balun in the Forest-- E_{θ} at 75 MHz	159
Figure B-12	Contour Plot of the Median Response of the Horizontal Dipole with Balun in the Forest-- E_{ϕ} at 75 MHz	161
Figure B-13	Contour Plot of the Median Response of the Horizontal Balanced Dipole in the Forest-- E_{θ} at 75 MHz	163
<u>Figure B-14</u>	Contour Plot of the Median Response of the Horizontal <u>Balanced Dipole</u> in the Forest-- E_{ϕ} at 75 MHz	165

Figure B-15	Contour Plot of the Median Response of the Horizontal Balanced Dipole in the Forest-- E_{θ} at 100 MHz.	167
Figure B-16	Contour Plot of the Median Response of the Horizontal Balanced Dipole in the Forest-- E_{ϕ} at 100 MHz.	169
Figure B-17	Contour Plot of the Median Response of the Vertical Sleeve Dipole in the Clearing-- E_{θ} at 100 MHz.	171
Figure B-18	Contour Plot of the Median Response of the Vertical Sleeve Dipole in the Forest-- E_{θ} at 100 MHz.	173
Figure B-19	Contour Plot of the Median Response of the Vertical Sleeve Dipole in the Forest-- E_{ϕ} at 100 MHz.	175
Figure B-20	Contour Plot of the Median Response of the Vertical Balanced Dipole in the Forest-- E_{θ} at 100 MHz.	177
Figure B-21	Contour Plot of the Median Response of the Vertical Balanced Dipole in the Forest-- E_{ϕ} at 100 MHz.	179

TABLES

Table 1	Statistical Parameters for the 75-MHz Dipole with Balun--in the Forest, E_{θ} at 6° Elevation.	34
Table 2	Statistical Parameters for the 75-MHz Dipole with Balun--in the Forest, E_{θ} at 14° Elevation.	35
Table 3	Statistical Parameters for the 75-MHz Dipole with Balun--in the Forest, E_{θ} at 25° Elevation.	36
Table 4	Statistical Parameters for the 75-MHz Dipole with Balun--in the Forest, E_{θ} at 33° Elevation.	37
Table 5	Statistical Parameters for the 75-MHz Dipole with Balun--in the Forest, E_{θ} at 45° Elevation.	38
Table 6	Statistical Parameters for the 75-MHz Dipole with Balun--in the Forest, E_{θ} at 55° Elevation.	39
Table 7	Statistical Parameters for the 75-MHz Dipole with Balun--in the Forest, E_{ϕ} at 5° Elevation.	40
Table 8	Statistical Parameters for the 75-MHz Dipole with Balun--in the Forest, E_{ϕ} at 13° Elevation.	41
Table 9	Statistical Parameters for the 75-MHz Dipole with Balun--in the Forest, E_{ϕ} at 25° Elevation.	42
Table 10	Statistical Parameters for the 75-MHz Dipole with Balun--in the Forest, E_{ϕ} at 33° Elevation.	43
Table 11	Statistical Parameters for the 75-MHz Dipole with Balun--in the Forest, E_{ϕ} at 45° Elevation.	44

Table 12	Statistical Parameters for the 75-MHz Dipole with Balun--in the Forest, E_{θ} at 55° Elevation.	45
Table 13	Comparison of Mean and Median Signal Strength for Antenna Set 1.	47
Table 14	Comparison of Mean and Median Signal Strength for Antenna Set 2.	48
Table 15	Standard Deviations about the Mean for the Horizontal Unbalanced Dipole in the Forest-- E_{θ} at 75 MHz	54
Table 16	Standard Deviations about the Mean for the Horizontal Unbalanced Dipole in the Forest-- E_{ϕ} at 75 MHz	56
Table 17	Relative Voltage Across 50-Ohm Loads at Pattern Maxima--Measurement Set 1.	61
Table 18	Relative Voltage Across 50-Ohm Loads at Pattern Maxima--Measurement Set 2.	61
Table 19	Relative Voltage into Matched Loads at Pattern Maxima	62
Table 20	Feed-Point Impedances for Antenna Set 1.	68
Table 21	Feed-Point Impedances for Antenna Set 2.	68
Table A-1	Standard Deviations about the Median for the Horizontal Unbalanced Dipole in the Clearing-- E_{θ} at 50 MHz	88
Table A-2	Standard Deviations about the Median for the Horizontal Unbalanced Dipole in the Clearing-- E_{ϕ} at 50 MHz	90
Table A-3	Standard Deviations about the Median for the Horizontal Unbalanced Dipole in the Forest-- E_{θ} at 50 MHz	92
Table A-4	Standard Deviations about the Median for the Horizontal Unbalanced Dipole in the Forest-- E_{ϕ} at 50 MHz	94
Table A-5	Standard Deviations about the Median for the Vertical Sleeve Dipole in the Clearing-- E_{θ} at 50 MHz	96

Table A-6	Standard Deviations about the Median for the Vertical Sleeve Dipole in the Clearing-- E_{ϕ} at 50 MHz	98
Table A-7	Standard Deviations about the Median for the Vertical Sleeve Dipole in the Forest-- E_{θ} at 50 MHz	100
Table A-8	Standard Deviations about the Median for the Horizontal Unbalanced Dipole in the Clearing-- E_{θ} at 75 MHz	102
Table A-9	Standard Deviations about the Median for the Horizontal Unbalanced Dipole in the Clearing-- E_{ϕ} at 75 MHz	104
Table A-10	Standard Deviations about the Median for the Horizontal Unbalanced Dipole in the Forest-- E_{θ} at 75 MHz	106
Table A-11	Standard Deviations about the Median for the Horizontal Unbalanced Dipole in the Forest-- E_{ϕ} at 75 MHz	108
Table A-12	Standard Deviations about the Median for the Vertical Sleeve Dipole in the Clearing-- E_{θ} at 75 MHz	110
Table A-13	Standard Deviations about the Median for the Vertical Sleeve Dipole in the Clearing-- E_{ϕ} at 75 MHz	112
Table A-14	Standard Deviations about the Median for the Vertical Sleeve Dipole in the Forest-- E_{θ} at 75 MHz	114
Table A-15	Standard Deviations about the Median for the Vertical Sleeve Dipole in the Forest-- E_{ϕ} at 75 MHz	116
Table A-16	Standard Deviations about the Median for the Horizontal Unbalanced Dipole in the Clearing-- E_{θ} at 100 MHz.	118
Table A-17	Standard Deviations about the Median for the Horizontal Unbalanced Dipole in the Clearing-- E_{ϕ} at 100 MHz.	120
Table A-18	Standard Deviations about the Median for the Horizontal Unbalanced Dipole in the Forest-- E_{θ} at 100 MHz.	122

Table A-19	Standard Deviations about the Median for the Horizontal Unbalanced Dipole in the Forest-- E_{ϕ} at 100 MHz.	124
Table A-20	Standard Deviations about the Median for the Vertical Sleeve Dipole in the Clearing-- E_{θ} at 100 MHz.	126
Table A-21	Standard Deviations about the Median for the Vertical Sleeve Dipole in the Clearing-- E_{ϕ} at 100 MHz.	128
Table A-22	Standard Deviations about the Median for the Vertical Sleeve Dipole in the Forest-- E_{θ} at 100 MHz.	130
Table A-23	Standard Deviations about the Median for the Vertical Sleeve Dipole in the Forest-- E_{ϕ} at 100 MHz.	132
Table B-1	Standard Deviations about the Median for the Horizontal Unbalanced Dipole in the Clearing-- E_{θ} at 50 MHz	138
Table B-2	Standard Deviations about the Median for the Horizontal Unbalanced Dipole in the Clearing-- E_{ϕ} at 50 MHz	140
Table B-3	Standard Deviations about the Median for the Horizontal Folded Dipole in the Forest-- E_{θ} at 50 MHz	142
Table B-4	Standard Deviations about the Median for the Horizontal Folded Dipole in the Forest-- E_{ϕ} at 50 MHz	144
Table B-5	Standard Deviations about the Median for the Vertical Sleeve Dipole in the Clearing-- E_{θ} at 50 MHz	146
Table B-6	Standard Deviations about the Median for the Vertical Sleeve Dipole in the Clearing-- E_{ϕ} at 50 MHz	148
Table B-7	Standard Deviations about the Median for the Vertical Folded Dipole in the Forest-- E_{θ} at 50 MHz	150

Table B-8	Standard Deviations about the Median for the Vertical Folded Dipole in the Forest-- E_{ϕ} at 50 MHz	152
Table B-9	Standard Deviations about the Median for the Horizontal Unbalanced Dipole in the Forest-- E_{θ} at 75 MHz	154
Table B-10	Standard Deviations about the Median for the Horizontal Unbalanced Dipole in the Forest-- E_{ϕ} at 75 MHz	156
Table B-11	Standard Deviations about the Median for the Horizontal Dipole with Balun in the Forest-- E_{θ} at 75 MHz	158
Table B-12	Standard Deviations about the Median for the Horizontal Dipole with Balun in the Forest-- E_{ϕ} at 75 MHz	160
Table B-13	Standard Deviations about the Median for the Horizontal Balanced Dipole in the Forest-- E_{θ} at 75 MHz	162
Table B-14	Standard Deviations about the Median for the Horizontal Balanced Dipole in the Forest-- E_{ϕ} at 75 MHz	164
Table B-15	Standard Deviations about the Median for the Horizontal Balanced Dipole in the Forest-- E_{θ} at 100 MHz.	166
Table B-16	Standard Deviations about the Median for the Horizontal Balanced Dipole in the Forest-- E_{ϕ} at 100 MHz.	168
Table B-17	Standard Deviations about the Median for the Vertical Sleeve Dipole in the Clearing-- E_{θ} at 100 MHz.	170
Table B-18	Standard Deviations about the Median for the Vertical Sleeve Dipole in the Forest-- E_{θ} at 100 MHz.	172
Table B-19	Standard Deviations about the Median for the Vertical Sleeve Dipole in the Forest-- E_{ϕ} at 100 MHz.	174
Table B-20	Standard Deviations about the Median for the Vertical Balanced Dipole in the Forest-- E_{θ} at 100 MHz.	176

Table B-21	Standard Deviations about the Median for the Vertical Balanced Dipole in the Forest-- E_0 at 100 MHz.	178
Table C-1	Median Transmitter Power Calculations.	188
Table C-2	Calculation of Transmitter Power for 99-Percent Reliability	190

ACKNOWLEDGMENTS

The authors wish to thank Mr. James D. Hice of Varian Associates (formerly with the Communication Laboratory of Stanford Research Institute), the personnel of the California Aircraft Engine Company of San Lorenzo, California (owners and operators of the modified B-25 aircraft used to tow the Xeledop), and the Military Research and Development Center of Bangkok, Thailand for assistance during the field-measurement phase of this work. The authors are pleased to acknowledge the contribution of Dr. John Taylor, Head of the Electrical Engineering Department of the University of South Carolina, who made the model computations of the radiation patterns presented in this report. The authors also wish to thank Mr. R. C. McCarty, formerly of the Mathematical Sciences Department of Stanford Research Institute, for his assistance on the statistical data-processing techniques.

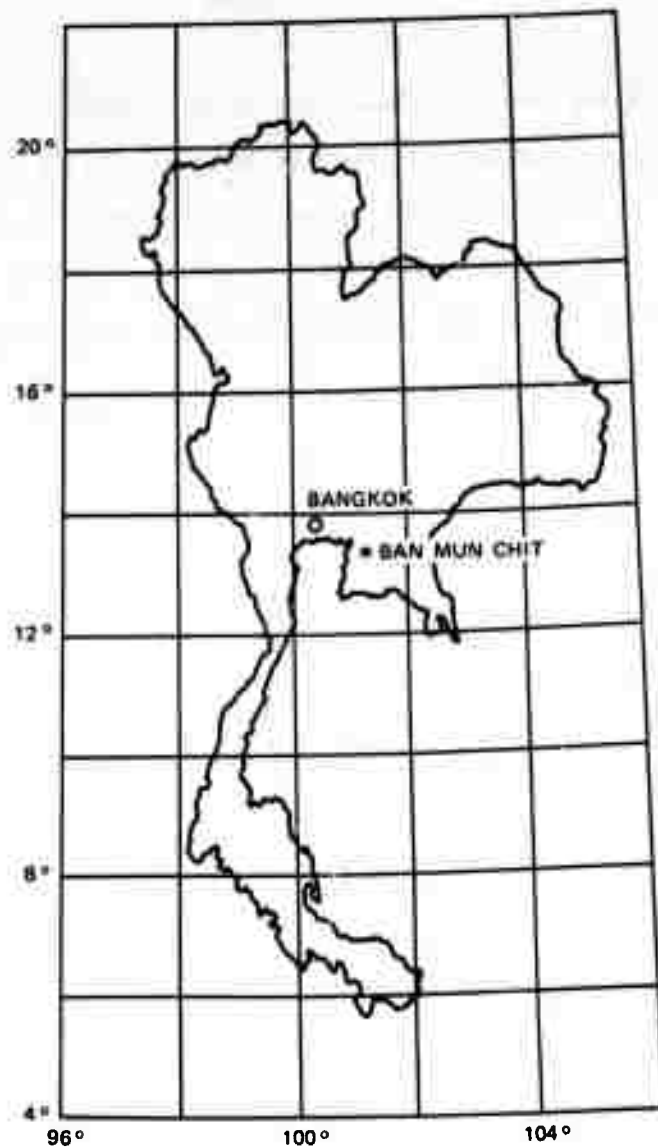
1 INTRODUCTION

Interest in the study of the effects of tropical environments on antenna performance has been stimulated because of the need for better communications when operating in these areas. This report is concerned with the effects of a tropical forest in Thailand on the radiation patterns and gains of simple VHF antennas located in and near the forest.

Although the patterns of VHF antennas operating under ideal conditions have been well documented, little documentation of the effects of typical ground and forested environments, as are encountered in daily use of VHF antennas, had been done until recently. Preliminary VHF antenna pattern measurements were performed under this contract during November 1965 in a eucalyptus grove near Newark, California.^{1*} Measurements of both HF and VHF antennas were performed in a tropical forest near the village of Ban Mun Chit (Chon Buri Province), Thailand (see Figure 1). The results of the VHF measurements are discussed in this report and the results of the HF measurements have been reported previously.²

The antennas described in this report were primarily simple horizontal dipoles and vertical sleeve dipoles, similar to those used for the measurements in California. In addition to these, patterns of antennas used for the manpack Xeledop measurements³ and those of a folded-dipole antenna kit for the AN/PRC-10 radio set also were measured.⁴

*References are given at the end of this report.



*Antenna pattern measurement site

TA-8663-55

FIGURE 1 MAP OF THAILAND SHOWING ANTENNA PATTERN MEASUREMENT SITE

The measurements indicate that scattering of the incident signal results from the uneven surface of the ground surrounding the antenna and additional scattering and signal attenuation is introduced when the antennas are situated in a forest. Because of the significant variation in the measured signal strength over a small azimuthal sector and in order to provide a more meaningful and useful data presentation, the data from these measurements were processed statistically. The median signal strengths over 10° azimuth sectors were determined and then plotted as contours of equal median signal strength as a function of the azimuth and elevation angles on azimuthal equal-area projections in order to provide the measured radiation patterns of the antennas. These contour plots are essentially the same presentation as was employed under this contract for the HF pattern data,^{2,5,6} except the actual data points were used for contouring the HF data whereas the median values for a small azimuthal interval at constant elevation angles were contoured for the VHF data.

In addition to the contour plots of the radiation patterns for the two polarizations, estimators of the standard deviation of the signal strength and a comparison of the average relative gains are provided. Also, the maximum median level of signal received on each antenna (while the Xeledop traversed a 10° azimuth sector at essentially constant elevation angle) was used to estimate the relative gain of all antennas measured on the same frequency.

In order to better understand these data, a computer model developed under this contract to predict the radiation patterns of HF antennas in a forest (as approximated by a lossy dielectric slab)⁷ was employed using input parameters pertinent to the VHF antennas. This model (like any other mathematical model) is potentially only as accurate as its input data (in this case the ground and vegetation electrical constants and an

estimate of the forest and antenna heights). To provide the data on the electrical constants of the ground and vegetation, open wire transmission line techniques (discussed elsewhere²) were devised to provide measured values of these parameters. The computer model proved to be useful for predicting the mean signal strength for some of the antennas but further study is required to provide a model that would be completely reliable for VHF antenna performance predictions.

The measurement antennas are described in Section II of this report. A description of the measurement site and the results of the open wire transmission line measurements of the foliage and the ground electrical constants are provided in Section III. The antenna pattern measurement equipment and the data processing techniques are described in Sections IV and V. A discussion and example presentations of the statistical parameters that were derived from these measurements are provided in Section VI. The feed point impedance of each antenna was measured while the antennas were located in their pattern measurement environment and these results are presented in Section VII. The mathematical model developed to predict the radiation patterns of HF antennas is described in Section VIII along with a discussion of the applications of the model to VHF antennas. The results of these measurements are discussed in Section IX and a summary of the major findings of this work along with recommendations for future studies is presented in Section X.

The antennas were measured in two sets and the data from these measurements are presented as contour plots of the median signal strength and tables of the estimated standard deviations in Appendices A and B. Finally, an example application problem is presented in Appendix C to assist the reader in interpreting and employing the data presented here. The particular example presented here shows that the forest can reduce the received signal as much as 20 dB when compared to an antenna located in a clearing.

II DESCRIPTIONS OF THE MEASURED ANTENNAS

Simple antennas with relatively predictable patterns (when over level, open terrain) were measured to determine the effect of surrounding foliage on the performance of these antennas. The antennas were scaled to be resonant at 50, 75,* or 100 MHz and were measured only on their design frequencies. The antennas were measured in two sets (see Section III). Twenty-five feet of RG-58/U coaxial transmission line was connected to the feed point of the antennas (except the folded dipoles) and then connected to RG-8/U coaxial transmission line which led to the equipment van containing the receiving and recording instrumentation.

A. Horizontal Unbalanced Dipole Antennas

The radiating elements of the horizontal unbalanced dipole antennas were constructed from 3/8-inch-diameter aluminum tubing scaled to 95 percent of $\lambda/4$, as shown in Figure 2. At the feed point, a constant distance between the elements was maintained with a Teflon spacer. These antennas were supported 10 feet above the ground with bamboo poles.

In Set 2, a North Hills Model 1100BB balun (75 Ω :75 Ω) was attached to the feed point of the 75-MHz antenna; this is referred to as a "horizontal dipole with balun" to distinguish it from the balanced dipoles described in Section II-C.

* For these measurements 75.1 MHz actually was used because 75.0 MHz is an international aeronautical frequency, however, 75.1 MHz is rounded to 75 MHz in this report.

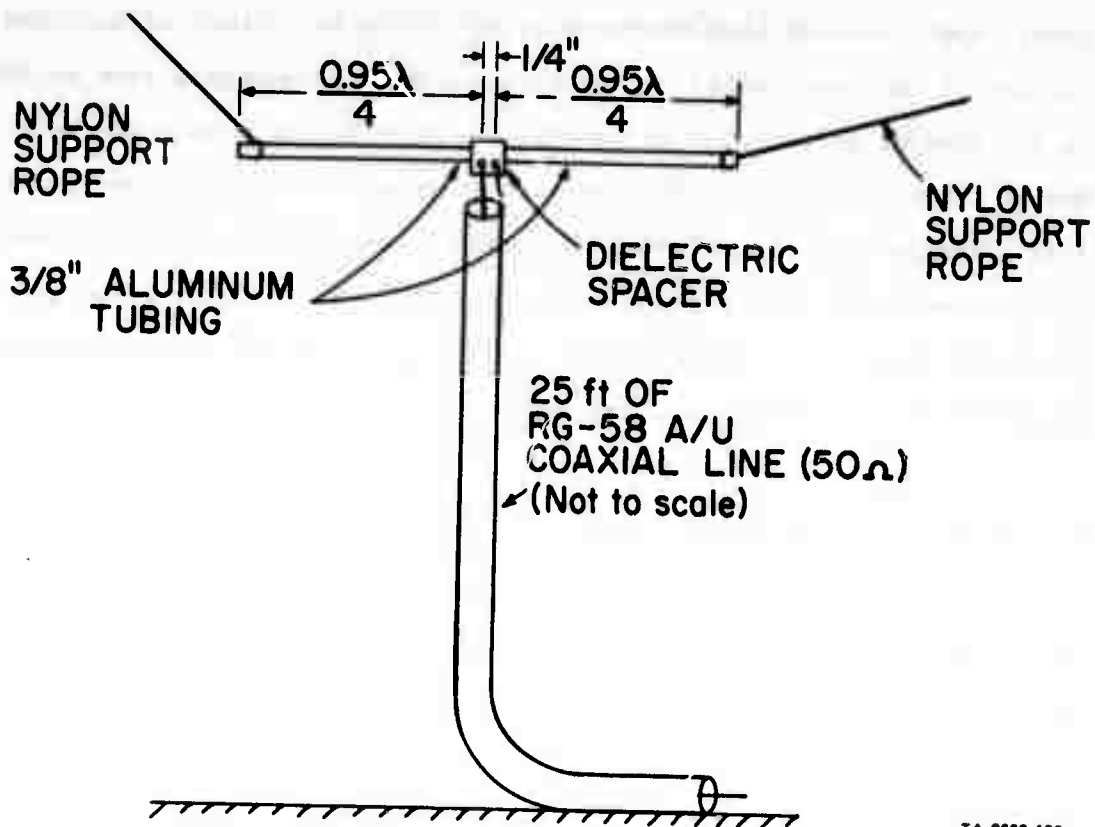


FIGURE 2 HORIZONTAL UNBALANCED DIPOLE ANTENNA

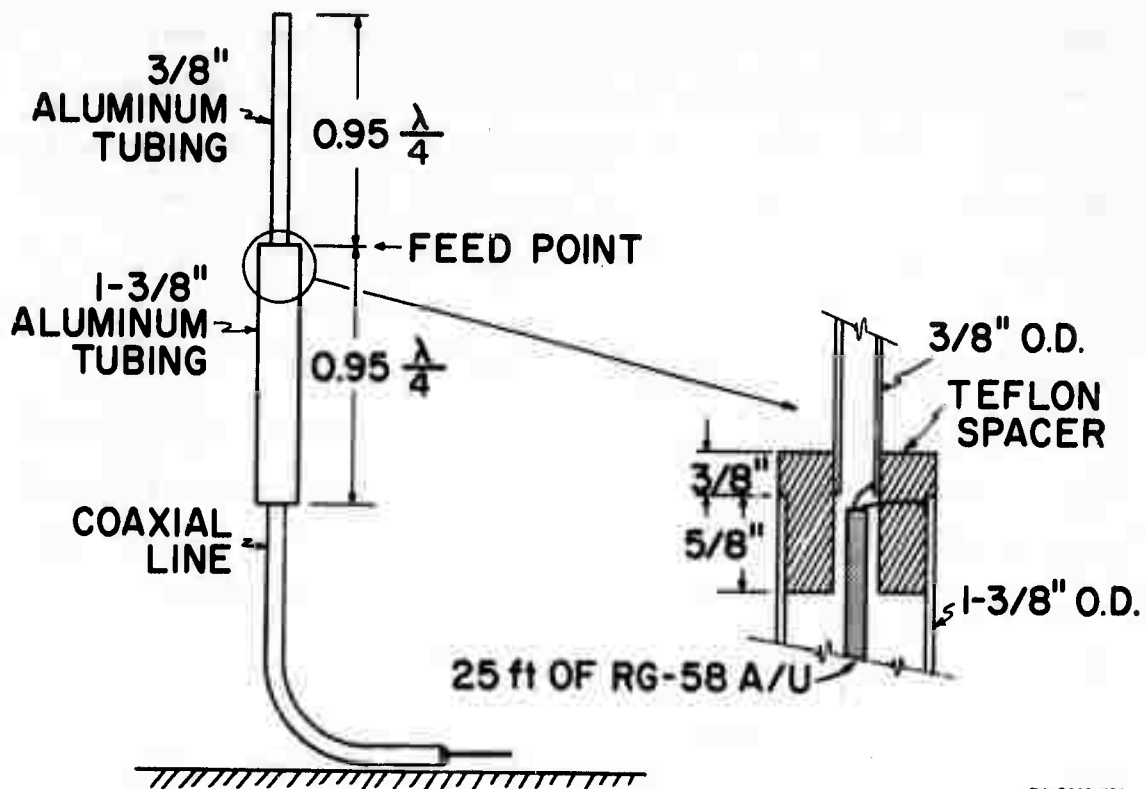
B. Vertical Sleeve Dipole Antennas

The vertical sleeve dipole antennas were constructed from 3/8-inch and 1-3/8-inch-diameter aluminum tubing, as shown in Figure 3. The radiating element was made of 3/8-inch-diameter tubing scaled for 95 percent of $\lambda/4$ and supported with a Teflon spacer from a sleeve of 1-3/8-inch-diameter tubing of the same length as the radiating element. The RG-58/U coaxial transmission line was brought up through the center of the sleeve to the base of the radiating element. The sleeve dipoles were supported with their feed points 10 feet above the ground with bamboo poles, as shown in the typical installation in Figure 4.

C. Horizontal and Vertical Balanced Dipole Antennas

The balanced dipole antennas were the same as those used for the manpack Xeledop measurements of signal strength as a function of range.^{3,9,10} These half-wave dipoles were designed to be portable, self-supporting, and adjustable. The antenna elements were telescoping automobile antennas that could be adjusted to operate from 50 to 100 MHz.

A 1:1 balun transformer (North Hills Model 1100BB) was mounted near the antenna feed point on a 2-foot support arm of phenolic material. This arm also served as a support to keep the RG-58/U coaxial transmission line perpendicular to the antenna elements for the first two feet beyond the antenna connection. The antenna support arm was fastened to a wooden mast section by a clamp, which allowed the antenna to be rotated to any desired orientation, as shown in Figure 5. The antenna mast was supported by an adjustable wooden tripod, with the feed point of the antenna located 10 feet above the ground. The length of the radiating elements was determined from previous measurements where they were adjusted to resonance over an open delta.³ These antenna lengths (for a feed-point height of 10 feet) for each frequency were:



TA-8663-239

FIGURE 3 VERTICAL SLEEVE DIPOLE ANTENNA

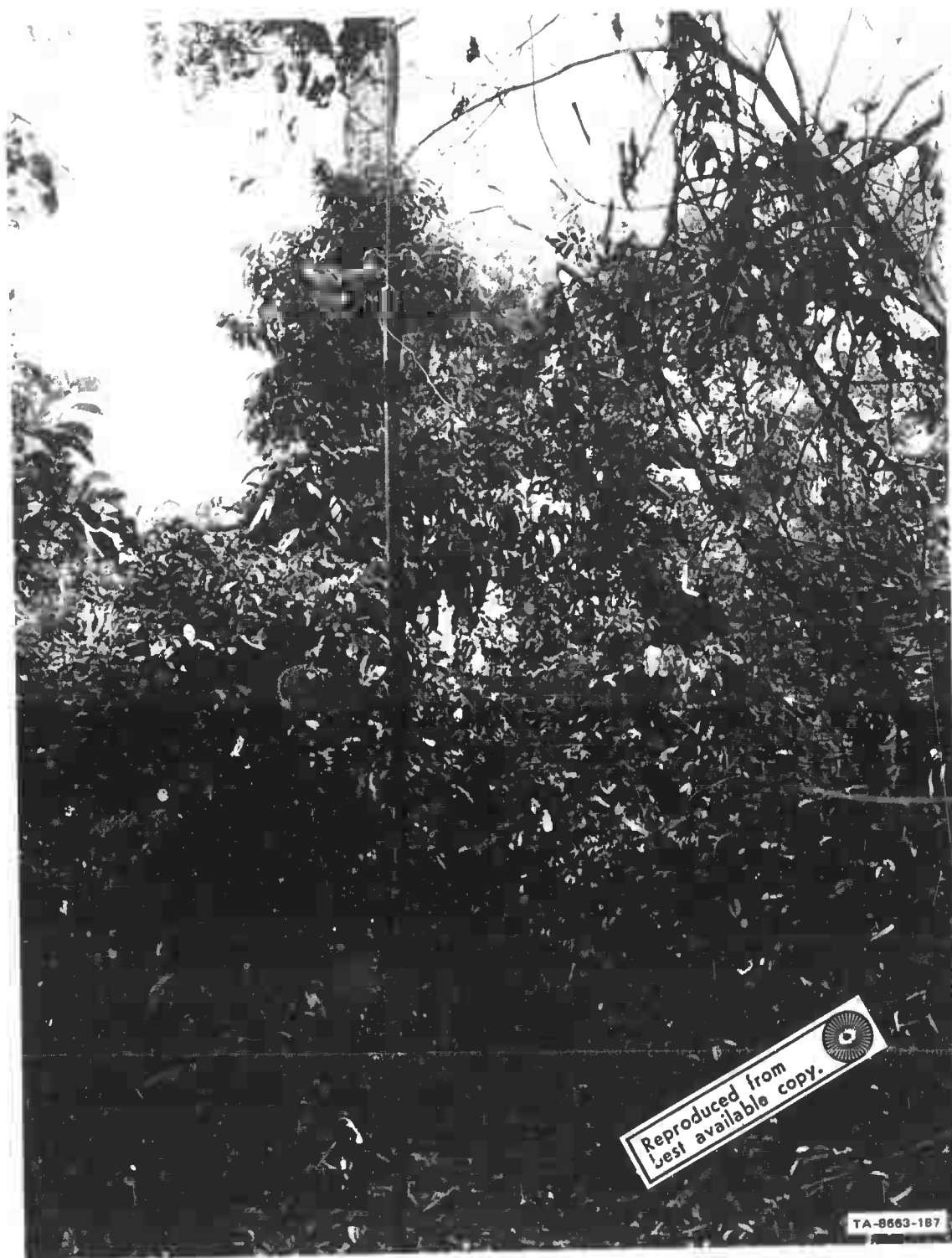


FIGURE 4 TYPICAL VERTICAL SLEEVE DIPOLE INSTALLATION



FIGURE 5 PHOTOGRAPH OF HORIZONTAL BALANCED DIPOLE INSTALLATION

50 MHz	112.5 inches
75 MHz	77.0 inches
100 MHz	60.5 inches.

D. Horizontal and Vertical Folded Dipole Antennas

The folded dipole antennas that were measured were part of a patrol antenna kit designed for the AN/PRC-10 radio sets. The nomenclature designation used for this kit is CDTC-V PATROL ANTENNA, MK III, PRC10. The measured antennas were two 48- to 54-MHz folded dipole antennas with 36 feet of 300- Ω "twin lead" (NR 214-056) transmission line. The twin lead was wound onto a small movie film reel for storage. A coaxial balun was mounted on the reel along with a coaxial connector for connecting the antenna to the radio set.^{4,11} These antennas were measured at 50 MHz while oriented in the horizontal configuration and while oriented in the vertical configuration; in both cases, the feed points of the antennas were 36 feet above the ground.

III DESCRIPTION OF THE MEASUREMENT SITE

A brief description of the tropical forest used for these measurements is presented below. A more comprehensive description can be found in Appendix G of Ref. 8, which describes the site documentation performed by the Environmental Sciences Division of the Joint Thai-U.S. Military Research and Development Center, Bangkok, Thailand.

The measurement site was located on the edge of a tapioca plantation, as shown in Figure 6. The antennas were located in and near the forest adjoining the tapioca field, as indicated in Figures 7 and 8.

The forest used for these measurements was mainly second growth. Scattered trees in the upper and middle story, remains of fallen trees, and decomposed stumps indicated that the forest had gone through a heavy exploitation in the past. A great number of large-sized trees of commercial value in the upper and middle stories had been removed; therefore the remaining trees were either species of negligible commercial value, or small trees associated with a dense undergrowth layer. Trees in the upper story were of an uneven height of over 75 feet, and the crown canopy was a discontinuous layer. There was relatively no separation in the lower stories. The greatest density of the vegetation was in the lowest story and undergrowth layer (from the ground up to 46 feet), and 88.7 percent of the trees were under 50 feet tall. The lowest story of the forest was about 20 to 46 feet high. Since some individual trees were lower than the undergrowth, there was no distinct line separating these two layers. In parts of the area, shrubs and trees in the lowest story were totally covered by a common climber which made the ground appear to be covered with a green sheet. Because of the dense undergrowth,

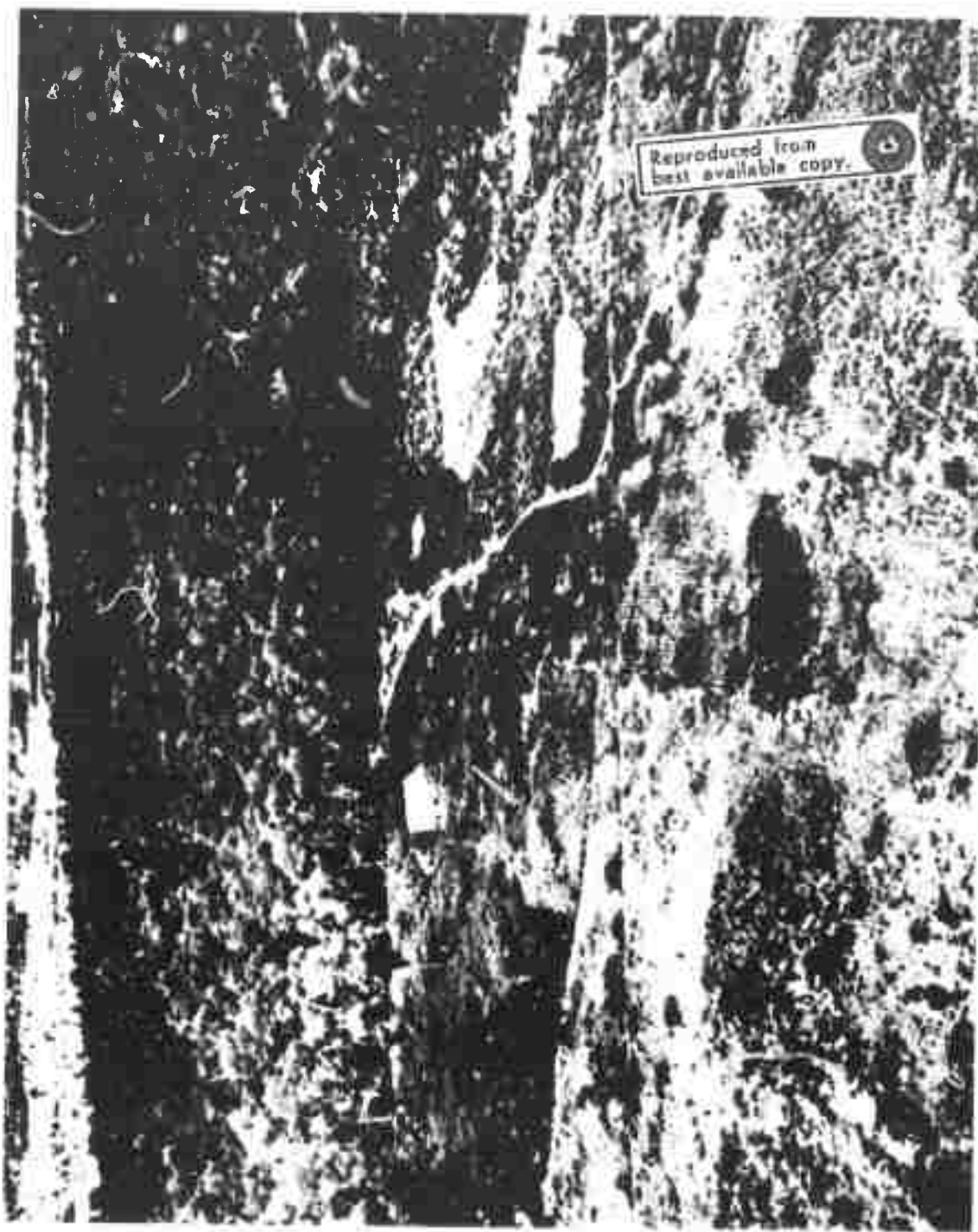
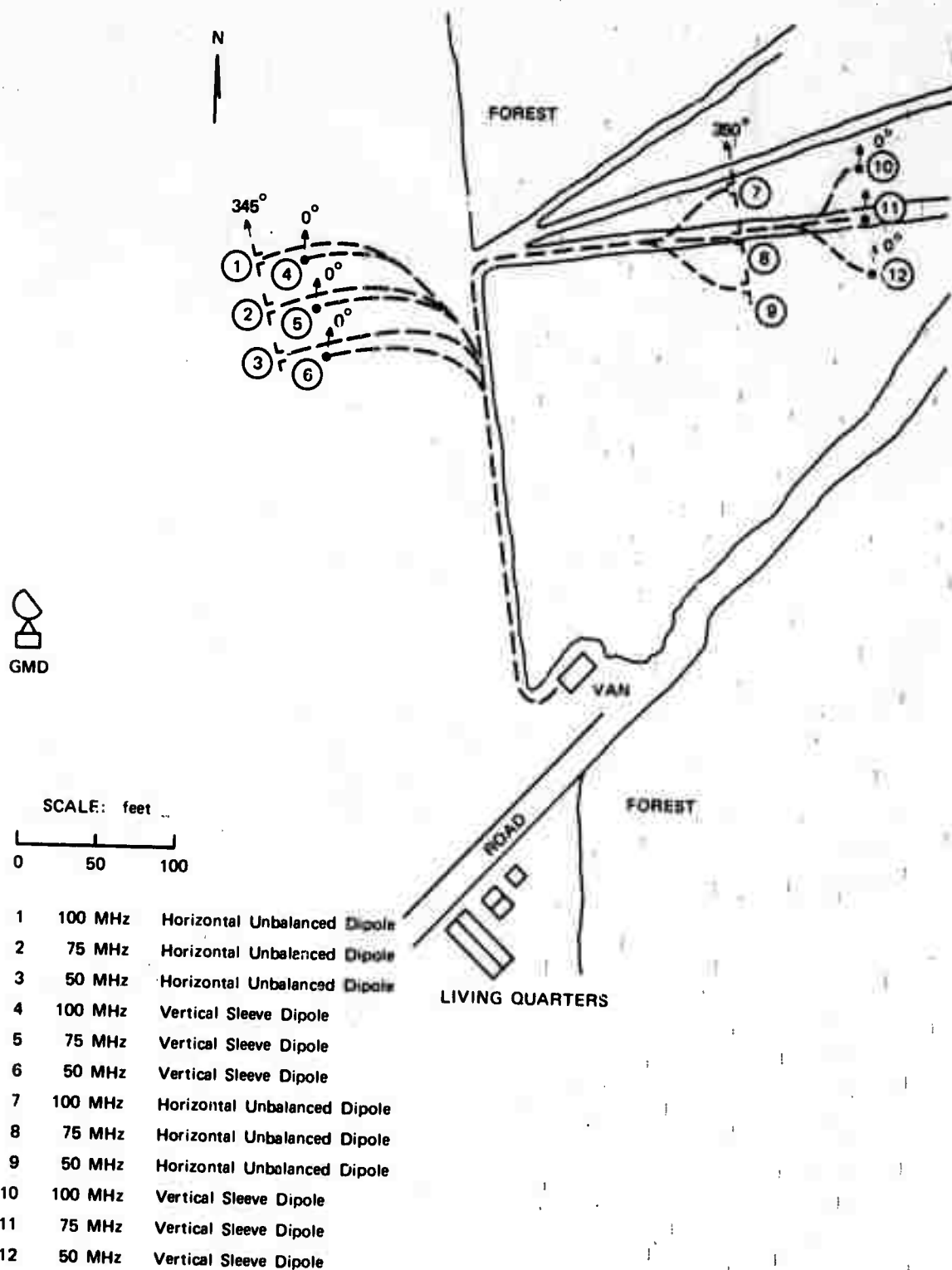
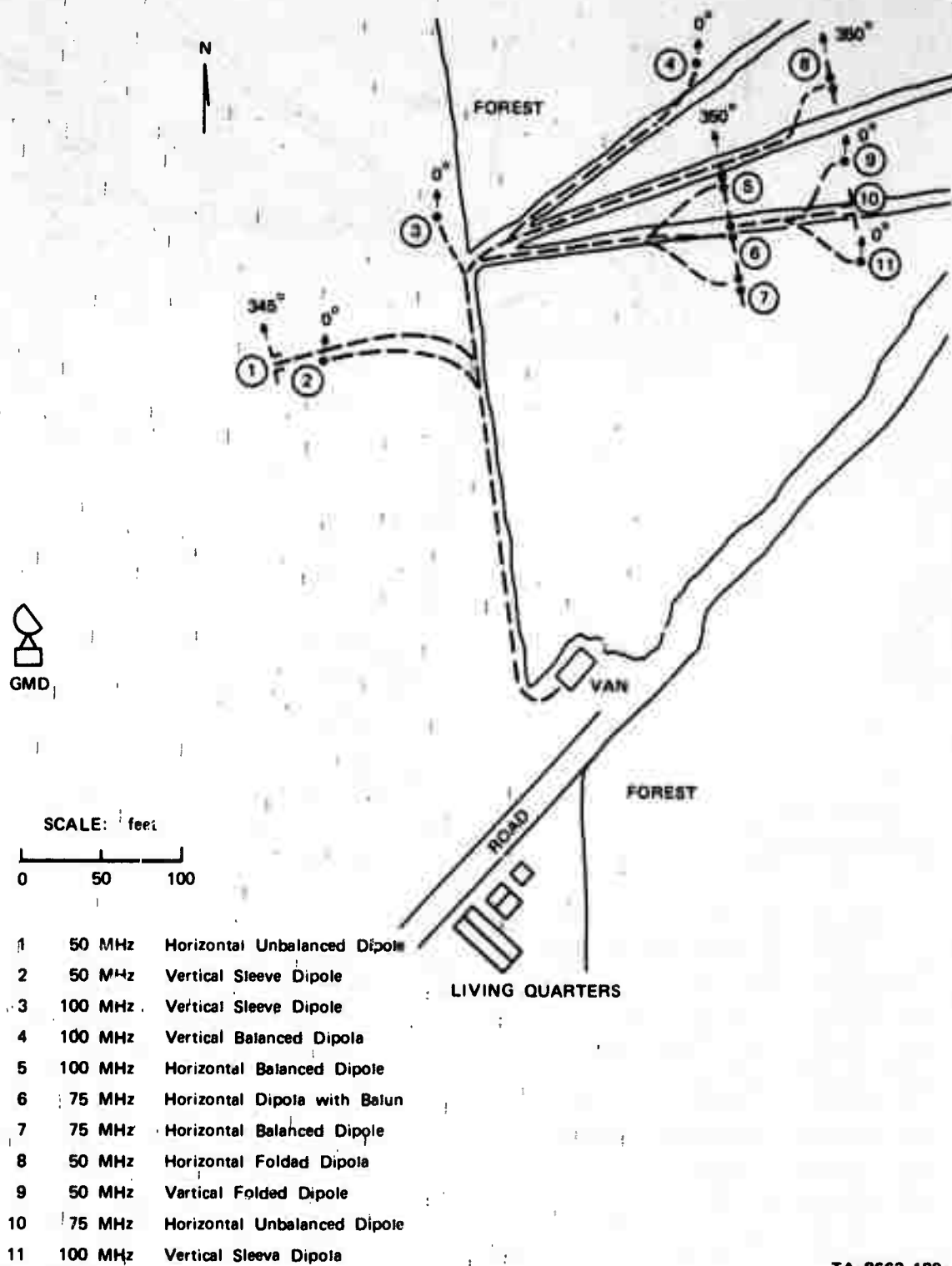


FIGURE 6 AERIAL PHOTOGRAPH OF ANTENNA MEASUREMENT SITE



TA-8663-19

FIGURE 7 SITE MAP FOR ANTENNA SET 1



TA-8663-189

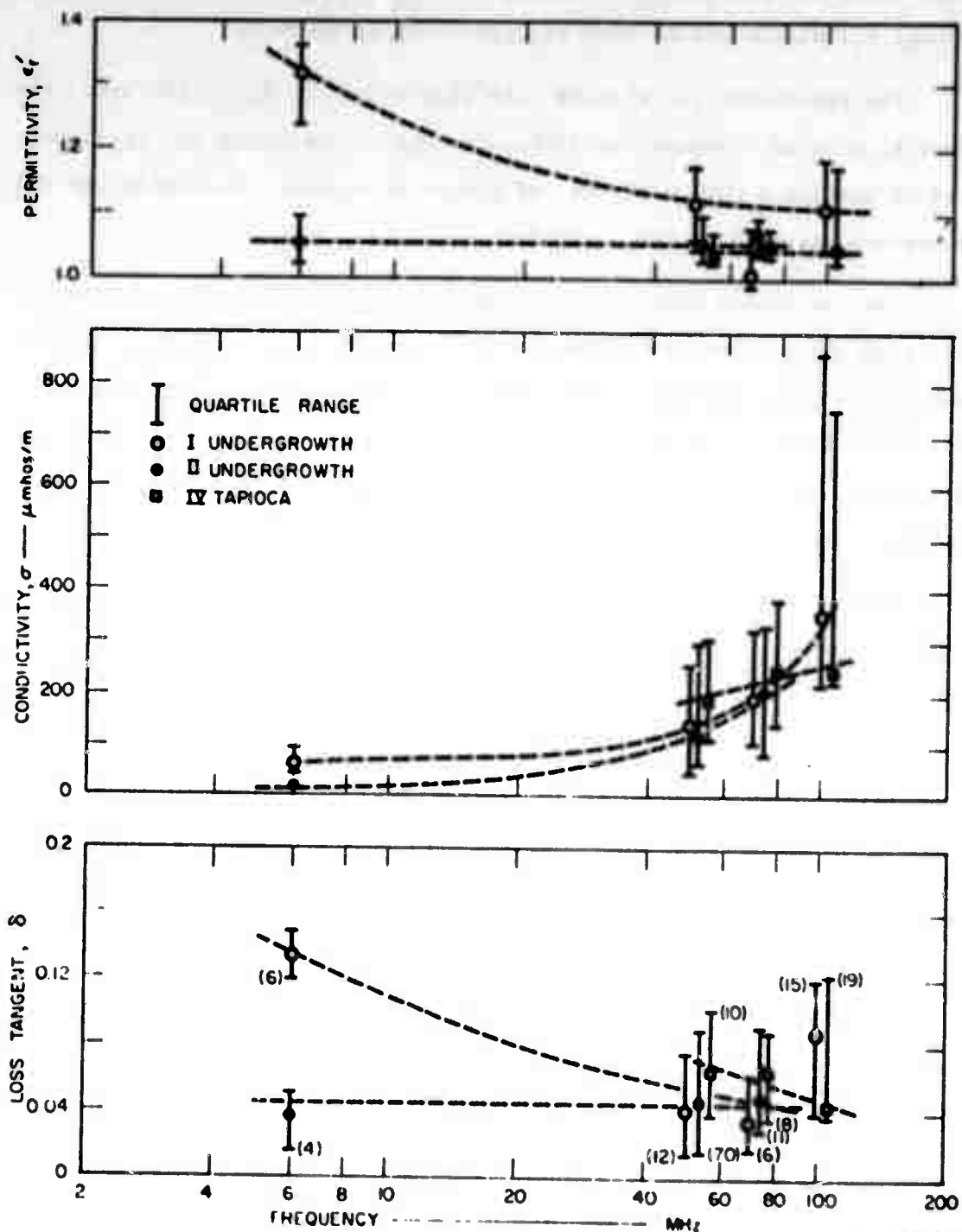
FIGURE 8 SITE MAP FOR ANTENNA SET 2

visibility was poor both vertically and horizontally. The average horizontal visibility was limited to approximately 30 feet.

The vegetation was removed from this site only where necessary for trails, coaxial transmission lines, passage of equipment and personnel, and to provide a couple of feet of clearance between the vegetation and radiating elements of the antennas.

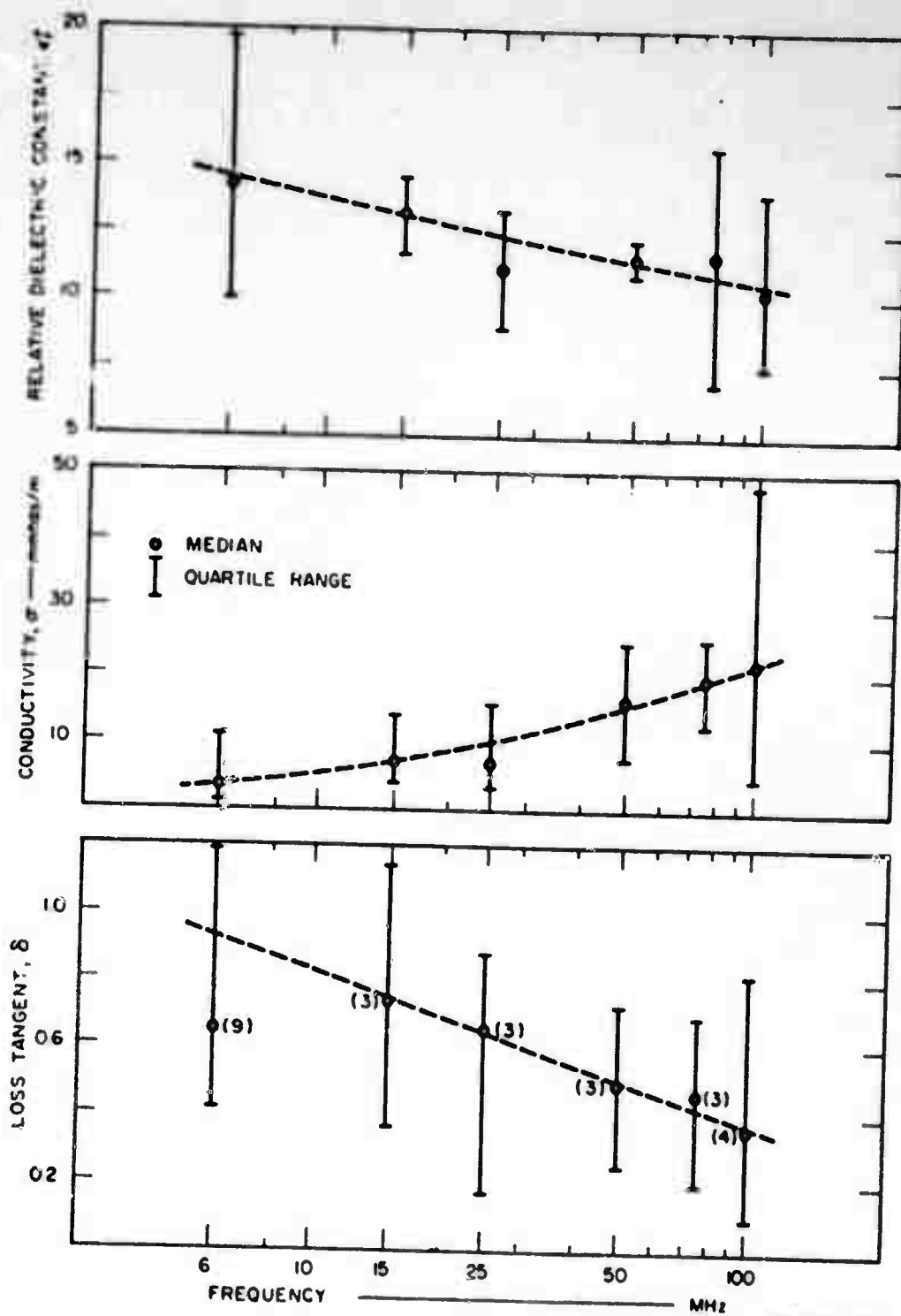
The electrical properties of the undergrowth at Ban Mun Chit were measured using open-wire transmission lines (OWLs) at different sites and in different seasons.⁸ The results of these measurements are presented in Figure 9, which shows the median values and quartile ranges as a function of frequency. The number of samples is indicated in parenthesis on the loss-tangent plot.

Ground constants also were measured at Ban Mun Chit using OWL probes. These results are summarized in Figure 10.



TA-8863-59

FIGURE 9 ELECTRICAL CONSTANTS OF FOLIAGE MEASURED AT BAN MUN CHIT



TA-8663-56

FIGURE 10 GROUND CONSTANTS MEASURED IN FOREST AT BAN MUN CHIT

IV PATTERN-MEASUREMENT EQUIPMENT

The antenna patterns were measured by towing a multifrequency special purpose transmitter (Xeledop) on a 300-foot dielectric rope behind an aircraft modified especially for this purpose. While the aircraft flew in circular orbits around the antennas being measured, the signals received by the measurement antennas on the ground were recorded digitally on magnetic tape and on analog strip-chart recorders together with the position of the aircraft as indicated by electronic tracking aides. The data for each antenna were then processed to provide contour plots of the median response of one antenna to one polarization for a given frequency as functions of azimuth and elevation angles. The instrumentation and field-measurement techniques are briefly described in this section, and the data processing is discussed in Section V.

A. The VHF Xeledop

The VHF Xeledop is a scaled-down version of the eight-frequency Xeledop that has been described in reports discussing previous HF measurements^{2,5,6,12} and in the open literature.¹³ Unlike the HF Xeledop, which uses sequentially keyed transmitters, the VHF Xeledop can operate either continuously on three frequencies (50, 75, and 100 MHz) or in a commutated mode. Continuous operation, as was used for these measurements, is made possible through the use of a passive, three-section multicoupler to match any or all of three transmitters to the dipole antenna. Tuned coupling transformers transform the reactive impedance of the short dipole to 50 Ω , and parallel-tuned traps provide isolation for the three transmitters. Thus, any one coupling transformer is loaded by the dipole but not by the other transmitters.¹⁴

The VHF Xeledop and its associated stabilizing equipment are shown in Figure 11. From top to bottom, these items are VHF Xeledop, fiberglass tail fin and balancing rod (for operation in the horizontal orientation), and drag cone (for operation in the vertical orientation). A similar VHF Xeledop was adapted for use on a backpack, and also was employed at Ban Mun Chit to obtain signal attenuation as a function of distance as the unit was carried on a special backpack down a forest trail.^{3,9,10,16}

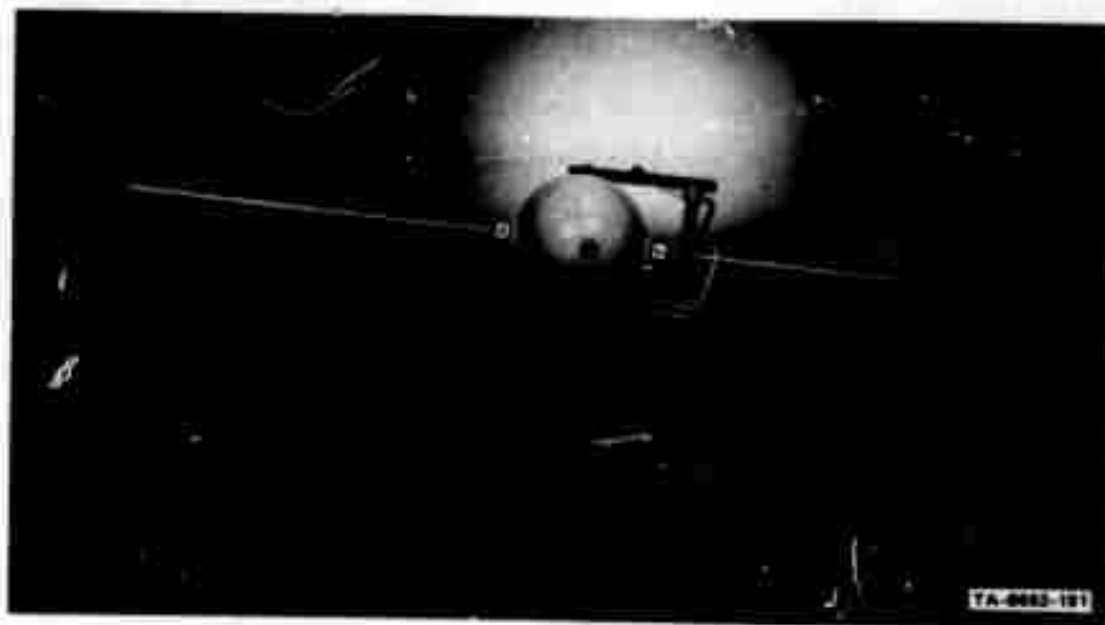


FIGURE 11 VHF XELEDOP AND STABILIZING HARDWARE

B. Aircraft Tracking and Guidance

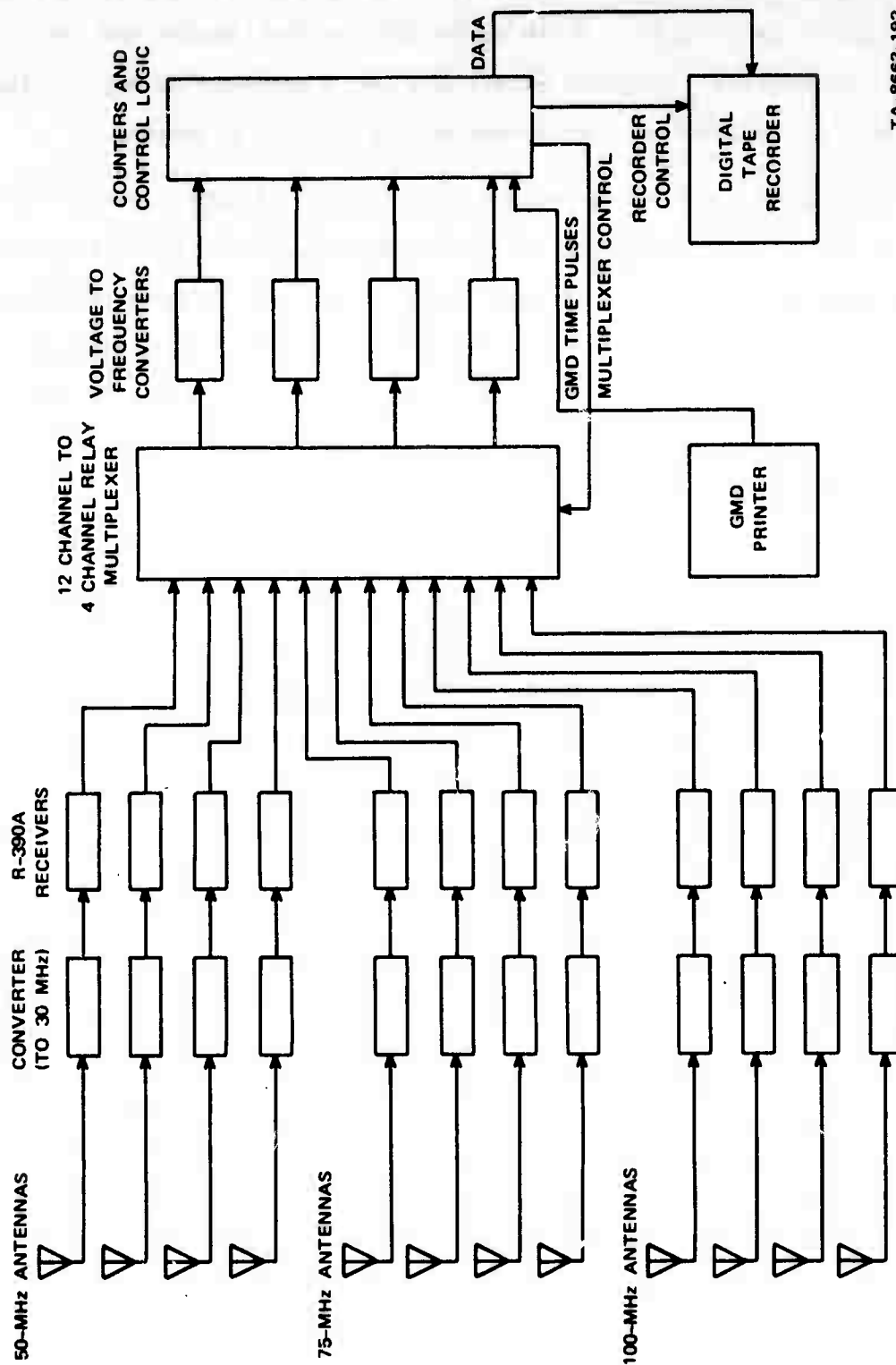
In addition to the Xeledop transmitter, the aircraft carries a low-power radio beacon transmitter and a modified APX-6 (IFF) transponder unit. Both are used for position information. The beacon is tracked by ground equipment, which provides azimuth and elevation information for data processing; the airborne transponder operates with a similar unit on the ground to indicate slant range for the pilot's information. The latter, displayed on a meter, is called the Pilot's Deviation Indicator (PDI).

The ground-tracking unit is a Rawin AN/GMD-1 Weather Balloon Tracker (referred to as the GMD). A steerable dish antenna tracks the aircraft beacon transmitter. Azimuth, elevation, and a sequence number (called GMD time) are printed on adding-machine paper every 6 seconds.

Although the operating frequency of the GMD is approximately 1.6 GHz, it has been found that metal and wooden towers--such as those normally found at a permanent antenna installation--do not interfere sufficiently with the signals to cause erratic operation of the tracking unit. However, the dish will start to "hunt" for the beacon if the signal is blocked by a large object or by numerous trees, as was the case when measurements were conducted in a conifer forest.⁶ To overcome this problem, the GMD was elevated on a 20-foot steel tower. With the GMD so situated, minor tracking problems occurred below about 15° elevation (breaking point between trees and sky), but reasonable tracking could be maintained down to 5° elevation. When tracking was lost, it was primarily the elevation angles that were erroneous; during these few occasions, it was necessary to rely on the pilot to maintain his orbit with the PDI, barometric altimeter, and ground reference points.

C. Receiving and Recording

A block diagram of the receiving and digital recording system is shown in Figure 12. The receiver consisted of crystal-controlled converters that translated the received frequencies of 50, 75, and 100 MHz to 30 MHz, so that the AGC voltage of the R-390A/URR receivers could be monitored by the recording system. The inputs to the converters were padded so that their input impedance would remain within 1.2:1 VSWR of 50 ohms. The AGC voltages were used as inputs to the digital recording equipment and, because this was the first major measurement program where the VHF measurement data were recorded on digital magnetic tape,



TA-8663-192

FIGURE 12 BLOCK DIAGRAM OF VHF RECEIVING AND RECORDING SYSTEM

were also monitored with analog strip-chart recorders as a backup and for on-line monitoring purposes.

The 12-channel-to-4-channel relay multiplexer was controlled by the control logic of the digital recording equipment. This unit connected four receivers on one frequency to the four voltage-to-frequency converters. The digital values were derived by counting the cycles of the four voltage-to-frequency converters over a period of 2.5 ms, and these digital values were written on a magnetic tape. Then, the multiplexer switched to the next group of four antennas, and the received signals were again sampled and recorded. Each block of data containing samples from all twelve antennas is referred to as a frame of data; this data frame was preceded by a preamble containing the GMD time during that sample (the GMD time was established by controlling an electronic counter with the relay that advanced the sequence counter on the GMD printer). Between every 32 frames, a record preamble was written, containing information such as the date the measurements were conducted, the run number, and an identifier to indicate if the system was being calibrated or if pattern measurement data were being recorded.

Calibration of the receiving and recording equipment was accomplished by means of a crystal-controlled signal generator with a 50- Ω output impedance, which operated on the three Xeledop frequencies. This signal was injected through a stepped attenuator into the system in place of the antenna (before the converter pads) and was stepped in 10-dB steps over a 40-dB range. The dynamic range of the recording system was extended to 80 dB by using push-button attenuators between the converter pads and the converters. The attenuation required to keep the recorders within the 40-dB calibrated range was then inserted by the operators (in 10- or 20-dB steps), and the value was recorded on the monitoring strip-chart recorders by the operators so that this attenuation could be compensated for during the data processing.

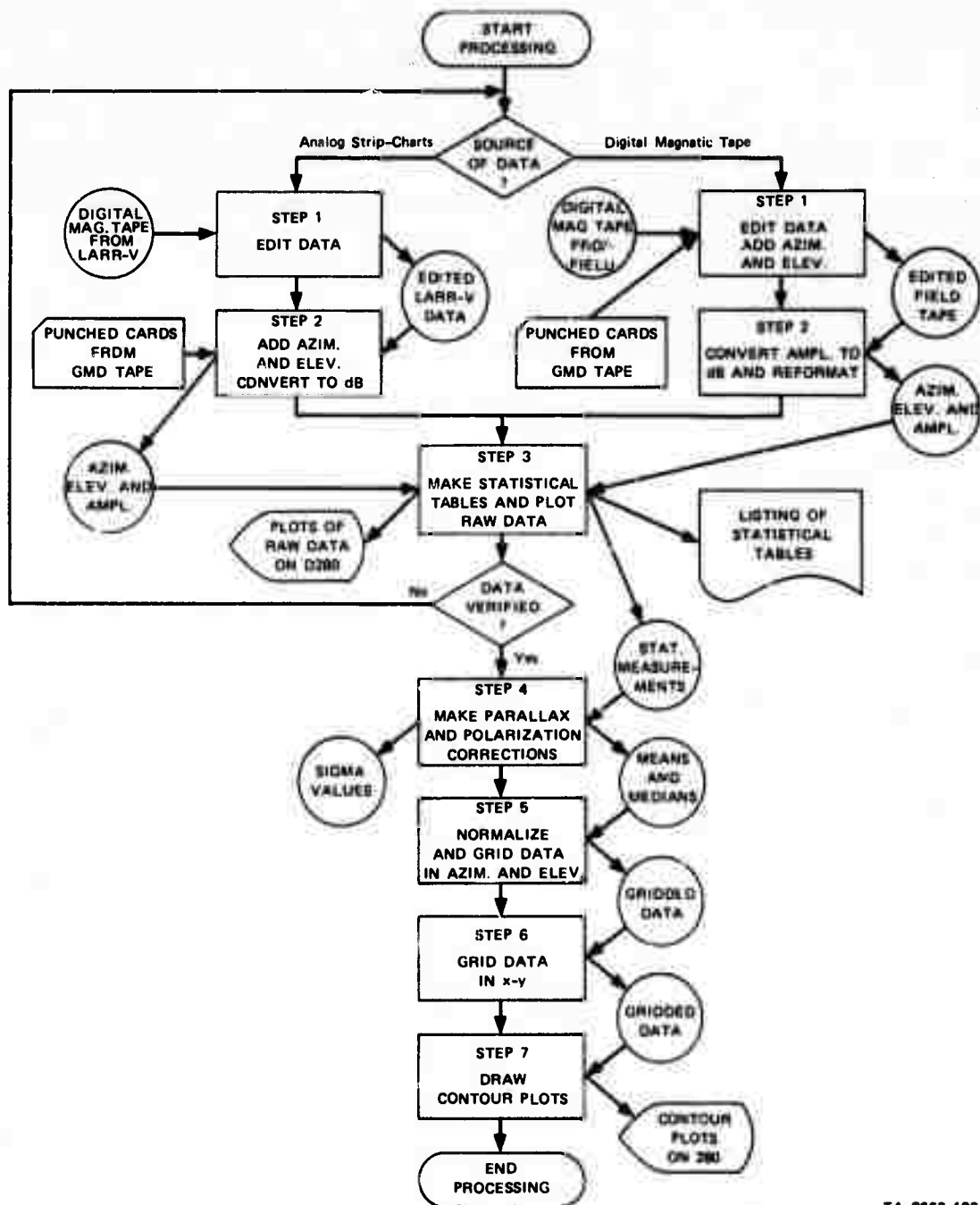
V DATA PROCESSING

The processing of the antenna pattern-measurement data was accomplished with semiautomatic scaling and plotting devices and a Control Data Corporation Model 3200 digital computer. Only the general steps in the data processing are outlined in this section, since the details of each computer program are not necessary to understand the final presentation of the processed data.

As the data flow chart in Figure 13 shows, the field data came from two sources. Digital magnetic tape recorded at the field site was the preferred data medium because it was directly usable by a digital computer. It was fortunate, however, that analog strip-chart recordings of the same data were made simultaneously, because the magnetic tape containing the horizontal polarization (E_{ϕ}) data for Set 1 was not readable on any of the four computers available. The disadvantage of strip-chart data is the necessity of manually scaling (analog-to-digital conversion) in order to transfer the data to a medium suitable as direct digital computer input. Because the scaling operation requires a human operator, the time and cost of data reduction increases as does the possibility of data scaling errors.

The analog strip-chart data for Set 1 (E_{ϕ}) were manually scaled by a semiautomatic data-scaling device, a Benson Lehner LARR-V. The LARR-V recorded the amplitude data and calibration levels in the form of x and y coordinates directly onto digital magnetic tape.

As the first step in processing the magnetic tape data from both sources an editing program corrected all obvious errors from the field data. The magnetic tapes recorded in the field frequently had records



TA-8663-183

FIGURE 13 FLOW CHART OF MAJOR STEPS IN VHF ANTENNA PATTERN DATA PROCESSING

with parity errors and missing characters. The data scaled from the strip-charts contained data scaling errors in the identifying data fields and in the data field indicating attenuation changes. The editing program for digital magnetic tape data rejected only amplitude values beyond the range of the analog-to-digital converters described in Section IV-C. With this program, it was attempted to recover as much data as possible from those records with parity errors and/or missing characters.

Neither source of field data contained azimuth or elevation values, but by means of the GMD time, recorded on both media, azimuth and elevation could be related to the amplitude sample points. Azimuth and elevation values and the GMD time, which were recorded every 6 seconds on the GMD tape at the same time the amplitude data were recorded (described in Section IV-B), were recorded on computer cards. Since the recording rate of the GMD was much slower than that of the digital recorder, approximately 60 frames of amplitude values were recorded between two consecutive GMD time counts, azimuth and elevation values for each amplitude frame were found by linear interpolation between the values provided by the GMD at 6-second intervals. Similarly, there were a number of amplitude values (ranging from 5 to 30 samples) scaled from the analog strip-charts for each GMD time (6 seconds), and the corresponding azimuth and elevation angles also were found by linear interpolation between the known values at each recorded GMD time.

The signal amplitude values from both sources of data had to be converted to decibels. Calibration values for each 10-dB step of the 40-dB calibrated range were recorded in the field for each channel (one antenna and frequency combination). Within each calibration step the intervening amplitude values were found by linear interpolation. This piecewise-linear function was interpolated to fit the calibration curve about as accurately as a least-squares curve-fitting technique. Amplitude values

outside the calibration range were rejected. The attenuation inserted by the operators at the time the data were recorded was added to the amplitude after it had been converted to decibels.

The analog strip-chart data were scaled and processed for one antenna/frequency channel at a time, while the data recorded on magnetic tape were processed for 12 antenna/frequency channels simultaneously. As a result, the edited magnetic tape data required reformatting to reduce tape handling operations on the computer. This was accomplished at Step 2 at the time the amplitude data were converted to dB (see Figure 13).

From Step 3 through Step 7 the data from both sources followed the same path. At Step 3 several statistical calculations were performed. The median, $\hat{\mu}'$, and the mean, $\hat{\mu}$, amplitudes were found for each 10° azimuth segment at each elevation angle of the transmitter. Estimators of the standard deviations about the median amplitude, $\hat{\sigma}'$, and the standard deviation about the mean amplitude, $\hat{\sigma}$, were derived from the square roots of the second moments about the median ($\sqrt{\hat{\mu}_2'}$) and about the mean ($\sqrt{\hat{\mu}_2}$) amplitudes. In addition to these, estimators were derived of the standard deviations of the samples above the median and mean (peaks), $\hat{\sigma}'_p$ and $\hat{\sigma}_p$, and of the standard deviations of the samples below the median and mean (nulls), $\hat{\sigma}'_n$ and $\hat{\sigma}_n$. These statistical estimators were printed in tabular form, a sample of which appears in Section VI (Tables 1 through 12), and were written on magnetic tape to serve as input to subsequent processing steps. To reduce the processing time of the data recorded originally on magnetic tape, where the number of amplitude values per orbit averaged 6000, only every third data point was used in the calculations. Every data point was used from the scaled analog strip-chart data which averaged 2000 points per orbit. Plots of amplitude versus azimuth for each transmitter elevation were also produced on the Control Data Corporation Model 280 Display System (a cathode-ray tube display device on-line with the

computer) in Step 3. These plots were compared with the analog strip-chart recordings to verify the accuracy of the scaled data. Examples of these plots are shown in Section VI-D (Figure 17). An overlooked attenuation change showed up clearly on these plots as a 10- or 20-dB discontinuity. When serious errors occurred on an antenna/frequency channel, the data for this channel were reprocessed from Step 1 with appropriate corrections. The computer program in Step 4 computed the azimuth and elevation of the transmitter with respect to the antenna instead of the location of the aircraft with respect to the GMD as was recorded in the field. The program then computed an actual slant range and added to the mean and median amplitudes from Step 3 a correction factor K:

$$K = 20 \log_{10} \left(R/R_n \right) ,$$

where R is the computed actual slant range and R_n is the normalizing slant range (typically 4 miles). When the Xeledop transmitter was oriented vertically, a factor of $20 \log_{10} \cos$ (elevation angle) was added to the amplitude to correct for the transmitting pattern of the Xeledop, which was assumed to be that of a Hertzian dipole, and produce the vertical polarization (E_θ) pattern. No correction was necessary on the horizontal polarization (E_ϕ) patterns.

The next two steps in the processing procedure prepared the data for contouring. The amplitude values were normalized so that the maximum observed estimated median value was 0 dB. The amplitude values at the intersection points of an azimuth-elevation grid were found by simple plane-surface interpolation. The grid was divided into 6-degree steps of azimuth from -174 degrees to +180 degrees and 2-degree steps of elevation from 2 to 60 degrees.

In Step 6 this azimuth-elevation grid was converted to Cartesian (x and y) coordinates required by the contouring program.* These gridded values were used in the final step to produce contour plots of amplitude as a function of azimuth and elevation. The plots were produced on 35-mm film on the Control Data Corporation Model 280 Display System. The azimuth and elevation grid lines on the plot were generated at the same time as the contour lines, thus avoiding the problem of overlaying and registration. These contour plots of estimated median amplitude (in dB relative to the maximum estimated median amplitude) produced by the process described above are described in more detail in Section VI-B and are presented in Appendices A and B of this report.

* A proprietary item purchased from Computer Laboratories, Inc., Houston, Texas.

VI STATISTICAL ESTIMATIONS FROM THE PATTERN DATA

The amplitude data were processed, as discussed in Section V, to provide tabulations of the estimated statistical parameters of the pattern data as well as contour plots of the estimated median amplitude. To be strictly correct one should refer to these calculations as estimated means, estimated medians, etc., but for simplicity these estimated statistical parameters will be referred to as means, medians, and standard deviations for the remainder of this report. Examples of these calculated estimators are shown in Tables 1 through 12 which show all the parameters calculated from the orbital data to make up the two (E_{θ} and E_{ϕ}) contour plots used to define the response of the 75-MHz horizontal dipole with balun located in the forest. Tables 1 through 6 are derived from the E_{θ} data and Tables 7 through 12 are derived from the E_{ϕ} data. The first column in the tables simply indicates the interval number (remember that the data are segmented into 10° azimuthal sectors, and these 10° sectors were considered to be the statistical samples). The next column gives the sample size or the number of valid points in the 10° interval. If there were no valid points in an interval (e.g., in a pattern null where the received signal dropped below the receiver sensitivity), a message indicating this was printed out. As discussed in Section V, every third point derived from the field tape was used for the statistical calculations. If less than 30 points were found in a 10° interval, the program would use every point in the interval--these cases are indicated with an asterisk in the "ss" column. The next two columns are the mean azimuth (relative to magnetic north) and mean elevation angles of the sample interval (these values have not been corrected for parallax). Examples of obvious elevation angle errors that have not been corrected can be

Table 1

STATISTICAL PARAMETERS FOR THE 75-MHz DIPOLE WITH BALUN—IN THE FOREST, 2° AT 4° ELEVATION

Interval	SF	Azimuth	Elevation	Median	Signs		Median-mean	Mean	Signs		Combined Signs
					Peaks	Nulls			Peaks	Nulls	
1	34	83.0	8.8	-35.23	1.87	3.25	0.33	-35.38	2.11	2.80	2.45
2	31	73.0	8.1	-35.71	4.07	3.50	-0.53	-35.18	4.15	2.81	2.88
3	11	61.0	8.1	-37.14	1.34	1.42	-0.22	-36.93	1.51	1.08	0.98
4	30	55.0	7.4	-37.38	3.31	1.87	-0.83	-36.74	3.27	2.00	1.63
5	34	42.0	5.4	-33.90	4.34	3.70	-0.28	-33.30	3.98	3.93	3.88
6	46	33.0	8.0	-31.90	2.88	4.87	0.28	-32.18	3.79	3.84	3.33
7	34	20.0	8.0	-36.42	3.88	3.33	-0.81	-35.82	3.26	3.69	3.33
8	39	15.0	8.0	-34.28	1.30	3.70	0.88	-34.94	2.81	3.10	2.93
9	49	5.0	6.2	-34.10	2.43	3.27	0.50	-34.28	2.17	2.27	2.18
10	43	283.0	5.4	-34.78	3.10	2.31	-0.21	-34.33	2.90	2.58	2.72
11	31	345.0	3.4	-34.28	3.94	3.43	2.21	-34.89	2.93	3.23	3.08
12	39	335.0	17.8	-33.80	2.40	2.47	0.19	-33.89	2.10	2.11	2.48
13	47	325.0	5.4	-32.38	3.14	1.87	-0.15	-32.23	2.00	1.88	1.88
14	50	315.0	2.4	-32.38	2.83	3.30	0.24	-32.40	2.88	3.28	3.03
15	43	305.0	5.4	-30.00	1.30	3.71	1.79	-31.76	3.13	4.08	3.82
16	44	295.0	6.7	-28.20	1.79	3.38	1.83	-27.13	3.71	3.42	3.80
17	33	285.0	5.4	-28.27	2.04	7.00	1.47	-29.74	2.93	7.20	4.90
18	46	275.0	3.4	-27.73	1.83	2.31	0.03	-27.79	1.93	2.29	2.10
19	40	265.0	5.4	-21.88	1.88	4.30	0.73	-22.45	1.34	4.98	3.79
20	41	255.0	3.4	-22.38	1.94	1.88	0.32	-23.70	2.13	2.71	4.79
21	37	245.0	3.4	-35.33	2.30	2.41	-0.18	-35.05	2.34	3.44	3.38
22	43	235.0	3.4	-34.28	2.88	3.54	-0.28	-33.49	2.70	2.85	2.44
23	39	225.0	18.7	-33.80	3.47	4.00	0.29	-34.09	3.41	2.83	2.41
24	41	215.0	5.4	-32.80	1.80	2.80	0.29	-33.08	1.77	2.83	2.11
25	33	205.0	3.4	-33.80	1.79	4.00	0.74	-34.54	1.88	3.83	2.88
26	13	195.0	5.4	-27.81	1.30	1.72	0.19	-27.80	1.44	1.33	1.43
27	19	185.0	3.4	-25.33	3.20	5.92	0.39	-23.73	3.80	7.54	5.84
28	37	175.0	3.4	-26.19	4.87	1.79	-1.18	-29.83	3.82	2.57	3.08
29	31	165.0	5.4	-31.71	1.71	2.30	0.23	-35.98	1.88	2.08	1.94
30	30	155.0	3.4	-36.90	8.52	1.71	-0.28	-36.22	2.38	1.83	2.08
31	22	145.0	3.4	-38.37	1.48	1.18	0.02	-38.38	1.05	1.18	1.07
32	18	135.0	3.4	-38.09	1.28	1.43	0.12	-38.71	1.19	1.21	1.20
33	09	125.0	6.0	-39.04	1.90	0.75	-0.47	-38.33	1.78	0.97	1.38
34	03	115.0	6.0	-32.71	2.49	2.78	0.08	-35.79	2.23	2.68	2.45
35	17	105.0	6.0	-38.33	1.41	1.27	-0.08	-38.25	1.33	1.21	1.38
36	30	95.0	8.0	-27.81	4.18	1.40	-1.08	-26.23	3.88	2.03	2.41
37	38	85.0	8.0	-23.80	2.63	3.07	-0.28	-23.41	3.33	3.13	2.18
38	29	75.0	7.0	-34.78	1.78	3.30	0.73	-35.48	2.30	2.78	2.68
39	23	65.0	7.0	-38.23	2.08	3.68	-0.08	-39.17	3.92	3.29	3.47
40	26	55.0	7.0	-27.13	2.96	1.53	-0.23	-28.61	2.68	1.91	2.23

Table 2

STATISTICAL PARAMETERS FOR THE 75-MHz DIPOLE WITH BALUN--IN THE FOREST, E. AT 14° ELEVATION

Interval	SS	Azimuth	Elevation	Median	Sigma		Median-Mean	Mean	Sigma		Combined Sigma
					Peaks	Nulls			Peaks	Nulls	
1	42	225.0	15.2	-32.00	2.16	3.97	0.71	-32.71	2.63	3.46	2.99
2	34	215.0	15.2	-32.50	3.75	4.15	0.10	-32.60	3.64	4.06	3.89
3	31	205.0	15.2	-35.50	7.08	2.53	-1.92	-33.58	5.17	4.19	4.58
4	41	195.0	14.2	-29.64	1.01	1.75	0.10	-29.74	0.88	1.66	1.21
5	51	185.0	14.2	-28.21	1.54	3.58	0.95	-29.06	2.06	3.16	2.54
6	49	175.0	13.1	-31.50	2.57	4.71	0.84	-32.34	3.05	4.30	3.60
7	41	165.0	13.1	-35.50	2.46	2.62	0.41	-35.91	2.53	2.43	2.45
8	39	155.0	13.1	-36.50	3.53	2.34	-0.49	-36.01	3.09	2.53	2.76
9	44	145.0	13.1	-33.50	4.21	3.13	-0.57	-32.63	3.57	3.47	3.48
10	36	135.0	13.6	-34.50	4.77	3.25	-0.64	-33.66	4.36	3.27	3.66
11	31	125.0	13.8	-36.50	7.09	2.50	-1.96	-34.54	5.50	4.16	4.74
12	38	115.0	14.3	-33.50	2.61	4.16	0.66	-34.16	2.93	3.80	3.27
13	34	105.0	14.3	-31.00	2.56	4.34	0.67	-31.67	2.71	3.97	3.27
14	34	95.0	14.3	-33.75	3.77	2.93	-0.38	-33.37	3.66	3.98	3.30
15	34	85.0	14.3	-35.00	3.42	3.53	0.15	-35.15	3.23	3.39	3.25
16	33	75.0	14.3	-35.50	1.53	2.56	0.16	-35.68	1.47	2.39	1.82
17	41	65.0	14.3	-32.00	4.49	3.90	-0.26	-31.74	4.26	4.03	4.09
18	45	55.0	14.3	-28.57	1.58	4.57	1.26	-29.85	2.21	3.93	2.94
19	39	45.0	14.3	-30.50	2.03	6.30	1.94	-32.44	3.41	5.02	4.08
20	40	35.0	14.3	-27.14	1.06	8.21	2.69	-29.83	3.23	7.47	4.91
21	44	25.0	13.2	-29.46	2.28	5.40	1.27	-30.73	3.18	4.84	3.89
22	26	15.0	13.1	-29.46	1.60	5.46	1.34	-30.60	2.44	5.67	3.70
23	44	5.0	13.2	-31.00	4.72	6.19	0.53	-31.53	4.57	6.02	5.14
24	45	355.0	14.0	-30.00	3.08	4.49	0.63	-30.63	3.10	4.31	3.62
25	46	345.0	14.0	-28.92	2.13	2.87	0.08	-29.00	1.88	2.81	2.28
26	47	335.0	14.0	-27.14	2.90	2.07	-0.35	-26.79	2.61	2.23	2.39
27	49	325.0	14.0	-24.84	1.04	0.65	-0.24	-24.40	0.82	0.72	0.16
28	48	315.0	14.0	-26.25	1.21	1.92	0.24	-26.49	1.33	1.86	1.51
29	46	305.0	14.0	-25.71	2.34	3.82	0.38	-26.07	2.36	3.55	2.51
30	47	295.0	14.0	-25.35	3.31	3.04	0.93	-25.38	3.03	3.01	2.99
31	47	285.0	14.0	-28.92	2.68	4.23	0.30	-29.22	2.66	3.99	3.25
32	36	275.0	14.0	-28.92	1.05	4.69	1.07	-28.99	1.61	5.14	2.94
33	42	265.0	14.0	-28.03	1.68	5.07	1.28	-29.29	2.52	4.92	3.51
34	47	255.0	14.0	-31.00	2.51	3.59	0.22	-31.22	2.50	3.40	2.90
35	36	245.0	14.0	-34.50	3.07	3.58	0.07	-34.57	2.87	3.52	3.13
36	21	235.0	14.0	-38.50	4.23	1.21	-0.60	-37.90	3.60	1.42	2.16
37	46	225.0	14.0	-35.25	3.76	1.45	-1.02	-34.23	2.99	2.33	2.62
38	40	215.0	14.0	-31.50	2.35	4.45	0.83	-32.33	2.94	4.06	3.41
39	24	205.0	14.0	-36.00	7.37	2.72	-2.17	-33.83	5.52	4.67	4.96

Table 3

STATISTICAL PARAMETERS FOR THE 75-MHz DIPOLE WITH BALUN--IN THE FOREST, E₀ AT 25° ELEVATION

Interval	SS	Azimuth	Elevation	Median	Sigma		Median-Mean	Mean	Sigma		Combined Sigma
					Peaks	Nulls			Peaks	Nulls	
1	39	255.0	24.9	-31.00	1.86	3.40	0.76	-31.76	2.19	2.78	2.43
2	39	245.0	24.9	-29.28	1.57	3.63	0.84	-30.12	2.02	3.45	2.62
3	40	235.0	24.9	-32.00	2.37	3.65	0.60	-32.60	2.60	3.63	3.01
4	39	225.0	24.9	-29.64	0.93	2.70	0.67	-30.51	1.43	2.17	1.73
5	40	215.0	24.9	-26.25	0.87	1.73	0.38	-26.63	0.94	1.62	1.23
6	40	205.0	24.9	-29.10	2.18	1.77	-0.18	-28.92	2.03	1.93	1.95
7	39	195.0	24.9	-28.21	2.63	5.36	1.05	-29.26	3.59	4.55	4.00
8	32	185.0	24.9	-28.21	3.41	5.82	0.86	-29.07	3.73	5.30	4.41
9	36	175.0	24.9	-29.28	1.68	5.15	1.20	-30.48	2.50	4.48	3.35
10	40	165.0	24.9	-28.03	1.68	3.12	0.60	-28.63	2.14	2.76	2.40
11	39	155.0	24.9	-28.57	2.01	3.20	0.25	-28.82	1.95	3.02	2.44
12	31	145.0	24.9	-34.50	3.15	2.78	-0.37	-34.13	2.81	2.69	2.70
13	29	135.0	24.9	-33.00	2.33	3.73	0.61	-33.61	2.82	3.15	2.93
14	33	125.0	24.9	-32.00	3.63	3.34	-0.37	-31.63	3.27	3.53	3.36
15	40	115.0	24.8	-30.50	1.90	1.95	0.00	-30.50	1.78	1.95	1.82
16	36	105.0	24.6	-34.25	4.23	3.00	-0.63	-33.62	3.80	3.45	3.57
17	37	95.0	24.6	-28.92	1.47	2.64	0.55	-29.47	1.60	2.42	1.94
18	32	85.0	24.6	-34.50	2.30	2.82	0.08	-34.58	2.41	2.75	2.53
19	33	75.0	24.6	-36.50	1.23	2.23	0.41	-38.91	1.43	1.87	1.62
20	24	65.0	24.6	-33.50	2.20	3.68	0.44	-33.94	2.30	3.28	2.68
21	38	55.0	24.6	-29.28	2.00	2.57	0.07	-29.35	1.81	2.52	2.10
22	39	45.0	24.6	-28.42	2.40	2.76	0.23	-26.65	2.33	2.55	2.51
23	38	35.0	24.6	-25.89	3.06	2.17	-0.40	-25.49	2.78	2.48	2.59
24	38	25.0	24.6	-24.82	1.85	1.80	-0.01	-24.81	1.84	1.81	1.80
25	39	15.0	24.8	-23.92	1.78	1.85	-0.12	-23.80	1.68	1.63	1.63
26	39	5.0	24.6	-25.71	2.01	2.35	0.10	-25.81	1.84	2.26	2.01
27	40	355.0	24.6	-23.57	1.68	2.98	0.20	-23.77	1.57	2.82	2.06
28	39	345.0	24.6	-20.71	1.74	2.46	0.27	-20.98	1.96	2.21	2.05
29	39	335.0	24.6	-22.50	1.55	1.27	-0.11	-22.39	1.46	1.27	1.34
30	39	325.0	24.6	-24.28	3.25	2.68	-0.15	-24.13	3.10	2.55	2.75
31	44	315.0	24.6	-23.57	1.65	3.12	0.25	-23.82	1.68	2.94	2.25
32	40	305.0	24.6	-29.10	3.54	4.77	0.46	-29.56	3.83	4.52	4.12
33	41	295.0	24.6	-27.85	2.04	2.21	-0.09	-27.77	1.97	2.16	2.04
34	31	285.0	24.6	-32.50	3.95	3.93	-0.09	-32.41	3.86	3.87	3.80
35	42	275.0	24.6	-28.27	1.05	0.83	-0.14	-28.43	0.92	0.74	0.80
36	42	265.0	24.6	-30.50	3.45	3.09	-0.19	-30.31	3.27	3.03	3.10
37	38	255.0	24.6	-33.00	2.72	3.39	-0.05	-32.95	2.87	2.92	2.77
38	40	245.0	24.6	-29.28	1.85	5.69	1.67	-30.95	3.05	4.59	3.69
39	38	235.0	24.6	-32.50	2.89	3.62	0.23	-32.73	2.94	3.42	3.13

Table 4

STATISTICAL PARAMETERS FOR THE 75-MHz DIPOLE WITH BALUN--IN THE FOREST, E_θ AT 33° ELEVATION

Interval	SS	Azimuth	Elevation	Median	Sigma		Median-Mean	Mean	Sigma		Combined Sigma
					Peaks	Nulls			Peaks	Nulls	
1	39	155.0	33.0	-28.42	2.43	3.11	0.15	-28.57	2.07	2.99	2.43
2	40	145.0	33.0	-25.00	2.50	2.32	-0.06	-24.94	2.45	2.08	2.22
3	38	135.0	32.1	-28.39	3.81	3.51	-0.18	-28.21	3.65	3.66	3.81
4	38	125.0	32.4	-29.10	2.10	2.90	0.21	-29.31	2.08	3.11	2.49
5	38	115.0	32.9	-27.85	0.93	2.43	0.21	-28.06	0.92	2.25	1.42
6	38	105.0	32.9	-32.85	5.04	2.08	-1.27	-31.58	4.51	2.77	3.43
7	39	95.0	32.9	-28.42	1.21	2.91	0.50	-26.92	1.49	2.90	2.11
8	36	85.0	32.9	-31.42	5.74	5.81	-0.55	-30.87	5.21	5.38	5.23
9	34	75.0	32.9	-35.23	2.74	2.40	0.07	-35.30	2.45	2.33	2.36
10	28	85.0	32.9	-32.14	1.98	4.23	0.59	-32.73	2.28	4.42	3.18
11	38	55.0	32.9	-29.28	2.38	5.07	1.12	-30.40	3.02	4.27	3.58
12	39	45.0	32.9	-24.64	1.34	1.38	0.13	-24.77	1.29	1.24	1.25
13	35	35.0	32.9	-21.78	0.75	1.77	0.47	-22.25	1.01	1.42	1.17
14	38	25.0	32.9	-18.48	0.55	1.37	0.26	-18.74	0.78	1.17	0.98
15	37	15.0	32.9	-18.78	0.87	1.01	-0.02	-18.78	0.85	0.91	0.87
16	40	5.0	32.9	-18.48	0.81	3.99	1.10	-19.58	1.53	4.08	2.44
17	38	355.0	32.9	-17.11	0.21	3.10	1.15	-18.26	1.18	2.96	1.83
18	37	345.0	32.9	-17.57	0.42	1.74	0.47	-18.04	0.88	1.68	1.05
19	39	335.0	32.9	-20.35	1.88	1.85	-0.10	-20.25	1.79	1.83	1.78
20	38	325.0	32.9	-22.85	1.04	0.92	0.04	-22.89	0.99	0.88	0.93
21	39	315.0	32.9	-22.85	2.18	3.00	0.14	-22.99	2.14	2.88	2.45
22	39	305.0	32.9	-22.85	0.64	0.90	0.19	-23.04	0.69	0.72	0.70
23	40	295.0	32.9	-23.21	0.86	1.17	0.17	-23.38	0.89	1.01	0.93
24	38	285.0	32.9	-25.53	1.91	1.74	-0.11	-25.42	1.80	1.84	1.80
25	39	275.0	32.9	-22.85	0.81	1.73	0.35	-23.20	0.96	1.43	1.17
28	40	265.0	32.9	-23.57	1.81	2.20	0.13	-23.70	1.61	2.09	1.81
27	42	255.0	32.9	-28.39	0.79	1.47	0.22	-28.81	0.88	1.51	1.14
28	27	245.0	32.9	-34.28	3.24	3.50	0.33	-34.81	3.11	3.21	3.09
29	32	235.0	32.9	-32.82	2.31	4.04	0.65	-33.26	2.83	3.62	3.17

Table 5

STATISTICAL PARAMETERS FOR THE 75-MHz DIPOLE WITH BALUN--IN THE FOREST, E_0 AT 45° ELEVATION

Interval	SS	Azimuth	Elevation	Median	Signs		Median-Mean	Mean	Signs		Combined Signs
					Peaks	Nulls			Peaks	Nulls	
No points in Interval 1											
No points in Interval 2											
No points in Interval 3											
No points in Interval 4											
No points in Interval 5											
No points in Interval 6											
No points in Interval 7											
8	15	285.0	44.6	-24.44	0.55	0.31	-0.07	-24.57	0.47	0.20	0.38
9	29	275.0	44.9	-28.43	0.43	0.52	-0.07	-28.35	0.56	0.41	0.48
10	27	265.0	44.9	-32.80	4.13	2.82	-0.77	-32.08	3.37	3.03	3.23
11	19	255.0	44.9	-37.61	2.51	1.44	-0.30	-37.31	2.23	1.55	1.81
12	30	245.0	44.9	-43.85	2.03	2.95	0.40	-44.20	2.13	2.61	2.33
13	29	235.0	44.9	-50.47	0.88	2.70	0.01	-51.38	1.51	2.51	1.87
14	29	225.0	44.9	-54.38	2.01	4.00	0.60	-54.87	2.43	3.53	2.97
15	25	215.0	44.9	-59.38	2.38	3.88	0.43	-59.70	1.94	4.78	2.89
16	31	205.0	44.9	-63.57	0.74	0.97	0.07	-63.84	0.83	0.81	0.73
17	32	195.0	45.2	-65.06	1.40	1.83	-0.01	-64.99	1.78	1.00	1.66
18	31	185.0	46.2	-69.90	1.79	1.34	-0.01	-70.04	1.79	1.38	1.51
19	31	175.0	46.2	-74.64	1.77	2.74	0.23	-74.91	1.80	2.58	2.13
20	32	165.0	46.2	-81.43	0.70	1.88	0.37	-81.89	0.89	1.97	0.86
21	31	155.0	46.2	-82.16	0.88	1.83	0.53	-82.67	1.03	1.84	1.23
22	31	145.0	46.2	-82.85	0.58	1.31	0.40	-83.25	0.66	1.18	0.85
23	28	135.0	45.8	-83.07	0.78	0.85	0.05	-83.82	0.58	0.61	0.57
24	30	125.0	45.8	-88.06	1.60	0.83	-0.34	-84.78	1.29	0.84	1.07
25	30	115.0	45.8	-92.50	1.17	1.13	-0.03	-92.47	1.14	1.04	1.07
26	31	105.0	45.8	-94.64	1.03	0.54	-0.48	-94.16	1.17	0.78	0.92
27	29	95.0	45.9	-93.21	0.88	1.03	0.08	-93.27	0.83	0.88	0.78
28	31	85.0	46.5	-93.57	1.38	0.88	-0.18	-93.41	1.23	0.88	1.08
29	28	75.0	46.5	-94.64	1.64	2.07	0.47	-95.11	1.76	2.32	2.08
30	35	65.0	45.8	-98.82	1.09	0.52	-0.38	-98.88	1.04	0.58	0.83
31	32	55.0	45.5	-100.47	1.13	1.02	0.21	-100.68	0.85	1.14	0.98
32	27	45.0	45.5	-97.14	1.73	1.93	0.77	-97.51	1.42	1.80	1.50
33	28	35.0	45.5	-93.35	0.88	0.61	-0.10	-93.25	0.77	0.83	0.88
34	26	25.0	45.5	-90.42	1.03	1.48	-0.04	-90.38	1.18	1.24	1.20
35	32	15.0	45.5	-84.64	1.30	2.27	0.22	-84.88	1.40	2.08	1.88
36	26	5.0	45.5	-18.24	1.13	0.83	-0.11	-18.13	1.03	1.03	1.03
37	32	355.0	45.5	-18.48	1.08	1.31	0.12	-18.60	0.85	1.21	1.05
38	29	345.0	45.5	-18.88	0.65	1.27	0.20	-17.02	0.63	1.13	0.82

Table 6

STATISTICAL PARAMETERS FOR THE 75-MHz DIPOLE WITH BALUN--IN THE FOREST, E₀ AT 55° ELEVATION

Interval	SS	Azimuth	Elevation	Median	Sigma		Median-Mean	Mean	Sigma		Combined Sigma
					Peaks	Nulls			Peaks	Nulls	
1	25	225.0	57.3	-35.23	1.26	1.53	-0.05	-35.16	1.23	1.24	1.21
2	22	215.0	57.3	-30.95	0.92	1.45	0.13	-31.06	0.92	1.32	1.07
3	26	205.0	56.5	-30.00	0.42	1.89	0.66	-30.66	0.71	1.70	1.07
4	22	195.0	55.2	-34.52	0.65	1.30	0.32	-34.64	0.62	1.21	0.95
5	28	185.0	54.1	-33.60	2.34	1.62	-0.37	-33.43	1.98	1.97	1.94
6	28	175.0	53.7	-31.90	1.12	0.86	-0.20	-31.70	0.93	0.61	0.85
7	27	165.0	53.2	-28.57	0.48	1.19	0.13	-28.70	0.45	1.06	0.66
8	28	155.0	53.6	-28.57	0.72	0.50	-0.14	-28.43	0.59	0.45	0.51
9	26	145.0	55.1	-29.46	0.91	0.71	-0.06	-29.36	0.84	0.78	0.80
10	23	135.0	56.5	-30.95	0.67	1.10	0.00	-30.95	0.67	0.61	0.73
11	25	125.0	57.6	-32.85	1.16	2.75	0.73	-33.56	1.32	2.36	1.72
12	22	115.0	57.6	-33.33	1.20	1.09	-0.09	-33.24	1.12	0.90	0.97
13	26	105.0	56.0	-33.33	0.75	1.04	0.03	-33.36	0.63	1.01	0.77
14	25	95.0	55.6	-31.42	1.15	0.83	-0.09	-31.33	1.06	0.66	0.61
15	2*	85.0	55.6	-38.60	0.00	0.00	0.00	-36.60	0.00	0.00	1.01
No points in Interval 16											
17	17	65.0	55.9	-36.19	2.10	0.80	-0.40	-35.79	1.72	1.08	1.33
18	26	55.0	57.4	-35.23	1.09	2.33	0.52	-35.75	1.26	2.10	1.59
19	19	45.0	57.6	-29.64	4.17	2.63	-0.93	-28.71	3.27	3.21	3.15
20	25	35.0	57.5	-22.65	0.76	1.62	0.40	-23.25	0.95	1.23	1.06
21	23	25.0	55.3	-21.07	1.46	1.03	0.11	-21.16	1.07	0.93	0.96
22	26	15.0	55.5	-19.39	0.37	0.53	0.18	-19.57	0.26	0.37	0.32
23	25	5.0	55.2	-19.39	0.58	0.35	-0.17	-19.22	0.42	0.30	0.35
24	26	355.0	55.1	-16.76	1.11	0.74	-0.22	-16.56	0.92	0.72	0.60
25	23	345.0	55.1	-19.09	0.98	0.99	0.17	-19.26	0.68	0.84	0.74
26	16	335.0	55.2	-19.65	0.31	0.51	0.09	-19.93	0.39	0.43	0.40
27	26	325.0	55.9	-20.35	0.65	0.50	-0.03	-20.32	0.62	0.44	0.51
28	20	315.0	54.7	-20.35	0.64	0.66	-0.10	-20.25	0.53	0.55	0.53
29	26	305.0	54.1	-18.46	0.46	0.69	-0.04	-18.44	0.42	0.37	0.36
30	27	295.0	54.2	-20.35	0.83	2.67	0.60	-21.15	1.54	2.26	1.65
31	25	265.0	53.9	-24.28	1.10	0.86	-0.01	-24.27	1.08	0.79	0.90
32	26	275.0	53.5	-23.92	0.83	1.50	0.25	-24.17	1.00	1.26	1.11
33	23	265.0	54.4	-23.92	0.75	0.59	-0.15	-23.77	0.61	0.56	0.57
34	23	255.0	54.6	-25.71	0.85	2.20	0.73	-26.44	1.34	1.46	1.37
35	16*	245.0	55.9	-29.10	0.71	1.64	0.22	-29.32	0.74	2.28	1.20
36	11	235.0	55.1	-37.14	2.66	1.12	-0.46	-36.66	2.23	1.48	1.76
37	42	225.0	55.1	-29.64	3.41	4.97	0.64	-30.46	3.90	4.26	4.01
38	23	215.0	54.2	-20.71	0.78	1.56	0.36	-21.09	0.93	1.35	1.06

* See text.

Table 7

STATISTICAL PARAMETERS FOR THE 75-MHZ DIPOLE WITH BALUN--IN THE FOREST, E₀ AT 5° ELEVATION

Interval	SS	Azimuth	Elevation	Median	Sigma		Median-Mean	Mean	Sigma		Combined Sigma
					Peaks	Nulls			Peaks	Nulls	
1	37	135.0	5.4	-34.28	2.26	2.98	0.17	-34.45	2.28	2.84	2.52
2	44	125.0	5.4	-33.09	2.08	4.05	0.81	-33.90	2.52	3.89	3.08
3	40	115.0	5.4	-31.42	2.44	3.27	0.04	-31.46	2.06	3.24	2.56
4	40	105.0	5.7	-32.85	1.83	4.71	1.27	-34.12	2.47	4.00	3.13
5	40	95.0	6.5	-30.47	1.63	4.50	0.93	-31.40	2.32	3.71	2.94
6	41	85.0	8.5	-24.28	2.08	7.06	1.63	-25.91	3.24	6.86	4.80
7	42	75.0	8.4	-27.32	2.07	1.76	-0.18	-27.14	1.91	1.92	1.89
8	47	65.0	7.8	-24.64	1.55	1.71	0.06	-24.70	1.40	1.65	1.50
9	43	55.0	6.6	-25.35	1.99	1.57	-0.20	-25.15	1.82	1.67	1.72
10	42	45.0	5.8	-23.39	2.43	4.53	1.00	-24.39	3.13	3.93	3.45
11	48	35.0	5.7	-20.89	1.72	4.09	0.85	-21.74	2.23	4.02	2.99
12	45	25.0	5.4	-23.57	2.64	2.28	-0.10	-23.47	2.55	2.15	2.32
13	43	15.0	5.9	-24.84	1.78	3.04	0.72	-25.36	2.12	2.40	2.22
14	46	5.0	6.2	-29.82	2.44	2.34	-0.11	-29.71	2.35	2.43	2.36
15	42	355.0	5.5	-34.28	7.37	3.60	-1.63	-32.65	6.24	4.63	5.31
16	46	345.0	5.5	-34.76	2.95	2.96	-0.04	-34.72	2.91	2.81	2.82
17	23	335.0	5.6	-35.71	3.09	2.88	-0.17	-35.54	2.92	2.88	2.83
18	44	325.0	5.6	-35.23	8.89	2.95	-2.45	-32.78	7.00	4.81	5.73
19	45	315.0	5.6	-25.35	2.60	1.48	-0.51	-24.84	2.32	1.77	1.99
20	40	305.0	5.6	-20.53	1.47	5.58	1.68	-22.21	2.76	5.04	3.66
21	41	295.0	5.6	-16.36	1.19	1.77	0.20	-16.56	1.29	1.58	1.40
22	39	285.0	5.6	-15.75	1.38	1.10	-0.08	-15.67	1.32	1.09	1.19
23	43	275.0	5.8	-12.72	0.67	2.74	0.74	-13.46	1.12	2.41	1.62
24	39	265.0	5.6	-14.54	2.04	0.95	-0.47	-14.07	1.86	1.18	1.45
25	39	255.0	5.8	-13.63	0.68	1.05	0.19	-13.82	0.76	0.88	0.81
26	39	245.0	5.6	-13.03	1.00	1.81	0.39	-13.42	1.23	1.53	1.35
27	43	235.0	5.6	-13.93	0.66	0.73	0.03	-13.96	0.54	0.70	0.60
28	43	225.0	5.6	-15.15	0.39	0.68	0.10	-15.25	0.34	0.59	0.44
29	43	215.0	5.6	-19.09	1.82	1.46	-0.36	-18.73	1.62	1.31	1.42
30	41	205.0	5.0	-20.71	1.25	3.21	0.99	-21.70	1.85	2.48	2.12
31	41	195.0	5.0	-23.21	2.75	4.09	0.73	-23.94	3.35	3.37	3.32
32	43	185.0	5.0	-25.71	1.51	2.14	0.12	-25.83	1.44	2.05	1.71
33	40	175.0	5.0	-32.62	3.49	3.51	0.01	-32.63	3.51	3.50	3.46
34	33	165.0	5.0	-30.00	1.50	4.01	1.12	-31.12	2.39	3.10	2.69
35	27	155.0	5.0	-36.68	2.58	2.50	0.09	-36.75	2.45	2.42	2.39
36	29	145.0	5.0	-36.19	2.03	2.29	0.18	-36.37	1.95	2.14	2.01
37	39	135.0	5.0	-35.23	3.90	2.88	-0.64	-34.59	3.50	3.04	3.20
38	30	125.0	5.0	-36.18	2.70	2.59	0.11	-36.30	2.79	2.49	2.59

Table 8

STATISTICAL PARAMETERS FOR THE 75-MHz DIPOLE WITH BALUN--IN THE FOREST, E₀ AT 13° ELEVATION

Interval	SS	Azimuth	Elevation	Median	Sigma		Median-Mean	Mean	Sigma		Combined Sigma
					Peaks	Nulls			Peaks	Nulls	
1	37	335.0	13.6	-31.90	2.42	4.86	0.64	-32.54	2.74	4.48	3.49
2	40	325.0	13.7	-19.85	1.87	5.97	1.61	-21.46	3.04	5.61	4.05
3	40	315.0	13.8	-20.53	1.08	0.98	-0.04	-20.50	1.05	1.01	1.02
4	37	305.0	13.8	-17.35	2.41	1.08	-0.66	-16.69	2.01	1.41	1.65
5	41	295.0	13.8	-13.82	0.85	1.40	0.23	-14.05	0.97	1.21	1.08
6	37	285.0	13.8	-12.35	1.54	3.17	0.73	-13.08	2.13	2.56	2.31
7	40	275.0	13.3	-11.17	0.52	0.38	-0.06	-11.11	0.46	0.29	0.36
8	40	265.0	13.3	-10.44	0.47	0.57	0.04	-10.47	0.51	0.53	0.52
9	38	255.0	13.4	-9.76	0.63	0.43	-0.11	-9.65	0.53	0.36	0.43
10	37	245.0	13.7	-10.95	1.74	0.80	-0.21	-10.74	1.56	0.85	1.15
11	37	235.0	13.7	-10.47	0.49	0.73	0.19	-10.66	0.50	0.55	0.52
12	40	225.0	13.7	-13.96	1.30	1.14	-0.06	-13.91	1.25	1.19	1.20
13	41	215.0	13.7	-17.05	0.91	0.65	-0.01	-17.04	0.90	0.59	0.71
14	39	205.0	13.7	-16.47	0.86	0.86	-0.03	-16.44	0.83	0.83	0.82
15	36	195.0	13.7	-19.41	0.64	1.01	0.13	-19.54	0.59	0.91	0.73
16	35	185.0	13.7	-20.35	1.87	5.36	1.46	-21.81	3.18	3.92	3.49
17	34	175.0	13.7	-25.53	1.82	1.73	-0.18	-25.35	1.67	1.86	1.74
18	38	165.0	13.7	-26.07	3.16	6.55	1.32	-27.39	3.83	5.72	4.59
19	33	155.0	13.7	-33.33	4.12	3.56	-0.06	-33.27	4.06	3.30	3.58
20	23	145.0	13.7	-35.23	3.97	2.80	-0.54	-34.69	3.65	3.02	3.23
21	29	135.0	13.7	-24.64	1.29	8.96	2.20	-26.84	2.85	9.92	5.21
22	40	125.0	13.7	-23.21	2.25	3.25	0.25	-23.46	2.24	3.05	2.60
23	39	115.0	13.7	-20.71	2.66	1.05	-0.77	-19.94	2.33	1.43	1.77
24	39	105.0	13.7	-19.70	1.86	1.19	-0.29	-19.41	1.62	1.27	1.42
25	40	95.0	13.7	-20.35	1.37	2.92	0.63	-20.98	1.69	2.53	2.03
26	36	85.0	13.7	-15.58	1.64	2.40	0.32	-15.91	1.90	2.16	2.00
27	41	75.0	13.7	-13.23	0.61	0.44	-0.08	-13.15	0.54	0.47	0.50
28	41	65.0	13.7	-13.23	0.53	0.31	-0.16	-13.07	0.40	0.32	0.36
29	38	55.0	13.7	-15.29	1.88	0.55	-0.60	-14.69	1.63	0.86	1.16
30	40	45.0	13.7	-14.41	1.50	0.70	-0.30	-14.11	1.23	0.87	1.02
31	41	35.0	13.7	-14.41	1.03	1.99	0.48	-14.89	1.38	1.59	1.46
32	37	25.0	13.7	-17.64	0.78	1.68	0.44	-18.08	1.11	1.30	1.19
33	38	15.0	13.7	-22.85	3.98	2.05	-0.68	-22.17	3.98	2.13	2.79
34	43	5.0	13.7	-22.50	1.57	0.82	-0.53	-21.97	1.20	0.87	1.01
35	40	355.0	13.7	-23.03	1.97	2.53	0.25	-23.28	2.03	2.51	2.22
36	45	345.0	13.7	-28.92	2.62	5.07	0.96	-29.88	3.29	4.39	3.80
37	36	335.0	13.7	-33.80	3.45	4.35	0.51	-34.31	3.38	4.17	3.67
38	43	325.0	13.7	-28.92	5.26	3.50	-0.95	-27.97	4.87	3.85	4.25

Table 9

STATISTICAL PARAMETERS FOR THE 75-MHz DIPOLE WITH BALUN--IN THE FOREST, E₀ AT 25° ELEVATION

Interval	SS	Azimuth	Elevation	Median	Sigma		Median-Mean	Mean	Sigms		Combined Sigms
					Peaks	Nulls			Peaks	Nulls	
1	38	5.0	25.8	-20.71	0.97	2.43	0.58	-21.29	1.33	2.08	1.66
2	39	355.0	26.2	-27.50	5.79	3.57	-0.99	-26.51	5.05	3.96	4.38
3	38	345.0	25.7	-25.53	1.86	2.14	0.16	-25.69	1.99	2.00	1.97
4	36	335.0	25.7	-33.80	2.42	3.58	0.51	-34.31	2.36	3.37	2.75
5	38	325.0	25.7	-26.96	3.10	3.81	-0.11	-26.85	3.00	3.88	3.42
6	39	315.0	25.7	-24.64	2.63	2.83	0.30	-24.94	2.51	2.55	2.50
7	36	305.0	25.7	-21.42	1.68	2.94	0.54	-21.96	1.90	2.52	2.15
8	39	295.0	25.7	-18.47	1.06	1.26	-0.03	-16.44	1.03	1.08	1.04
9	35	285.0	25.7	-18.52	1.61	0.95	-0.32	-18.20	1.34	1.16	1.23
10	38	275.0	25.7	-16.47	0.71	0.37	-0.23	-16.24	0.52	0.39	0.45
11	37	265.0	25.7	-11.76	0.83	2.63	0.39	-12.15	1.03	2.27	1.51
12	39	255.0	25.7	-11.76	0.87	0.38	-0.13	-11.63	0.75	0.41	0.55
13	37	245.0	24.7	-10.00	0.32	1.00	0.20	-10.20	0.41	0.82	0.58
14	39	235.0	24.7	-12.50	0.93	0.49	-0.14	-12.36	0.79	0.58	0.67
15	35	225.0	24.7	-12.50	0.38	2.23	0.72	-13.22	0.90	1.78	1.24
16	38	215.0	24.7	-16.78	0.97	0.97	0.01	-16.79	0.78	0.96	0.84
17	39	205.0	24.7	-16.42	0.83	0.76	0.10	-16.52	0.63	0.67	0.64
18	37	195.0	24.7	-16.42	0.54	0.56	-0.01	-16.41	0.53	0.34	0.40
19	37	185.0	24.7	-20.35	2.06	1.15	-0.13	-20.22	1.95	1.12	1.46
20	38	175.0	24.7	-23.57	1.77	1.17	-0.15	-23.42	1.63	1.07	1.28
21	36	165.0	24.7	-23.92	2.47	1.31	-0.52	-23.40	2.04	1.64	1.80
22	37	155.0	24.7	-30.47	3.01	3.99	0.20	-30.67	2.94	3.82	3.30
23	26	145.0	24.7	-31.67	3.09	4.86	0.83	-32.49	3.72	4.27	3.90
24	34	135.0	24.7	-30.47	4.19	4.23	-0.23	-30.24	3.97	4.15	4.01
25	39	125.0	24.7	-22.85	1.34	2.04	0.30	-23.15	1.34	1.78	1.52
26	34	115.0	24.7	-16.76	1.36	1.75	0.04	-16.80	1.19	1.72	1.42
27	37	105.0	24.7	-14.41	0.57	0.67	0.04	-14.45	0.45	0.63	0.52
28	33	95.0	24.7	-15.58	0.72	0.55	-0.12	-15.46	0.81	0.52	0.55
29	36	85.0	24.7	-12.50	0.84	2.26	0.66	-13.16	1.39	1.78	1.54
30	36	75.0	24.7	-11.76	0.94	1.00	0.16	-11.92	0.70	0.87	0.78
31	36	65.0	24.7	-12.94	1.43	0.94	-0.20	-12.74	1.25	0.97	1.09
32	38	55.0	24.7	-10.88	0.31	1.60	0.48	-11.38	0.62	1.40	0.94
33	19	45.0	24.7	-10.88	0.00	0.64	0.23	-11.11	0.29	0.44	0.36
No points in Interval 34											
No points in Interval 35											
No points in Interval 36											
No points in Interval 37											
No points in Interval 38											

Table 10

STATISTICAL PARAMETERS FOR THE 75-MHz DIPOLE WITH BALUN--IN THE FOREST, E₀ AT 33° ELEVATION

Interval	SS	Azimuth	Elevation	Median	Sigma		Median-Mean	Mean	Sigma		Combined Sigma
					Peaks	Nulls			Peaks	Nulls	
1	41	35.0	32.9	-17.27	0.52	0.77	0.09	-17.36	0.53	0.68	0.60
2	37	25.0	32.9	-19.69	1.10	0.94	-0.09	-19.60	1.02	0.66	0.92
3	37	15.0	32.9	-22.14	0.99	0.97	-0.09	-22.05	0.90	0.96	0.92
4	35	5.0	32.9	-24.64	2.99	2.26	-0.37	-24.27	2.72	2.45	2.54
5	26	355.0	33.3	-29.82	2.19	3.10	0.34	-30.16	2.41	2.93	2.61
6	33	345.0	33.9	-33.33	3.18	3.63	0.25	-33.58	2.79	3.62	3.11
7	37	335.0	34.2	-35.23	1.54	2.71	0.52	-35.75	1.67	2.41	1.96
8	32	325.0	34.2	-33.80	4.43	3.32	-0.65	-33.15	3.80	3.66	3.66
9	34	315.0	33.4	-32.85	4.39	4.64	0.27	-33.13	4.63	4.36	4.44
10	38	305.0	32.1	-31.87	2.52	4.40	0.66	-32.52	3.23	3.73	3.43
11	42	295.0	32.1	-21.96	0.63	2.43	0.69	-22.65	1.39	1.99	1.65
12	39	285.0	33.5	-23.57	1.89	1.15	-0.40	-23.17	1.55	1.36	1.43
13	35	275.0	33.8	-20.71	1.56	0.88	-0.35	-20.36	1.28	1.02	1.14
14	35	265.0	34.9	-18.78	0.98	0.67	0.02	-18.80	0.77	0.85	0.79
15	37	255.0	33.5	-19.09	1.03	1.54	0.02	-19.11	0.65	1.53	1.10
16	40	245.0	32.3	-19.09	1.06	0.43	-0.16	-18.93	0.94	0.47	0.66
17	38	235.0	32.3	-19.09	0.62	0.44	-0.05	-19.04	0.56	0.43	0.49
18	37	225.0	32.5	-18.78	0.95	1.12	0.03	-18.61	0.93	1.09	0.99
19	38	215.0	33.4	-21.78	1.98	0.52	-0.62	-21.16	1.58	0.98	1.23
20	36	205.0	33.7	-18.94	1.83	1.62	-0.09	-18.85	1.75	1.70	1.70
21	36	195.0	33.7	-17.57	0.66	1.51	0.35	-17.92	0.88	1.28	1.05
22	37	185.0	33.7	-20.71	0.72	0.86	0.00	-20.71	0.63	0.68	0.73
23	36	175.0	33.7	-26.25	3.38	2.37	-0.37	-25.66	3.06	2.69	2.64
24	33	165.0	33.7	-36.19	4.03	2.08	-0.73	-35.46	3.56	2.37	2.68
25	24	155.0	33.7	-34.76	3.19	4.14	0.44	-35.20	3.36	3.73	3.42
26	28	145.0	33.7	-35.23	2.05	2.05	0.00	-35.23	1.61	2.05	1.89
27	20	135.0	33.7	-33.80	2.86	4.14	0.55	-34.36	3.22	3.84	3.42
28	36	125.0	33.7	-35.53	1.18	2.80	0.66	-26.19	1.68	2.46	2.01
29	34	115.0	33.7	-21.96	1.24	5.19	1.37	-23.33	2.12	5.96	3.45
30	14	105.0	33.7	-17.57	0.71	1.44	0.24	-17.81	0.81	1.25	1.01
31	15	95.0	33.7	-18.46	0.61	0.51	-0.06	-16.42	0.55	0.47	0.50
32	14	85.0	33.7	-18.94	2.52	1.47	-0.53	-18.40	2.06	1.92	1.96
33	35	75.0	33.7	-18.66	0.47	0.85	0.24	-16.90	0.59	0.62	0.60
34	38	65.0	33.7	-18.78	0.57	0.64	0.03	-18.81	0.39	0.61	0.46
35	37	55.0	31.7	-17.27	0.72	0.81	0.08	-17.35	0.58	0.74	0.64
36	37	45.0	32.4	-16.66	0.43	0.57	0.08	-16.74	0.40	0.49	0.44
37	31	35.0	33.0	-16.48	0.59	0.88	0.17	-18.65	0.60	0.73	0.65
38	35	25.0	34.0	-20.00	0.85	0.89	0.02	-20.02	0.57	0.87	0.68

Table 11

STATISTICAL PARAMETERS FOR THE 75-MHz OIPOLE WITH BALUN--IN THE FOREST, E₀ AT 45° ELEVATION

Interval	SS	Azimuth	Elevation	Median	Sigma		Median-Mean	Mean	Sigma		Combined Sigma
					Peaks	Nulls			Peaks	Nulls	
1	29	265.0	46.5	-13.63	0.39	0.99	0.29	-13.92	0.60	0.72	0.65
2	33	255.0	45.2	-15.15	0.63	0.59	-0.04	-15.11	0.59	0.54	0.56
3	31	245.0	44.1	-17.57	1.27	2.12	0.30	-17.87	1.52	1.86	1.66
4	32	235.0	42.6	-19.69	0.40	0.84	0.16	-19.85	0.40	0.69	0.52
5	31	225.0	42.6	-21.07	1.12	0.70	-0.18	-20.89	0.95	0.73	0.82
6	38	215.0	43.0	-21.60	1.55	0.91	-0.24	-21.36	1.54	1.03	1.23
7	32	205.0	44.3	-24.64	1.22	2.77	0.68	-25.32	1.56	2.44	1.90
8	33	195.0	46.5	-29.28	2.59	0.83	-0.64	-28.64	2.24	1.24	1.67
9	23	185.0	46.5	-31.42	1.79	5.50	1.36	-32.78	2.51	4.89	3.41
10	30	175.0	46.5	-26.42	1.24	5.26	1.48	-27.90	2.33	4.85	3.29
11	31	165.0	46.5	-25.71	0.92	0.93	-0.01	-25.70	0.91	0.79	0.83
12	31	155.0	45.5	-28.21	2.23	1.38	0.08	-28.29	1.68	1.30	1.48
13	23	145.0	45.5	-35.71	2.15	2.23	0.31	-36.02	1.95	1.95	1.90
14	23	135.0	45.5	-35.23	4.78	2.83	-1.34	-33.89	3.42	3.39	3.33
15	36	125.0	45.5	-25.71	1.17	3.34	0.60	-26.31	1.60	2.99	2.24
16	21	115.0	45.5	-25.00	3.14	1.12	-0.99	-24.01	2.15	1.87	1.96
17	31	105.0	46.5	-19.09	0.42	0.73	0.13	-19.22	0.46	0.62	0.53
18	27	95.0	46.9	-18.18	0.60	0.48	0.00	-18.18	0.60	0.37	0.45
19	27	85.0	46.9	-16.96	0.96	1.39	0.19	-17.15	1.00	1.24	1.10
20	25	75.0	46.5	-16.06	0.61	1.29	0.19	-16.25	0.69	1.11	0.86
21	28	65.0	45.7	-16.66	0.56	0.50	-0.16	-16.50	0.41	0.39	0.39
22	30	55.0	45.7	-17.57	0.47	1.05	0.14	-17.71	0.48	0.93	0.67
23	20	45.0	45.7	-15.45	0.49	1.00	0.06	-15.51	0.44	0.94	0.60
24	25	35.0	45.8	-14.84	0.45	0.40	-0.05	-14.79	0.41	0.28	0.32
25	26	25.0	46.5	-15.75	0.53	0.91	0.19	-15.94	0.63	0.72	0.66
26	25	15.0	46.5	-16.66	0.46	0.49	0.01	-16.70	0.41	0.45	0.42
27	30	5.0	46.5	-16.81	0.34	0.50	0.05	-16.86	0.38	0.46	0.42
28	22	355.0	46.5	-20.00	1.50	2.82	0.50	-20.50	1.56	2.74	2.00
29	26	245.0	46.5	-26.07	1.33	2.61	0.55	-26.62	1.59	2.23	1.84
30	27	335.0	46.5	-31.42	4.33	2.49	-0.94	-30.48	3.56	3.05	3.22
31	28	325.0	46.5	-28.75	1.23	6.50	2.22	-30.96	3.16	5.21	4.00
32	24	315.0	46.5	-28.39	3.41	1.69	-0.70	-27.69	2.93	2.25	2.53
33	26	305.0	46.5	-21.42	0.65	0.86	-0.01	-21.41	0.64	0.68	0.65
34	25	295.0	46.5	-18.78	0.87	0.94	0.06	-18.84	0.80	0.90	0.83
35	28	285.0	46.5	-19.24	0.50	0.59	0.05	-19.29	0.55	0.54	0.53
36	28	275.0	46.5	-16.66	0.93	0.97	0.03	-16.69	0.86	0.94	0.88
37	28	265.0	46.5	-15.45	0.43	0.73	0.22	-15.67	0.40	0.55	0.47
38	28	255.0	46.5	-15.15	0.49	0.59	-0.04	-15.11	0.46	0.42	0.42
39	29	245.0	46.5	-16.96	1.02	0.80	-0.13	-16.83	0.89	0.86	0.86
40	29	235.0	46.5	-18.18	0.49	0.58	0.07	-18.25	0.46	0.51	0.48

Table 12

STATISTICAL PARAMETERS FOR THE 75-MHz DIPOLE WITH BALUN--IN THE FOREST, E. AT 55° ELEVATION

Interval	SS	Azimuth	Elevation	Median	Sigma		Median-Mean	Mean	Sigma		Combined Sigma
					Peaks	Nulls			Peaks	Nulls	
1	28	175.0	54.5	-20.71	0.56	0.74	0.14	-20.85	0.49	0.81	0.53
2	27	185.0	54.4	-22.50	0.86	0.91	0.10	-22.60	0.81	0.82	0.70
3	28	155.0	55.8	-25.00	0.44	1.11	0.41	-25.41	0.51	0.83	0.63
4	24	145.0	54.5	-29.82	1.98	6.28	1.90	-31.72	3.73	4.73	4.12
5	24	135.0	55.4	-27.67	3.09	8.63	2.10	-29.77	4.46	8.62	5.97
8	24	125.0	55.4	-22.14	0.38	1.59	0.27	-22.41	0.50	1.37	0.88
7	23	115.0	55.4	-20.00	0.70	1.58	0.22	-20.22	0.82	1.38	1.04
8	30	105.0	55.4	-18.78	0.92	0.60	0.00	-18.78	0.59	0.60	0.59
9	20	95.0	55.4	-16.21	1.33	1.18	-0.08	-18.13	1.25	1.25	1.22
10	29	85.0	54.8	-12.42	0.39	1.09	0.34	-12.78	0.47	1.11	0.68
11	21	75.0	54.6	-13.33	1.31	0.37	-0.51	-12.82	0.89	0.81	0.72
12	19	85.0	54.6	-11.81	0.35	0.42	0.12	-11.93	0.29	0.31	0.29
13	23	55.0	54.6	-12.42	0.37	0.32	0.08	-12.50	0.20	0.24	0.21
14	26	45.0	55.2	-12.72	0.35	0.40	0.05	-12.77	0.17	0.35	0.22
15	23	35.0	58.2	-13.63	0.76	0.68	-0.16	-13.47	0.82	0.43	0.50
16	19	25.0	57.4	-16.36	0.77	0.44	-0.06	-16.30	0.72	0.38	0.51
17	21	15.0	57.5	-18.96	0.38	0.51	-0.03	-16.93	0.35	0.31	0.32
18	21	5.0	57.2	-17.27	0.34	0.70	0.16	-17.43	0.36	0.58	0.45
19	22	355.0	58.9	-18.18	0.74	1.18	0.01	-18.19	0.55	1.17	0.73
20	22	345.0	58.8	-19.54	0.68	1.82	0.40	-19.94	1.04	1.32	1.14
21	22	335.0	58.4	-23.21	0.82	0.46	-0.13	-23.08	0.71	0.43	0.55
22	21	325.0	56.4	-24.28	1.39	4.54	1.28	-25.58	2.48	3.55	2.90
23	21	315.0	58.4	-28.92	2.92	3.02	0.07	-28.99	2.89	2.95	2.73
24	20	305.0	56.4	-22.50	1.89	0.97	-0.32	-22.17	1.38	1.29	1.30
25	21	295.0	56.4	-18.78	0.94	0.90	0.13	-18.91	0.77	0.77	0.75
26	22	285.0	56.4	-18.18	0.65	0.46	-0.13	-18.05	0.54	0.41	0.46
27	22	275.0	56.6	-15.15	1.29	1.14	-0.05	-15.09	1.24	1.19	1.19
28	18	265.0	57.1	-13.03	0.52	0.49	-0.04	-12.99	0.48	0.43	0.44
29	22	255.0	58.4	-12.12	0.38	0.32	0.07	-12.19	0.19	0.25	0.21
30	26	245.0	56.4	-11.51	0.35	0.51	0.13	-11.84	0.25	0.38	0.30
31	21	235.0	54.7	-12.42	0.37	0.85	0.22	-12.64	0.34	0.47	0.40
32	21	225.0	58.0	-13.63	0.37	0.51	0.17	-13.80	0.30	0.34	0.31
33	23	215.0	56.2	-13.63	0.35	0.36	0.10	-13.73	0.26	0.25	0.25
34	22	205.0	51.8	-13.63	0.47	0.56	-0.11	-13.52	0.36	0.38	0.36
35	25	195.0	54.8	-16.06	1.02	1.24	0.08	-18.14	0.96	1.18	1.03
36	23	185.0	54.7	-19.09	1.10	1.17	0.08	-19.17	1.00	1.09	1.03
37	25	175.0	54.8	-21.42	0.96	0.93	0.01	-21.43	0.92	0.93	0.91
38	23	185.0	56.7	-24.28	1.05	1.17	0.00	-24.28	0.91	1.17	1.00

seen in Table 1--e.g., intervals 12 and 23 (these angles were corrected before the data were contoured). The next three columns give the median, $\hat{\mu}'$, the standard deviations of the points greater than the median (peaks), $\hat{\sigma}'_p$, and the standard deviations of the points less than the median (nulls), $\hat{\sigma}'_n$. The next column is the difference between the median and mean for the interval. The next three columns are the arithmetic mean, $\hat{\mu}$, of the amplitude points (note that these values were computed by summing the decibel values--it can be shown that this is actually the geometric mean) and the standard deviations of the points above and below the mean, $\hat{\sigma}_p$ and $\hat{\sigma}_n$. The last column is the total standard deviation of the sample points about the median, $\hat{\sigma}'$. It is not possible to present the complete sets of tables for all of the antennas in this report, but the data are summarized in the following sections of this chapter.

A. Comparison of Mean and Median Amplitudes

The median indicates the amplitude value that divides the distribution of data so that half of the points are below this value and half are above this value. The median is readily obtained with the data expressed in decibels, whereas the arithmetic mean if calculated directly with the amplitude values expressed in decibels (as was done here) results in a mean of the logarithmic values or a geometric mean--the resulting geometric mean is smaller than the arithmetic mean (unless all values in the sample are equal). In order to provide an indication of the similarity between the mean and median of the data for each constant-elevation orbit, the number of 10° intervals in which the absolute difference between the mean and the median exceeded 1 dB were counted and are presented in Tables 13 and 14. The elevation angles indicated are nominal but the actual orbits were generally within 2° of these nominal values. The fractions in the table are such that the numerator indicates

Table 13

COMPARISON OF MEAN AND MEDIAN SIGNAL STRENGTH FOR ANTENNA SET 1

Antenna Type	Frequency (MHz)	Polarization	Fraction of Intervals where Absolute Difference of Mean and Median Exceed 1 dB for Elevation Angle Indicated							
			5°	10°	15°	25°	35°	45°	55°	Total (percent)
Horizontal Unbalanced Dipole--in Clearing	50	E_θ	5/38	3/37	5/28	4/40	2/36	2/38	1/40	8.6
		E_ϕ	2/37	--	0/27	2/37	1/37	0/37	--	2.7
Horizontal Unbalanced Dipole--in Forest	50	E_θ	5/38	2/37	8/40	8/39	4/38	1/37	4/40	11.9
		E_ϕ	3/37	--	4/33	4/38	2/37	2/37	--	8.2
Vertical Sleeve Dipole--in Clearing	50	E_θ	2/38	4/37	3/40	3/40	1/36	0/38	0/40	4.8
		E_ϕ	3/25	--	2/37	1/38	3/37	3/38	--	6.9
Vertical Sleeve Dipole--in Forest	50	E_θ	5/38	9/37	6/40	5/40	2/38	2/38	0/40	10.3
Horizontal Unbalanced Dipole--in Clearing	75	E_θ	11/28	15/37	7/40	11/40	5/31	3/38	2/40	21.2
		E_ϕ	7/37	--	2/37	3/38	5/37	1/38	--	9.6
Horizontal Unbalanced Dipole--in Forest	75	E_θ	4/38	4/37	8/40	10/40	4/38	0/38	2/40	11.8
		E_ϕ	5/38	--	1/37	3/36	1/37	4/38	--	7.5
Vertical Sleeve Dipole--in Clearing	75	E_θ	5/38	7/37	2/40	1/40	0/38	0/38	1/40	5.9
		E_ϕ	8/37	--	17/37	7/38	1/37	3/38	--	19.4
Vertical Sleeve Dipole--in Forest	75	E_θ	7/38	7/37	13/34	14/40	9/38	11/36	13/40	28.1
		E_ϕ	1/27	--	12/37	3/38	2/37	0/38	--	10.2
Horizontal Unbalanced Dipole--in Clearing	100	E_θ	8/38	13/33	6/40	10/40	6/26	2/38	3/36	19.1
		E_ϕ	8/37	--	2/37	2/38	2/37	2/38	--	8.6
Horizontal Unbalanced Dipole--in Forest	100	E_θ	3/38	4/37	5/40	6/40	6/38	1/38	2/40	10.0
		E_ϕ	6/37	--	5/37	3/38	2/37	2/38	--	9.6
Vertical Sleeve Dipole--in Clearing	100	E_θ	8/34	1/31	2/40	11/40	0/38	6/38	2/40	8.4
		E_ϕ	0/28	--	10/37	3/38	3/37	3/38	--	10.7
Vertical Sleeve Dipole--in Forest	100	E_θ	2/37	7/37	4/40	7/40	3/38	3/32	6/40	12.1
		E_ϕ	0/14	--	3/35	3/38	1/32	0/32	--	4.6

Table 14

COMPARISON OF MEAN AND MEDIAN SIGNAL STRENGTH FOR ANTENNA SET 2

Antenna Type	Frequency (MHz)	Polarization	Fraction of Intervals where Absolute Difference of Mean and Median Exceed 1 dB for Elevation Angle Indicated							
			5°	10°	15°	25°	35°	45°	55°	Total (percent)
Horizontal Unbalanced Dipole--in Clearing	50	E_θ	2/40	--	6/39	5/39	1/29	1/38	1/38	7.7
		E_ϕ	2/38	--	1/38	3/38	1/38	D/40	2/38	3.9
Horizontal Folded Dipole--in Forest	50	E_θ	12/40	--	5/39	4/39	3/29	D/38	2/38	11.7
		E_ϕ	2/38	--	4/38	1/38	2/38	1/40	1/38	4.8
Vertical Sleeve Dipole--in Clearing	50	E_θ	5/53	--	5/39	1/39	1/29	1/38	1/38	6.3
		E_ϕ	1/38	--	10/38	1/38	2/38	3/40	0/38	7.5
Vertical Folded Dipole--in Forest	50	E_θ	14/37	--	12/39	4/39	0/29	D/38	D/38	13.6
		E_ϕ	4/38	--	5/38	3/38	5/38	4/40	0/38	9.1
Horizontal Unbalanced Dipole--in Forest	75	E_θ	5/40	--	6/39	13/39	5/28	13/38	14/38	25.2
		E_ϕ	6/38	--	5/28	2/38	10/27	4/40	0/29	13.5
Horizontal Dipole w/Balun--in Forest	75	E_θ	5/40	--	11/39	3/39	4/29	0/31	0/37	10.7
		E_ϕ	7/38	--	4/38	0/33	1/38	4/40	3/38	8.4
Horizontal Balanced Dipole--in Forest	75	E_θ	20/40	--	16/38	15/39	8/29	4/38	3/38	29.7
		E_ϕ	9/36	--	0/38	3/38	3/38	7/27	3/23	12.5
Horizontal Balanced Dipole--in Forest	100	E_θ	8/40	--	13/39	7/39	7/23	2/38	2/38	18.0
		E_ϕ	7/34	--	3/37	6/38	6/38	3/40	2/38	12.0
Vertical Sleeve Dipole--in Clearing	100	E_θ	5/37	--	3/37	4/38	1/29	0/29	0/34	6.4
Vertical Sleeve Dipole--in Forest	100	E_θ	8/39	--	9/37	10/39	2/25	5/38	2/37	15.8
		E_ϕ	0/31	--	1/38	0/38	0/35	1/38	0/36	D.9
Vertical Balanced Dipole--in Forest	100	E_θ	11/40	--	10/39	2/39	0/29	3/38	1/36	12.2
		E_ϕ	1/38	--	1/38	2/38	10/38	7/40	1/38	9.5

the number of intervals in which the absolute value of the difference between the median and mean exceeded 1 dB, and the denominator is the number of 10° of azimuth sample spaces in each orbit (a denominator greater than 36 indicates that there was an overlap in the orbit and a denominator less than 36 indicates that there was no data in a portion of the orbit). These differences were both positive and negative; thus, a statement about the mean always being greater or less than the median cannot be made. Although the table indicates only the percent of occurrences of the difference exceeding 1 dB, further checking of the samples indicated that the difference exceeded 2 dB for less than 5 percent of the sample--even the differences of the mean and median of the response of the 75-MHz horizontal balanced dipole in the forest, which had 29.7 percent of the differences greater than 1 dB, exceeded 2 dB for only 4 percent of the samples.

From the data presented here it appears reasonable to assume that the estimated median can be used as an estimate of the mean amplitude for the data from this site.

B. Pattern Contour Plots

The antenna patterns are presented in the form of contours of the computed medians plotted on an azimuthal equal-area projection. This display may appear at first glance to be unnecessarily complicated; however, these plots have several advantages that will be discussed following an explanation of the way to read them.

Each contour map shows all the amplitude data taken on one antenna for one polarization at one frequency, in the form of median amplitudes of 10° azimuth intervals. The plot can be visualized in several ways. For example, one may picture placing a large hemisphere over the antenna being measured, then drawing the median field strength contours on its

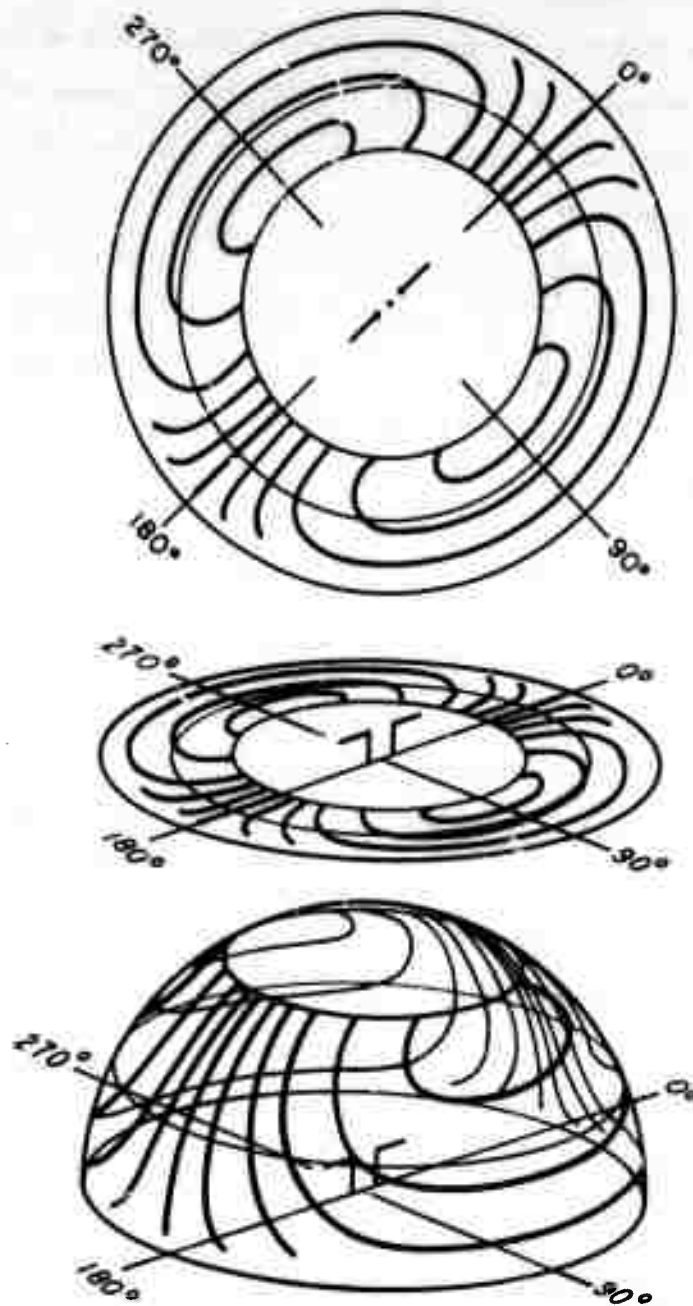
surface. The contour plots are two-dimensional maps of this hemisphere regarded from above (see Figure 14). Hence, the zenith is at the center of the plot; azimuth angles appear as radials; and elevation angles are concentric circles.* The outer rim of the plot is the horizon, or 0° elevation. The azimuth angles numbered around the rim of the plot are in degrees relative to the principal axis of the horizontal dipole antennas or magnetic north for the vertical antennas. As an example, for the horizontal unbalanced dipoles in the clearing, 0° azimuth on the plots is actually 345° as indicated on the site map in Figure 7 by arrows labeled in degrees magnetic.[†] The relationship of contour-plot azimuth to each horizontal dipole antenna is also shown by the diagram in the center of the plot.

The contour interval is 3 dB, with the largest observed median amplitude (over a 10° azimuthal interval) for each plot was established as 0 dB. The 0-dB point is not shown, because its exact position is misleading without detailed knowledge regarding the aircraft orbits, but its true location can easily be inferred from the other contours.

The plot has merits both intrinsically as a data display and extrinsically through its adaptability to the Xeledop measurement technique. As a data display, it has the advantage of clearly showing, statistically, the characteristics of the antenna response in one diagram. It also emphasizes the average energy distribution as a function of solid angle, a better measure of the usefulness of any antenna for communications than azimuthal beamwidth.

*The azimuthal equal-area projection allows equal solid angles to be represented as equal areas on the plot, whereas, if a stereographic projection were used, the lower elevation would be closer together than the higher elevation angles. An excellent discussion of these plots can be found in Ref. 16.

[†]The magnetic declination in Thailand is less than 1° ; consequently, for practical purposes, magnetic and true bearings are the same.



TA-8663-60

FIGURE 14 A CONTOUR PLOT AS A MAP OF A HEMISPHERE

In addition to having these advantages as a display, the contour plots are very well adapted to the way in which the data were taken. Since the aircraft did not fly perfect orbits about each antenna, the elevation angles actually measured varied during any given orbit and from one set of antennas to another. Thus it is neither accurate nor adequate simply to plot the measured amplitude as a function of azimuth on a polar chart. Some means of interpolating between the data taken at the various elevation angles is required, because the angles actually measured changed from one set of orbits to the next. The contour-plot program does this by finding surfaces (contours) of constant average received signal indicated by the available amplitude data. Once the program has found this surface (drawn the contour plot), polar cuts can easily be taken at any constant elevation angle of interest.

Contour plots of the mean signal strength of the 75-MHz horizontal dipole in the forest (Figures 15 and 16) were produced using the techniques discussed in this section of this report. The standard deviation about the mean, $\hat{\sigma}$ was calculated, gridded, and tabulated as discussed in Section VI-C. Comparing the contour plots of the mean and median (Figures 15 and 16 with Figures A-10 and A-11), and comparing the tables of the standard deviations about the mean, $\hat{\sigma}$ (Tables 15 and 16), with those of the standard deviation about the median, $\hat{\sigma}'$ (Tables A-10 and A-11), one can see that the mean and median are quite similar.

Several other cases of the median and mean were compared and from these comparisons and the data provided in Section VI-A, it was concluded that the median amplitudes could be plotted and used as a reasonable estimate of the mean amplitude if necessary.

C. Estimated Standard Deviations of the Amplitude about the Median

The estimated standard deviations about the median, $\hat{\sigma}'$, were computed over the same 10° azimuth intervals as the medians were computed. These values were then gridded in a regular array of constant azimuth- and elevation-angle increment, by using the gridding portion of the pattern-contouring program (again, a linear interpolation was used so as not to create any extraneous peak values). These values were tabulated and are shown in Tables A-1 through A-23 and Tables B-1 through B-21, opposite the corresponding contour plot of the median signal strength in Appendices A and B. The azimuth angles have been normalized so that 0° in the tables is the same as the 0° used for the contour plots of the median amplitude (thus 90° on the table is 90° on the contour plot and -90° in the table is 270° on the contour plot).

These tables show that $\hat{\sigma}'$ for the dipoles increases in the areas of the nulls of the dipole. If it is remembered that $\hat{\sigma}'$ was computed by comparing all of the points in a 10° interval, one will realize that the $\hat{\sigma}'$ values also include the deterministic pattern function of the dipole. Thus, the $\hat{\sigma}'$ values would be smaller if this pattern factor were eliminated. The general trend that can be determined from these tables is that $\hat{\sigma}'$ tends to decrease with increasing elevation angle.

D. Effect of Variation of Slant Range

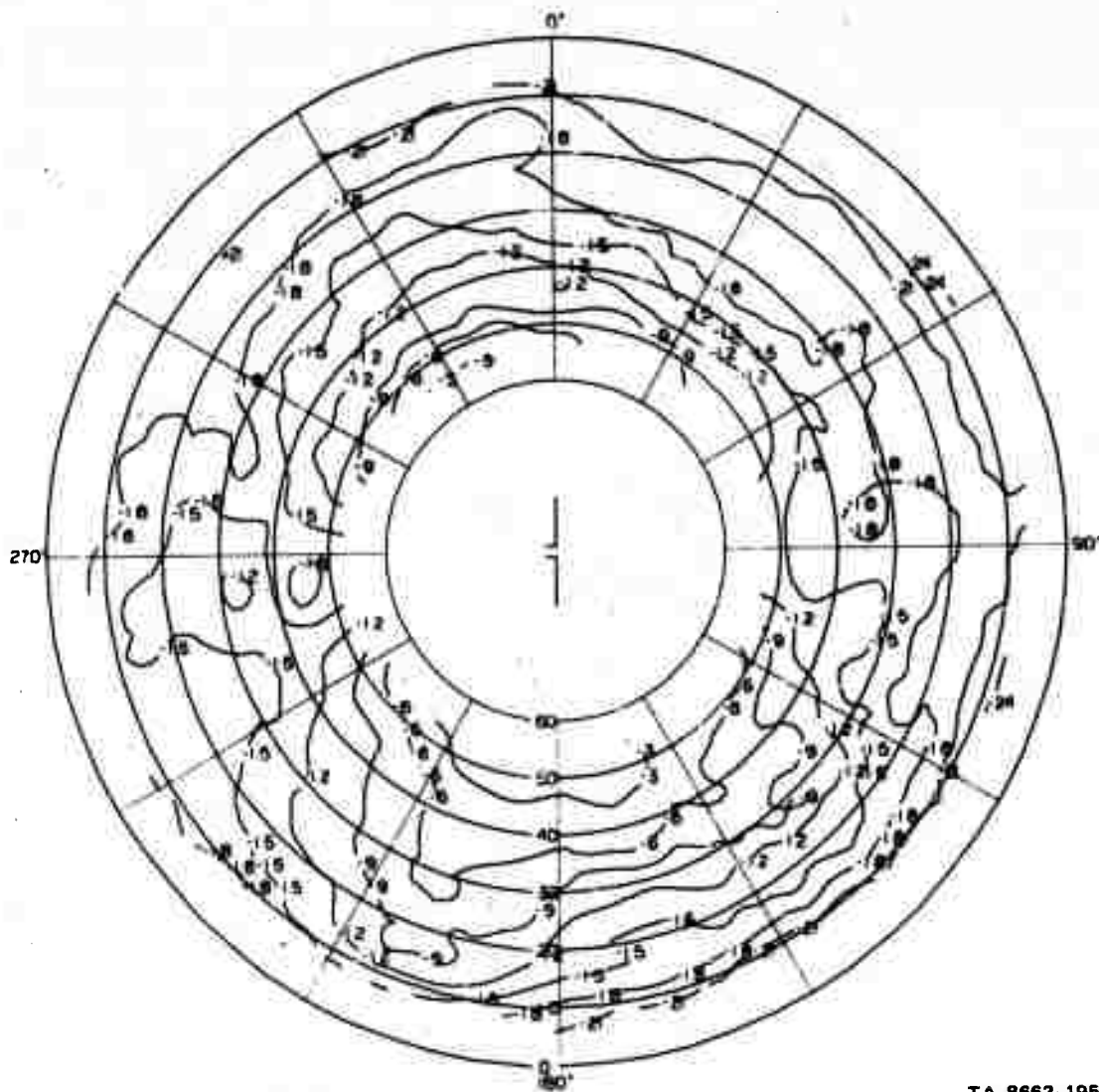
The criterion for determining the distance between the transmitting and receiving antennas required for far-field measurements when conducting antenna pattern measurements is usually expressed by the relationship

$$R = 2D^2/\lambda \quad ,$$

Table 15

STANDARD DEVIATIONS ABOUT THE MEAN FOR THE HORIZONTAL UNBALANCED DIPOLE
IN THE FOREST-- E_{θ} AT 75 MHz

Elevation Azimuth	10.0	15.0	20.0	25.0	30.0	35.0	40.0	45.0	50.0
-170.0	3.09	2.94	2.71	2.65	2.13	1.71	1.41	1.14	0.57
-160.0	3.04	2.41	2.69	2.35	1.50	1.27	1.40	1.27	0.74
-150.0	2.92	3.05	3.11	3.34	2.63	1.50	1.60	1.85	1.17
-140.0	3.32	3.90	3.70	3.93	3.12	1.70	1.75	1.64	0.98
-130.0	2.24	2.54	2.78	2.64	2.48	2.21	1.84	1.40	0.68
-120.0	2.46	2.92	2.80	2.79	2.61	2.45	2.23	1.67	0.75
-110.0	2.95	3.41	2.94	2.71	2.49	2.37	2.14	2.05	1.63
-100.0	3.64	2.86	2.96	2.96	2.39	2.08	2.05	2.15	1.91
-90.0	3.79	2.84	3.12	3.15	2.27	1.69	1.99	2.10	1.90
-80.0	3.69	3.66	3.24	3.18	2.65	2.01	2.11	2.10	2.37
-70.0	3.60	2.93	2.95	3.03	3.34	2.98	2.50	2.30	1.91
-60.0	3.19	2.41	2.83	3.00	3.04	2.37	2.38	2.19	1.64
-50.0	3.34	2.92	2.82	2.87	2.64	2.07	1.82	1.49	1.15
-40.0	3.13	3.16	3.13	3.20	2.78	1.86	1.58	1.32	0.57
-30.0	3.07	2.75	2.83	2.66	2.18	1.64	1.82	1.94	1.15
-20.0	3.16	3.26	3.12	3.14	3.01	2.50	2.24	2.00	0.89
-10.0	2.64	2.92	3.00	3.06	3.48	2.78	2.57	1.87	0.62
0.0	2.43	3.10	3.00	2.92	3.44	2.83	2.30	1.39	0.71
10.0	2.69	2.77	2.80	2.86	2.78	1.98	1.56	1.40	0.55
20.0	2.47	2.53	2.72	2.77	2.41	1.91	1.23	1.20	0.63
30.0	2.29	2.76	2.84	2.96	2.50	2.67	1.63	1.20	0.75
40.0	2.58	3.18	3.32	3.41	2.80	2.51	1.44	1.32	0.87
50.0	2.30	3.52	3.43	3.63	2.67	2.47	1.64	1.70	1.09
60.0	2.31	3.12	3.33	3.27	2.19	2.8	1.76	1.93	1.33
70.0	2.25	3.16	3.07	2.91	2.66	2.45	2.20	2.28	1.54
80.0	2.13	3.03	2.76	2.46	2.69	2.85	2.73	2.42	1.86
90.0	2.25	2.70	2.71	2.62	2.60	2.73	2.53	2.52	2.13
100.0	2.21	3.21	3.29	3.25	2.92	2.54	2.30	2.56	2.52
110.0	2.20	3.37	3.27	3.19	2.85	3.01	2.31	2.26	1.67
120.0	2.21	3.12	3.08	3.13	2.82	2.78	2.14	1.76	0.98
130.0	2.48	2.95	2.83	2.44	1.38	1.50	1.24	1.69	1.02
140.0	2.88	3.41	3.10	2.97	1.88	1.20	1.13	1.14	0.83
150.0	2.69	3.19	3.24	3.17	2.46	1.30	1.14	0.93	0.71
160.0	2.38	3.25	3.28	3.18	2.43	1.55	1.23	0.97	0.68
170.0	2.31	3.23	3.33	3.43	2.34	1.02	1.10	0.93	0.63
180.0	2.76	3.31	3.18	3.17	2.44	1.56	1.39	1.31	0.77



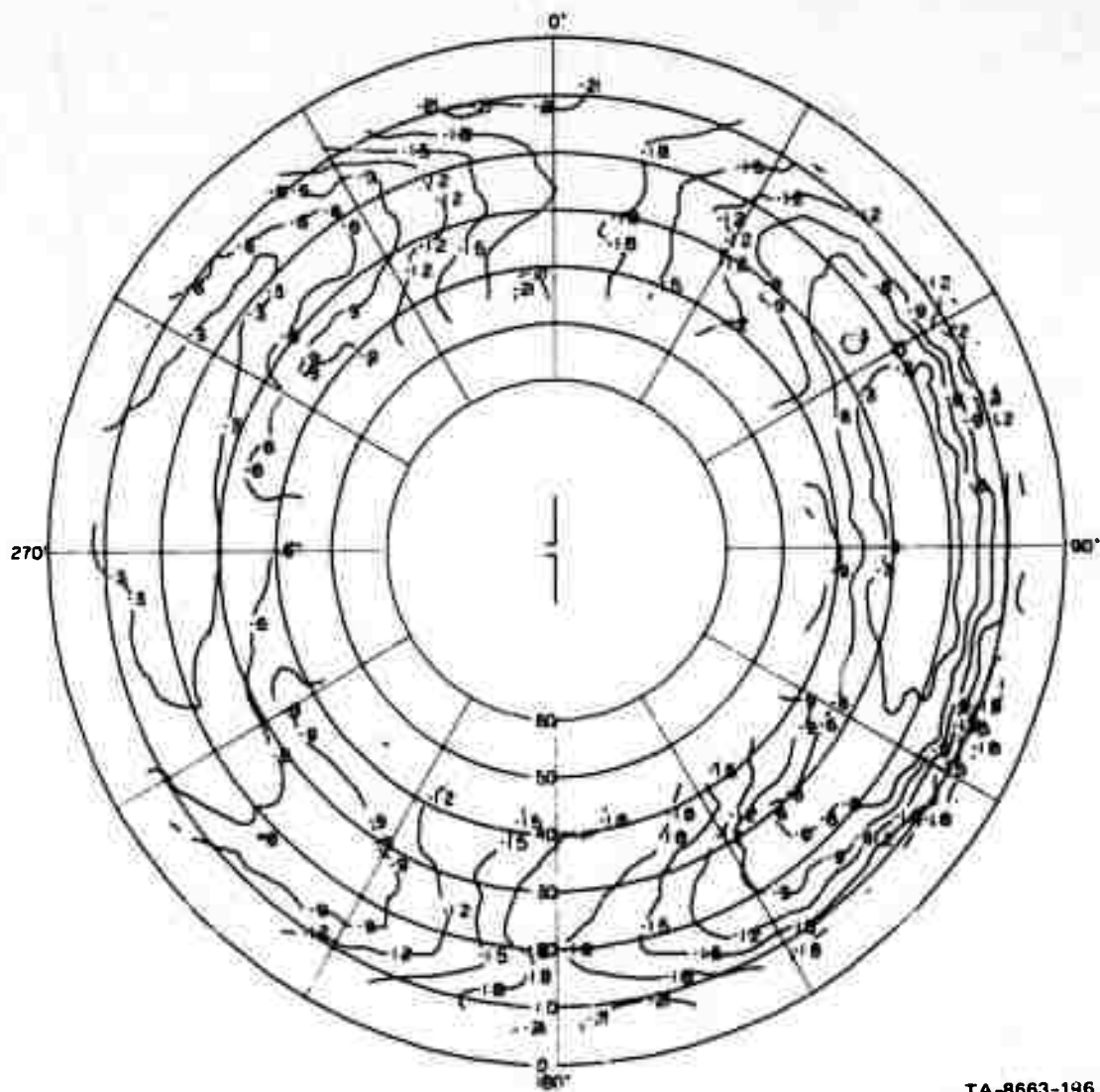
TA-8663-195

FIGURE 15 CONTOUR PLOT OF THE MEAN RESPONSE OF THE HORIZONTAL UNBALANCED DIPOLE IN THE FOREST— E_{θ} AT 75 MHz

Table 16

STANDARD DEVIATIONS ABOUT THE MEAN FOR THE HORIZONTAL UNBALANCED DIPOLE
IN THE FOREST-- E_0 AT 75 MHz

Elevation Azimuth	10.0	15.0	20.0	25.0	30.0	35.0	40.0	45.0	50.0
-170.0	1.98	1.82	2.32	2.83	3.14	2.51	2.33	2.06	--
-160.0	2.34	1.74	1.53	1.64	1.72	1.72	1.79	1.49	--
-150.0	2.26	1.48	1.55	1.26	1.00	1.12	1.10	1.29	--
-140.0	2.34	1.68	1.59	1.37	1.18	0.87	0.92	0.92	--
-130.0	1.94	1.70	1.54	1.33	1.14	0.90	0.93	0.89	--
-120.0	1.36	0.88	0.82	0.60	0.93	1.02	0.89	0.68	--
-110.0	1.23	0.96	0.88	1.01	1.33	1.36	1.14	0.71	--
-100.0	0.73	0.73	0.82	1.02	1.07	1.05	0.97	0.67	--
-90.0	0.81	0.67	0.79	0.87	0.64	0.60	0.68	0.65	--
-80.0	1.08	0.89	0.78	0.70	0.83	1.03	1.01	0.85	--
-70.0	1.02	0.80	0.81	0.87	1.06	1.23	1.07	0.73	--
-60.0	1.18	1.10	1.18	1.25	1.19	1.18	1.00	0.58	--
-50.0	1.36	1.40	1.48	1.13	1.17	1.16	1.22	0.92	--
-40.0	1.98	1.75	1.43	1.10	1.11	1.46	1.28	1.08	--
-30.0	2.53	1.71	1.44	1.72	1.99	2.05	1.66	1.39	--
-20.0	2.99	3.32	3.46	3.58	2.64	1.90	1.96	2.16	--
-10.0	2.70	3.06	3.51	3.37	2.50	1.97	2.19	2.28	--
0.0	2.81	3.03	3.63	3.66	2.91	2.37	2.39	2.50	--
10.0	3.21	3.38	4.19	4.45	3.64	2.69	2.65	2.83	--
20.0	3.42	3.38	3.50	2.95	2.55	2.22	2.37	2.30	--
30.0	2.56	2.46	2.54	2.30	2.10	2.13	1.92	1.77	--
40.0	1.91	1.82	1.55	1.66	1.94	1.80	1.60	1.50	--
50.0	1.95	1.69	1.33	1.27	1.43	1.44	1.22	1.12	--
60.0	2.51	2.11	1.15	1.18	1.17	1.12	0.98	1.06	--
70.0	2.09	2.15	1.11	1.08	0.84	0.78	1.22	1.02	--
80.0	1.72	2.03	0.98	0.96	0.76	0.66	1.81	2.30	--
90.0	2.05	1.79	0.74	0.78	0.72	0.74	2.26	3.24	--
100.0	1.82	1.67	0.64	0.53	0.64	0.76	1.76	2.63	--
110.0	1.47	1.43	0.75	0.70	0.71	0.79	1.08	1.41	--
120.0	1.61	1.20	1.00	1.01	0.79	0.77	1.04	1.15	--
130.0	2.09	1.61	1.34	1.24	1.01	1.09	1.48	1.44	--
140.0	2.05	1.90	1.60	0.99	1.34	1.46	1.96	2.09	--
150.0	1.74	1.55	1.67	1.51	1.82	1.95	2.51	2.60	--
160.0	2.57	2.81	2.65	2.58	2.56	2.97	2.59	2.19	--
170.0	2.50	3.62	3.00	2.43	2.48	2.99	3.07	2.98	--
180.0	1.83	3.13	3.18	3.04	3.21	3.00	2.55	1.94	--



TA-8663-196

FIGURE 16 CONTOUR PLOT OF THE MEAN RESPONSE OF THE HORIZONTAL UNBALANCED DIPOLE IN THE FOREST— E_{ϕ} AT 75 MHz

where D is the longest dimension of the antenna being measured. The dimension D is usually obtained quite readily for linear antennas by measuring the length of the radiators of the antenna being measured or the height of the antenna above ground, but the effect of erecting the antenna in foliage was not fully understood and it appeared reasonable that the surrounding foliage could increase the effective aperture of the antenna.⁷ For this reason, a set of orbits was flown at radii of 3, 4, and 6 miles and at a constant elevation angle of 15° . (Note that the majority of the pattern-measurement data and all data comprising the contour plots was measured at a 4-mile slant range.)

Examples of the measured signal strength as a function of azimuth angle for the E_ϕ response of the 100-MHz horizontal unbalanced dipole in the forest are shown in Figure 17. Azimuth angle decreases from left to right because these plots are derived from plots of the raw data and orbits were flown counterclockwise. These plots show a relatively high repeatability of the lobe and null structure of the amplitude pattern. In some instances it can be seen that the azimuthal location of a null is not exactly repeatable, but it must be remembered that the azimuth data are recorded at time intervals of 6 s and intermediate points must be interpolated, and that the elevation angle was only as constant as the pilot could maintain (the range of the elevation angle was 14.5° to 16.8° for the three orbits) his orbits.

A cursory check of these plots indicates that the data at the three ranges are quite similar and the 4-mile slant range was large enough for these measurements to define the depth of the nulls and to acquire enough sample points to define the patterns.

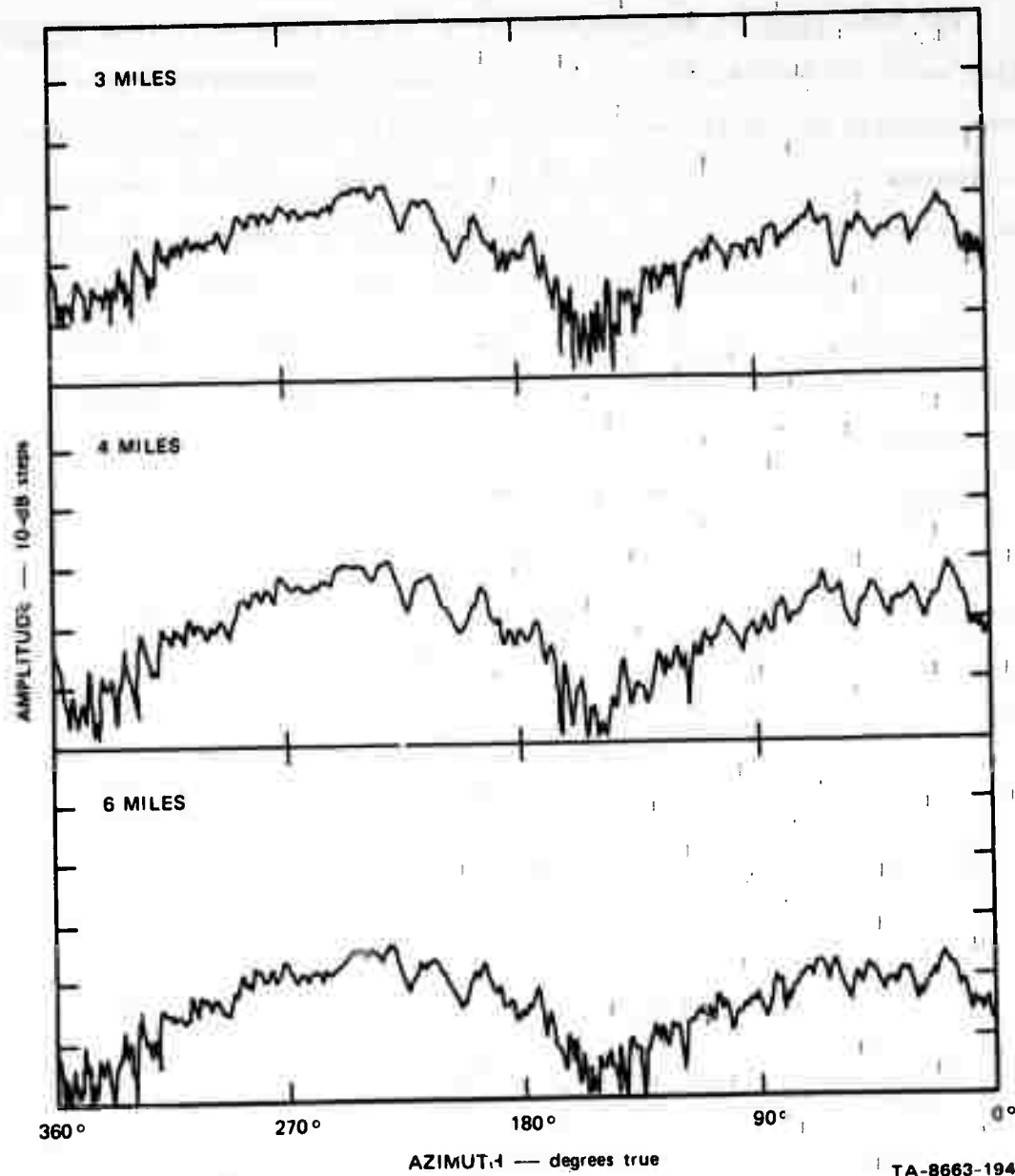


FIGURE 17 COMPARISON OF E_{θ} RESPONSE FOR THE 100 MHz UNBALANCED DIPOLE ANTENNA IN THE FOREST AT 3-, 4-, AND 6-MILE SLANT RANGES AT 15 DEGREES ELEVATION

E. Relative Gains

The term relative gain is used here to distinguish it from absolute gain, which is usually derived theoretically and expressed relative to some absolute reference level--e.g., isotropic. Since the receivers are calibrated in parallel and the input impedances are known, the gains of the various antennas in both polarizations can be compared, or related. But, the power of the Xeledop is not known and, therefore, absolute gains cannot be derived from the measured data without assuming the gain of one antenna (see the following section for further comments on absolute gain). Since absolute gain cannot be derived from the measured data it is also not possible to make comparisons between frequencies.

In order to make the relative gain information more useful and meaningful, these values are tabulated in terms of the relative voltage across 50- Ω loads (Tables 17 and 18) and the relative voltage into matched loads (Table 19).

The relative voltages presented in Tables 17 and 18 are a comparison of the maximum median value computed over the 10° azimuth sectors used to produce the contour plots. These values, which have been normalized to the unbalanced dipoles in the clearing for a given frequency, are presented in two separate tables to facilitate distinguishing the antenna sets during pattern measurement and the information is presented in the tables in the same order as the antenna patterns are presented in the appendices. Note that these tables do not present comparisons of the maximum observed values but of the maximum computed median. It should also be emphasized that these values are not necessarily the maximum obtainable response of the antenna but are the maximum median values that were computed from the data in the 0° -to- 50° elevation range of the measurements--i.e., the maximum response of one-quarter-wavelength-high Hertzian dipole would be at the zenith, whereas there would be a null at

Table 17

RELATIVE VOLTAGE ACROSS 50-OHM LOADS AT PATTERN MAXIMA--
MEASUREMENT SET 1

Measurement and Design Frequency (MHz)	Antenna Type and Location	Relative Voltage		E_{θ}/E_{ϕ} (dB)
		E_{θ} (dB)	E_{ϕ} (dB)	
50	Horizontal unbalanced dipole in clearing	-7.4	0.0	-7.4
	Horizontal unbalanced dipole in forest	-1.0	-3.3	+2.3
	Vertical sleeve dipole in clearing	-7.8	-17.4	+9.6
	Vertical sleeve dipole in forest	-7.0	--	--
75	Horizontal unbalanced dipole in clearing	-3.6	0.0	-3.6
	Horizontal unbalanced dipole in forest	-9.6	-10.2	+0.6
	Vertical sleeve dipole in clearing	-8.6	-16.8	+8.2
	Vertical sleeve dipole in forest	-13.0	-27.2	+14.2
100	Horizontal unbalanced dipole in clearing	-2.4	0.0	-2.4
	Horizontal unbalanced dipole in forest	-6.0	-6.6	+0.6
	Vertical sleeve dipole in clearing	-5.3	-20.3	+15.2
	Vertical sleeve dipole in forest	-9.7	-21.8	+12.1

Table 18

RELATIVE VOLTAGE ACROSS 50-OHM LOADS AT PATTERN MAXIMA--
MEASUREMENT SET 2

Measurement and Design Frequency (MHz)	Antenna Type and Location	Relative Voltage		E_{θ}/E_{ϕ} (dB)
		E_{θ} (dB)	E_{ϕ} (dB)	
50	Horizontal unbalanced dipole in clearing	-7.9	-0.7	-7.2
	Horizontal folded dipole in forest	+2.4	+2.8	-0.4
	Vertical sleeve dipole in clearing	-4.5	-15.4	+10.9
	Vertical folded dipole in forest	+1.2	-13.6	+14.8
75	Horizontal unbalanced dipole in forest	-15.0	-13.3	-1.7
	Horizontal dipole with balun in forest	-12.4	-8.5	-3.9
	Horizontal balanced dipole in forest	-13.4	-9.0	-4.4
100	Horizontal balanced dipole in forest	-8.0	-3.1	-4.9
	Vertical sleeve dipole in clearing	-3.9	--	--
	Vertical sleeve dipole in forest	-4.6	-22.4	+17.8
	Vertical balanced dipole in forest	-8.0	-25.4	+17.4

Table 19

RELATIVE VOLTAGE INTO MATCHED LOADS AT PATTERN MAXIMA

Measurement and Design Frequency (MHz)	Antenna Type and Location	Measurement Set	Potential Error*	Relative Gain* (dB)	
				E_g	E_s
30	Horizontal unbalanced dipole in clearing	1		-7.4	0.0
	Horizontal unbalanced dipole in forest	1		-1.0	+3.2
	Horizontal folded dipole in forest	2		+2.0	+3.0
	Vertical folded dipole in forest	1		+1.4	-13.4
	Vertical sleeve dipole in clearing	2	X	-0.4	-13.3
	Horizontal unbalanced dipole in clearing	2		-7.0	-0.7
	Vertical sleeve dipole in clearing	1	X	-2.7	-13.3
	Vertical sleeve dipole in forest	1	X	-4.4	--
75	Horizontal unbalanced dipole in clearing	1		-3.8	0.0
	Vertical sleeve dipole in clearing	1		-4.0	-13.3
	Horizontal dipole with balun in forest	2	X	-12.8	-6.7
	Horizontal balanced dipole in forest	2		-12.5	-9.1
	Horizontal unbalanced dipole in forest	1		-9.4	-10.1
	Vertical sleeve dipole in forest	1		-9.8	-24.0
	Horizontal unbalanced dipole in forest	2	X	-14.8	-13.1
100	Horizontal unbalanced dipole in clearing	1		-2.3	0.0
	Vertical sleeve dipole in clearing	1	X	-1.8	-17.0
	Vertical sleeve dipole in forest	2	X	-2.0	-19.8
	Vertical sleeve dipole in clearing	2	X	-2.2	--
	Horizontal balanced dipole in forest	2		-8.3	-3.4
	Horizontal unbalanced dipole in forest	1		-6.2	-6.8
	Vertical sleeve dipole in forest	1	X	-6.6	-18.4
	Vertical balanced dipole in forest	2		-8.2	-25.6

* Potential amplitude errors greater than 7.3 dB due to type measurement errors.

All gains on one frequency normalized to set the horizontal unbalanced dipole in clearing equal to 0.0 dB.

the zenith for a one-half-wavelength-high Hertzian dipole. The location of these observed maxima can be inferred from the contour plots of the antennas in the appendices of this report. The values in Tables 17 and 18 have been corrected for the attenuation of the coaxial feed line from the antenna to the measurement van and the values for both tables were then normalized to the value measured for the E_{ϕ} response of the horizontal unbalanced dipole antenna in the clearing (measured in Set 1) for the three frequencies.

The last column of Tables 17 and 18 tabulate the difference between the maximum of the vertical (E_{θ}) polarization response and the maximum of the horizontal (E_{ϕ}) polarization response, with a plus sign indicating that the E_{θ} response was greater. For example, for the 50-MHz horizontal unbalanced dipole in the clearing, the E_{ϕ} maximum was 7.2 dB higher than the E_{θ} maximum, while the E_{θ} maximum was 10.9 dB higher than the E_{ϕ} maximum for the 50-MHz vertical sleeve dipole in the clearing.

The most accurate values in Tables 17 and 18 would be those comparing the two polarization components of the same antenna since the same receiver was used for these measurements. When comparing between different antennas, the variation of receiver input impedance must be accounted for, the neglect of which can cause an error of up to 2 dB.

Table 19 presents relative power gains into matched loads, which were derived from the values from Tables 17 and 18 through the following procedure:

- (1) The mismatch loss to 50 Ω for each antenna at each measured frequency was estimated from the impedance data provided in Section VII.
- (2) These estimated losses were added to each of the maximum received signal values to estimate the power that would have been delivered to a matched load.

- (3) To simplify comparisons, the E_ϕ response for the horizontal unbalanced dipole in the clearing was chosen as a 0-dB reference for each frequency, and all of the relative gain values for that frequency were normalized to this reference.

The resulting values include the 2-dB errors from Tables 17 and 18 plus an error in the mismatch-loss estimates. These losses are determined from antenna impedance, which was measured by a technique that finds the magnitude and angle of the reflection coefficient, with an accuracy of about ± 5 percent in the magnitude, $|\rho|$ as it increases from 0 to 1 (or the VSWR as it increases from 1 to infinity), the relative gain estimates suffer a small error at low antenna VSWR and a large error for high antenna VSWR--all due to a constant 5-percent error in $|\rho|$. Although the effect of this error is minimized by the technique outlined in Section VII, it should still be noted that such an error is present. In Table 19 those values for which the sum of the errors, including the voltage gain errors, is potentially in excess of 3 dB have been indicated by an "X." Potential errors of the unmarked values are less than 3 dB.

F. Comments on Absolute Gains

It was indicated in the previous section that the absolute gain (gain above isotropic) of the measured antennas can usually be estimated by calculating the absolute gain of one of the antennas at a particular frequency and then referring all the other gains on this frequency to the calculated value by using the relative-gain data from pattern measurements--as was done in Ref. 12.

The method attempted was to use the relationship,⁷

$$G_{iso}(\theta, \phi) = G_{fs} + 20 \log_{10} F(\theta, \phi) - 10 \log_{10} (R_a/R_d) ,$$

where

G_{fs} = Gain of a half-wavelength dipole in free space relative to an isotropic radiator (2.15 dB)

$F(\theta, \phi)$ = The field-imaging factor

R_a = Measured antenna feed-point resistance

R_d = Antenna feed-point resistance in free space (73Ω for a half-wavelength dipole).

The field-imaging factors, $F(\theta, \phi)$ can be calculated by the mathematical model described in Section VIII and it is only necessary to add 2.15 dB and correct for the antenna impedance to estimate the absolute gains of these antennas. The term (R_a/R_d) includes both the effect of the change in ease or difficulty in driving the antenna as installed (relative to free space), and the effect of losses in the ground and antenna wire. R_a can be defined to equal the sum of an effective radiation resistance (R_r) and an effective loss resistance (R_ℓ). Then,

$$10 \log_{10}(R_a/R_d) = 10 \log_{10}\left(\frac{R_r + R_\ell}{R_r}\right) + 10 \log_{10}(R_r/R_d) \quad ,$$

where the first term is the antenna efficiency, and the second term is the relative ease or difficulty in maintaining the free-space input current to an equivalent lossless radiating element. This expression may be termed the ground proximity loss (or gain for the case where $R_a < R_d$).

The method outlined above was used to provide calculated elevation-plane patterns (gain as a function of elevation) of the dipole antennas measured in the clearing and the forest. These calculated elevation-plane patterns were then compared to the elevation-plane patterns derived from the measured data and a constant was determined that should be added

to the relative gains in order to convert them to absolute gains. Since several dipole antennas were measured on a given frequency, several constants could be determined and compared for reasonableness. The range of these correction values was 16 dB (i.e., an accuracy of ± 8 dB was the best that could be provided for the estimated absolute gains). Because of the large discrepancies observed it was decided not to attempt to provide estimates of the absolute gains of these antennas.

If an estimate of the absolute gain must be obtained for these antennas, the most reasonable approximation appears to be a value of +5 dB added to each of the gains presented in Table 19. Example calculations employing this technique are presented in Appendix C of this report.

VII IMPEDANCE MEASUREMENTS

The impedance of each antenna was measured after it was erected for the pattern measurements to determine the amount of mismatch between the antenna and the 50- Ω (1.2 VSWR maximum) receiver input terminals, and to acquire a better understanding of the effect of the forest on the antenna feed-point impedance. These measurements were made with an Alford automatic impedance plotter, which can be used to provide a rapid and continuous display of the impedance at the antenna feed point over a reasonably wide frequency range. This impedance plotter has been used at HF to provide displays of the antenna impedance as a function of frequency.^{2,5,6}

The plotter measures impedances by finding the reflection coefficient (compared to 50 Ω) of the load and displays the value on a Smith-chart bezel on an oscilloscope. The accuracy of the plotter is expressed as a percentage of the reflection coefficient (± 5 percent, $\pm 5^\circ$); hence, the resistance and reactance measurements near the rim of the chart (values with high VSWR) are not precise. Inaccuracy also results from several parts of the plotter being frequency-sensitive, and previous experience indicated that the erroneous readings can be obtained when made at the critical frequency of the coaxial feed line from the antenna to the plotter. At VHF it was found that these inaccuracies increased to the extent that reliable measurements could not be performed in the field without calibrating every frequency of interest. For this reason, the impedance of each antenna was measured only at the design frequency of the antenna. These values are tabulated in Tables 20 and 21.

Table 20

FEED-POINT IMPEDANCES FOR ANTENNA SET 1

Antenna Type and Location	Measurement Frequency (MHz)	Impedance (ohms)
Horizontal unbalanced dipole in clearing	50	$50 + j15$
Horizontal unbalanced dipole in forest	50	$60 + j10$
Vertical sleeve dipole in clearing	50	$150 + j170$
Vertical sleeve dipole in forest	50	$100 + j120$
Horizontal unbalanced dipole in clearing	75	$45 + j30$
Horizontal unbalanced dipole in forest	75	$50 + j40$
Vertical sleeve dipole in clearing	75	$180 + j170$
Vertical sleeve dipole in forest	75	$100 + j150$
Horizontal unbalanced dipole in clearing	100	$35 + j20$
Horizontal unbalanced dipole in forest	100	$40 + j20$
Vertical sleeve dipole in clearing	100	$30 + j90$
Vertical sleeve dipole in forest	100	$140 + j150$

Table 21

FEED-POINT IMPEDANCES FOR ANTENNA SET 2

Antenna Type and Location	Measurement Frequency (MHz)	Impedance (ohms)
Horizontal unbalanced dipole in clearing	50	$50 + j15$
Horizontal folded dipole in forest	50	$70 + j20$
Vertical sleeve dipole in clearing	50	$150 + j170$
Vertical folded dipole in forest	50	$35 + j10$
Horizontal unbalanced dipole in forest	75	$50 + j40$
Horizontal dipole with balun in forest	75	$70 + j15$
Horizontal balanced dipole in forest	75	$70 + j20$
Horizontal balanced dipole in forest	100	$40 + j5$
Vertical sleeve dipole in clearing	100	$100 + j100$
Vertical sleeve dipole in forest	100	$50 + j100$
Vertical balanced dipole in forest	100	$38 + j12$

VIII COMPUTER-MODELING OF THE VHF ANTENNA RADIATION PATTERNS

The computer program developed for predicting the directivity pattern of HF antennas in forests⁷ was used for the VHF antennas measured at Ban Mun Chit using input data applicable to the VHF case.⁸ Although it was not anticipated that the model would be useful for describing the VHF patterns in detail because of the scattering observed during the U.S. tests,¹ it did seem important to determine if the model could provide a reasonable prediction of the average VHF directivity patterns (i.e., to determine if the predicted patterns compared reasonably well with the contour plots obtained by statistically processing the data from the field measurements).

A. Description of the Model

Only a brief description of the model will be provided here since a detailed description is provided in Ref. 7. The model approximates the forest and ground as layers of dielectric slabs, as shown in Figure 18. The upper layer is the space above the forest, characterized by ϵ_0 and μ_0 , the permittivity and permeability of free space. The center region is the forest, characterized by a complex dielectric constant,

$$\epsilon_1 = \epsilon_1' - j\epsilon_1''$$

and the lower region is the ground below the forest, characterized by a complex dielectric constant,

$$\epsilon_2 = \epsilon_2' - j\epsilon_2''$$

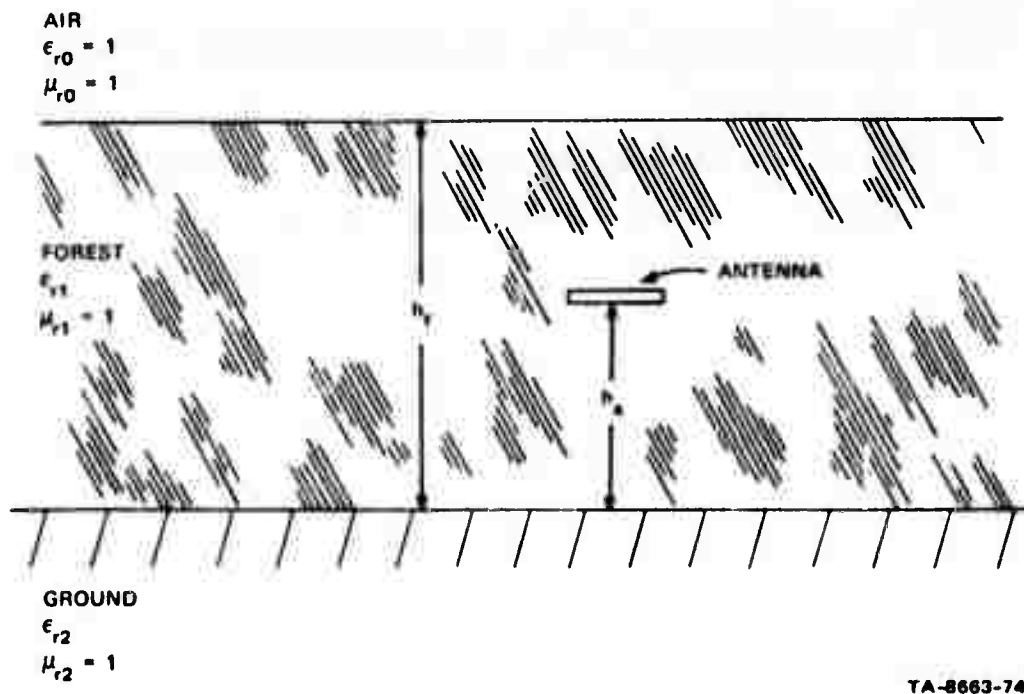


FIGURE 18 IDEALIZED LOSSY DIELECTRIC SLAB MODEL

Each region is assumed to be homogeneous and to possess the magnetic permeability of free space. The antenna is a Hertzian dipole.

B. Antenna Radiation Patterns

The multilayer slab model was used to calculate the expected radiation patterns of the dipole antennas measured at Ban Mun Chit. The measured foliage and ground constants presented in Figures 9 and 10 were used to define the forest and ground in the model.

In order to simplify the comparison of the measured and computed data, the computed pattern was referenced to the measured patterns. This was accomplished by estimating the mean elevation angle of the lowest -3 dB contour on the measured patterns--i.e., by visually estimating the average location of the -3 dB contour in the vicinity of 90° from the

dipole axis for the E_ϕ response and in the vicinity of 0° from the dipole axis for the E_θ response. The program then determined the azimuth angles at which the -6, -9, and -12 dB contours intersected certain elevation angles. These contours were then plotted by hand on the plots of the measured data. In other words, the elevation of the -3 dB contour of the calculated pattern near 0° or 90° azimuth was predetermined (i.e., the measured and calculated values were forced to agree at this one point), and then the remaining contours were referenced to this point. Physically, this procedure is similar to adding a constant gain or loss to an antenna through the use of an amplifier or an attenuator.

The calculated patterns are shown as dashed lines on the patterns of the measured data presented in Appendices A and B. Only one-half of the calculated pattern is shown, since the remaining pattern would be an inverted image of the portion provided.

IX DISCUSSION OF RESULTS

The data presented in this report are the results of exploratory measurements of the effect of tropical vegetation on the performance of simple VHF antennas. The measured signal-strength data were processed statistically to provide contour plots of the antenna radiation patterns. No special mathematical models were developed to predict the radiation patterns of these VHF antennas, but the multilayered slab model developed previously for HF antenna pattern predictions was tested to evaluate its utility at VHF.

A. Measured Antenna Radiation Patterns

The patterns of the antennas discussed in this section are presented in Appendices A and B of this report and they are discussed in this section primarily in order of increasing frequency instead of the order in which they are presented in the appendices.

The 50-MHz horizontal unbalanced dipole antenna was measured while located in the clearing during both measurement sets (Figures A-1 and A-2, and B-1 and B-2, respectively). The contour plots of the median signal strength resulting from the two measurements of this antenna compare quite favorably, as do the values for the relative gain (the E_0 values are within 0.7 dB of each other and the E_θ values are within 0.5 dB). The estimated standard deviations about the median, $\hat{\sigma}'$, are also quite similar for these two measurements (see Tables A-1 and A-2, and B-1 and B-2, respectively). The standard deviation tends to increase in the nulls of the radiation pattern, particularly for the E_θ responses (see Tables A-2 and B-2). This is a result of the data-processing

techniques (as indicated in Section VI) and not a phenomenon of the antenna itself. Generally, $\hat{\sigma}'$ was greater for the E_{θ} (vertically polarized) response than for the E_{ϕ} response (horizontally polarized).

When the 50-MHz horizontal unbalanced dipole was measured in the forest, the maximum of the E_{θ} response of the antenna occurred at higher elevation angles and the lobes of the E_{ϕ} response encompassed a smaller elevation sector than when the same type of antenna was located in the clearing. Although $\hat{\sigma}'$ was not greatly affected it was slightly higher for the antenna in the forest.

Patterns of the 50-MHz vertical sleeve dipole were measured during both measurement sets while the antenna was located in the clearing. The E_{θ} response of this antenna was fairly omnidirectional at the higher elevation angles (above 30°), but the radiation pattern did not repeat as well for the two sets of measurements as those of the 50-MHz horizontal unbalanced dipole in the clearing. When the same type of antenna was located in the forest, the normally omnidirectional radiation pattern became somewhat perturbed (see Figure A-7). For elevation angles below about 30° the patterns were not very omnidirectional for the antenna in the clearing or the forest.

The 75-MHz horizontal unbalanced dipole was measured while it was located in the clearing during measurement Set 1. The resulting E_{θ} and E_{ϕ} radiation patterns (Figures A-8 and A-9) from these measurements were slightly more complex than those from the 50-MHz unbalanced dipole in the clearing and the $\hat{\sigma}'$ values were generally higher for the 75-MHz dipole, particularly for the E_{θ} responses. This type of antenna also was measured at two different locations in the forest (see Figures A-10 and A-11 and Figures B-9 and B-10); and, though there are slight differences between the resulting patterns, the lobes occur at nearly the same elevation

angles for both locations. The $\hat{\sigma}'$ values for the location in Set 2 are generally slightly higher than those from Set 1.

The 75-MHz horizontal unbalanced dipole in the forest, measured in Set 1; and the horizontal dipole with a balun in the forest, measured in Set 2, were actually the same antenna at the same location measured with and without a balun. The resulting patterns have some discrepancies, which are possibly due to the orbits used for the measurements not being exactly duplicated and possibly because of the impedance mismatch caused by the 75- Ω :75- Ω balun but more likely caused by the antenna not being installed identically for the two measurement sets. The $\hat{\sigma}'$ values for the two antennas are within 0.5 dB of each other. The E_{θ} patterns for this antenna appears to be affected by the insertion of the balun more than the E_{ϕ} patterns, and this is what one might expect because the balun controls (and tends to minimize) the currents flowing on the outside of the cable shield.

Contour plots were produced for the estimated mean and the estimated median signal strength of the 75-MHz horizontal unbalanced dipole in the forest measured in Set 1. The E_{ϕ} patterns for the mean and median compare quite favorably (Figures 1' and A-11), whereas there are more differences between the mean and median for the E_{θ} patterns (Figures 15 and A-10). The estimated standard deviation about the mean, $\hat{\sigma}$, and the estimated standard deviation about the median, $\hat{\sigma}'$, were also calculated and gridded for this antenna. The values for $\hat{\sigma}$ and $\hat{\sigma}'$ are quite similar for the pattern data from this antenna and other examples that were checked, and it was thus assumed that the estimated median response was representative of the estimated mean response. Thus, the estimated median response was used to generate the contour plots employed to describe the "smoothed" response of the antennas measured at this site.

Similar 75-MHz vertical sleeve dipoles were measured while installed in the clearing and in the forest. The E_{θ} radiation pattern of these antennas remained fairly omnidirectional at the higher elevation angles, but there were perturbations in the pattern at the lower elevation angles for the antenna located in the forest.

Similar 100-MHz unbalanced dipoles were measured while located in the clearing and in the forest. In this case, the forest tended to increase $\hat{\theta}'$ for the E_{θ} response but caused a decrease in $\hat{\theta}'$ for the E_{ϕ} response.

The response of similar 100-MHz vertical sleeve dipoles was measured in two locations in the clearing--one was separated from the clearing-tree interface and the other was fairly close to this interface. It can be seen that the response of the one near the clearing-tree interface is fairly smooth (see Figure B-17) compared to that of the one further out of the clearing (Figure A-20). From the values of $\hat{\theta}'$ and from the median signal response, it appears that the forest-clearing interface may have helped smooth the E_{θ} radiation pattern of this antenna. Also, it may be noted that the antenna farther out in the clearing exhibited a deeper, more symmetrical null at the higher elevation angles.

The patterns of the 100-MHz vertical sleeve dipole were measured while the antenna was situated in two locations in the forest. The median-signal-strength plots for this antenna show perturbations and irregularities not common to the two locations, but the values of $\hat{\theta}'$ are similar.

Generally, there was not a significant change in the values of $\hat{\theta}'$ as the measurement frequency was increased from 50 MHz to 100 MHz, but the median radiation pattern of the antennas became more complex; which is partially caused by the increased electrical height of the antennas as the frequency was increased. It appears reasonable to assume that if,

as in Ref. 1, a calculation of the change in signal strength as a function of azimuth were made, the average change in signal strength for constant small increments of azimuth would increase as the frequency was increased.

As a means of establishing the significance of the forest on the scattering one could compare the data from the antennas in the clearing and in the forest and find that there are only minor differences in the standard deviations for the two locations. Measurements of VHF antennas were performed under another contract in rough terrain near Livermore, California¹⁷ and, although the deterministic pattern factors of the antennas were affected by the hillsides on which the antennas were located, the standard deviations were actually slightly higher than those resulting from the measurements presented in this report. The data from the Livermore measurements showed that $\hat{\sigma}'$ tended to increase as the incident signal was composed of a direct wave and a wave reflected from the hill. Thus, it appears that the reflected waves from the trees add in and out of phase and can possibly cause the signal variations observed in the Thailand forest.

B. Relative Gain Results

In Set 1, essentially the same types of antennas (half-wave resonant horizontal and vertical dipoles) were measured simultaneously in and out of the forest. The horizontal dipoles in the clearing produced the maximum received signal, and when both horizontal and vertical dipoles were operated on the same frequency and in the same types of environment (i.e., clearing or forest), the horizontal dipole exhibited the greater received signal by about $6 \text{ dB} \pm 3 \text{ dB}$ when the comparison is made without regard to the polarization of the incident signal. By comparing the maximum relative responses of these two types of antennas (on the same frequency and

in the same type of terrain) for the same transmitted polarization (i.e., E_θ or E_ϕ) it can be observed that the horizontal dipole response to E_θ exceeded that of the vertical dipole by about $3 \text{ dB} \pm 3 \text{ dB}$ in both the clearing and the forest, whereas the maximum E_ϕ response for the horizontal dipole exceeded that of the vertical dipole by about $17.5 \text{ dB} \pm 3 \text{ dB}$.

The most accurate relative-gain data for both Sets 1 and 2 are the E_θ/E_ϕ values for the same antenna. An examination of these data in Tables 17 and 18 indicates that for the horizontally polarized antennas, $E_\theta/E_\phi \approx -5 \text{ dB} \pm 3 \text{ dB}$ in the clearing and $-2 \text{ dB} \pm 3 \text{ dB}$ in the forest, whereas the corresponding values for the vertically polarized antennas are $+12 \text{ dB} \pm 4 \text{ dB}$ and $+15 \text{ dB} \pm 3 \text{ dB}$ for clearing and forest, respectively. The E_θ/E_ϕ ratio typically increased about 3 dB for both horizontally and vertically polarized antennas when the same type of antenna was moved from the clearing to forest. Data at 6 MHz showed that the E_θ/E_ϕ ratio increased by approximately 8 dB when horizontal dipoles were moved from the clearing to the forest at this site. It should be noted that when the E_θ/E_ϕ ratio was calculated, the maximum response for E_θ was usually at a different azimuth and elevation than the E_ϕ maximum. No pronounced frequency trends are apparent at VHF.

C. Measured Antenna Feed-Point Impedance

When reviewing the measured impedance data, one must remember that often different antennas of identical dimensions were measured instead of relocating the same physical structure. This factor could have considerable effect on the reactive part of the impedance. But if these data are used cautiously, the impedance data provide an indication of the effects that the forest would create on matching the antennas to a radio set. It can be seen in Tables 20 and 21 that the impedance of the horizontal unbalanced dipoles varied only slightly when measured in the

clearing and the forest, but the location of the vertical sleeve dipoles greatly affected their observed feed-point impedance. The horizontal dipole would probably be the easier antenna to match to a radio set for use in forests.

D. Comparison of Measured and Calculated Patterns

The calculated and measured median patterns discussed in this section are presented as contour plots in Appendices A and B at the end of this report. The measured patterns are shown as solid lines and the calculated patterns are shown as dashed lines on the contour plots. The data are not necessarily discussed in the order in which the figures are presented in the appendices but are discussed in order of increasing frequency.

The highest correlation between the measured and calculated patterns at 50 MHz can be seen in the E_{θ} response of the horizontal unbalanced dipole in the clearing, measured in both sets (Figures A-1 and B-1). However, calculated E_{ϕ} response of this antenna does not resemble the measured data as well as the calculated and measured E_{θ} data.

The calculated and measured patterns of the 50-MHz unbalanced dipole in the forest are again quite similar--in fact, the two patterns are within 3 dB of each other (Figures A-3 and A-4). But the calculated patterns of the 50-MHz horizontal folded dipole in the forest had almost no resemblance to the measured patterns and were not plotted (Figures B-3 and B-4).

The measured and calculated patterns of the 75-MHz unbalanced dipole antenna in the clearing are fairly similar but do not compare as well as those of the 50-MHz unbalanced dipole in the clearing. Of the two

polarization responses of the antenna, the patterns for the E_θ response show the most resemblance (Figure A-9). When the 75-MHz unbalanced dipole was located in the forest, the similarity between the calculated and measured data was still quite poor.

The calculated and measured patterns of the 100-MHz unbalanced dipole in the clearing are quite similar for the portion of the E_θ pattern that was calculated. The patterns for this antenna in the forest are again similar. But the patterns of the balanced dipole are quite dissimilar--primarily because of the deep null toward 300° in both measured patterns.

From the examples of calculated and measured patterns provided in this report, it appears that the slab model can predict the average patterns of simple VHF dipole to ± 3 dB in some cases. But more example cases should be studied before any definite conclusion can be made. Obviously, the model cannot predict the "fine structure" of the pattern, but if more data were available it appears that one could place a figure of merit on the model regarding prediction of the effect of the macroscopic features of the forest. In the absence of a more refined model, a standard deviation of the scattering caused by the microscopic features of the forest could be employed to complete the model, so that the probability of the signal strength exceeding a certain level at a given range in a given solid angle from a transmitting antenna could be predicted.

X SUMMARY AND RECOMMENDATIONS

These exploratory measurements on the performance of VHF antennas immersed in a tropical forest provide insight into some of the problems of the field communicator operating VHF radios in a tropical forest.

The pattern-measurement data indicate that the forest at Ban Mun Chit was apparently more isotropic than the forest previously considered at Newark, California.¹ Although there were pattern perturbations and fairly rapid fadings observed in the data from Ban Mun Chit, these fadings (presumably caused by the predominantly vertical tree trunks) were not as extensive as those observed at Newark where, it might be noted, the forest was composed mostly of tall vertical tree trunks.

The rapid variation of signal strength as a function of the azimuth angle indicated that these data should be processed statistically in order to provide a more consolidated and understandable display of the data. The data were processed so as to provide statistical estimates over 10° azimuth sectors, as derived from the measured signal strength as a function of the azimuth angle. The estimated median signal strength was then contoured to provide patterns of the relative median signal strength as a function of azimuth and elevation. In addition to this, the estimated standard deviations were tabulated for 10° increments of azimuth and 5° increments of elevation. The statistical estimators show that the mean and median signal strength are quite similar for these data. The radiation pattern data indicate that the median signal strength is generally representative of that expected for the antenna structures. The pattern data from the dipole antennas indicated that the maximum signal strength occurred at higher elevation angles when the antennas

were located in the forest than when they were located in the clearing. The patterns of the vertical-sleeve dipole antennas and the vertical dipole antennas, which should have fairly omnidirectional azimuthal patterns, became quite perturbed when located in the forest.

The number of antennas measured exceeded the number of available receiving and recording channels, which required that the antennas be measured as two sets. While measuring these two sets, measurements were duplicated on several antennas in the same locations. A high degree of repeatability in the median signal strengths was observed for the two sets of measurements.

Horizontal dipoles typically exhibited about 6 dB more gain than vertical dipoles when a comparison of relative maximum median response was made without regard to the polarization of the incident signal. The maximum median response of a horizontal dipole for E_{θ} exceeded that of a vertical dipole by only about 3 dB, whereas for E_{ϕ} the difference increased to 17.5 dB for antennas in both clearing and forest. The ratio of E_{θ}/E_{ϕ} for the horizontal dipoles was about -5 dB, whereas for the vertical dipoles a ratio of +12 dB was more typical when the antennas were in the clearing. This ratio was observed to increase by about 3 dB for both vertical and horizontal dipoles when the antennas were moved from clearing to forest.

The feed-point impedance of the antennas was measured while they were in their pattern-measurement situations and these data show that the surrounding foliage affected the impedance of the vertical dipole antennas more than that of the horizontal dipole antennas.

The computer program developed for predicting the radiation patterns of HF antennas in a homogeneous, isotropic forest was used with the parameters to define the forest and horizontal dipole antennas measured at VHF at Ban Mun Chit. The resulting calculated patterns compare

favorably with the measured median patterns for the unbalanced dipole antennas. The largest discrepancies between the measured and modeled patterns resulted from the 75-MHz antennas. The model, although it will calculate the average pattern, still requires further development before it will predict the significant variations in the patterns or a statistical estimator of the variations caused by scattering at VHF.

In order to better understand the effects of forests on VHF antennas, it is recommended that the following programs should be considered:

- (1) Measurement of another set of simple dipole antennas at a constant electrical height--i.e., $\lambda/4$ in order to maintain a more constant ideal pattern as the frequency is varied.
- (2) More patterns should be measured in different forests so as to gain a better understanding of the effect that these differing forests have on the patterns.
- (3) From the various forests, statistical distributions of the "scattering functions" for the various forests should be determined for the computer model.

Appendix A

CONTOUR PLOTS OF THE ESTIMATED MEDIAN AMPLITUDES
AND TABLES OF STANDARD DEVIATIONS FOR ANTENNA SET 1

Appendix A

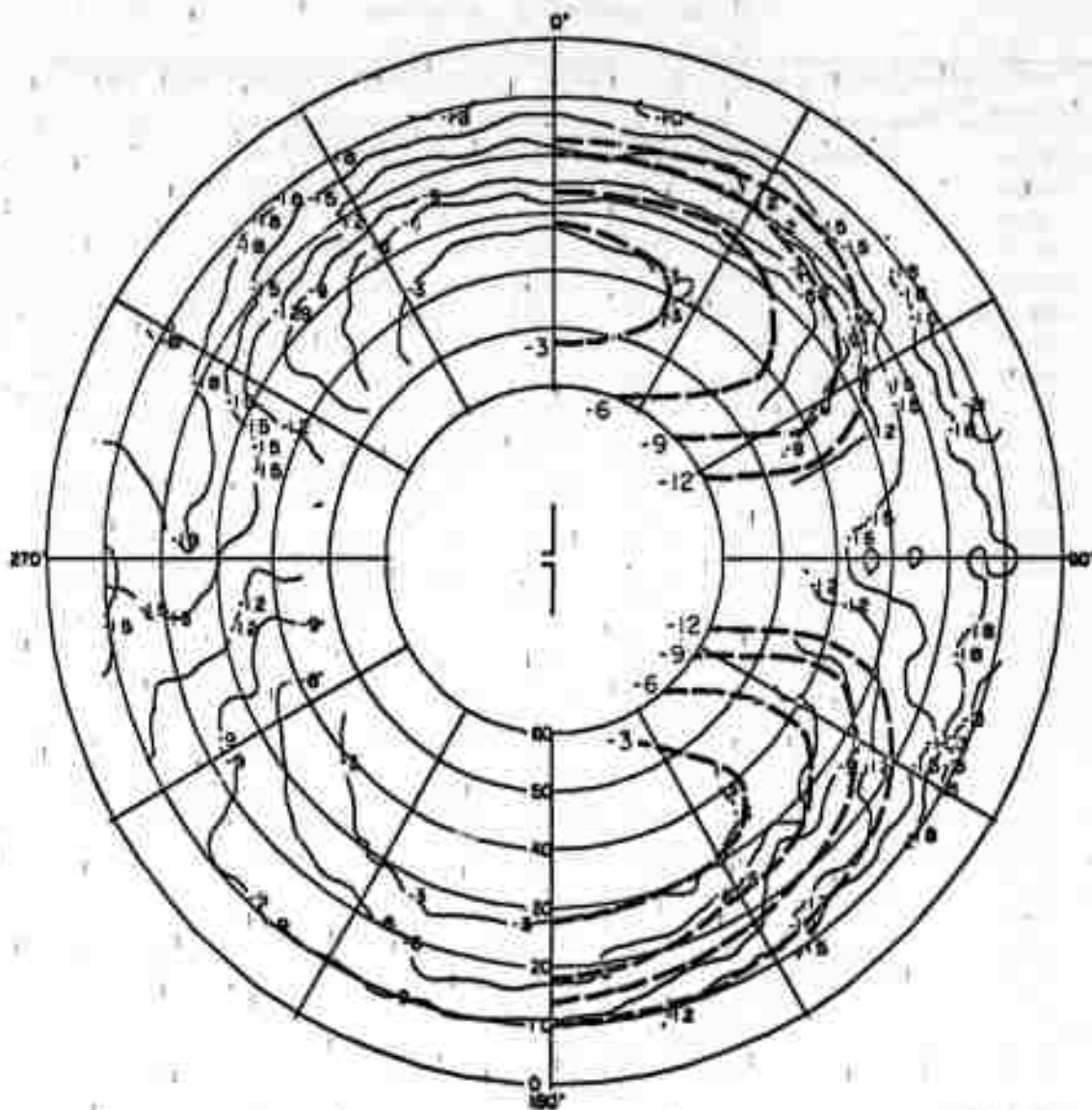
CONTOUR PLOTS OF THE ESTIMATED MEDIAN AMPLITUDES AND TABLES OF STANDARD DEVIATIONS FOR ANTENNA SET 1

This appendix contains the contour plots of the estimated median signal strength (as described in Section VI-B) and tables of the standard deviation of the signal strength about the median as described in Section VI-C for Antenna Set 1 (see Figure 7). For each contour plot presented, a table of standard deviations is presented on the opposite page. The data are grouped in order of increasing frequency, and within the frequency group the data for horizontal dipoles are presented first, and then the data for the vertical sleeve dipoles. The title indicates: the antenna type, the antenna location, the measurement polarization (using the same notation as defined in Section V--i.e., E_{θ} is vertical polarization and E_{ϕ} is horizontal polarization), and the measurement frequency which is also the design frequency of the antenna. Where the calculated patterns are available, they are shown as dashed lines on the contour plots.

Table A-1

STANDARD DEVIATIONS ABOUT THE MEDIAN FOR THE HORIZONTAL UNBALANCED DIPOLE
IN THE CLEARING--E₀ AT 50 MHz

Elevation Azimuth	10.0	15.0	20.0	25.0	30.0	35.0	40.0	45.0	50.0
-170.0	1.75	1.01	0.83	0.57	0.61	0.76	0.70	0.69	0.71
-160.0	1.18	0.86	0.82	0.72	0.58	0.56	0.79	0.91	1.00
-150.0	1.16	0.92	0.84	0.79	0.72	0.83	0.95	1.19	1.08
-140.0	1.03	0.81	0.78	0.64	0.77	0.98	0.92	0.80	0.79
-130.0	0.92	0.82	0.85	0.89	0.78	0.63	0.90	1.09	1.07
-120.0	1.48	1.11	1.25	1.03	0.90	0.83	0.96	0.97	1.23
-110.0	1.78	1.59	1.55	1.40	1.29	1.29	0.97	0.79	1.03
-100.0	3.37	2.65	2.13	2.13	1.89	1.79	1.43	1.27	1.42
-90.0	1.71	1.79	2.07	2.40	1.77	1.02	1.82	2.44	2.12
-80.0	2.14	2.43	2.04	1.74	2.08	2.34	2.10	1.76	1.41
-70.0	2.24	1.75	1.99	1.89	2.37	2.62	2.20	1.77	1.62
-60.0	1.83	2.21	2.18	2.26	2.47	2.74	2.29	2.35	2.02
-50.0	2.74	2.33	2.19	2.01	2.04	1.86	1.71	1.47	1.58
-40.0	2.02	2.13	2.03	2.47	2.08	1.59	1.30	1.09	0.73
-30.0	1.62	1.32	1.63	1.72	1.45	1.16	0.83	0.59	0.50
-20.0	2.24	1.03	1.39	1.39	1.03	0.78	0.66	0.55	0.50
-10.0	2.60	2.84	1.44	0.95	0.76	0.89	0.80	0.78	0.68
0.0	2.01	0.36	1.16	0.88	0.74	0.72	0.86	0.80	0.71
10.0	2.59	2.32	1.27	1.24	0.98	1.00	0.94	1.21	1.02
20.0	1.87	1.23	1.41	1.13	0.86	0.87	0.86	0.65	0.63
30.0	1.86	0.77	1.25	0.98	0.84	0.85	0.74	0.69	0.83
40.0	2.45	3.08	2.07	1.63	1.29	0.86	0.86	0.99	1.13
50.0	2.96	1.95	2.09	1.98	1.82	1.25	1.11	0.54	1.05
60.0	2.17	2.28	2.07	2.23	2.23	2.70	1.53	0.97	1.58
70.0	1.01	1.65	1.92	1.85	1.94	1.41	1.78	1.89	1.99
80.0	1.89	1.96	1.98	2.07	2.47	3.30	2.59	2.48	2.31
90.0	2.88	2.51	2.61	3.00	2.81	1.68	2.25	2.77	2.51
100.0	2.35	2.94	2.54	2.51	2.68	3.02	2.12	1.40	1.72
110.0	1.17	2.26	2.23	1.76	1.72	1.28	1.44	1.30	1.29
120.0	2.05	2.37	2.38	2.96	2.15	1.06	1.13	0.91	0.97
130.0	3.29	2.54	2.40	1.75	1.20	0.67	0.88	0.86	0.64
140.0	2.70	2.62	2.28	2.34	1.76	1.51	1.00	0.84	0.67
150.0	2.02	1.49	1.44	1.15	0.97	0.57	0.73	0.71	0.59
160.0	1.31	0.93	1.12	0.78	0.55	0.61	0.62	0.52	0.53
170.0	1.54	1.11	0.96	0.92	0.64	0.54	0.54	0.52	0.44
180.0	1.54	1.05	0.92	0.77	0.68	0.68	0.60	0.58	0.53



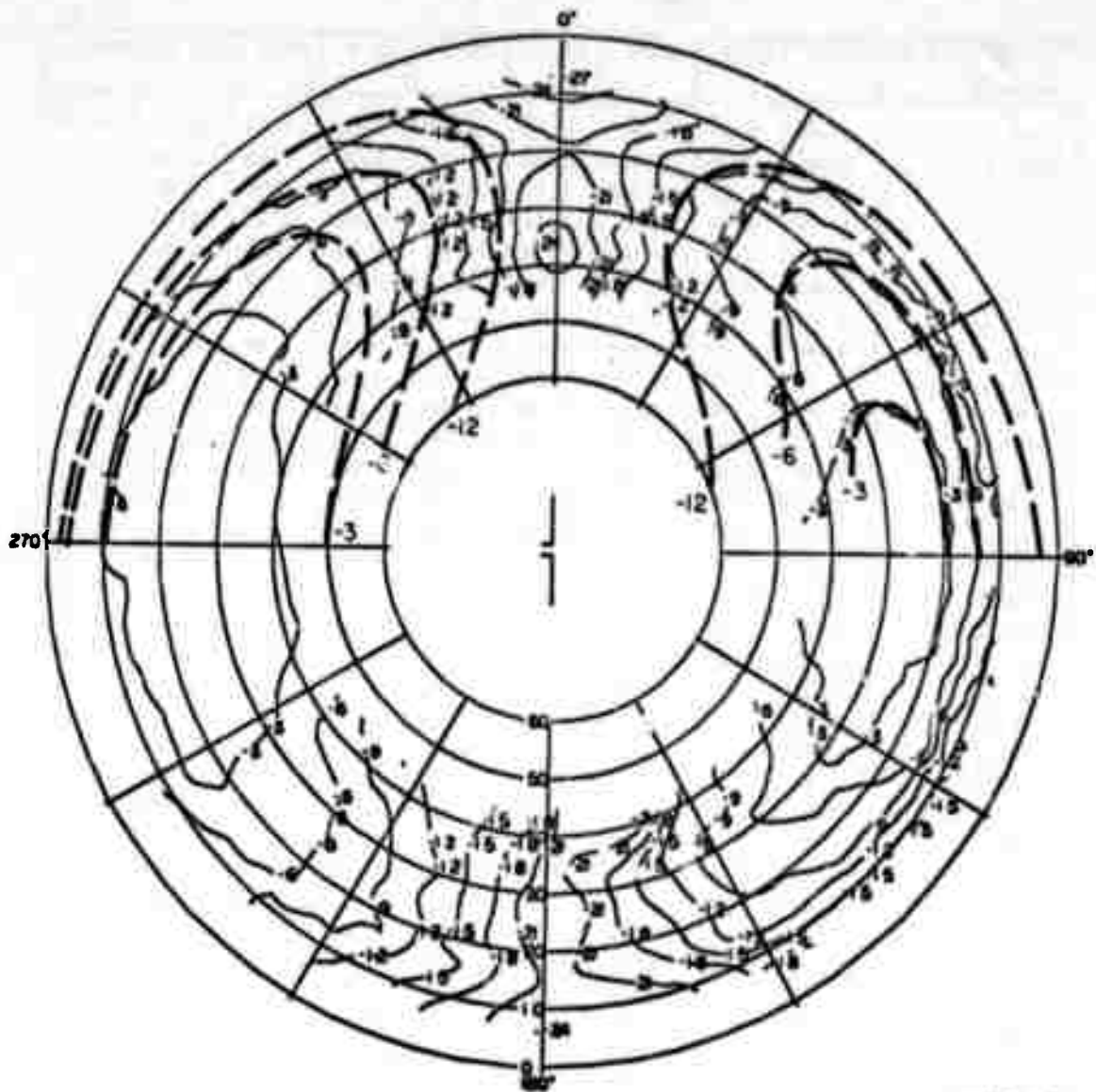
TA-8663-197

FIGURE A-1 CONTOUR PLOT OF THE MEDIAN RESPONSE OF THE HORIZONTAL UNBALANCED DIPOLE IN THE CLEARING— E_θ AT 50 MHz

Table A-2

STANDARD DEVIATIONS ABOUT THE MEDIAN FOR THE HORIZONTAL UNBALANCED DIPOLE
IN THE CLEARING--E₀ AT 50 MHz

Elevation Azimuth	10.0	15.0	20.0	25.0	30.0	35.0	40.0	45.0	50.0
-170.0	2.84	2.12	2.40	2.91	2.70	2.12	1.94	--	--
-160.0	1.72	1.16	1.77	2.03	1.88	1.32	1.33	0.67	--
-150.0	1.01	1.28	1.27	1.22	1.19	0.77	0.83	0.65	--
-140.0	0.88	0.98	0.96	0.95	0.85	0.74	0.76	0.91	--
-130.0	0.59	0.29	0.61	0.56	0.60	0.55	0.77	0.84	--
-120.0	0.43	0.39	0.44	0.56	0.57	0.69	0.73	0.81	--
-110.0	0.37	0.39	0.36	0.42	0.41	0.51	0.41	0.26	--
-100.0	0.53	0.18	0.20	0.16	0.19	0.13	0.21	0.24	--
-90.0	0.51	0.16	0.16	0.12	0.22	0.19	0.19	0.22	--
-80.0	0.41	0.28	0.40	0.24	0.30	0.23	0.21	0.15	--
-70.0	0.62	0.58	0.66	0.85	0.48	0.27	0.34	0.41	--
-60.0	0.58	0.54	0.54	0.29	0.43	0.24	0.40	0.50	--
-50.0	0.88	0.96	0.91	0.90	0.69	0.60	0.50	0.44	--
-40.0	0.90	0.62	0.64	0.93	0.70	0.57	0.55	0.67	--
-30.0	1.30	0.92	0.86	0.66	0.82	0.72	0.92	0.70	--
-20.0	1.88	2.16	2.28	1.39	2.15	1.71	1.53	1.20	--
-10.0	1.49	1.93	2.57	4.19	3.15	2.33	2.40	2.02	--
0.0	1.30	1.05	1.97	1.77	2.38	2.79	2.64	2.61	--
10.0	1.56	1.67	1.70	1.87	2.30	2.77	2.26	2.32	--
20.0	1.42	1.15	1.38	2.02	1.47	1.33	1.58	1.58	--
30.0	1.31	1.02	0.90	0.53	0.69	0.90	0.88	0.71	--
40.0	1.11	0.78	0.64	0.85	0.77	0.80	0.76	0.91	--
50.0	1.01	0.47	0.61	0.57	0.74	0.94	0.65	0.51	--
60.0	1.12	0.95	0.84	0.90	0.76	0.58	0.50	0.33	--
70.0	1.07	1.17	0.79	0.48	0.57	0.68	0.56	0.50	--
80.0	0.96	0.85	0.69	0.52	0.48	0.37	0.39	0.34	--
90.0	1.35	0.59	0.55	0.66	0.43	0.29	0.26	0.13	--
100.0	1.86	1.40	0.75	0.66	0.40	0.24	0.24	0.27	--
110.0	1.43	0.83	0.55	0.40	0.27	0.14	0.31	0.43	--
120.0	1.43	0.96	0.59	0.24	0.17	0.24	0.33	0.38	--
130.0	1.23	0.93	0.78	1.01	0.83	0.82	0.56	0.60	--
140.0	1.50	0.74	0.93	0.66	0.77	0.61	0.73	0.63	--
150.0	1.66	1.56	1.26	1.58	1.20	1.36	1.19	1.67	--
160.0	2.17	1.83	1.69	1.06	1.15	1.74	2.42	3.75	--
170.0	3.61	3.87	2.45	1.97	2.65	3.64	3.42	3.43	--
180.0	3.29	1.93	2.37	2.68	3.83	4.29	3.19	2.03	--



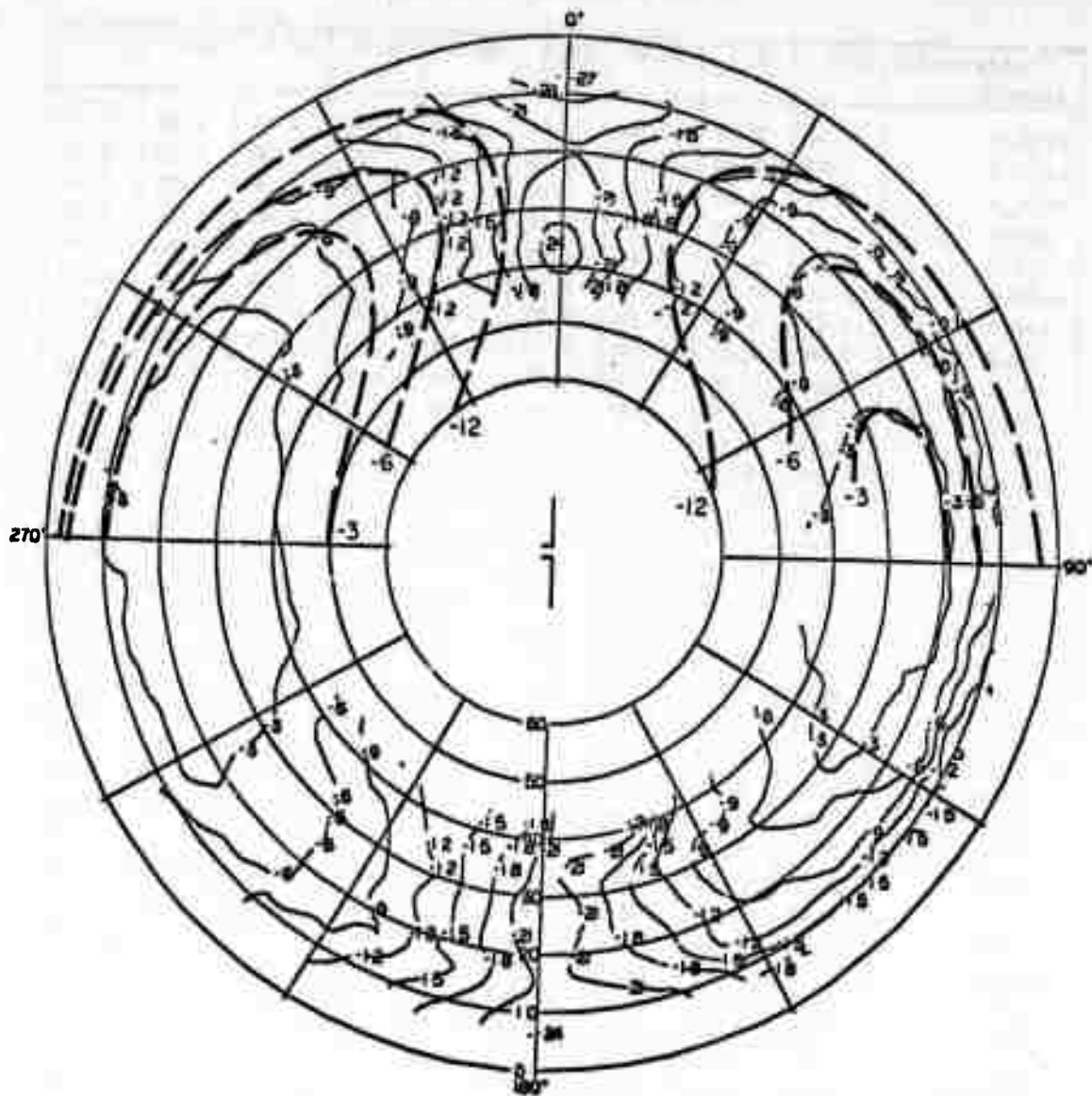
TA-8663-198

FIGURE A-2 CONTOUR PLOT OF THE MEDIAN RESPONSE OF THE HORIZONTAL UNBALANCED DIPOLE IN THE CLEARING— E_{ϕ} AT 50 MHz

Table A-3

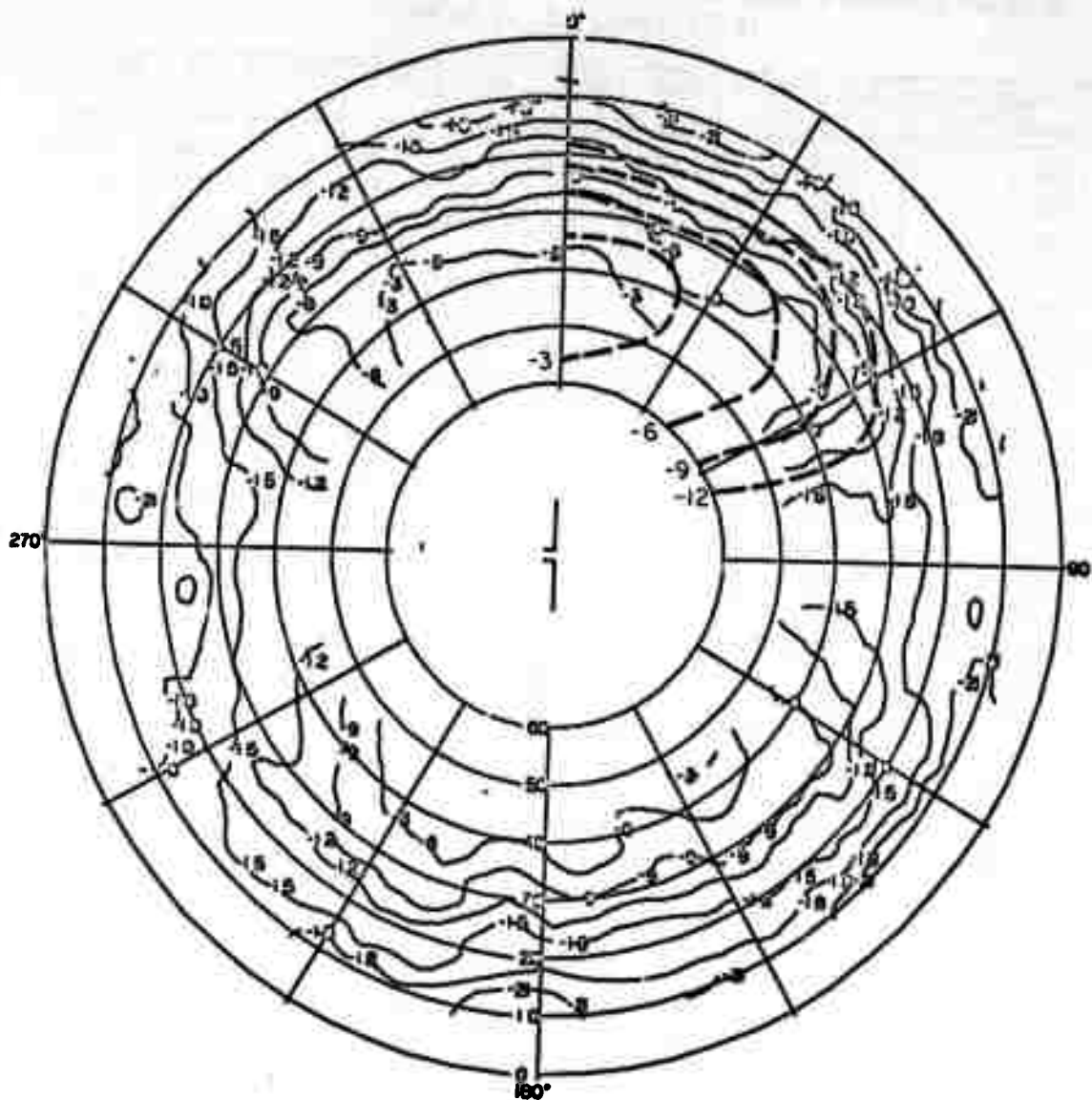
STANDARD DEVIATIONS ABOUT THE MEDIAN FOR THE HORIZONTAL UNBALANCED DIPOLE
IN THE FOREST-- E_{θ} AT 50 MHz

Elevation Azimuth	10.0	15.0	20.0	25.0	30.0	35.0	40.0	45.0	50.0
-170.0	2.36	2.57	2.92	3.51	3.07	1.84	1.37	1.21	0.97
-160.0	2.95	2.49	2.47	2.48	1.90	1.37	1.36	1.19	0.67
-150.0	3.08	2.81	2.54	2.29	1.61	1.28	1.30	1.21	0.65
-140.0	2.76	2.34	2.28	2.19	1.91	1.47	1.44	1.37	0.80
-130.0	2.22	2.13	2.63	2.79	3.10	2.33	2.19	1.95	1.45
-120.0	2.84	3.26	3.09	3.08	3.27	2.38	2.22	2.08	2.04
-110.0	2.70	3.60	3.43	3.27	3.58	2.26	2.25	2.01	2.01
-100.0	3.06	2.74	2.60	2.43	3.41	3.01	2.60	2.44	1.91
-90.0	3.01	2.09	2.38	2.36	3.01	3.01	2.99	2.98	2.28
-80.0	2.50	2.39	2.60	3.00	3.46	3.14	3.37	3.47	3.30
-70.0	2.47	3.23	3.20	3.42	4.09	3.45	3.03	2.61	2.23
-60.0	2.68	2.48	2.56	2.21	2.69	2.51	2.24	1.49	2.30
-50.0	3.72	2.54	2.25	1.92	1.97	2.14	1.62	1.50	1.90
-40.0	2.26	1.86	1.79	1.96	1.68	1.30	1.41	1.37	1.29
-30.0	1.77	1.49	1.86	1.85	1.41	1.24	1.04	0.82	0.78
-20.0	3.37	2.59	2.25	1.91	1.21	0.81	0.76	0.61	0.68
-10.0	3.27	2.79	2.59	2.43	1.37	0.69	0.64	0.56	0.66
0.0	2.62	2.22	2.13	1.91	1.30	0.94	1.00	1.16	1.07
10.0	2.39	2.17	1.98	1.81	1.20	1.13	1.20	1.11	0.86
20.0	2.13	1.95	1.88	1.80	1.19	1.18	1.31	1.66	1.13
30.0	2.56	2.02	1.92	1.80	1.76	2.01	2.04	1.81	1.09
40.0	2.90	2.03	1.91	1.65	1.73	1.95	2.03	1.80	0.99
50.0	2.33	2.13	1.96	1.80	1.65	1.67	1.45	1.29	0.88
60.0	2.22	2.32	2.43	2.26	1.82	2.02	1.73	1.73	1.44
70.0	2.37	2.36	2.95	3.69	2.77	2.68	2.16	2.36	2.36
80.0	2.67	3.00	3.54	4.21	3.23	2.91	2.16	2.17	2.27
90.0	2.83	3.02	3.13	3.19	2.70	2.63	2.05	1.97	2.16
100.0	2.43	2.61	2.49	2.41	2.05	2.08	2.23	2.28	2.49
110.0	2.40	2.27	2.11	1.86	1.55	1.86	2.55	2.76	2.55
120.0	2.10	2.21	2.26	2.09	1.98	2.04	2.43	2.55	1.97
130.0	2.12	2.71	2.59	2.71	2.06	1.68	1.76	2.33	1.62
140.0	2.64	2.67	2.58	2.44	1.94	1.76	1.45	1.43	0.95
150.0	2.04	2.25	2.48	2.38	1.87	1.15	0.99	0.96	0.90
160.0	2.10	3.18	3.30	3.72	3.22	1.56	1.53	1.77	1.33
170.0	2.63	3.89	3.60	3.42	2.60	1.43	1.26	1.16	0.93
180.0	2.04	2.72	3.20	3.39	2.71	1.10	1.34	1.34	1.05



TA-8663-198

FIGURE A-2 CONTOUR PLOT OF THE MEDIAN RESPONSE OF THE HORIZONTAL UNBALANCED DIPOLE IN THE CLEARING— E_{ϕ} AT 50 MHz



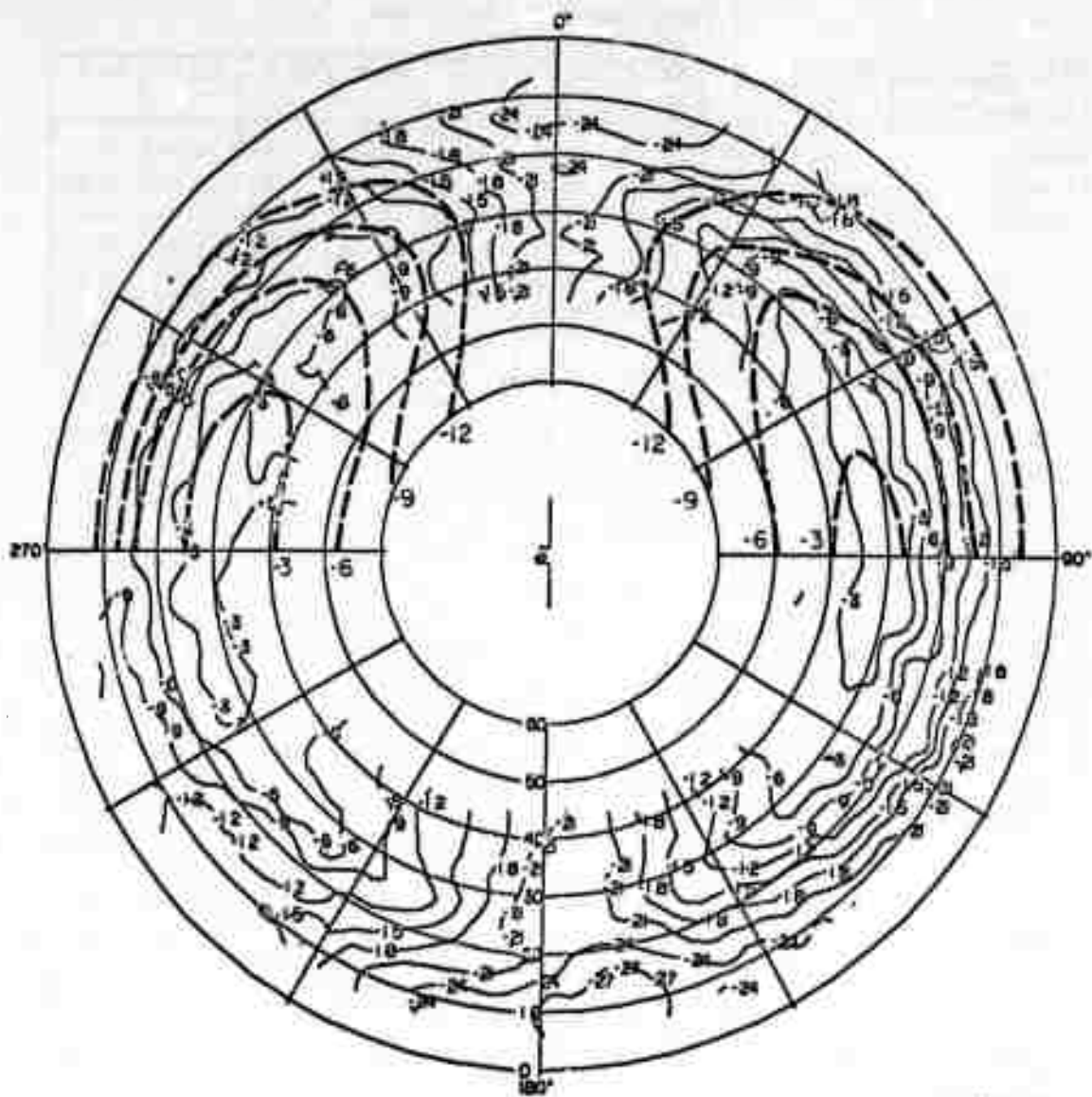
TA-8663-199

FIGURE A-3 CONTOUR PLOT OF THE MEDIAN RESPONSE OF THE HORIZONTAL UNBALANCED DIPOLE IN THE FOREST— E_0 AT 50 MHz

Table A-4

STANDARD DEVIATIONS ABOUT THE MEDIAN FOR THE HORIZONTAL UNBALANCED DIPOLE
IN THE FOREST-- E_{ϕ} AT 50 MHz

Elevation Azimuth	10.0	15.0	20.0	25.0	30.0	35.0	40.0	45.0	50.0
-170.0	--	2.35	2.75	3.08	2.35	1.37	1.72	1.86	--
-160.0	2.02	1.95	2.26	2.99	2.52	1.64	1.69	2.18	--
-150.0	2.31	1.78	1.53	1.54	1.20	0.87	0.91	1.01	--
-140.0	0.76	0.75	1.12	1.04	0.90	0.81	0.87	1.03	--
-130.0	1.24	1.21	1.00	0.84	0.67	0.66	0.60	0.64	--
-120.0	1.25	1.13	1.03	0.79	0.62	0.38	0.38	0.34	--
-110.0	0.87	0.70	0.81	0.73	0.57	0.45	0.40	0.36	--
-100.0	0.90	0.58	0.54	0.40	0.37	0.39	0.43	0.40	--
-90.0	0.91	0.56	0.65	0.38	0.38	0.46	0.55	0.67	--
-80.0	1.23	0.81	0.73	0.37	0.40	0.49	0.44	0.42	--
-70.0	0.94	0.66	0.60	0.32	0.38	0.48	0.50	0.56	--
-60.0	0.88	0.55	0.60	0.50	0.58	0.57	0.67	0.81	--
-50.0	0.94	1.03	1.05	1.07	0.82	0.55	0.62	0.67	--
-40.0	0.99	0.95	1.08	1.00	1.08	0.76	0.72	0.74	--
-30.0	1.27	1.10	1.07	1.23	1.08	1.14	0.99	1.40	--
-20.0	2.48	2.60	2.03	1.70	1.36	1.75	1.60	1.12	--
-10.0	2.87	2.99	3.46	3.89	3.33	2.98	3.05	3.50	--
0.0	2.64	2.62	3.33	3.61	3.44	3.09	3.15	2.84	--
10.0	2.66	2.57	3.36	3.33	2.70	2.29	2.49	2.68	--
20.0	3.24	3.09	2.78	2.59	1.98	1.70	1.57	1.45	--
30.0	3.07	3.14	2.66	2.06	1.44	1.24	1.12	0.94	--
40.0	2.05	2.03	1.42	1.25	0.92	0.85	0.94	0.96	--
50.0	1.45	1.20	0.90	1.01	0.68	0.72	0.89	0.96	--
60.0	1.60	1.83	1.07	0.91	0.69	0.66	0.77	0.86	--
70.0	1.81	1.59	0.70	0.64	0.41	0.45	0.44	0.46	--
80.0	1.45	1.41	0.37	0.44	0.21	0.27	0.28	0.29	--
90.0	1.62	1.74	0.54	0.51	0.26	0.21	0.25	0.32	--
100.0	2.50	2.08	0.71	0.61	0.34	0.34	0.35	0.33	--
110.0	2.37	2.31	0.93	0.81	0.48	0.48	0.45	0.34	--
120.0	2.02	1.76	0.97	0.84	0.44	0.43	0.47	0.37	--
130.0	1.36	0.99	0.79	0.77	0.72	0.55	0.78	0.65	--
140.0	1.95	1.29	1.23	1.13	1.20	1.17	1.57	1.50	--
150.0	2.93	2.35	2.07	1.70	1.78	2.05	2.26	2.24	--
160.0	2.40	2.43	2.20	1.84	2.22	2.38	2.41	2.20	--
170.0	1.97	1.50	2.33	2.73	3.41	3.05	2.54	2.12	--
180.0	2.29	2.41	2.52	2.90	2.60	1.93	1.82	1.23	--



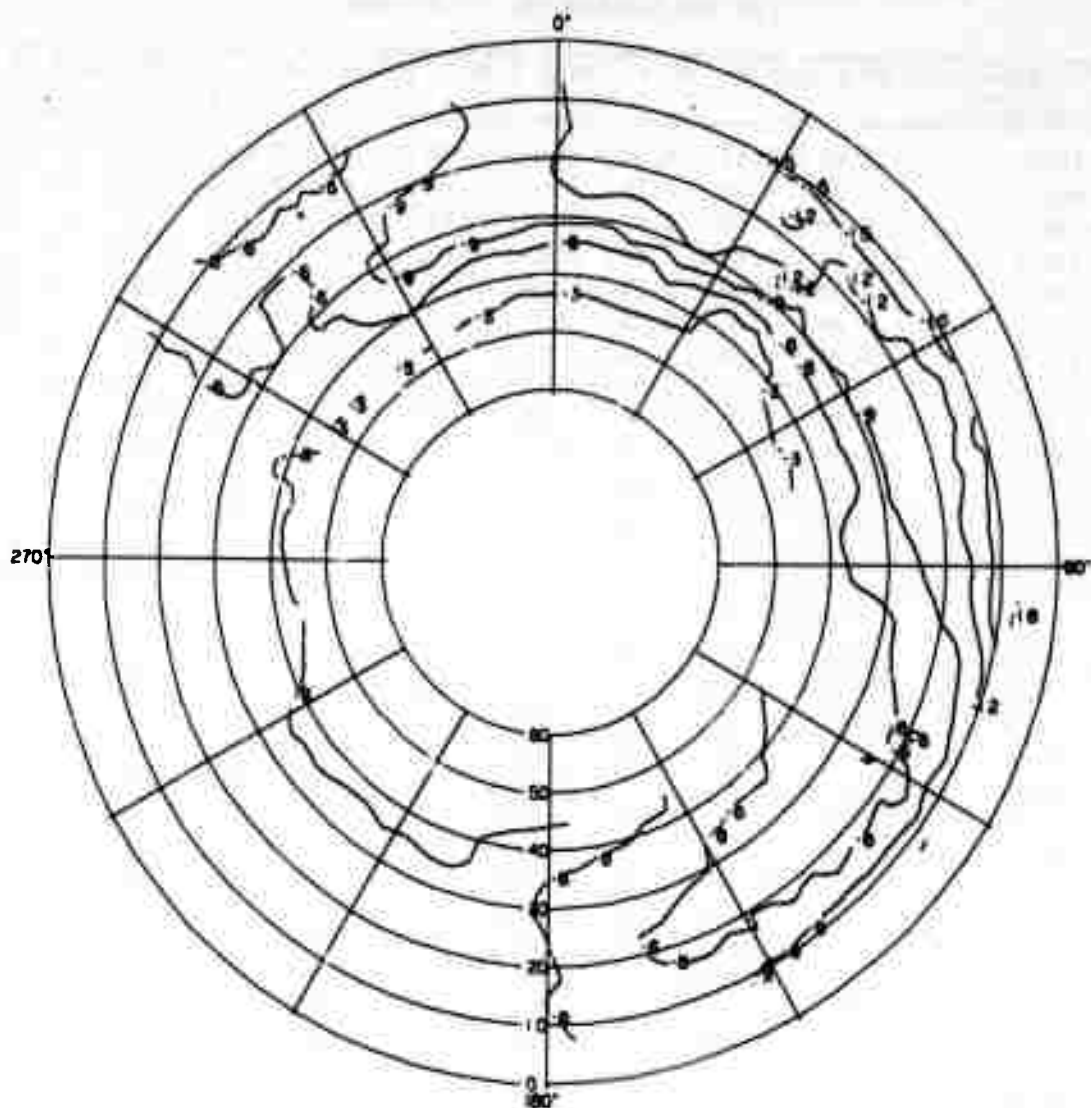
TA-8663-200

FIGURE A-4 CONTOUR PLOT OF THE MEDIAN RESPONSE OF THE HORIZONTAL UNBALANCED DIPOLE IN THE FOREST— E_{ϕ} AT 50 MHz

Table A-5

STANDARD DEVIATIONS ABOUT THE MEDIAN FOR THE VERTICAL SLEEVE DIPOLE
IN THE CLEARING--E_θ AT 50 MHz

Elevation Azimuth	10.0	15.0	20.0	25.0	30.0	35.0	40.0	45.0	50.0
-170.0	0.67	0.49	0.52	0.52	0.51	0.46	0.49	0.39	0.21
-160.0	0.64	0.46	0.46	0.43	0.32	0.30	0.28	0.32	0.12
-150.0	0.76	0.49	0.46	0.45	0.31	0.26	0.20	0.22	0.13
-140.0	0.54	0.45	0.42	0.44	0.29	0.25	0.17	0.15	0.18
-130.0	0.80	0.30	0.34	0.33	0.23	0.24	0.21	0.27	0.38
-120.0	0.98	0.33	0.29	0.30	0.25	0.29	0.32	0.35	0.32
-110.0	0.66	0.32	0.32	0.34	0.49	0.56	0.48	0.36	0.20
-100.0	0.53	0.35	0.40	0.44	0.69	0.63	0.49	0.39	0.14
-90.0	0.66	0.49	0.45	0.42	0.48	0.43	0.36	0.32	0.13
-80.0	0.66	0.54	0.44	0.36	0.24	0.26	0.38	0.38	0.19
-70.0	0.59	0.54	0.65	0.69	0.66	0.47	0.42	0.38	0.23
-60.0	0.98	0.73	0.91	1.11	1.06	0.58	0.48	0.45	0.21
-50.0	1.91	1.36	1.35	1.06	0.90	0.45	0.50	0.50	0.17
-40.0	1.54	1.58	1.83	2.30	2.20	0.84	0.82	0.70	0.27
-30.0	0.86	1.80	2.34	2.87	3.11	1.29	1.01	0.85	0.48
-20.0	1.69	2.28	2.37	2.17	2.02	0.95	0.86	0.66	0.38
-10.0	1.52	2.18	2.03	2.04	1.56	0.67	0.58	0.44	0.23
0.0	1.45	1.88	2.14	2.44	1.91	0.49	0.44	0.36	0.17
10.0	2.97	2.35	2.30	2.19	1.39	0.40	0.39	0.41	0.16
20.0	3.50	2.66	2.47	2.35	1.45	0.70	0.51	0.44	0.18
30.0	3.45	2.07	2.14	2.08	1.27	0.88	0.59	0.49	0.22
40.0	3.26	2.06	2.04	2.02	0.94	0.92	0.48	0.45	0.25
50.0	3.04	2.37	2.30	2.16	1.02	0.89	0.39	0.41	0.24
60.0	3.16	3.00	2.59	2.29	0.93	0.89	0.34	0.44	0.21
70.0	2.96	2.36	2.35	2.29	1.13	1.14	0.59	0.48	0.20
80.0	2.53	1.66	1.84	1.87	1.26	1.18	0.73	0.68	0.19
90.0	2.65	1.58	1.46	1.46	1.20	1.40	1.05	0.84	0.35
100.0	2.59	1.13	1.09	1.01	0.92	1.14	0.91	0.90	0.61
110.0	1.86	0.74	0.69	0.68	0.30	0.49	0.71	0.85	0.71
120.0	1.29	0.46	0.53	0.52	0.25	0.53	0.46	0.55	0.63
130.0	1.29	0.67	0.55	0.52	0.23	0.57	0.64	0.58	0.83
140.0	1.52	0.62	0.52	0.44	0.46	0.97	1.17	1.29	1.19
150.0	1.38	0.59	0.54	0.48	1.03	1.56	1.41	1.37	0.87
160.0	0.90	0.63	0.64	0.59	1.36	1.68	1.38	1.04	0.56
170.0	1.00	0.88	0.82	0.81	1.35	1.34	1.18	1.14	0.59
180.0	1.17	0.79	0.80	0.84	1.05	0.96	0.90	0.79	0.30



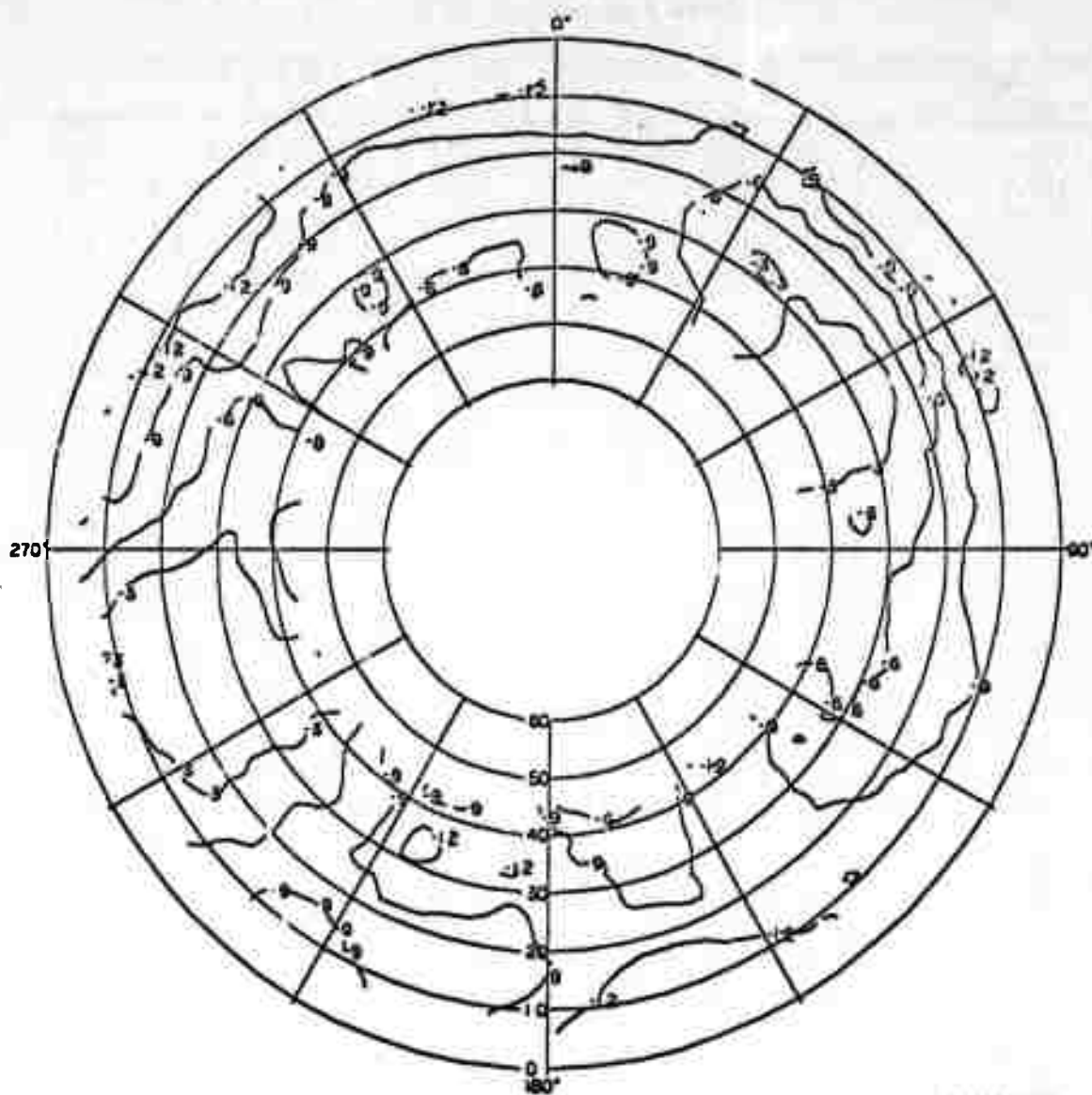
TA-8663-201

FIGURE A-5 CONTOUR PLOT OF THE MEDIAN RESPONSE OF THE VERTICAL SLEEVE DIPOLE IN THE CLEARING— E_{θ} AT 50 MHz

Table A-6

STANDARD DEVIATIONS ABOUT THE MEDIAN FOR THE VERTICAL SLEEVE DIPOLE
IN THE CLEARING-- E_{ϕ} AT 50 MHz

Elevation Azimuth	10.0	15.0	20.0	25.0	30.0	35.0	40.0	45.0	50.0
-170.0	1.62	1.80	2.14	2.48	2.62	2.51	2.55	2.79	--
-160.0	1.78	1.48	1.72	1.67	1.60	1.83	2.00	2.29	--
-150.0	1.68	1.62	1.67	1.65	1.91	1.59	1.42	1.04	--
-140.0	2.18	1.84	1.80	1.80	2.07	1.80	1.56	1.47	--
-130.0	2.14	1.60	1.42	1.36	1.01	1.08	1.69	1.78	--
-120.0	1.36	1.20	1.14	1.02	0.75	1.01	0.95	1.22	--
-110.0	0.77	0.60	0.82	0.63	0.63	0.62	0.68	0.85	--
-100.0	1.82	1.22	1.23	0.79	0.79	0.90	1.03	1.30	--
-90.0	2.74	1.96	1.78	1.15	1.11	1.27	1.20	1.29	--
-80.0	1.83	1.66	1.53	1.15	1.07	1.22	1.32	1.36	--
-70.0	0.97	1.19	1.02	1.05	1.32	1.97	2.39	2.75	--
-60.0	1.26	1.43	1.54	1.85	1.84	2.21	2.09	2.01	--
-50.0	1.66	1.64	1.83	2.03	1.96	2.13	1.98	2.12	--
-40.0	1.90	1.84	1.51	1.53	1.72	1.86	1.58	1.68	--
-30.0	2.05	1.82	1.42	1.44	1.16	1.14	1.15	0.91	--
-20.0	1.85	2.04	1.59	1.39	0.87	0.66	0.60	0.75	--
-10.0	1.69	1.69	1.47	1.54	0.87	0.81	1.00	1.00	--
0.0	2.07	2.21	2.04	1.85	1.54	1.74	1.72	2.06	--
10.0	2.07	2.21	2.22	2.28	2.09	1.73	1.79	1.69	--
20.0	1.77	1.72	1.97	2.03	1.64	1.25	1.53	1.43	--
30.0	1.45	1.22	1.25	1.19	0.89	0.94	1.28	1.62	--
40.0	1.03	1.01	0.92	0.85	0.60	0.59	0.83	0.97	--
50.0	0.91	0.88	1.09	1.20	0.74	0.55	0.48	0.32	--
60.0	1.25	1.43	1.62	1.57	1.00	0.67	0.56	0.25	--
70.0	1.49	1.61	1.76	1.61	0.85	0.69	0.77	0.72	--
80.0	1.56	1.53	1.66	1.68	0.95	0.91	1.13	1.35	--
90.0	1.80	1.94	1.89	1.78	1.35	1.19	1.49	1.60	--
100.0	1.82	1.79	1.78	1.69	1.25	1.27	1.26	1.10	--
110.0	1.90	2.05	1.81	1.75	1.47	1.20	1.39	1.54	--
120.0	1.55	1.66	1.75	1.77	1.68	1.61	1.55	1.60	--
130.0	1.47	1.53	1.57	1.49	1.47	1.34	1.31	1.17	--
140.0	1.74	1.77	1.71	1.72	1.46	1.34	1.39	1.10	--
150.0	1.47	1.66	1.53	1.43	1.74	1.93	1.84	1.38	--
160.0	0.82	1.24	1.29	1.33	2.06	2.51	2.19	1.92	--
170.0	0.99	1.93	1.84	1.65	1.89	2.09	1.86	1.03	--
180.0	1.49	2.52	2.28	2.35	2.73	2.54	2.03	1.54	--



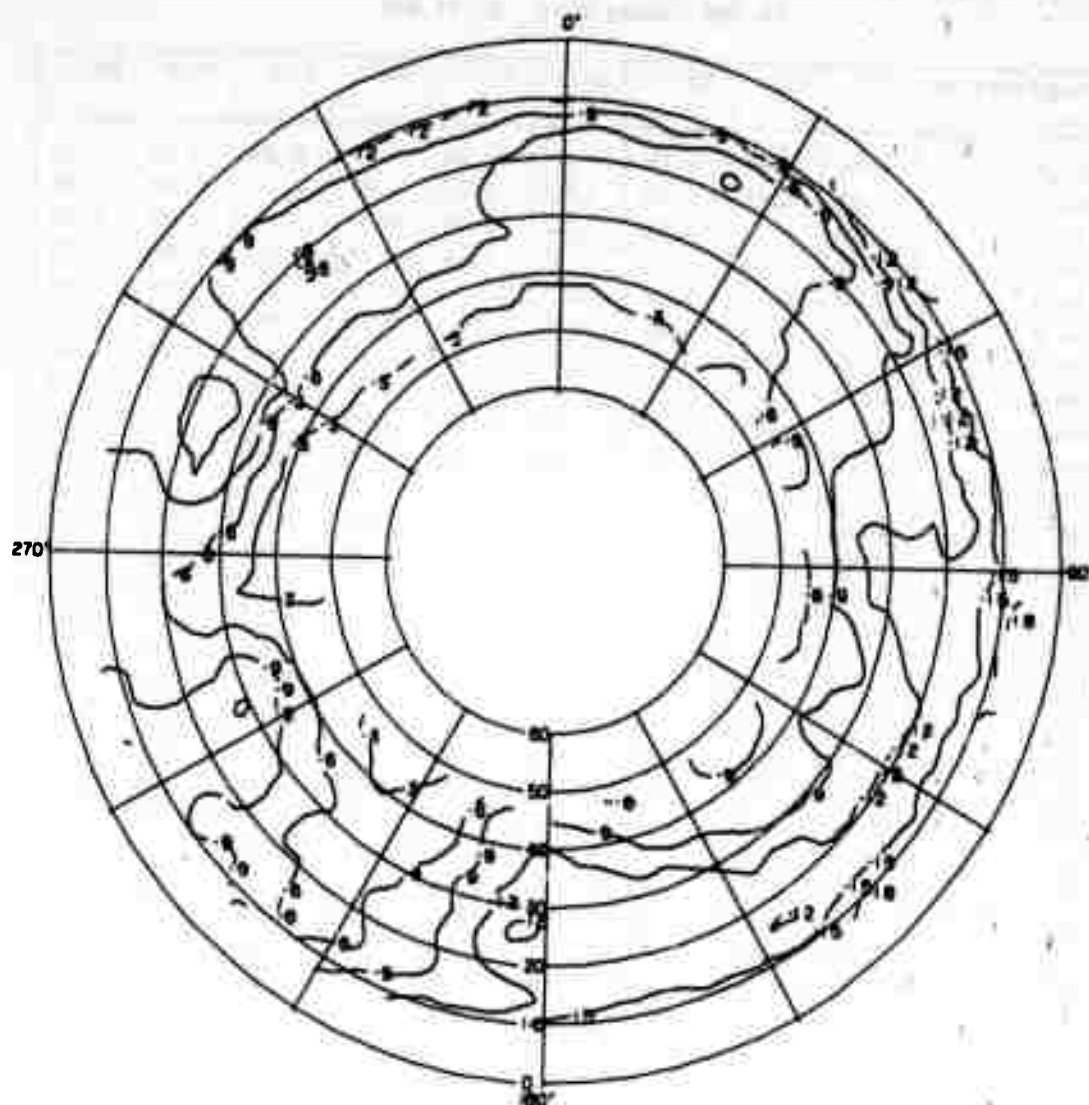
TA-8663-202

FIGURE A-6 CONTOUR PLOT OF THE MEDIAN RESPONSE OF THE VERTICAL SLEEVE DIPOLE IN THE CLEARING— E_{ϕ} AT 50 MHz

Table A-7

STANDARD DEVIATIONS ABOUT THE MEDIAN FOR THE VERTICAL SLEEVE DIPOLE
IN THE FOREST-- E_{θ} AT 50 MHz

Elevation Azimuth	10.0	15.0	20.0	25.0	30.0	35.0	40.0	45.0	50.0
-170.0	2.31	2.43	2.32	2.38	2.51	2.27	1.94	1.38	1.16
-160.0	2.77	2.06	1.95	1.97	1.65	1.23	1.32	1.07	1.03
-150.0	2.23	1.42	1.69	1.89	1.20	0.92	0.98	0.84	0.55
-140.0	2.39	1.96	1.88	1.77	1.37	1.38	1.24	0.98	0.52
-130.0	3.56	2.95	2.77	2.55	2.05	1.70	1.54	1.59	0.96
-120.0	3.84	3.40	3.20	3.34	2.60	1.70	1.77	1.71	1.01
-110.0	3.08	2.66	2.95	2.91	2.89	2.52	2.15	1.80	0.91
-100.0	3.62	2.95	2.65	2.33	2.30	2.30	1.78	1.54	1.00
-90.0	3.34	2.92	2.60	2.64	1.72	1.09	0.99	0.75	0.64
-80.0	3.04	2.52	2.79	2.87	1.87	0.80	0.69	0.64	0.66
-70.0	2.79	2.50	2.43	2.42	1.60	0.86	0.82	0.78	0.73
-60.0	2.69	2.31	2.59	2.44	1.50	0.88	0.80	0.78	0.85
-50.0	3.92	3.21	2.52	2.04	1.15	0.68	0.79	0.70	0.63
-40.0	2.87	2.83	2.54	2.05	1.21	1.13	0.83	0.67	0.49
-30.0	2.25	2.12	2.07	2.04	1.33	0.73	0.79	0.81	0.68
-20.0	2.82	2.13	1.92	1.57	0.91	0.70	0.63	0.55	0.57
-10.0	2.95	2.09	1.86	1.50	0.83	0.78	0.63	0.47	0.44
0.0	2.26	1.90	1.75	1.47	0.69	0.64	0.54	0.54	0.55
10.0	2.07	1.55	1.45	1.46	1.07	0.97	0.77	0.99	0.79
20.0	1.94	1.18	1.23	1.39	1.30	1.47	1.16	0.96	0.64
30.0	1.91	1.24	1.54	1.74	1.37	1.24	0.86	0.92	0.67
40.0	2.37	1.75	1.82	2.07	1.63	1.29	0.84	1.00	1.26
50.0	2.21	2.17	2.06	1.83	1.27	1.28	1.19	1.15	1.18
60.0	1.87	2.85	2.60	2.20	1.32	1.29	1.53	1.65	1.37
70.0	2.03	2.73	2.48	2.30	1.61	1.72	2.06	2.27	1.80
80.0	2.02	2.55	2.61	2.40	1.69	1.87	1.84	1.87	1.43
90.0	2.13	2.84	2.80	2.66	1.77	1.69	1.16	1.08	0.46
100.0	1.86	2.92	2.98	3.03	2.41	2.16	1.32	1.18	0.81
110.0	1.68	2.68	2.89	3.07	2.34	1.91	1.26	1.29	0.95
120.0	2.33	3.19	2.99	2.75	1.88	2.03	1.48	1.13	1.04
130.0	2.62	3.08	2.75	2.61	1.77	1.53	1.44	1.60	1.34
140.0	2.07	2.40	2.34	2.13	1.10	0.83	0.94	1.13	1.14
150.0	1.93	2.01	1.98	1.58	1.29	1.44	1.13	0.98	0.97
160.0	1.50	2.62	2.64	2.83	2.47	1.56	1.40	0.95	0.75
170.0	1.68	2.73	2.66	2.76	2.57	1.95	1.87	1.68	1.11
180.0	1.51	2.06	2.32	2.38	2.75	2.71	2.35	2.24	1.33



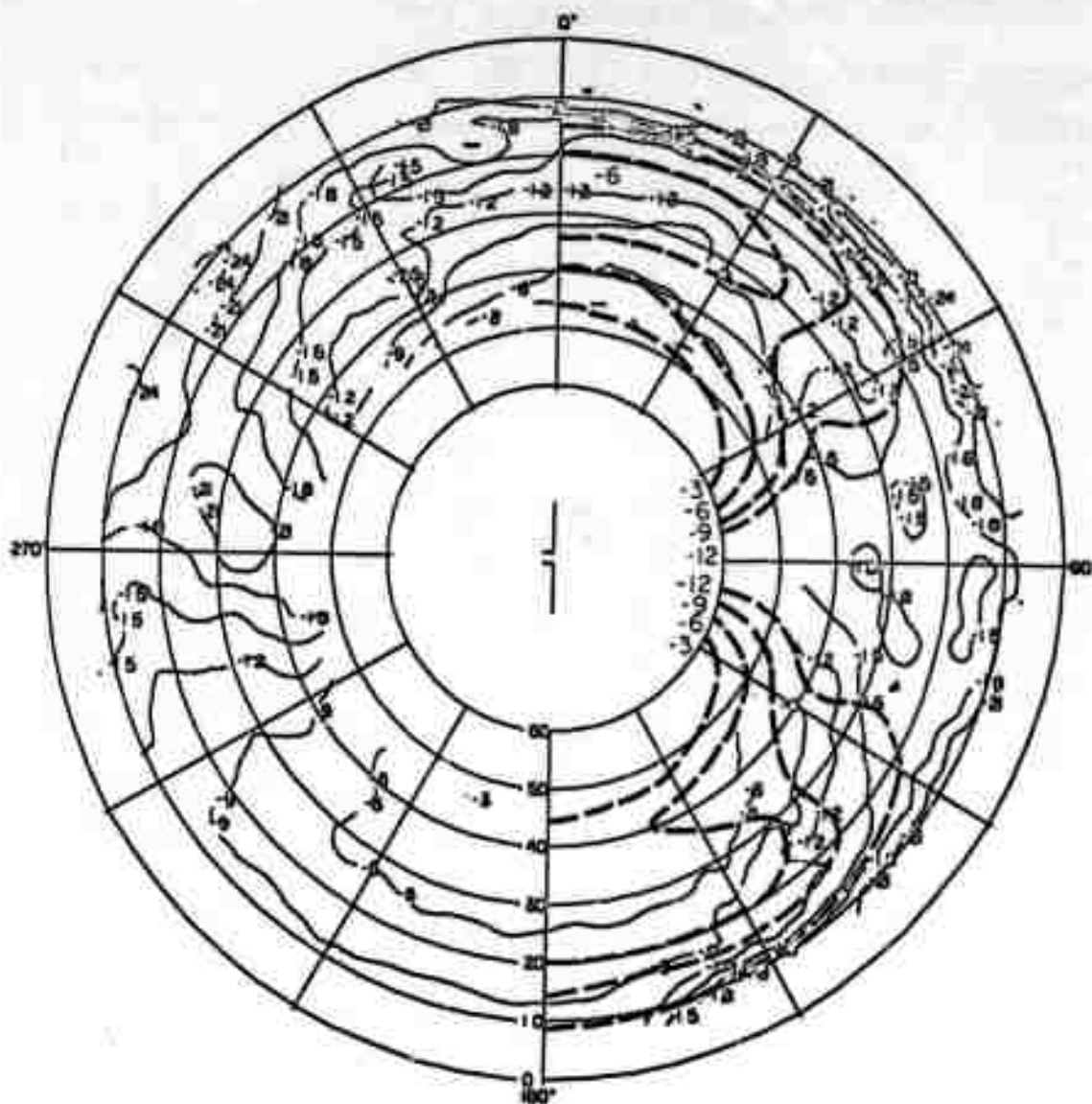
TA-8663-203

FIGURE A-7 CONTOUR PLOT OF THE MEDIAN RESPONSE OF THE VERTICAL SLEEVE DIPOLE IN THE FOREST— E_0 AT 50 MHz

Table A-8

STANDARD DEVIATIONS ABOUT THE MEDIAN FOR THE HORIZONTAL UNBALANCED DIPOLE
IN THE CLEARING--E₉ AT 75 MHz

Elevation Azimuth	10.0	15.0	20.0	25.0	30.0	35.0	40.0	45.0	50.0
-170.0	1.41	1.48	1.02	0.63	0.64	0.81	0.86	0.90	0.80
-160.0	1.80	1.68	1.20	1.05	0.82	0.88	0.93	0.99	0.81
-150.0	1.26	1.12	1.18	1.07	0.84	0.73	0.86	1.05	0.79
-140.0	1.90	1.40	1.19	1.04	0.80	0.74	0.94	0.99	0.75
-130.0	2.83	1.19	1.24	1.13	1.12	1.32	1.26	1.09	0.80
-120.0	1.52	1.22	1.59	2.01	1.54	1.44	1.62	1.49	1.58
-110.0	2.82	1.61	2.00	1.60	2.33	2.16	3.04	3.18	2.53
-100.0	2.30	3.53	3.08	2.95	4.66	5.76	3.45	2.54	2.64
-90.0	2.46	4.51	4.41	3.95	3.85	3.09	3.61	3.97	4.14
-80.0	3.15	4.70	5.09	5.44	4.76	3.60	2.76	2.26	2.51
-70.0	4.14	4.98	5.02	5.92	4.03	2.36	2.11	1.87	2.30
-60.0	5.20	4.76	4.33	3.76	2.86	1.84	1.60	1.39	1.32
-50.0	4.50	3.10	3.53	3.84	3.01	1.93	1.60	1.14	0.91
-40.0	5.75	4.16	3.18	2.72	2.36	2.24	1.52	1.38	0.92
-30.0	4.75	3.48	2.55	1.90	1.53	1.47	1.28	1.07	0.78
-20.0	4.01	1.63	1.79	2.03	1.55	1.30	1.06	0.97	0.66
-10.0	4.44	0.56	1.47	1.33	1.27	1.06	1.05	0.86	0.52
0.0	4.32	2.66	2.12	2.23	1.46	1.23	1.08	0.92	0.56
10.0	5.84	3.78	3.22	2.29	1.38	1.24	1.17	1.16	0.61
20.0	4.43	3.32	2.65	2.19	1.65	1.23	1.48	1.40	0.75
30.0	6.33	3.99	3.18	2.27	2.26	2.07	1.72	1.53	0.85
40.0	6.20	2.93	3.70	3.34	3.54	2.60	2.20	1.07	0.82
50.0	4.43	3.93	4.22	5.50	4.68	5.30	2.95	1.62	1.37
60.0	3.99	3.87	4.28	3.89	3.18	2.38	2.52	3.12	2.16
70.0	3.95	3.60	4.28	5.03	3.39	1.98	2.49	2.96	2.64
80.0	3.55	4.60	3.97	4.20	2.61	1.66	2.22	2.37	2.23
90.0	2.97	1.76	4.33	6.03	4.44	1.95	1.96	2.29	2.17
100.0	6.90	7.06	5.24	3.97	3.11	2.55	1.96	1.74	1.86
110.0	4.64	7.40	5.37	5.01	4.34	4.52	2.66	1.60	1.30
120.0	4.97	4.72	4.67	4.36	3.80	2.93	2.40	1.95	1.30
130.0	4.99	2.96	3.40	2.71	1.80	1.10	1.52	1.11	0.95
140.0	2.94	2.45	2.10	2.17	1.51	1.30	1.13	0.99	0.79
150.0	2.77	1.29	1.49	1.40	1.03	0.72	0.85	0.86	0.73
160.0	3.44	2.07	1.44	1.19	0.89	0.96	0.91	0.93	0.79
170.0	--	1.21	1.10	0.93	0.75	0.85	0.91	1.00	0.88
180.0	--	1.04	0.99	0.73	0.69	0.85	0.88	0.84	0.76



TA-8663-204

FIGURE A-8 CONTOUR PLOT OF THE MEDIAN RESPONSE OF THE HORIZONTAL UNBALANCED DIPOLE IN THE CLEARING— E_{θ} AT 75 MHz

Table A-9

STANDARD DEVIATIONS ABOUT THE MEDIAN FOR THE HORIZONTAL UNBALANCED DIPOLE
IN THE CLEARING--E₀ AT 75 MHz

Elevation Azimuth	10.0	15.0	20.0	25.0	30.0	35.0	40.0	45.0	50.0
-170.0	3.35	2.12	2.74	3.81	4.59	4.35	3.02	--	--
-160.0	2.26	1.16	1.97	1.86	2.42	2.01	2.36	1.67	--
-150.0	2.06	1.61	1.49	1.28	1.60	1.90	1.64	0.91	--
-140.0	1.34	0.90	0.89	0.93	1.14	1.07	1.24	1.56	--
-130.0	0.68	0.41	0.59	0.45	0.55	0.57	1.02	1.26	--
-120.0	0.59	0.29	0.45	0.73	0.50	0.55	0.87	1.06	--
-110.0	0.41	0.18	0.30	0.38	0.40	0.32	0.69	0.86	--
-100.0	0.55	0.16	0.26	0.31	0.46	0.64	0.78	0.50	--
-90.0	0.53	0.28	0.34	0.30	0.35	0.48	0.77	1.27	--
-80.0	0.58	0.66	0.52	0.49	0.47	0.47	0.55	0.64	--
-70.0	0.51	0.47	0.57	0.40	0.64	0.52	0.75	0.93	--
-60.0	0.63	0.66	1.00	1.42	1.18	0.78	0.87	0.87	--
-50.0	0.61	0.55	0.81	1.29	1.31	1.32	1.07	0.56	--
-40.0	0.60	0.68	0.81	0.91	1.07	1.00	1.28	1.44	--
-30.0	1.35	1.28	1.25	1.33	1.56	2.36	1.69	1.25	--
-20.0	3.20	2.04	2.03	1.88	1.80	1.91	2.23	1.59	--
-10.0	4.40	3.91	2.94	2.25	3.12	3.80	3.77	2.57	--
0.0	4.65	4.70	3.82	3.55	4.02	4.20	5.15	6.02	--
10.0	4.79	4.21	3.84	4.69	4.68	5.04	4.44	4.58	--
20.0	2.32	2.55	2.63	2.48	2.98	3.99	3.00	2.35	--
30.0	1.88	3.08	1.91	1.16	1.64	2.24	1.90	1.33	--
40.0	1.45	0.69	0.79	1.20	1.56	1.62	1.42	1.15	--
50.0	0.89	0.39	0.63	0.85	1.16	1.57	1.41	1.43	--
60.0	1.94	0.84	0.59	0.60	0.72	0.76	0.94	1.21	--
70.0	4.14	1.06	0.55	0.34	0.41	0.56	0.84	1.14	--
80.0	2.50	1.07	0.73	0.62	0.51	0.55	0.70	1.03	--
90.0	1.29	1.08	1.01	1.35	0.77	0.41	0.59	0.47	--
100.0	1.49	1.15	0.91	0.92	0.68	0.39	0.70	0.91	--
110.0	2.16	1.50	0.92	0.50	0.50	0.60	0.52	0.49	--
120.0	3.79	2.14	1.21	0.83	0.53	0.43	0.51	0.74	--
130.0	2.94	1.02	1.09	0.95	0.75	0.66	0.57	0.32	--
140.0	2.07	0.58	1.02	0.81	0.86	0.76	0.74	0.85	--
150.0	2.12	1.74	1.25	1.56	1.33	1.56	1.25	1.13	--
160.0	1.78	0.61	1.00	0.66	0.78	1.13	1.37	1.68	--
170.0	3.80	2.39	2.24	2.47	1.66	1.83	2.36	3.43	--
180.0	5.23	3.62	2.76	2.91	3.44	3.66	2.65	1.92	--

Table A-10

STANDARD DEVIATIONS ABOUT THE MEDIAN FOR THE HORIZONTAL UNBALANCED DIPOLE
IN THE FOREST--E AT 75 MHz

Elevation Azimuth	10.0	15.0	20.0	25.0	30.0	35.0	40.0	45.0	50.0
-170.0	3.29	3.15	2.86	2.80	2.22	1.77	1.45	1.18	0.60
-160.0	3.28	2.60	2.90	2.45	1.52	1.29	1.47	1.34	0.77
-150.0	3.07	3.34	3.42	3.72	3.01	1.63	1.70	1.94	1.20
-140.0	3.38	4.26	4.10	4.46	3.61	1.89	1.89	1.74	1.01
-130.0	2.31	2.57	2.85	2.70	2.58	2.33	1.84	1.46	0.89
-120.0	2.52	2.95	2.85	2.87	2.71	2.56	2.31	1.73	0.77
-110.0	3.01	3.51	3.03	2.79	2.34	2.39	2.20	2.11	1.67
-100.0	3.71	2.87	3.05	3.04	2.47	2.13	2.10	2.21	1.03
-90.0	3.85	2.90	3.19	3.22	2.37	1.77	2.04	2.14	1.96
-80.0	3.75	3.73	3.30	3.26	2.71	2.05	2.16	2.15	2.51
-70.0	3.64	2.98	3.01	3.08	3.40	3.03	2.55	2.37	2.00
-60.0	3.28	2.48	2.89	3.03	3.06	2.41	2.44	2.24	1.68
-50.0	3.43	3.04	2.92	3.00	2.77	2.16	1.89	1.56	1.19
-40.0	3.22	3.23	3.22	3.31	2.92	1.96	1.66	1.41	0.61
-30.0	3.13	2.81	2.91	2.72	2.27	1.73	1.94	2.04	1.18
-20.0	3.25	3.33	3.18	3.20	3.24	2.79	2.42	2.11	0.92
-10.0	2.70	2.97	3.06	3.12	3.63	2.91	2.70	1.96	0.63
0.0	2.49	3.14	3.04	2.95	2.47	2.87	2.35	1.45	0.75
10.0	2.77	2.81	2.82	2.87	2.81	2.04	1.61	1.45	0.58
20.0	2.53	2.55	2.76	2.81	2.45	1.97	1.27	1.24	0.64
30.0	2.31	2.82	2.92	3.05	2.60	2.77	1.69	1.25	0.77
40.0	2.61	3.34	3.47	3.58	2.93	2.63	1.50	1.36	0.91
50.0	2.41	3.65	3.57	3.81	2.75	2.53	1.66	1.73	1.12
60.0	2.42	3.21	3.44	3.56	2.21	2.33	1.76	1.64	1.34
70.0	2.31	3.28	3.16	3.00	2.73	2.49	2.21	2.30	1.56
80.0	2.22	3.13	2.86	2.53	2.78	2.92	2.77	2.46	1.89
90.0	2.31	3.80	2.83	2.76	2.74	2.87	2.60	2.58	2.15
100.0	2.22	3.31	3.41	3.40	3.07	2.67	2.36	2.62	2.54
110.0	2.20	3.45	3.34	3.23	2.89	3.07	2.34	2.31	1.69
120.0	2.26	3.18	3.14	3.20	2.87	2.82	2.19	1.79	1.00
130.0	2.54	3.03	2.90	2.49	1.41	1.55	1.41	1.77	1.08
140.0	2.99	3.56	3.19	3.03	1.89	1.22	1.17	1.21	0.86
150.0	2.72	3.31	3.38	3.25	2.50	1.34	1.18	0.97	0.74
160.0	2.50	3.48	3.45	3.34	2.56	1.62	1.27	1.00	0.69
170.0	2.36	3.34	3.51	3.68	2.53	1.02	1.12	0.95	0.65
180.0	2.85	3.39	3.28	3.31	2.55	1.59	1.42	1.33	0.79

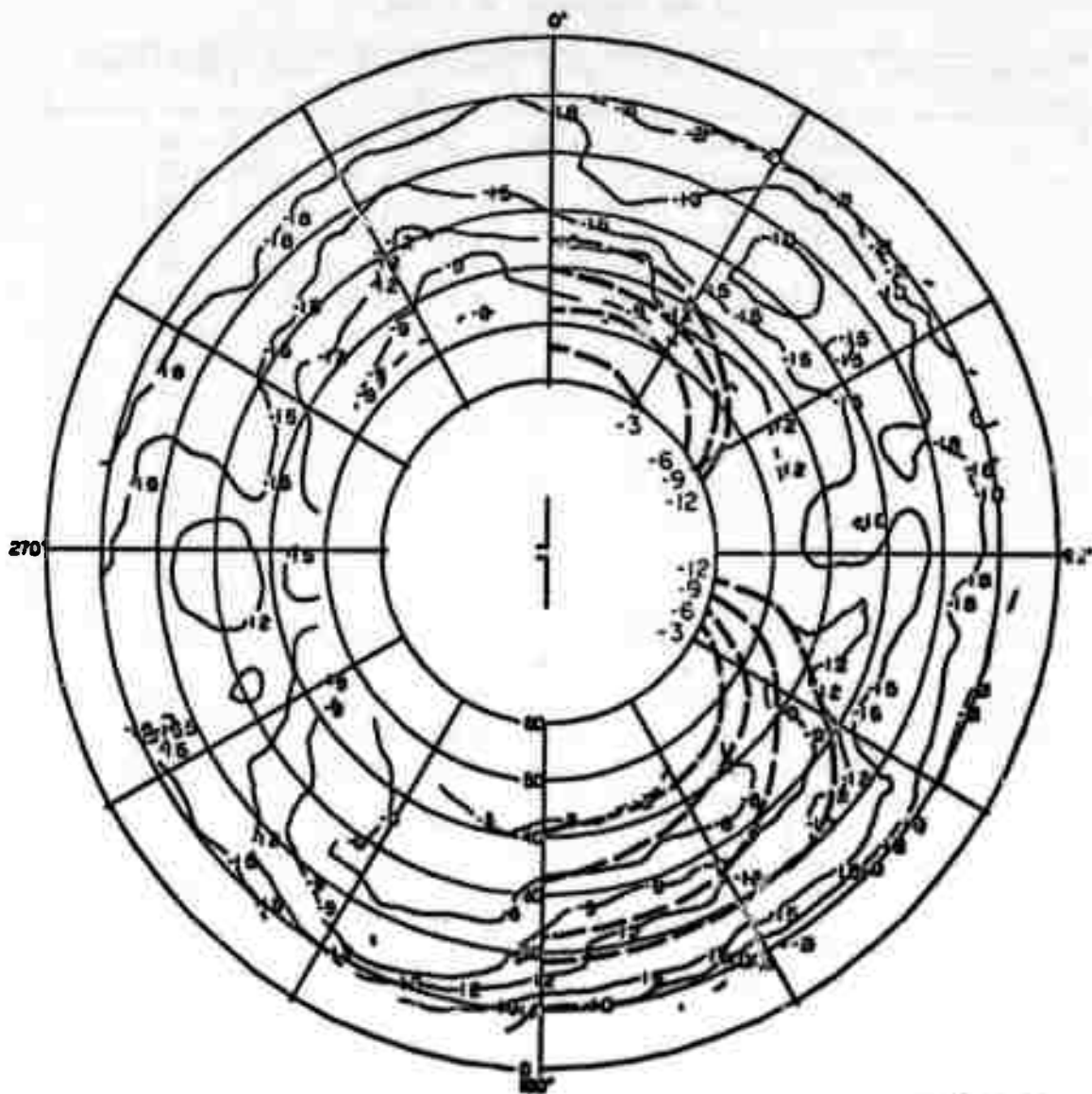
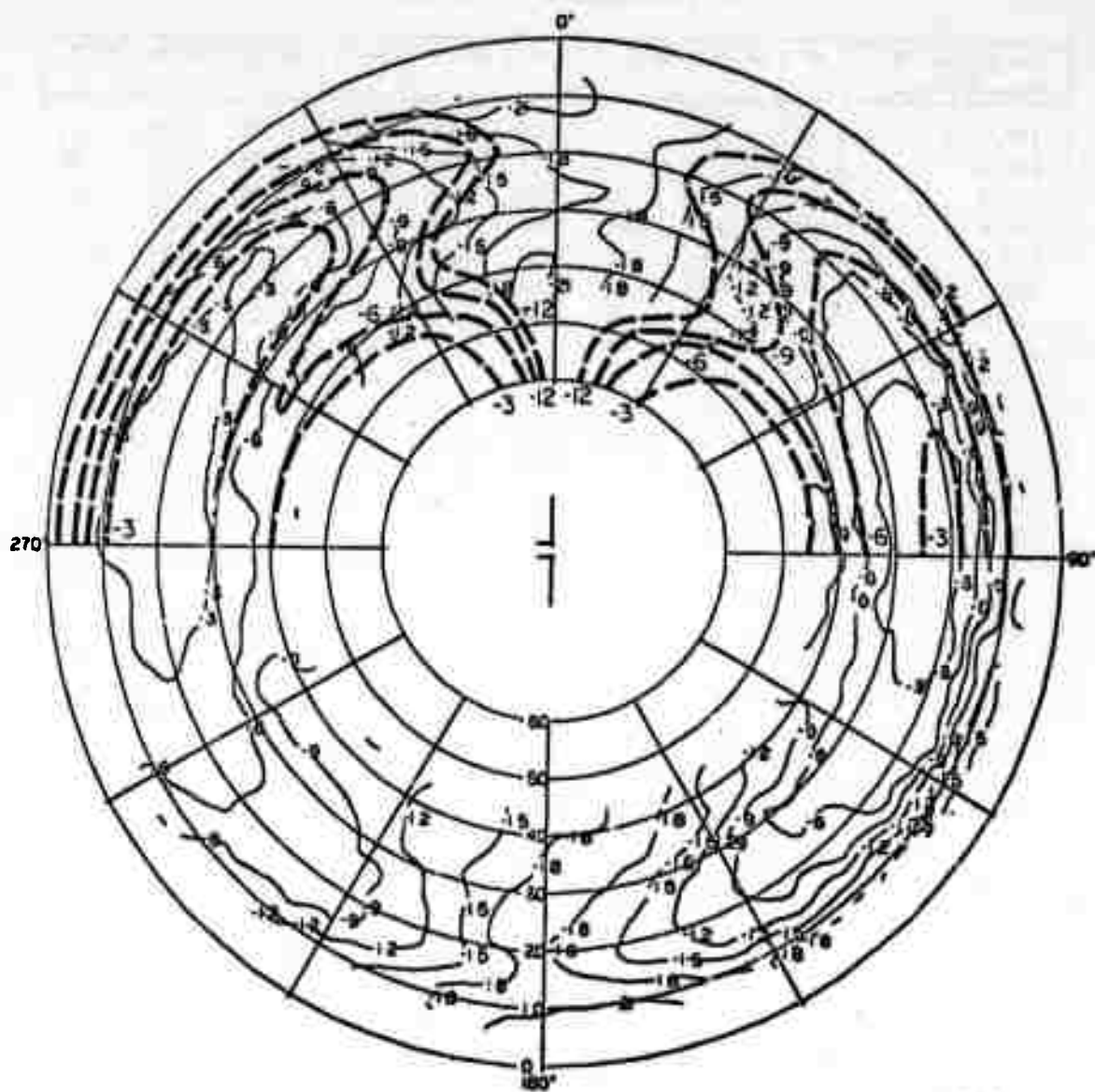


Table A-11

STANDARD DEVIATIONS ABOUT THE MEDIAN FOR THE HORIZONTAL UNBALANCED DIPOLE
IN THE FOREST-- E_0 AT 75 MHz

Elevation Azimuth	10.0	15.0	20.0	25.0	30.0	35.0	40.0	45.0	50.0
-170.0	2.08	1.88	2.36	2.86	3.22	2.63	2.39	2.07	--
-160.0	2.44	1.83	1.59	1.67	1.73	1.73	1.83	1.50	--
-150.0	2.34	1.51	1.60	1.31	1.03	1.13	1.12	1.30	--
-140.0	2.40	1.72	1.63	1.44	1.24	0.90	0.94	0.93	--
-130.0	1.99	1.72	1.56	1.34	1.17	0.94	0.97	0.90	--
-120.0	1.46	0.91	0.84	0.60	0.97	1.06	0.93	0.68	--
-110.0	1.30	0.99	0.91	1.03	1.40	1.43	1.18	0.72	--
-100.0	0.75	0.77	0.86	1.08	1.12	1.08	1.01	0.68	--
-90.0	0.83	0.71	0.83	0.91	0.67	0.61	0.71	0.66	--
-80.0	1.10	0.90	0.79	0.74	0.90	1.12	1.06	0.87	--
-70.0	1.04	0.82	0.83	0.91	1.12	1.30	1.13	0.77	--
-60.0	1.20	1.15	1.23	1.30	1.21	1.22	1.05	0.67	--
-50.0	1.41	1.47	1.54	1.14	1.18	1.20	1.26	0.99	--
-40.0	2.05	1.81	1.47	1.12	1.13	1.51	1.31	1.11	--
-30.0	2.64	1.78	1.50	1.83	2.09	2.12	1.71	1.42	--
-20.0	3.08	3.40	3.68	3.87	2.84	1.96	2.04	2.29	--
-10.0	3.73	3.11	3.66	3.54	2.64	2.04	2.30	2.43	--
0.0	2.87	3.09	3.79	3.82	3.02	2.41	2.47	2.61	--
10.0	3.30	3.44	4.27	4.54	3.75	2.79	2.75	2.96	--
20.0	3.57	3.49	3.55	2.98	2.59	2.30	2.45	2.40	--
30.0	2.64	2.53	2.57	2.34	2.16	2.19	1.98	1.80	--
40.0	1.94	1.88	1.58	1.70	1.98	1.85	1.63	1.52	--
50.0	1.99	1.74	1.37	1.31	1.46	1.47	1.23	1.13	--
60.0	2.55	2.15	1.18	1.22	1.20	1.15	0.99	1.07	--
70.0	2.16	2.24	1.16	1.12	0.87	0.80	1.24	1.04	--
80.0	1.86	2.15	1.03	1.00	0.79	0.68	1.83	2.32	--
90.0	2.17	1.88	0.76	0.81	0.75	0.77	2.31	3.29	--
100.0	1.85	1.74	0.66	0.54	0.66	0.78	1.83	2.71	--
110.0	1.56	1.49	0.78	0.73	0.74	0.82	1.13	1.46	--
120.0	1.75	1.26	1.03	1.06	0.83	0.79	1.09	1.23	--
130.0	2.21	1.65	1.35	1.25	1.02	1.13	1.56	1.52	--
140.0	2.15	1.93	1.64	1.00	1.36	1.48	2.04	2.18	--
150.0	1.77	1.62	1.76	1.61	1.92	2.00	2.65	2.80	--
160.0	2.67	2.93	2.78	2.74	2.68	3.03	2.67	2.28	--
170.0	2.60	3.73	3.10	2.50	2.51	3.03	3.14	3.09	--
180.0	1.87	3.16	3.22	3.09	3.29	3.09	2.61	2.00	--



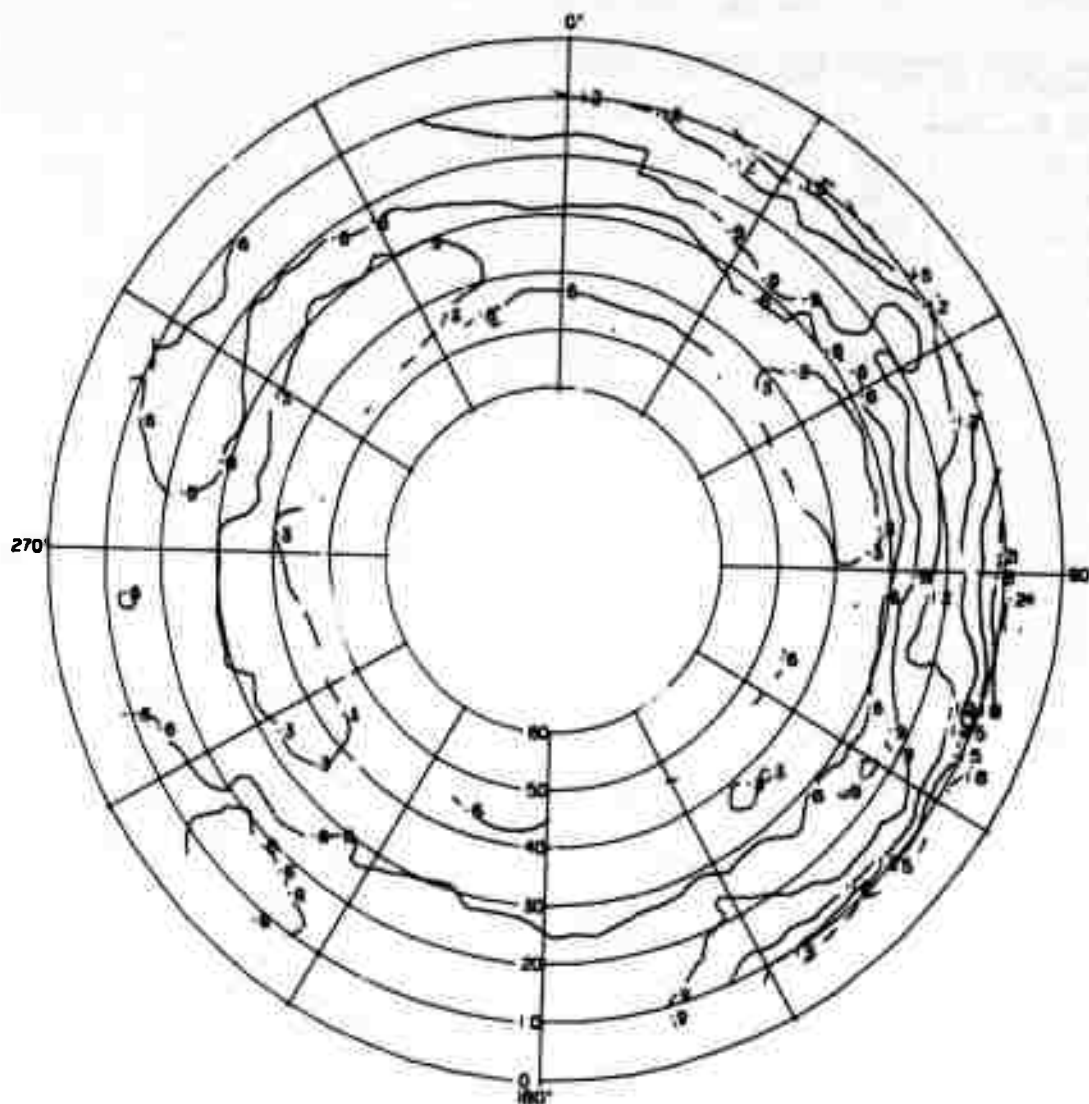
TA-8663-207

FIGURE A-11 CONTOUR PLOT OF THE MEDIAN RESPONSE OF THE HORIZONTAL UNBALANCED DIPOLE IN THE FOREST— E_{ϕ} AT 75 MHz

Table A-12

STANDARD DEVIATIONS ABOUT THE MEDIAN FOR THE VERTICAL SLEEVE DIPOLE
IN THE CLEARING--E AT 75 MHz

Elevation Azimuth	10.0	15.0	20.0	25.0	30.0	35.0	40.0	45.0	50.0
-170.0	1.54	1.30	1.31	1.21	0.86	0.96	0.98	0.89	1.31
-160.0	1.80	1.56	1.47	1.37	1.00	0.99	0.98	0.92	1.16
-150.0	2.08	1.84	1.66	1.59	1.15	1.00	0.94	0.93	1.13
-140.0	1.91	1.49	1.43	1.38	0.91	0.83	0.83	0.91	0.91
-130.0	2.12	1.19	1.11	1.08	0.66	0.71	0.75	0.74	0.79
-120.0	1.96	1.07	1.05	0.99	0.73	0.67	0.70	0.60	0.77
-110.0	1.54	1.08	1.19	1.35	1.14	0.76	0.75	0.75	0.68
-100.0	1.51	1.24	1.30	1.44	1.21	0.83	0.90	0.90	0.70
-90.0	1.70	1.38	1.46	1.33	1.24	1.08	0.94	0.84	0.56
-80.0	2.33	1.78	1.73	1.71	1.53	1.03	0.92	0.79	0.49
-70.0	2.48	2.05	1.79	1.69	1.25	0.91	0.88	0.83	0.70
-60.0	2.02	1.51	1.53	1.35	1.02	0.79	0.77	0.70	0.69
-50.0	1.59	1.44	1.33	1.19	0.89	0.75	0.69	0.66	0.94
-40.0	2.68	1.33	1.17	1.14	0.81	0.62	0.61	0.63	0.93
-30.0	2.86	1.42	1.36	1.31	0.80	0.56	0.65	0.67	1.47
-20.0	3.07	0.90	0.99	0.97	0.96	0.92	0.93	1.02	1.75
-10.0	3.04	1.15	1.08	1.14	1.10	0.98	1.00	1.06	1.59
0.0	2.57	1.32	1.29	1.38	0.94	0.84	0.88	0.93	1.13
10.0	2.82	1.34	1.42	1.37	0.78	0.82	0.79	0.91	1.13
20.0	2.72	2.23	1.87	1.49	0.96	1.19	0.85	0.80	1.01
30.0	3.37	2.42	2.11	1.94	1.54	1.38	1.00	1.10	0.83
40.0	3.33	1.75	2.01	2.20	1.76	1.72	1.09	1.07	0.93
50.0	2.20	1.44	1.75	2.02	1.45	1.40	0.83	0.67	0.58
60.0	3.34	1.82	1.71	1.66	0.99	0.92	0.53	0.57	0.48
70.0	5.42	2.16	1.75	1.57	0.67	0.88	0.61	0.64	0.60
80.0	4.13	2.35	2.37	1.96	0.95	0.88	0.68	0.60	0.63
90.0	2.99	2.92	3.02	3.22	2.14	0.87	0.67	0.71	0.78
100.0	3.37	3.07	3.29	3.76	2.94	0.84	0.81	0.88	0.82
110.0	2.79	2.16	2.42	2.30	1.60	0.74	0.70	0.84	0.53
120.0	2.16	1.64	1.80	1.90	1.07	0.60	0.63	0.67	0.65
130.0	2.21	1.74	1.64	1.75	1.03	0.71	0.70	0.72	0.71
140.0	2.45	2.52	2.08	1.64	0.55	0.61	0.71	0.69	0.78
150.0	3.36	2.19	1.81	1.45	0.71	0.83	0.83	0.91	0.98
160.0	2.82	1.35	1.41	1.38	0.99	0.69	0.68	0.65	1.01
170.0	1.74	1.17	1.24	1.32	0.71	0.57	0.67	0.68	1.08
180.0	1.98	1.26	1.17	1.19	0.87	0.79	0.78	0.82	1.28



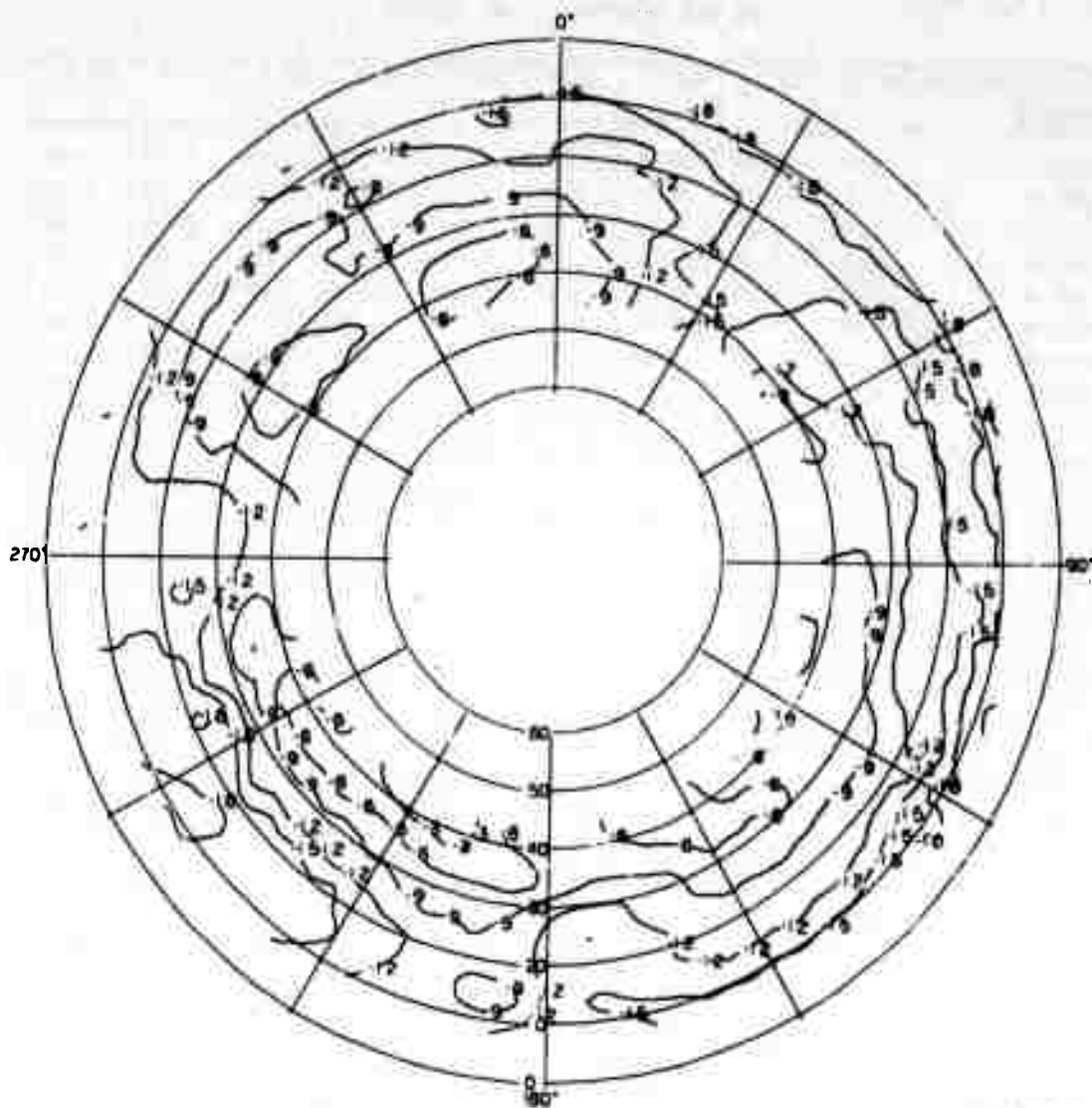
TA-8663-208

FIGURE A-12 CONTOUR PLOT OF THE MEDIAN RESPONSE OF THE VERTICAL SLEEVE DIPOLE IN THE CLEARING— E_{θ} AT 75 MHz

Table A-13

STANDARD DEVIATIONS ABOUT THE MEDIAN FOR THE VERTICAL SLEEVE DIPOLE
IN THE CLEARING--E₀ AT 75 MHz

Elevation Azimuth	10.0	15.0	20.0	25.0	30.0	35.0	40.0	45.0	50.0
-170.0	3.04	1.75	2.25	2.31	2.08	2.11	2.26	3.34	--
-160.0	2.67	2.35	2.21	2.31	1.19	0.81	0.81	1.23	--
-150.0	2.80	3.30	2.90	2.07	1.39	1.01	0.96	1.22	--
-140.0	3.82	3.77	3.39	3.02	1.97	1.18	1.28	1.51	--
-130.0	4.36	3.95	4.08	3.48	2.43	1.93	1.88	2.23	--
-120.0	4.03	3.80	3.98	3.03	2.33	2.16	2.35	2.13	--
-110.0	4.44	4.16	3.49	2.41	2.56	2.36	2.89	2.61	--
-100.0	3.31	3.30	3.91	3.86	3.66	3.46	3.79	3.91	--
-90.0	3.37	3.39	3.72	3.88	4.18	3.95	3.42	2.70	--
-80.0	4.06	3.22	2.93	2.94	3.12	2.70	2.22	1.32	--
-70.0	2.98	1.58	1.67	1.97	1.82	1.57	1.72	1.26	--
-60.0	2.12	1.34	0.99	1.18	1.13	1.12	1.26	1.17	--
-50.0	2.03	2.37	1.61	1.22	1.31	1.25	1.34	1.48	--
-40.0	2.65	2.71	1.96	1.51	1.45	1.27	1.51	1.68	--
-30.0	2.94	2.54	1.55	1.57	1.70	1.71	1.40	1.07	--
-20.0	3.18	2.83	1.54	1.71	1.57	1.40	1.17	0.97	--
-10.0	3.76	3.79	2.30	2.07	1.35	1.40	1.39	1.57	--
0.0	3.94	4.14	3.01	3.16	1.71	1.52	2.10	2.32	--
10.0	4.21	4.73	3.84	3.58	2.98	3.12	2.78	2.64	--
20.0	4.38	4.37	4.07	3.99	3.84	3.98	3.68	3.52	--
30.0	4.31	4.23	3.85	3.96	3.76	3.57	3.83	3.53	--
40.0	3.98	4.11	3.42	3.36	3.13	3.29	3.48	3.60	--
50.0	4.18	3.97	3.40	2.93	2.64	2.84	3.06	2.99	--
60.0	4.19	4.40	4.16	4.40	3.49	2.65	2.26	1.88	--
70.0	4.43	4.30	4.49	4.88	3.46	2.47	2.15	2.12	--
80.0	4.53	4.07	4.21	3.99	2.69	2.48	2.25	2.65	--
90.0	4.18	4.88	4.43	4.12	2.31	2.16	1.84	2.27	--
100.0	4.61	4.69	4.34	3.76	1.73	1.68	1.85	2.16	--
110.0	4.47	4.96	4.03	3.32	1.71	1.55	1.65	1.68	--
120.0	4.31	4.39	3.92	3.83	1.74	1.61	1.82	2.04	--
130.0	3.90	3.48	3.25	3.28	1.61	1.63	1.89	2.37	--
140.0	2.92	2.58	2.61	2.43	1.10	1.36	1.73	2.53	--
150.0	2.94	2.79	2.65	2.16	1.37	1.58	1.42	1.84	--
160.0	3.44	3.72	3.15	3.01	2.38	1.65	1.27	1.46	--
170.0	4.37	4.08	3.99	3.93	2.64	1.67	2.71	3.18	--
180.0	4.71	3.88	3.44	3.04	2.29	2.42	3.45	4.92	--



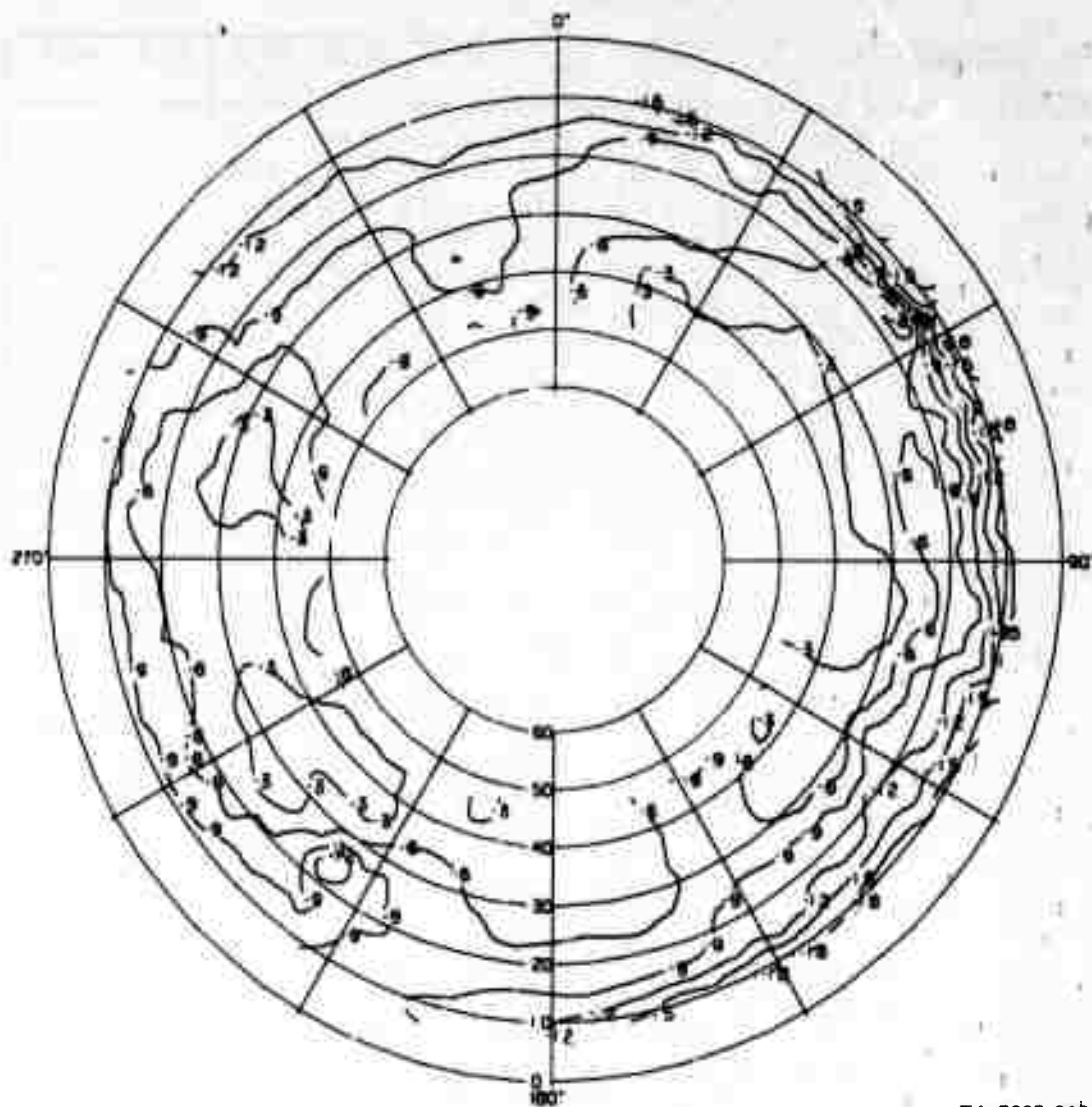
TA-8663-209

FIGURE A-13 CONTOUR PLOT OF THE MEDIAN RESPONSE OF THE VERTICAL SLEEVE DIPOLE IN THE CLEARING— E_{ϕ} AT 75 MHz

Table A-14

STANDARD DEVIATIONS ABOUT THE MEDIAN FOR THE VERTICAL SLEEVE DIPOLE
IN THE FOREST--E AT 75 MHz

Elevation Azimuth	10.0	15.0	20.0	25.0	30.0	35.0	40.0	45.0	50.0
-170.0	3.89	4.34	4.38	4.21	4.23	3.36	3.09	2.14	1.68
-160.0	3.32	4.36	4.51	4.88	4.47	3.06	2.65	1.70	1.56
-150.0	3.48	4.21	4.14	4.10	2.97	2.05	2.29	2.08	1.82
-140.0	3.88	3.93	4.10	4.19	3.27	2.29	2.10	1.74	1.83
-130.0	3.57	4.39	4.27	4.37	2.78	2.19	2.18	2.12	2.90
-120.0	4.52	4.76	4.55	4.07	2.38	2.19	2.45	2.67	3.00
-110.0	5.22	4.96	4.65	4.72	3.51	2.84	2.92	2.90	3.43
-100.0	4.27	4.28	4.51	4.69	3.87	3.53	3.26	3.25	4.01
-90.0	3.76	4.35	4.42	4.16	2.95	2.54	2.57	2.42	2.80
-80.0	3.91	4.96	4.29	3.69	2.17	1.98	2.12	2.27	3.04
-70.0	3.54	3.62	3.32	2.80	1.66	2.05	2.26	2.77	3.63
-60.0	3.31	2.67	3.04	3.47	2.41	2.04	2.39	2.68	3.02
-50.0	3.39	3.53	3.64	3.98	3.18	2.45	2.71	2.97	3.11
-40.0	3.36	4.02	3.92	3.94	3.44	2.90	2.87	3.07	3.18
-30.0	3.58	3.75	3.75	3.63	3.05	2.53	2.57	2.29	2.38
-20.0	3.66	3.89	3.80	3.87	3.54	3.00	2.53	2.44	2.17
-10.0	3.86	3.85	3.68	3.91	4.19	3.75	3.37	3.57	2.97
0.0	4.23	3.25	3.68	3.98	4.26	4.24	3.85	4.09	3.99
10.0	2.68	3.50	3.89	4.19	4.04	3.31	2.79	2.81	2.75
20.0	3.70	3.88	3.63	3.53	2.99	2.36	1.27	1.36	1.57
30.0	4.12	3.23	3.16	2.96	2.36	2.84	2.31	2.43	2.38
40.0	3.39	2.45	2.85	3.06	2.86	2.79	3.15	3.77	3.71
50.0	3.73	2.97	2.81	3.01	3.06	2.88	3.75	3.89	4.03
60.0	3.23	3.18	3.05	2.72	2.70	3.23	4.23	4.52	4.59
70.0	2.28	2.95	3.14	3.09	3.35	3.22	3.84	4.21	4.65
80.0	2.10	2.99	3.20	3.91	3.74	3.26	3.24	3.50	4.09
90.0	3.05	3.03	3.03	3.33	3.00	2.89	2.61	2.81	3.47
100.0	3.10	3.15	2.98	2.56	2.09	2.21	2.16	2.34	3.13
110.0	3.15	4.38	3.95	3.52	3.16	2.78	2.84	2.56	2.98
120.0	2.83	4.00	4.11	4.01	4.05	4.01	3.85	3.04	3.25
130.0	2.26	3.82	3.97	4.18	3.85	3.90	3.94	4.20	3.29
140.0	2.61	4.08	3.93	3.85	3.22	2.93	3.08	3.21	1.67
150.0	3.31	4.08	4.10	3.95	3.59	3.37	3.30	3.45	3.08
160.0	3.22	4.39	4.45	4.47	4.18	3.51	3.62	3.63	3.59
170.0	3.57	4.69	4.68	4.70	4.70	4.05	3.75	3.66	3.48
180.0	4.09	4.84	4.84	4.96	4.54	3.98	3.68	3.52	3.15



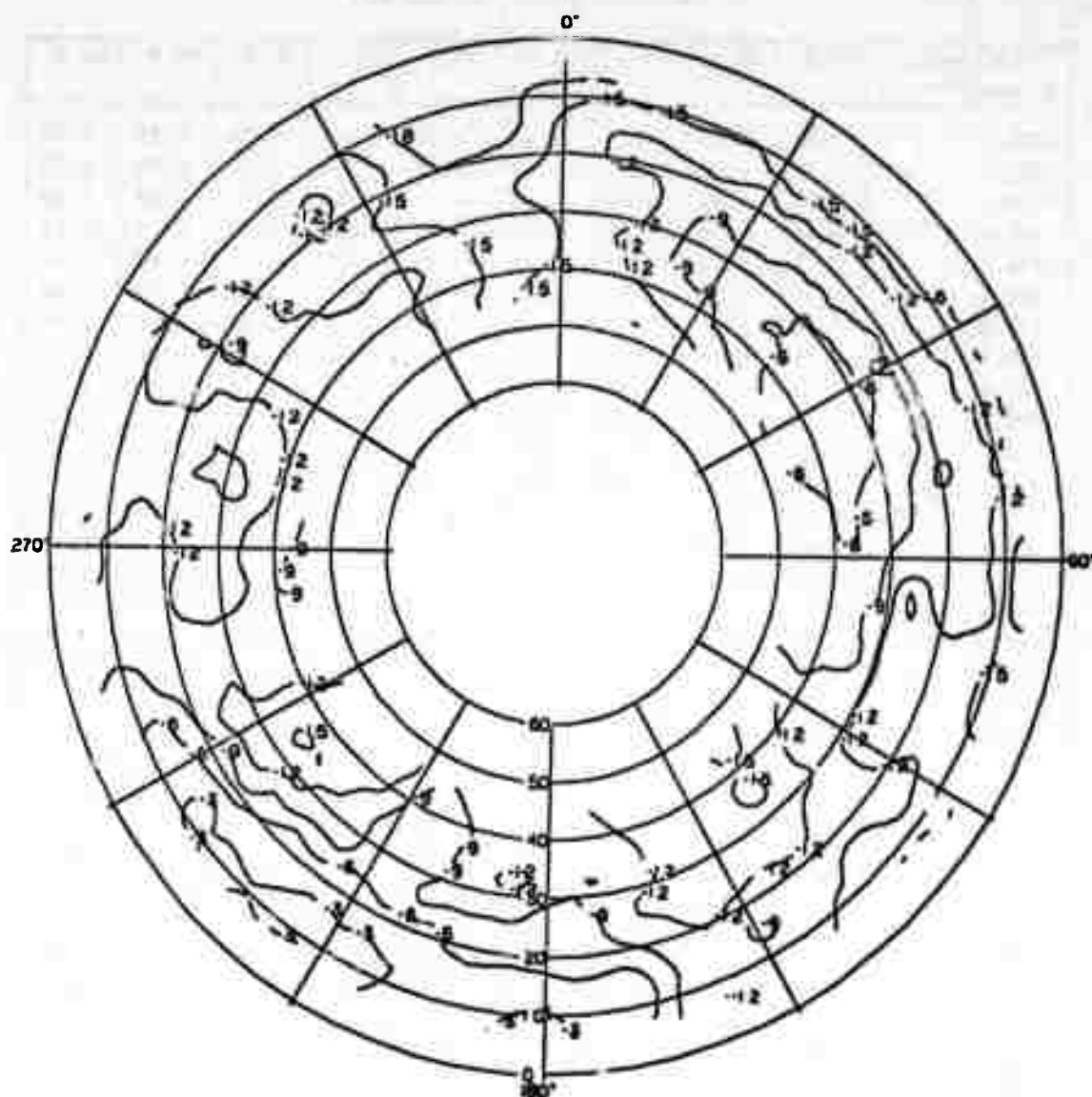
TA-8663-210

FIGURE A-14 CONTOUR PLOT OF THE MEDIAN RESPONSE OF THE VERTICAL SLEEVE DIPOLE IN THE FOREST— E_0 AT 75 MHz

Table A-15

STANDARD DEVIATIONS ABOUT THE MEDIAN FOR THE VERTICAL SLEEVE DIPOLE
IN THE FOREST--E₀ AT 75 MHz

Elevation Azimuth	10.0	15.0	20.0	25.0	30.0	35.0	40.0	45.0	50.0
-170.0	3.90	4.34	3.45	2.91	2.40	2.03	1.68	--	--
-160.0	3.36	2.97	2.91	2.84	2.49	2.18	1.89	--	--
-150.0	1.60	1.13	1.74	2.15	1.91	1.90	2.10	--	--
-140.0	1.78	1.61	1.70	1.68	2.27	2.63	2.22	--	--
-130.0	2.69	2.66	2.57	2.16	2.13	2.21	2.33	--	--
-120.0	3.67	3.33	3.27	2.85	2.93	2.63	2.51	2.18	--
-110.0	4.28	3.90	3.93	3.14	3.03	2.84	2.93	2.57	--
-100.0	4.06	4.27	3.91	2.92	2.87	2.58	2.50	2.27	--
-90.0	3.12	3.55	3.68	2.65	2.59	2.37	1.99	1.63	--
-80.0	3.91	3.87	3.23	1.90	2.08	1.82	1.84	1.83	--
-70.0	3.66	3.53	4.06	2.94	2.61	2.18	1.82	1.50	--
-60.0	4.38	5.66	4.42	2.42	2.56	1.89	1.83	1.68	--
-50.0	4.31	4.03	4.11	2.70	2.39	1.96	1.99	2.15	--
-40.0	2.60	2.17	2.80	2.70	2.63	2.22	2.08	1.87	--
-30.0	1.65	2.28	2.28	2.40	2.16	2.10	2.14	2.01	--
-20.0	2.43	3.72	3.10	2.51	2.12	2.53	2.33	2.19	--
-10.0	3.26	3.52	3.31	3.06	2.40	2.53	2.44	2.48	--
0.0	3.39	3.59	2.98	2.31	1.98	2.18	2.36	2.25	--
10.0	1.79	1.88	2.33	2.50	2.57	2.77	2.56	2.18	--
20.0	2.24	2.39	2.42	2.41	2.40	2.57	2.10	1.57	--
30.0	2.74	3.24	3.17	2.63	1.54	1.60	1.76	1.76	--
40.0	2.88	3.27	3.04	3.09	1.72	1.64	1.53	1.57	--
50.0	2.99	3.42	3.14	3.27	1.65	1.53	1.42	1.41	--
60.0	3.26	3.83	3.31	2.90	1.22	1.13	1.27	1.31	--
70.0	3.30	3.34	2.79	2.56	1.12	0.92	1.18	1.29	--
80.0	2.49	2.25	2.45	2.70	1.76	1.59	1.61	1.86	--
90.0	2.05	2.09	2.70	2.75	2.59	2.35	2.64	3.04	--
100.0	2.06	2.17	2.65	2.36	2.53	3.23	3.68	3.99	--
110.0	2.22	3.23	3.15	2.71	2.89	3.75	3.80	4.43	--
120.0	2.67	3.56	3.46	3.05	2.82	3.18	3.35	3.43	--
130.0	3.16	4.80	4.08	3.56	3.29	3.72	3.27	2.94	--
140.0	2.94	3.74	3.49	3.08	2.89	2.84	2.55	2.45	--
150.0	2.80	2.63	3.16	3.03	2.60	2.66	2.59	2.44	--
160.0	4.09	5.01	3.94	3.50	2.82	2.50	2.44	2.19	--
170.0	2.75	3.18	3.29	3.41	2.45	2.06	2.49	2.98	--
180.0	1.83	2.44	2.74	2.49	1.65	1.60	1.73	1.84	--



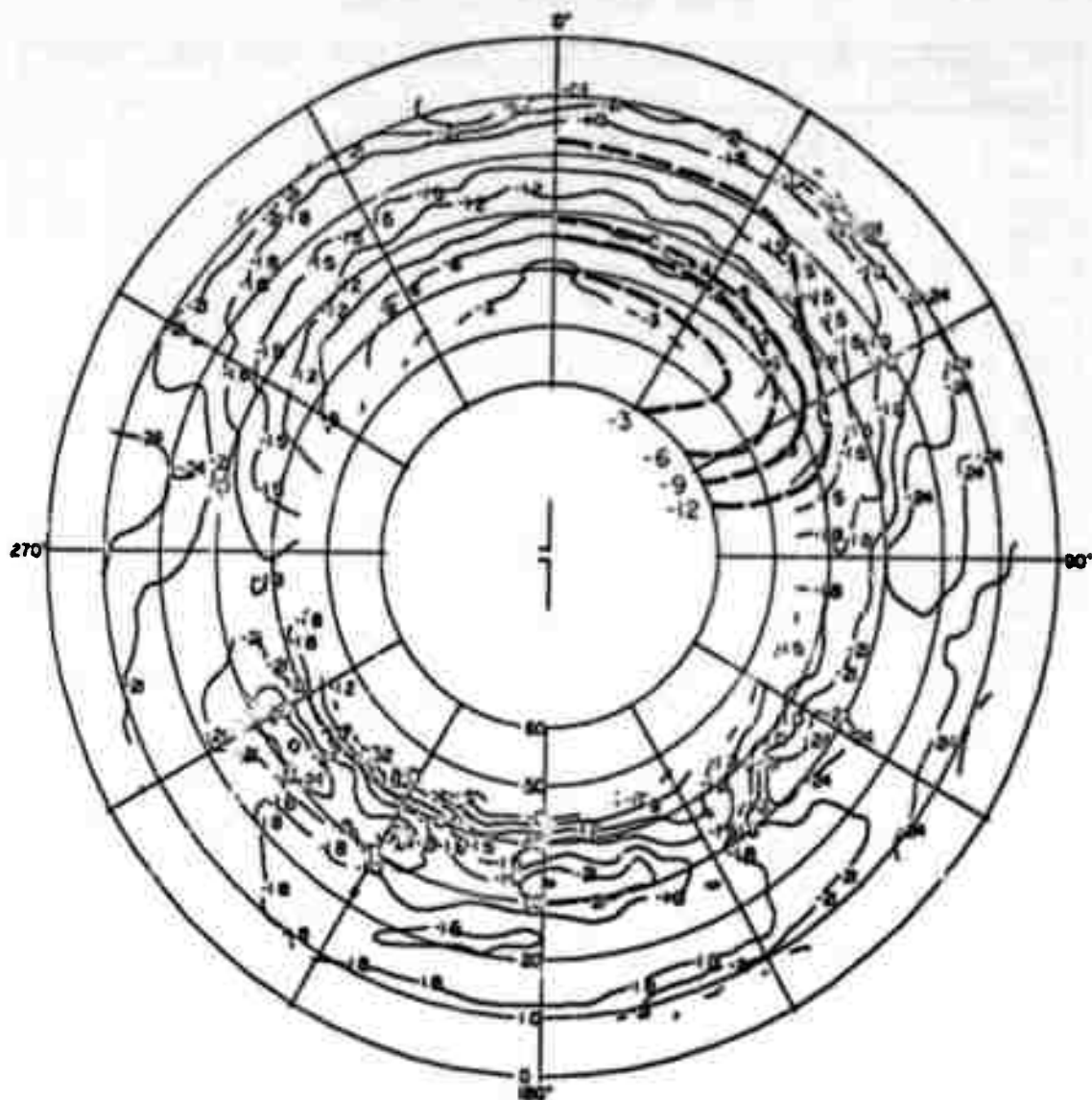
TA-8663-211

FIGURE A-15 CONTOUR PLOT OF THE MEDIAN RESPONSE OF THE VERTICAL SLEEVE DIPOLE IN THE FOREST— E_{ϕ} AT 75 MHz

Table A-16

STANDARD DEVIATIONS ABOUT THE MEDIAN FOR THE HORIZONTAL UNBALANCED DIPOLE
IN THE CLEARING--E AT 100 MHz

Elevation Azimuth	10.0	15.0	20.0	25.0	30.0	35.0	40.0	45.0	50.0
-170.0	7.97	2.65	2.04	1.34	0.89	0.94	0.79	0.81	0.86
-160.0	3.32	1.79	1.58	1.14	1.11	1.64	1.20	0.83	0.92
-150.0	2.23	1.60	1.44	1.28	0.79	6.44	0.87	1.48	1.25
-140.0	2.34	1.95	1.83	1.39	0.54	0.11	0.74	1.11	1.18
-130.0	3.29	3.92	2.88	1.99	1.02	0.20	0.74	0.86	0.85
-120.0	3.67	7.79	3.63	4.60	3.69	0.10	1.07	0.98	1.35
-110.0	4.43	3.56	4.40	5.72	3.17	3.67	2.39	2.48	2.83
-100.0	4.18	4.13	4.16	4.23	4.08	2.64	3.04	4.20	4.07
-90.0	3.51	3.94	3.80	3.3	3.24	3.01	3.14	3.34	3.41
-80.0	2.73	3.54	3.34	4.18	-.37	2.42	2.64	1.95	2.42
-70.0	3.40	2.63	2.63	1.98	1.09	4.01	2.53	2.00	1.72
-60.0	3.49	2.50	2.25	2.22	2.52	3.28	1.88	1.35	1.01
-50.0	4.34	2.06	1.77	1.58	1.21	1.03	1.15	0.93	0.80
-40.0	3.07	1.84	1.50	1.25	0.85	0.72	0.64	0.55	0.51
-30.0	2.61	1.23	1.48	1.34	0.89	0.53	0.56	0.59	0.61
-20.0	2.71	1.59	1.58	1.45	1.00	0.84	0.63	0.50	0.42
-10.0	2.88	3.26	1.97	1.33	0.78	0.57	0.60	0.66	0.56
0.0	3.03	1.77	1.75	1.32	0.97	0.73	0.71	0.62	0.51
10.0	3.57	1.60	1.68	1.80	1.36	0.98	0.81	0.68	0.61
20.0	5.20	2.31	1.93	1.67	1.31	0.93	0.84	0.87	0.74
30.0	3.15	1.90	1.99	1.93	1.58	1.10	0.96	0.87	0.63
40.0	4.26	1.77	2.31	2.48	1.91	1.15	0.95	0.72	0.50
50.0	3.75	2.85	3.06	2.48	2.15	1.73	1.19	0.67	0.62
60.0	4.09	4.14	3.92	3.88	3.03	2.22	1.45	1.21	1.28
70.0	3.94	3.39	4.41	5.96	4.12	1.26	2.22	2.34	1.96
80.0	4.76	3.88	3.90	3.51	4.68	4.94	3.65	3.58	3.00
90.0	4.33	3.27	3.68	3.82	4.22	3.73	3.83	4.28	4.00
100.0	4.05	4.60	3.86	3.88	3.64	3.22	2.94	2.40	2.58
110.0	3.97	4.38	3.79	3.05	3.07	3.60	2.72	2.03	1.74
120.0	3.99	3.65	3.82	3.98	3.53	2.73	1.98	1.87	1.33
130.0	2.90	3.38	3.23	3.40	2.43	0.34	1.20	0.93	0.93
140.0	3.49	2.72	2.76	2.72	1.86	0.95	0.93	0.78	0.82
150.0	4.21	2.10	2.32	1.98	1.26	0.93	0.60	0.76	0.87
160.0	3.86	3.04	2.39	2.16	1.11	0.45	0.78	0.88	0.91
170.0	3.05	1.94	1.80	1.47	0.61	0.15	0.45	0.44	0.78
180.0	2.81	3.01	2.04	1.26	0.44	0.09	0.37	0.77	0.85



TA-8663-212

FIGURE A-16 CONTOUR PLOT OF THE MEDIAN RESPONSE OF THE HORIZONTAL UNBALANCED DIPOLE IN THE CLEARING— E_θ AT 100 MHz

Table A-17

STANDARD DEVIATIONS ABOUT THE MEDIAN FOR THE HORIZONTAL UNBALANCED DIPOLE
IN THE CLEARING--E_z AT 100 MHz

Elevation Azimuth	10.0	15.0	20.0	25.0	30.0	35.0	40.0	45.0	50.0
-170.0	3.81	2.48	3.46	3.04	3.65	3.86	2.60	--	--
-160.0	2.16	1.79	2.42	2.97	3.56	3.14	2.51	1.12	--
-150.0	1.81	1.02	1.56	1.72	2.55	2.58	2.08	0.61	--
-140.0	1.23	1.08	1.11	1.19	1.89	2.31	1.66	0.97	--
-130.0	1.08	0.97	0.99	0.98	1.45	1.65	1.39	0.45	--
-120.0	0.84	0.65	0.93	1.11	1.36	1.46	1.13	0.63	--
-110.0	0.81	0.66	0.94	1.63	1.24	1.03	0.88	0.37	--
-100.0	0.82	0.46	0.74	0.92	1.24	1.05	0.74	0.38	--
-90.0	0.91	0.40	0.62	0.91	0.94	0.82	0.71	0.75	--
-80.0	0.98	0.52	0.77	0.97	0.77	0.64	0.59	0.40	--
-70.0	1.09	1.02	0.81	0.60	0.66	0.56	0.53	0.48	--
-60.0	0.80	0.89	0.87	0.69	0.78	0.72	0.69	0.43	--
-50.0	1.27	1.47	1.15	0.72	1.01	0.94	0.87	0.50	--
-40.0	1.74	1.51	1.40	1.31	1.42	1.38	1.02	0.76	--
-30.0	2.56	2.05	2.14	1.72	1.77	1.37	1.21	0.93	--
-20.0	3.74	4.43	3.46	2.39	2.40	2.18	2.03	1.38	--
-10.0	5.45	3.93	3.38	3.40	3.25	3.05	3.34	2.49	--
0.0	3.77	3.84	3.90	3.95	4.01	4.13	4.39	5.19	--
10.0	3.98	3.47	3.85	3.82	3.96	3.70	3.34	3.49	--
20.0	2.22	2.29	3.05	5.34	3.11	1.87	1.68	1.56	--
30.0	2.27	1.15	1.72	1.06	1.00	1.03	1.03	0.95	--
40.0	1.46	1.66	1.20	1.22	1.30	1.15	0.86	0.71	--
50.0	1.42	0.76	0.92	1.15	1.31	1.78	1.04	0.61	--
60.0	2.98	1.14	0.87	0.89	1.06	1.04	0.69	0.36	--
70.0	3.91	1.18	0.90	0.88	0.85	0.78	0.68	0.51	--
80.0	2.75	1.52	1.08	1.00	0.91	0.86	0.69	0.50	--
90.0	1.47	0.85	1.11	1.27	1.05	1.16	0.70	0.46	--
100.0	2.03	1.29	1.29	1.72	1.25	0.50	0.40	0.38	--
110.0	2.44	2.48	1.68	1.54	1.54	1.97	1.11	0.82	--
120.0	2.96	1.72	1.50	0.77	2.42	3.43	2.05	1.10	--
130.0	3.24	1.70	1.71	1.74	1.88	1.91	1.58	0.89	--
140.0	2.38	1.98	2.03	2.51	2.15	1.80	1.61	1.14	--
150.0	3.93	3.21	2.45	1.50	2.04	2.86	2.20	2.00	--
160.0	4.78	3.77	3.05	2.41	3.11	3.67	2.96	2.22	--
170.0	6.37	6.89	4.84	4.51	3.48	3.30	3.87	4.56	--
180.0	6.32	6.62	5.11	3.47	3.27	3.24	3.06	1.90	--

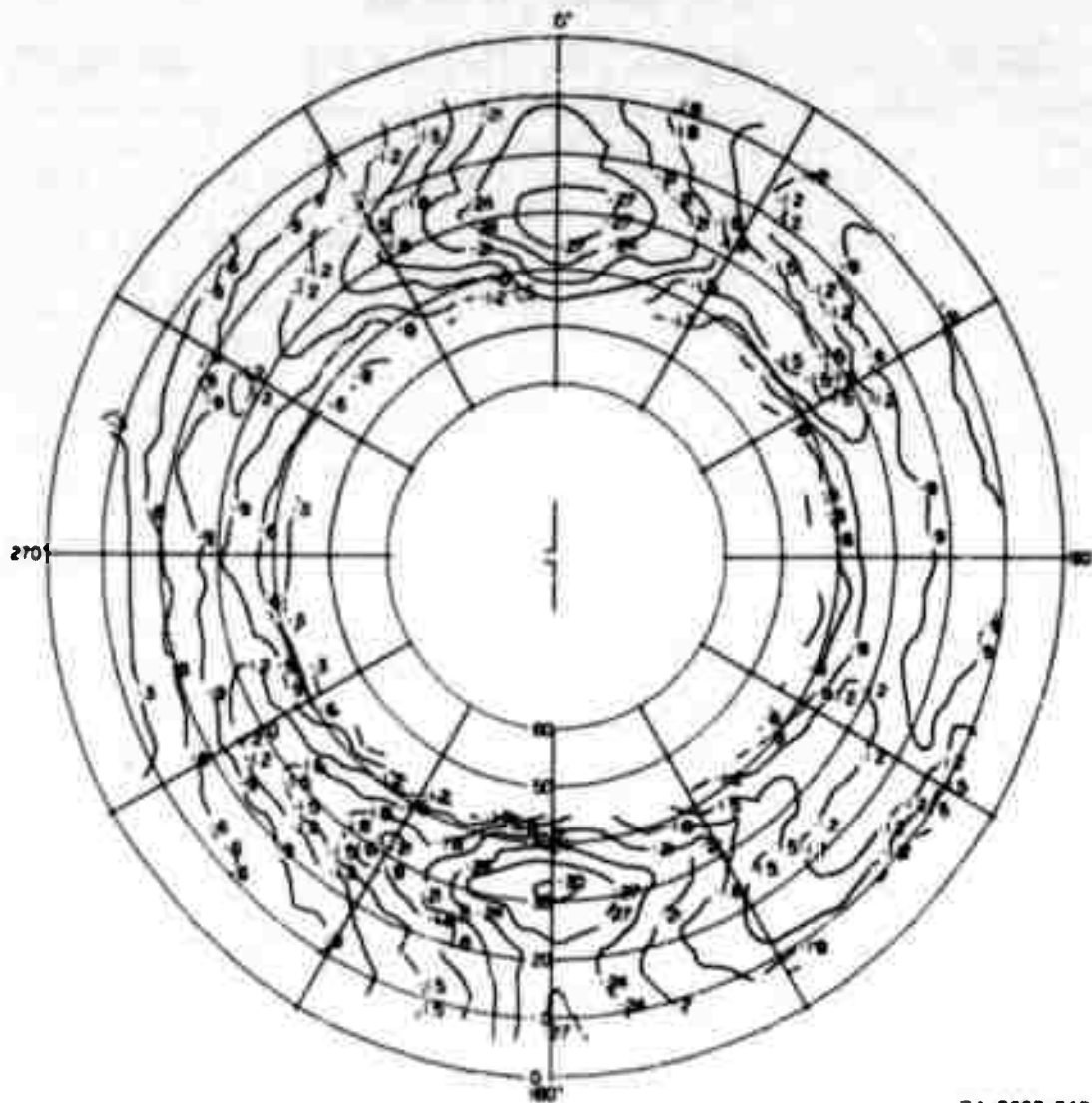
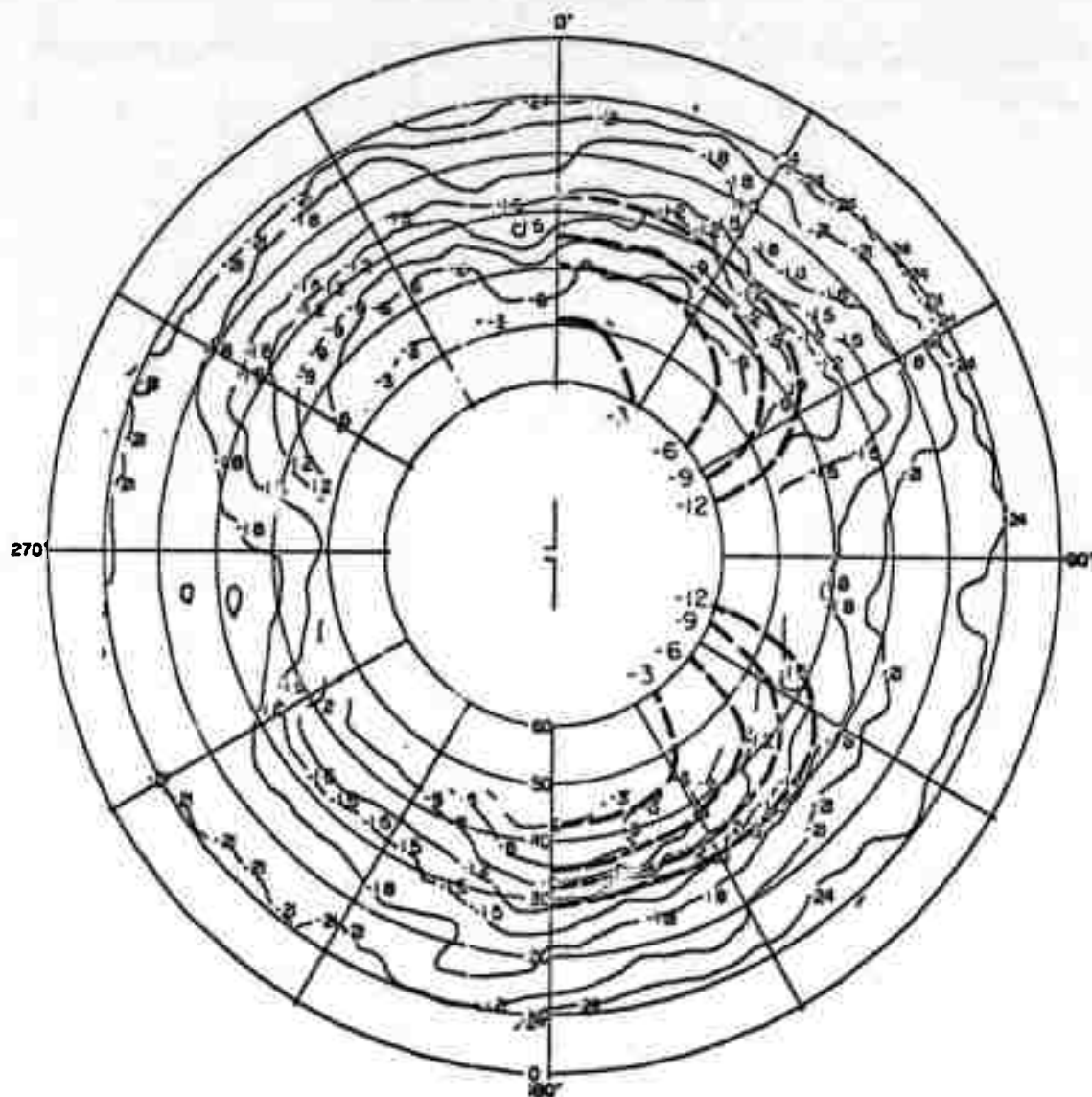


FIGURE A-17 CONTOUR PLOT OF THE MEDIAN RESPONSE OF THE HORIZONTAL UNBALANCED DIPOLE IN THE CLEARING— E_{ϕ} AT 100 MHz

Table A-18

STANDARD DEVIATIONS ABOUT THE MEDIAN FOR THE HORIZONTAL UNBALANCED DIPOLE
IN THE FOREST-- θ AT 100 MHz

Elevation Azimuth	10.0	15.0	20.0	25.0	30.0	35.0	40.0	45.0	50.0
-170.0	3.46	3.35	3.12	3.73	3.21	1.69	1.47	1.29	0.72
-160.0	3.46	3.15	3.12	3.13	3.45	2.97	2.15	1.57	0.62
-150.0	2.77	2.80	2.98	2.95	3.54	2.91	2.48	1.92	0.76
-140.0	2.88	3.51	3.37	3.34	3.49	2.60	2.15	1.87	0.92
-130.0	2.91	3.70	3.44	3.37	2.61	1.77	1.66	1.27	0.87
-120.0	3.28	3.32	3.44	3.26	2.90	2.47	2.23	2.24	1.59
-110.0	3.27	3.08	3.29	3.45	3.65	2.78	2.60	2.59	1.99
-100.0	3.37	3.33	3.28	3.43	3.32	2.54	2.88	2.88	2.43
-90.0	3.15	3.11	3.13	2.91	3.11	3.16	2.94	3.05	2.73
-80.0	2.68	3.25	3.19	3.27	3.42	3.07	2.93	2.40	1.68
-73.0	3.04	3.03	3.16	3.61	3.66	3.08	2.67	2.56	2.02
-60.0	3.12	2.90	2.98	2.68	2.15	1.69	1.72	1.49	1.72
-50.0	3.15	3.23	2.94	2.84	1.82	1.33	1.16	0.89	0.90
-40.0	2.97	2.87	2.89	2.95	1.99	1.30	1.16	1.20	0.86
-30.0	3.66	3.07	3.01	2.60	1.50	1.07	1.14	1.21	0.80
-20.0	2.93	4.02	3.70	3.73	2.47	1.40	1.51	1.34	0.94
-10.0	2.60	3.13	3.16	3.13	2.80	2.21	1.71	0.95	0.80
0.0	2.76	3.04	1.22	3.12	2.34	1.59	1.44	1.26	0.74
10.0	3.38	3.58	3.08	2.79	1.79	1.35	1.02	0.77	0.52
20.0	3.31	3.43	3.12	2.65	1.27	1.35	0.88	1.05	0.71
30.0	2.45	3.08	3.20	3.33	2.34	2.28	1.34	1.13	0.77
40.0	2.26	3.52	3.69	3.92	2.86	2.35	1.42	1.22	1.27
50.0	3.03	3.62	3.39	3.04	1.77	1.54	1.12	1.19	1.78
60.0	3.01	3.42	3.18	2.52	1.41	1.50	1.36	1.04	2.12
70.0	2.84	3.24	3.19	3.46	2.62	2.64	2.66	2.53	2.38
80.0	2.72	3.15	3.45	3.80	3.63	3.60	3.76	3.69	2.84
90.0	2.77	3.76	3.71	3.45	3.42	3.47	3.31	3.51	2.45
100.0	3.03	3.66	3.55	3.54	3.36	3.38	2.60	2.52	1.87
110.0	2.53	2.99	3.27	3.48	3.31	3.03	2.22	2.23	1.64
120.0	2.71	3.12	2.98	2.90	2.75	2.92	2.13	2.02	1.19
130.0	2.59	2.48	2.81	2.80	2.92	2.55	2.14	1.99	1.36
140.0	1.85	2.65	2.75	2.92	3.02	2.36	1.95	1.87	1.29
150.0	2.19	3.12	3.06	3.20	2.93	1.85	1.59	1.18	0.78
160.0	2.17	2.80	2.76	2.57	2.01	1.45	1.40	1.18	0.55
170.0	2.41	2.65	2.54	2.53	1.93	1.56	1.27	1.08	0.67
180.0	2.39	2.72	2.44	2.12	1.25	1.05	1.21	1.17	0.85



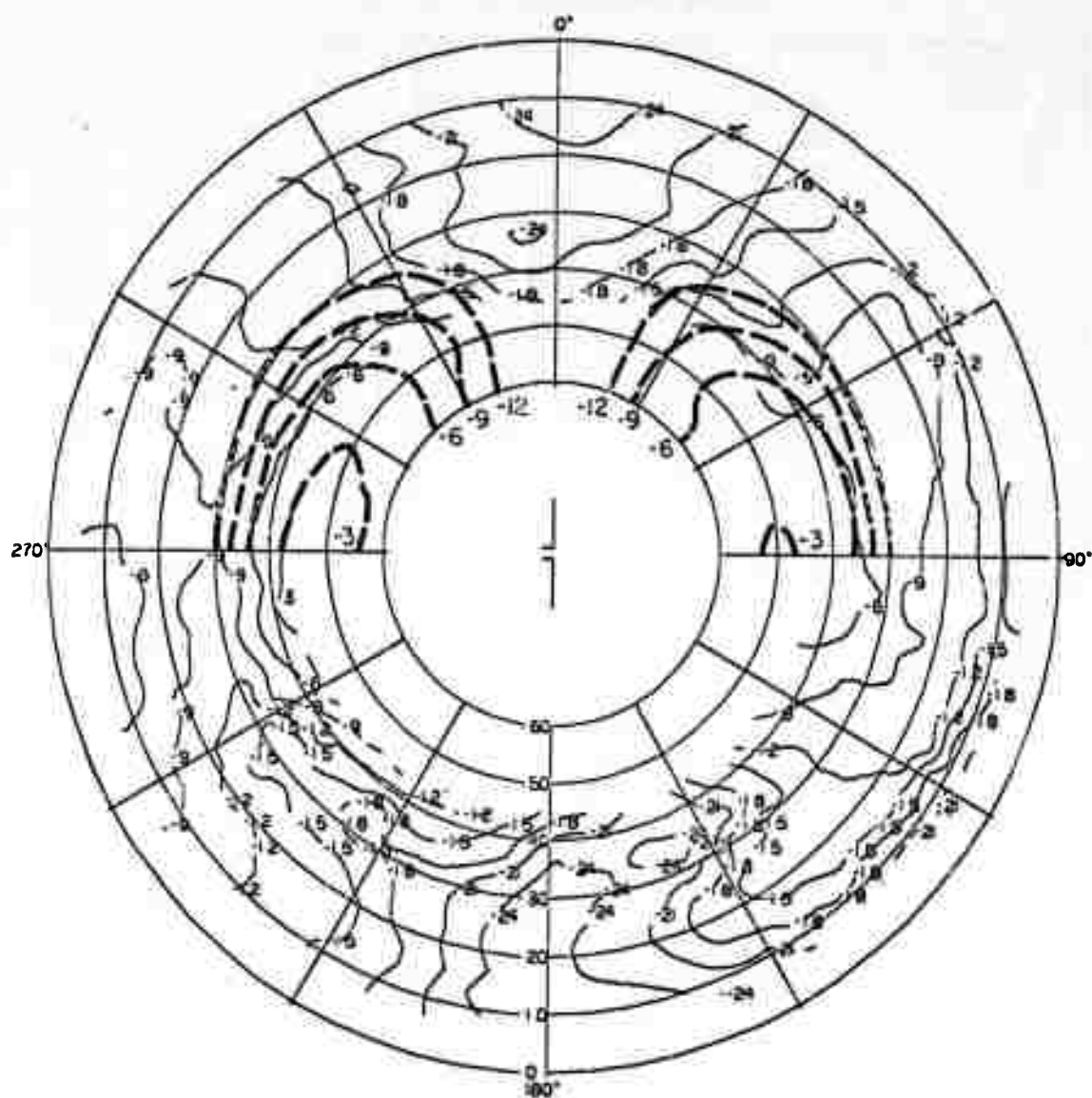
TA-8663-214

FIGURE A-18 CONTOUR PLOT OF THE MEDIAN RESPONSE OF THE HORIZONTAL UNBALANCED DIPOLE IN THE FOREST— E_{θ} AT 100 MHz

Table A-19

STANDARD DEVIATIONS ABOUT THE MEDIAN FOR THE HORIZONTAL UNBALANCED DIPOLE
IN THE FOREST-- E_{ϕ} AT 100 MHz

Elevation Azimuth	10.0	15.0	20.0	25.0	30.0	35.0	40.0	45.0	50.0
-170.0	3.88	3.97	3.73	3.56	3.28	2.40	1.82	0.97	--
-160.0	4.12	3.81	3.60	3.78	2.61	1.43	1.48	0.87	--
-150.0	2.37	1.78	2.23	2.24	1.81	1.40	1.12	0.45	--
-140.0	2.25	1.91	1.99	1.89	1.82	1.61	1.24	0.63	--
-130.0	2.48	2.45	2.27	1.91	1.97	1.58	1.57	0.91	--
-120.0	2.14	2.57	2.19	1.64	1.98	1.76	1.48	0.97	--
-110.0	1.54	2.02	2.08	1.76	1.56	0.85	1.04	0.57	--
-100.0	1.15	1.60	1.93	1.95	1.65	0.84	0.85	0.40	--
-90.0	1.19	1.51	1.36	1.47	1.65	0.95	0.82	0.46	--
-80.0	1.16	1.22	1.28	1.58	1.56	1.02	0.97	0.72	--
-70.0	1.42	1.27	1.47	1.61	1.46	0.99	0.85	0.64	--
-60.0	1.61	1.34	1.15	1.08	1.05	0.76	0.85	0.71	--
-50.0	1.22	1.16	1.14	1.31	1.35	1.20	1.15	0.80	--
-40.0	1.71	1.38	1.31	1.72	1.97	1.72	1.54	1.27	--
-30.0	2.59	2.40	2.66	2.93	2.76	2.35	1.87	1.64	--
-20.0	3.08	3.25	3.44	3.25	3.14	2.72	2.35	1.97	--
-10.0	3.36	3.47	3.34	3.16	2.64	2.69	3.01	3.75	--
0.0	3.31	3.40	3.49	3.75	3.20	3.55	4.00	4.49	--
10.0	3.68	3.78	3.97	3.89	3.70	3.15	3.39	3.30	--
20.0	2.81	2.61	3.29	3.49	3.06	2.38	2.39	1.94	--
30.0	3.03	2.91	2.93	2.96	2.21	1.59	1.15	1.04	--
40.0	3.40	3.29	2.72	2.25	1.60	1.18	0.94	0.77	--
50.0	2.87	2.85	1.84	1.55	0.95	0.97	0.73	0.58	--
60.0	2.84	2.81	1.45	1.29	0.70	0.73	0.63	0.58	--
70.0	3.02	2.72	1.42	1.46	0.81	0.70	0.70	0.72	--
80.0	2.81	2.85	1.77	1.82	1.21	0.96	0.69	0.69	--
90.0	2.65	2.75	1.87	1.94	1.32	1.15	0.67	0.61	--
100.0	2.60	2.40	1.57	1.71	1.18	1.08	0.82	0.87	--
110.0	2.54	2.46	1.64	1.48	1.17	1.19	1.15	1.32	--
120.0	2.36	1.95	1.53	1.52	1.36	1.50	1.34	1.21	--
130.0	1.92	1.57	1.30	1.19	1.68	1.58	1.59	1.50	--
140.0	2.59	2.16	1.87	1.61	2.19	2.52	2.48	1.95	--
150.0	2.94	2.95	2.54	1.76	2.52	2.99	2.68	2.22	--
160.0	2.22	2.43	2.94	2.85	2.84	2.71	3.06	3.21	--
170.0	2.58	3.33	3.45	4.08	3.64	2.73	2.46	2.30	--
180.0	3.11	3.95	3.43	3.07	2.68	2.27	2.16	1.87	--



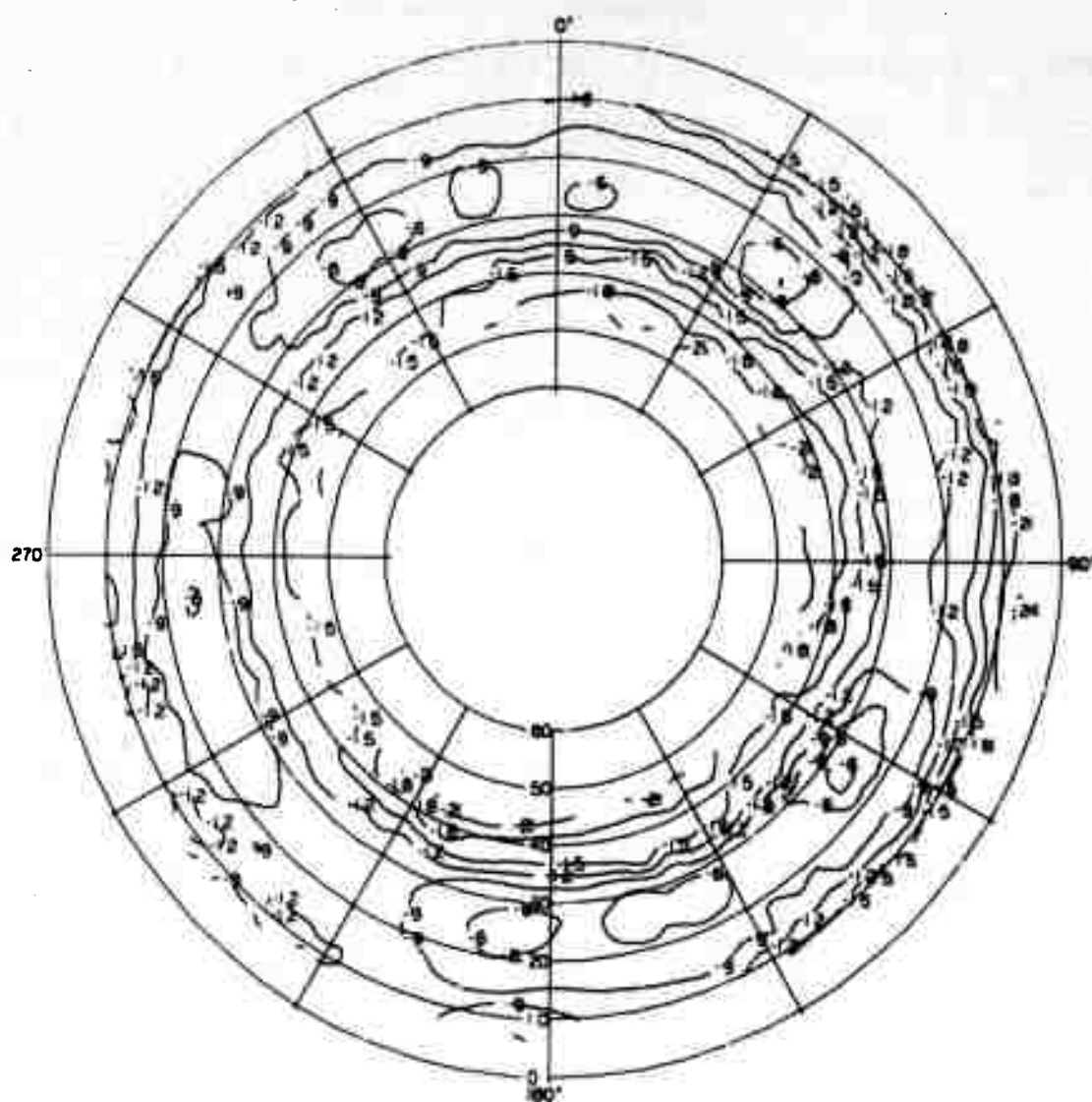
TA-8663-215

FIGURE A-19 CONTOUR PLOT OF THE MEDIAN RESPONSE OF THE HORIZONTAL UNBALANCED DIPOLE IN THE FOREST— E_{ϕ} AT 100 MHz

Table A-20

STANDARD DEVIATIONS ABOUT THE MEDIAN FOR THE VERTICAL SLEEVE DIPOLE
IN THE CLEARING-- E_{θ} AT 100 MHZ

Elevation Azimuth	10.0	15.0	20.0	25.0	30.0	35.0	40.0	45.0	50.0
-170.0	1.43	1.45	1.71	1.83	1.67	1.20	1.61	1.04	2.47
-160.0	1.79	1.55	1.81	2.06	1.92	0.95	1.53	1.65	1.81
-150.0	2.27	1.82	1.91	2.30	1.98	1.27	1.78	1.88	2.27
-140.0	1.91	1.73	1.82	1.59	1.46	1.24	2.12	2.77	2.71
-130.0	1.71	1.71	1.70	1.86	1.76	1.47	1.91	1.77	2.43
-120.0	2.05	1.65	1.71	1.76	1.76	1.08	1.41	1.37	2.08
-110.0	2.20	1.50	1.65	1.68	2.04	1.57	1.34	1.18	2.09
-100.0	2.09	1.67	1.67	1.71	1.95	1.32	1.23	1.21	2.19
-90.0	1.60	1.41	1.30	1.56	1.59	0.99	1.02	0.99	2.07
-80.0	1.49	1.35	1.39	1.36	1.46	1.04	1.01	1.04	1.66
-70.0	0.64	1.01	1.26	1.47	1.56	1.04	1.15	1.28	2.47
-60.0	0.50	1.56	1.72	1.93	1.76	1.14	1.16	1.26	2.50
-50.0	1.09	1.41	1.53	1.64	1.48	1.11	1.34	1.68	2.39
-40.0	1.68	1.88	1.88	2.28	1.94	1.12	1.41	1.92	2.75
-30.0	2.32	1.80	2.21	2.60	2.26	1.36	1.75	2.06	2.65
-20.0	2.42	2.15	2.21	2.20	2.08	1.75	1.78	1.87	2.01
-10.0	2.29	2.10	2.03	2.10	2.10	1.61	1.73	1.78	1.98
0.0	1.91	1.95	1.88	2.10	1.77	1.24	1.80	2.19	2.36
10.0	2.18	1.72	2.06	1.85	1.71	1.76	2.05	2.04	2.23
20.0	2.12	2.50	2.40	2.77	2.34	2.01	2.05	2.05	1.78
30.0	2.24	2.62	2.51	2.62	1.97	1.83	1.94	2.04	2.08
40.0	2.82	2.40	2.52	2.33	1.67	1.45	1.93	2.28	2.35
50.0	3.62	3.02	3.02	3.09	2.57	2.81	2.31	2.35	2.18
60.0	3.98	2.94	3.33	3.78	3.71	3.79	2.88	2.36	1.93
70.0	3.14	2.71	3.18	3.63	3.52	3.25	2.55	2.94	1.89
80.0	3.28	3.40	3.23	3.09	2.26	2.20	1.86	2.13	1.77
90.0	3.83	3.74	3.40	2.98	1.83	1.76	1.95	1.83	1.62
100.0	3.91	4.13	3.81	3.22	1.57	1.58	1.99	2.00	1.90
110.0	3.57	3.29	3.30	3.55	2.43	1.53	1.97	3.00	2.46
120.0	1.92	1.51	2.19	2.95	2.29	1.53	1.64	2.08	1.80
130.0	1.81	1.12	1.13	1.27	0.88	1.19	1.29	1.31	1.49
140.0	2.22	1.40	1.36	1.49	1.31	1.58	1.78	2.07	2.25
150.0	2.47	1.41	1.56	1.77	1.49	1.56	1.95	2.24	2.75
160.0	2.50	1.38	1.43	1.47	1.34	1.50	1.85	2.33	3.03
170.0	2.28	1.73	1.86	2.05	1.75	1.57	1.82	2.11	2.83
180.0	2.31	1.37	1.77	2.15	1.75	1.06	1.38	1.67	2.58



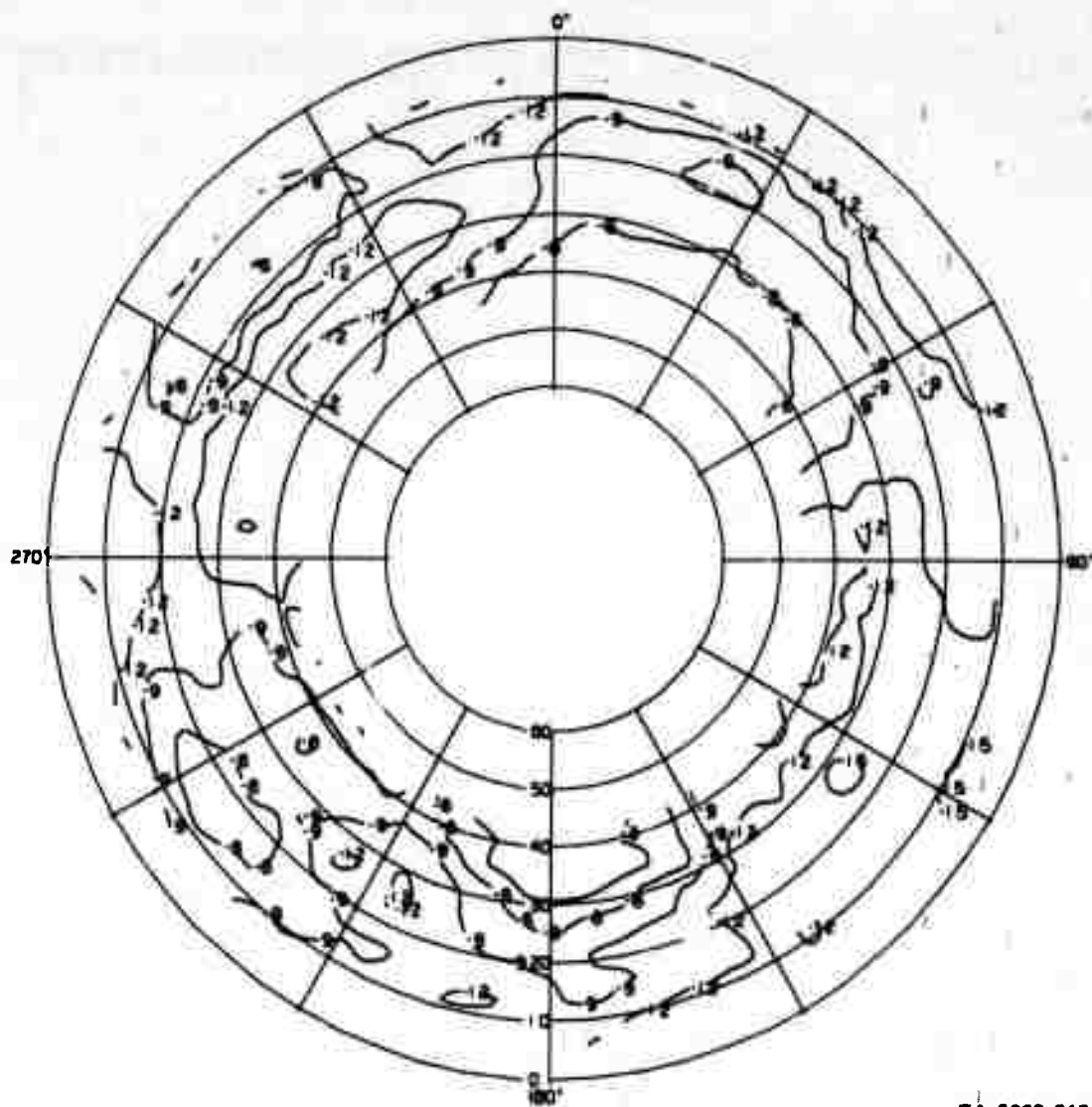
TA-8663-216

FIGURE A-20 CONTOUR PLOT OF THE MEDIAN RESPONSE OF THE VERTICAL SLEEVE DIPOLE IN THE CLEARING— E_0 AT 100 MHz

Table A-21

STANDARD DEVIATIONS ABOUT THE MEDIAN FOR THE VERTICAL SLEEVE DIPOLE
IN THE CLEARING--E₀ AT 100 MHz

Elevation Azimuth	10.0	15.0	20.0	25.0	30.0	35.0	40.0	45.0	50.0
-170.0	3.34	2.97	2.89	2.75	1.78	1.87	1.58	0.86	--
-160.0	2.98	3.15	3.13	2.88	2.58	2.69	2.88	2.14	--
-150.0	2.91	3.33	2.89	2.64	2.89	3.15	3.07	2.77	--
-140.0	2.65	2.54	2.85	2.11	2.26	2.59	2.25	1.85	--
-130.0	3.17	3.10	2.69	1.16	1.27	1.50	1.78	1.83	--
-120.0	3.51	3.41	2.98	1.81	2.18	2.31	2.11	2.38	--
-110.0	2.67	2.62	3.13	2.29	2.45	3.00	2.73	2.73	--
-100.0	3.25	3.84	3.36	2.61	2.82	3.28	2.92	3.00	--
-90.0	2.94	3.88	3.67	2.81	2.60	2.88	3.06	3.53	--
-80.0	2.48	2.89	2.85	2.46	2.38	2.33	2.46	2.80	--
-70.0	2.75	2.81	2.72	2.45	2.46	2.54	2.59	2.73	--
-60.0	2.46	2.21	2.29	2.82	2.69	2.81	2.71	3.80	--
-50.0	2.26	2.40	2.20	2.31	2.57	2.64	2.78	2.81	--
-40.0	2.78	2.62	2.46	2.54	2.71	2.43	2.43	2.28	--
-30.0	3.35	3.47	3.20	3.04	2.60	2.29	2.14	2.07	--
-20.0	3.01	3.30	3.37	3.20	2.46	1.99	1.87	1.39	--
-10.0	3.07	3.26	3.22	3.24	2.86	2.24	1.74	1.44	--
0.0	3.11	2.94	2.80	2.65	1.96	1.60	1.56	1.55	--
10.0	2.73	2.77	2.44	2.17	1.24	1.06	1.17	1.22	--
20.0	2.72	2.92	2.58	2.73	1.78	1.36	1.20	1.07	--
30.0	3.89	2.81	2.84	2.69	1.59	1.43	1.15	1.07	--
40.0	2.80	3.08	3.18	3.11	1.88	1.76	1.47	1.40	--
50.0	3.05	3.34	3.62	3.58	2.44	2.30	2.04	2.06	--
60.0	3.25	2.99	3.54	3.91	2.46	1.96	2.21	2.55	--
70.0	3.51	3.72	3.98	4.01	2.38	1.92	2.08	2.39	--
80.0	3.74	4.72	4.20	3.68	2.40	2.38	2.12	2.09	--
90.0	3.47	3.96	3.48	3.48	2.48	2.72	2.37	2.28	--
100.0	3.15	3.47	3.09	2.95	2.48	2.85	2.63	2.43	--
110.0	2.41	3.49	3.08	2.64	2.16	2.44	2.78	2.70	--
120.0	1.93	3.14	2.67	2.48	2.14	2.80	2.89	2.93	--
130.0	1.99	2.45	2.54	2.50	2.47	2.88	2.77	2.42	--
140.0	2.26	2.23	2.42	2.32	2.59	3.09	2.83	2.03	--
150.0	3.24	3.16	2.64	2.33	2.36	2.81	2.67	2.10	--
160.0	2.70	3.71	3.48	3.00	1.71	1.69	2.00	2.02	--
170.0	2.71	3.29	3.08	2.88	1.29	1.24	1.04	0.99	--
180.0	3.52	3.43	2.95	2.46	1.02	0.93	0.84	0.68	--



TA-8663-217

FIGURE A-21 CONTOUR PLOT OF THE MEDIAN RESPONSE OF THE VERTICAL SLEEVE DIPOLE IN THE CLEARING— E_{ϕ} AT 100 MHz

Table A-22

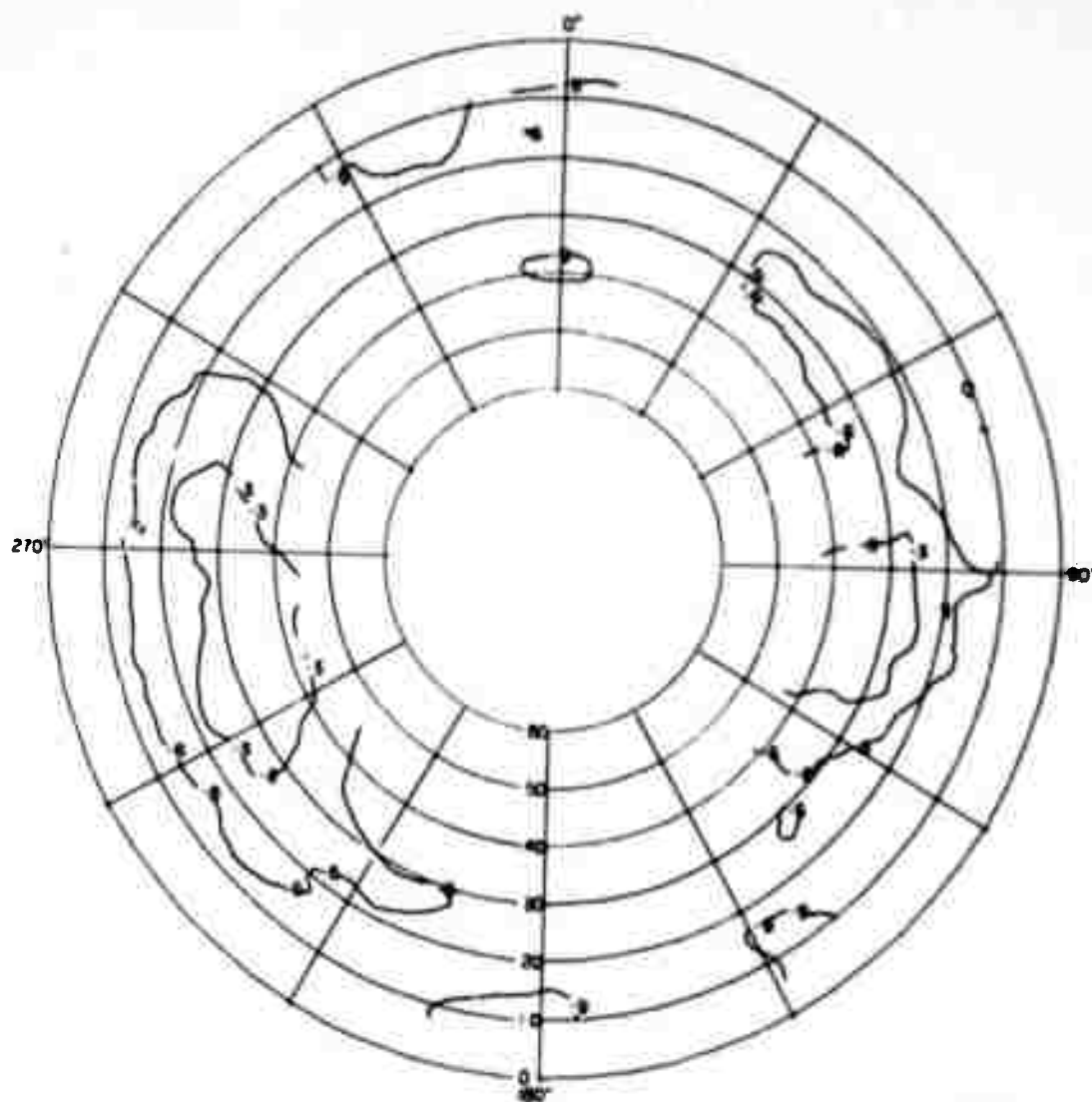
STANDARD DEVIATIONS ABOUT THE MEDIAN FOR THE VERTICAL SLEEVE DIPOLE
IN THE FOREST--E₀ AT 100 MHz

Elevation Azimuth	10.0	15.0	20.0	25.0	30.0	35.0	40.0	45.0	50.0
-170.0	2.80	2.61	2.60	2.52	2.43	2.45	2.32	2.39	2.18
-160.0	3.12	2.55	2.62	2.59	2.92	2.79	2.39	2.21	2.39
-150.0	3.03	2.88	2.80	2.83	2.95	2.45	2.24	1.89	1.55
-140.0	2.75	2.44	2.67	2.76	2.43	1.93	1.89	1.91	1.51
-130.0	2.63	2.35	2.40	2.43	1.84	1.72	1.91	2.18	2.00
-120.0	2.82	2.50	2.33	2.19	1.65	1.57	1.68	1.76	1.80
-110.0	2.98	2.53	2.36	2.20	1.95	1.87	1.80	1.91	2.08
-100.0	3.08	2.18	2.14	2.09	2.23	2.13	2.04	2.14	2.14
-90.0	2.01	1.75	1.92	1.99	2.16	2.00	1.98	1.84	1.73
-80.0	2.18	1.51	1.68	2.00	2.28	2.09	2.13	2.06	1.93
-70.0	3.27	2.15	2.50	2.73	2.73	2.32	2.13	2.05	2.48
-60.0	3.17	2.83	2.60	2.60	2.29	1.91	2.03	2.33	2.89
-50.0	2.49	2.92	2.72	2.37	1.31	1.29	1.74	1.96	2.45
-40.0	2.65	2.41	2.54	2.61	2.24	2.36	2.14	1.96	2.24
-30.0	2.83	2.63	2.60	2.63	2.65	2.43	2.12	2.11	2.25
-20.0	2.73	2.71	2.57	2.42	1.71	1.44	1.82	2.03	1.89
-10.0	2.78	2.58	2.62	2.58	2.17	2.16	2.34	2.22	2.04
0.0	2.55	2.93	2.83	2.93	3.17	3.04	3.04	2.96	2.36
10.0	2.30	3.00	2.92	2.77	2.31	2.17	2.32	2.19	2.00
20.0	2.60	2.72	2.93	2.73	1.86	1.67	1.94	1.34	1.90
30.0	3.15	2.83	2.58	2.56	1.84	1.97	1.62	1.47	1.22
40.0	3.04	2.48	2.45	2.25	1.72	1.92	1.48	1.17	1.52
50.0	2.78	2.43	2.35	2.24	1.90	1.76	1.02	0.75	1.32
60.0	2.66	2.63	2.56	2.46	2.03	2.00	1.42	1.39	1.69
70.0	2.60	2.89	2.67	2.58	2.42	2.48	2.18	2.19	2.13
80.0	2.30	2.57	2.71	2.68	2.93	3.00	2.47	2.31	2.15
90.0	1.90	2.48	2.77	3.02	3.18	3.28	2.30	2.25	2.39
100.0	1.84	2.81	2.76	3.07	2.96	2.67	1.62	1.62	2.10
110.0	2.15	2.69	2.70	2.49	2.16	2.25	1.46	1.37	1.84
120.0	1.82	2.30	2.38	2.27	2.10	2.32	1.98	1.70	1.49
130.0	1.66	2.72	2.64	2.67	2.02	1.88	1.49	1.33	1.57
140.0	1.74	2.26	2.24	2.33	2.19	2.35	2.51	2.47	2.25
150.0	1.50	2.18	2.17	2.21	2.48	2.92	3.07	3.14	2.51
160.0	1.61	2.20	2.41	2.42	2.57	3.00	3.16	3.21	3.21
170.0	1.52	2.44	2.49	2.63	2.36	2.42	2.96	3.71	3.64
180.0	2.24	2.69	2.73	2.85	2.22	1.68	2.11	2.49	3.05

Table A-23

STANDARD DEVIATIONS ABOUT THE MEDIAN FOR THE VERTICAL SLEEVE DIPOLE
IN THE FOREST--E₀ AT 100 MHz

Elevation Azimuth	10.0	15.0	20.0	25.0	30.0	35.0	40.0	45.0	50.0
-170.0	1.76	1.98	1.98	1.98	1.76	1.22	0.44	0.56	--
-160.0	2.02	2.34	2.49	2.56	1.85	1.32	1.10	0.63	--
-150.0	2.06	3.15	2.45	2.05	1.51	1.06	0.81	0.59	--
-140.0	1.71	2.56	2.38	2.11	1.50	1.31	1.21	0.93	--
-130.0	1.19	1.89	2.03	2.41	1.90	1.47	1.48	1.44	--
-120.0	1.04	1.70	1.80	2.09	1.64	1.35	1.32	1.10	--
-110.0	1.63	1.84	1.87	1.56	1.43	1.10	1.26	0.87	--
-100.0	2.09	2.53	2.37	1.67	1.72	1.37	1.27	1.07	--
-90.0	2.34	2.83	2.53	2.04	1.97	1.63	1.59	1.41	--
-80.0	1.51	1.91	2.02	2.04	2.08	1.88	1.69	1.34	--
-70.0	1.19	1.80	1.79	1.84	1.87	1.72	1.54	1.28	--
-60.0	1.01	1.75	1.73	1.62	1.49	1.11	1.25	0.96	--
-50.0	1.11	1.68	1.67	1.56	1.61	1.25	1.05	0.95	--
-40.0	1.20	1.57	1.84	1.77	1.44	1.03	1.08	1.09	--
-30.0	0.99	1.07	1.53	1.66	1.21	0.77	1.01	1.09	--
-20.0	1.21	1.18	1.51	1.84	1.34	1.29	1.20	1.04	--
-10.0	1.97	2.71	2.37	2.07	1.39	1.26	0.76	0.92	--
0.0	1.81	1.93	1.90	1.57	0.76	0.65	0.92	0.89	--
10.0	1.26	1.22	1.63	1.91	1.32	0.94	1.00	1.07	--
20.0	1.15	1.15	1.70	1.96	1.63	1.29	1.13	1.25	--
30.0	1.32	1.61	2.04	2.01	1.73	1.68	1.32	1.27	--
40.0	1.39	1.76	2.11	1.86	1.76	1.82	1.58	1.45	--
50.0	1.07	0.92	1.67	1.78	1.80	1.49	1.43	1.45	--
60.0	0.75	0.49	1.59	1.78	1.90	1.41	1.35	1.30	--
70.0	0.94	0.80	1.81	1.94	2.00	1.72	1.28	1.15	--
80.0	1.16	1.45	2.06	2.09	1.87	1.65	1.12	1.04	--
90.0	--	1.63	1.93	1.76	1.48	1.56	0.97	0.74	--
100.0	--	1.54	1.77	1.72	1.45	1.37	1.08	0.85	--
110.0	--	1.46	1.68	1.79	1.46	1.12	1.31	1.36	--
120.0	--	0.90	1.18	1.21	1.21	1.20	1.50	1.61	--
130.0	--	0.79	0.79	0.94	1.29	1.25	1.53	1.80	--
140.0	--	0.79	0.80	0.98	1.43	1.61	1.39	1.77	--
150.0	--	0.71	0.91	0.80	1.49	1.79	1.45	0.98	--
160.0	--	1.25	1.36	1.40	1.72	1.61	1.38	1.17	--
170.0	--	1.36	1.49	1.52	0.94	0.53	0.97	1.02	--
180.0	--	1.42	1.44	1.32	0.90	0.75	0.88	1.10	--



TA-8863-219

FIGURE A-23 CONTOUR PLOT OF THE MEDIAN RESPONSE OF THE VERTICAL SLEEVE DIPOLE IN THE FOREST— E_{ϕ} AT 100 MHz

Appendix B

**CONTOUR PLOTS OF THE ESTIMATED MEDIAN AMPLITUDES
AND TABLES OF STANDARD DEVIATIONS FOR ANTENNA SET 2**

Appendix B

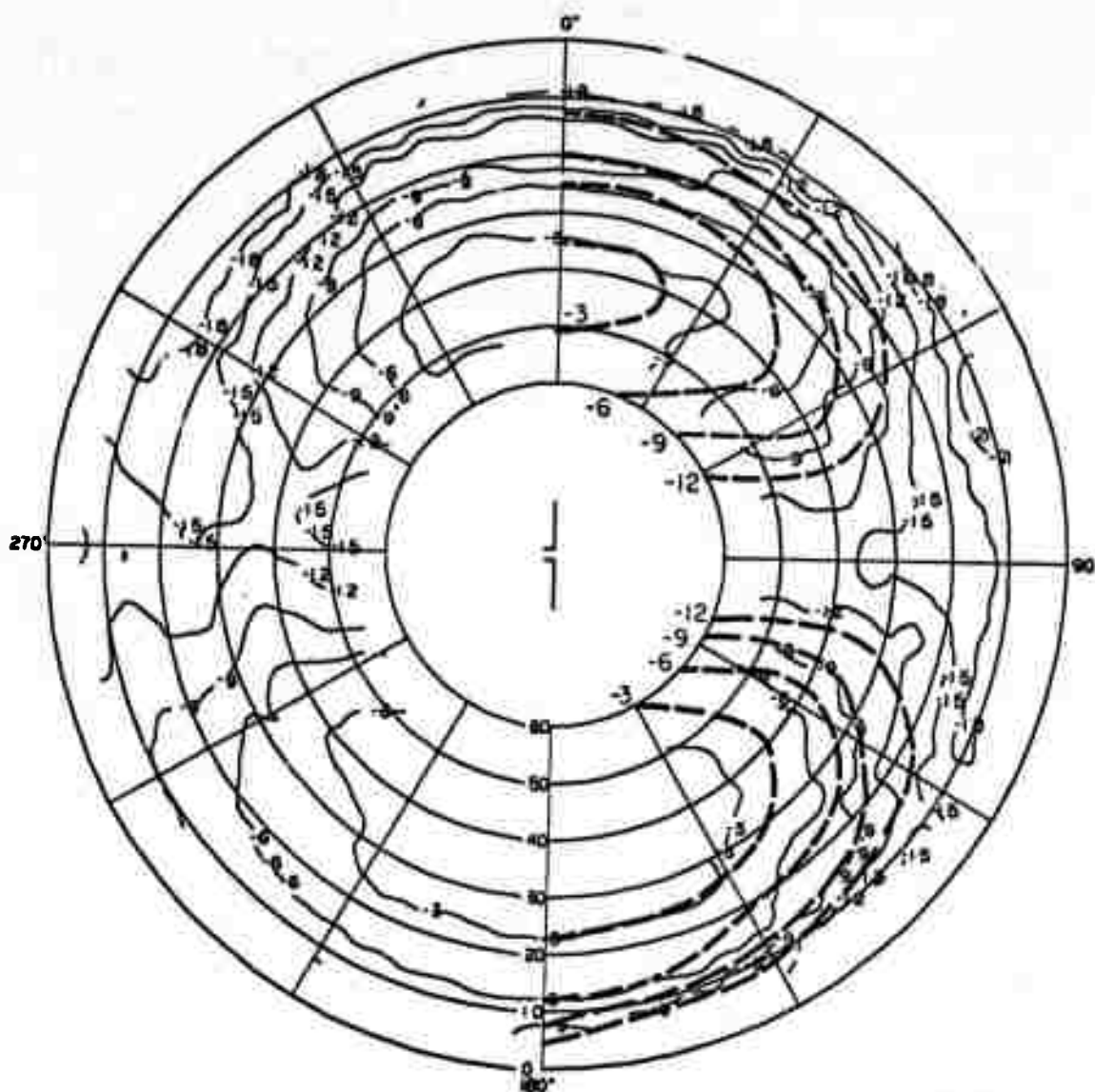
CONTOUR PLOTS OF THE ESTIMATED MEDIAN AMPLITUDES AND TABLES OF STANDARD DEVIATIONS FOR ANTENNA SET 2

This appendix contains the contour plots of the estimated median signal strength (as described in Section VI-B) and tables of the standard deviation of the signal strength about the median as described in Section VI-C for Antenna Set 2 (see Figure 8). For each contour plot presented, a table of standard deviations is presented on the opposite page. The data are grouped in order of increasing frequency, and within the frequency groups the data for horizontal antennas are presented first, and then the data for the vertical antennas. The title indicates the antenna type, the antenna location, the measurement polarization (using the same notation as defined in Section V--i.e., E_{θ} is vertical polarization and E_{ϕ} is horizontal polarization), and the measurement frequency which is also the design frequency of the antenna. Where the calculated patterns are available, they are shown as dashed lines on the contour plots.

Table B-1

STANDARD DEVIATIONS ABOUT THE MEDIAN FOR THE HORIZONTAL UNBALANCED DIPOLE
IN THE CLEARING--E_θ AT 50 MHz

Elevation Azimuth	10.0	15.0	20.0	25.0	30.0	35.0	40.0	45.0	50.0
-170.0	1.05	0.84	0.78	0.62	0.68	0.71	0.73	0.90	0.74
-160.0	0.97	0.89	0.86	0.88	0.80	0.79	0.73	0.56	0.96
-150.0	1.12	0.99	1.00	0.87	0.85	0.75	0.81	0.89	0.96
-140.0	1.31	1.43	1.04	0.73	0.91	0.95	0.91	0.82	0.96
-130.0	1.20	0.95	0.86	0.44	0.91	1.23	1.24	1.30	1.00
-120.0	1.26	1.14	1.10	1.12	1.41	1.24	1.36	1.56	1.24
-110.0	1.37	1.06	1.90	2.05	1.83	1.96	1.43	1.41	1.56
-100.0	2.01	1.65	1.89	2.69	1.69	1.10	1.14	0.92	1.32
-90.0	2.16	2.15	2.43	1.75	1.79	0.80	1.61	1.76	1.57
-80.0	2.66	3.18	2.71	2.33	2.40	2.76	2.18	2.10	1.35
-70.0	2.88	3.15	2.79	2.19	2.24	1.82	1.91	1.73	1.96
-60.0	2.21	2.83	2.64	2.58	2.58	2.95	2.02	1.82	2.06
-50.0	1.90	2.38	2.50	2.15	2.01	1.37	1.31	1.26	1.31
-40.0	1.99	2.57	2.57	2.67	2.04	1.53	1.29	1.16	0.88
-30.0	2.27	2.55	2.19	1.78	1.60	1.28	0.87	0.67	0.61
-20.0	2.37	1.76	1.59	1.25	0.88	0.61	0.55	0.40	0.65
-10.0	2.62	2.18	1.62	0.86	0.83	0.79	0.70	0.69	0.58
0.0	2.24	1.26	1.49	0.73	0.70	0.45	0.69	0.66	0.67
10.0	2.55	2.64	1.68	0.98	0.80	0.84	0.89	1.28	0.97
20.0	2.00	1.45	1.72	0.89	0.87	0.76	0.74	0.49	0.67
30.0	2.61	2.30	2.12	0.70	0.91	0.71	0.73	0.91	0.83
40.0	3.51	3.47	3.02	1.92	1.39	1.03	0.84	0.94	1.04
50.0	2.73	4.58	3.06	1.58	1.63	0.95	0.95	0.70	0.76
60.0	1.90	2.82	3.06	3.34	2.12	2.13	1.31	0.74	1.47
70.0	1.18	1.50	2.16	2.04	2.10	1.31	1.66	1.92	2.50
80.0	2.20	2.54	2.52	2.91	2.30	2.08	2.28	3.10	2.62
90.0	2.24	2.99	3.01	3.18	2.55	1.96	2.28	2.84	2.68
100.0	2.17	3.48	3.30	3.28	2.68	2.70	2.22	1.61	1.69
110.0	2.53	2.80	2.45	1.23	1.84	1.23	1.53	1.66	1.52
120.0	3.05	2.64	2.46	2.44	1.59	1.39	1.11	1.05	0.95
130.0	2.80	1.64	1.80	1.00	1.25	0.87	0.79	0.89	0.70
140.0	2.96	2.75	2.10	1.55	1.19	1.50	0.95	0.72	0.71
150.0	2.36	1.00	1.26	0.64	0.89	0.69	0.73	0.57	0.55
160.0	1.74	0.89	1.05	0.86	0.70	0.58	0.49	0.49	0.47
170.0	1.55	1.01	0.86	0.71	0.70	0.65	0.53	0.44	0.44
180.0	1.32	0.77	0.79	0.71	0.73	0.63	0.62	--	0.54



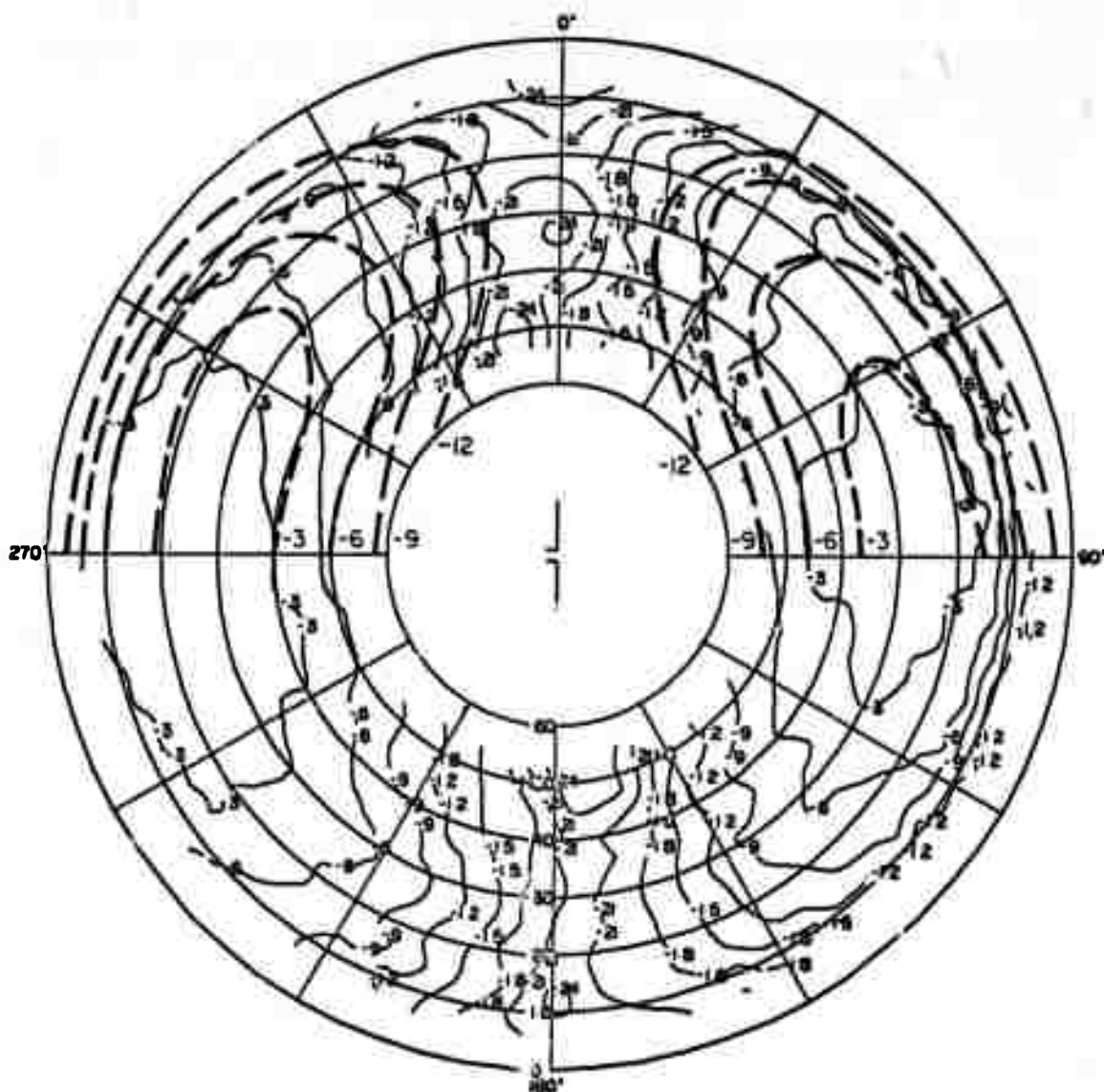
TA-8663-220

FIGURE B-1 CONTOUR PLOT OF THE MEDIAN RESPONSE OF THE HORIZONTAL UNBALANCED DIPOLE IN THE CLEARING— E_0 AT 50 MHz

Table B-2

STANDARD DEVIATIONS ABOUT THE MEDIAN FOR THE HORIZONTAL UNBALANCED DIPOLE
IN THE CLEARING--E_c AT 50 MHz

Elevation Azimuth	5.0	10.0	15.0	20.0	25.0	30.0	35.0	40.0	45.0
-170.0	--	3.16	2.95	2.50	1.54	1.93	1.43	1.45	1.43
-160.0	0.0	2.09	1.57	1.47	0.87	1.27	1.25	1.14	0.94
-150.0	--	1.26	0.88	0.96	0.54	0.78	0.86	0.84	0.88
-140.0	0.0	0.97	0.76	0.67	0.48	0.47	0.52	0.67	0.71
-130.0	--	0.82	0.51	0.59	0.57	0.46	0.61	0.90	0.91
-120.0	--	0.69	0.54	0.50	0.45	0.44	0.54	0.55	0.36
-110.0	--	0.65	0.47	0.38	0.28	0.35	0.30	0.37	0.31
-100.0	--	0.44	0.27	0.32	0.29	0.41	0.57	0.43	0.33
-90.0	--	0.37	0.36	0.33	0.21	0.41	0.50	0.45	0.35
-80.0	--	0.59	0.49	0.42	0.41	0.40	0.39	0.43	0.45
-70.0	--	0.71	0.55	0.55	0.42	0.44	0.51	0.52	0.54
-60.0	--	0.67	0.57	0.61	0.37	0.57	0.56	0.60	0.55
-50.0	--	1.04	1.01	0.87	1.17	1.04	0.80	0.70	0.60
-40.0	--	1.03	0.64	0.95	1.05	0.93	0.90	0.81	0.83
-30.0	--	1.56	1.11	1.50	1.02	1.08	1.03	1.38	1.11
-20.0	0.0	2.55	2.35	2.42	2.35	2.68	1.95	2.33	2.56
-10.0	--	2.47	3.89	3.53	4.16	4.28	3.90	3.25	2.79
0.0	--	2.53	3.28	3.44	3.48	3.32	3.38	3.05	3.19
10.0	--	2.39	2.29	2.59	3.12	2.20	2.40	2.20	1.70
20.0	--	1.70	1.32	1.17	1.62	1.46	1.64	1.03	0.71
30.0	--	1.27	0.86	0.67	0.50	0.76	0.77	0.69	0.79
40.0	--	1.29	0.52	0.56	0.33	0.43	0.64	0.62	0.53
50.0	--	1.29	0.65	0.63	0.60	0.49	0.44	0.58	0.64
60.0	--	1.13	0.63	0.60	0.54	0.59	0.91	0.62	0.41
70.0	--	1.06	0.71	0.62	0.37	0.44	0.32	0.36	0.48
80.0	0.0	1.01	0.91	0.68	0.49	0.32	0.24	0.32	0.35
90.0	--	1.49	0.63	0.58	0.19	0.32	0.29	0.34	0.41
100.0	--	1.93	0.81	0.73	0.61	0.41	0.32	0.35	0.41
110.0	--	1.60	0.80	0.70	0.44	0.35	0.28	0.35	0.33
120.0	--	1.10	0.62	0.63	0.41	0.57	0.60	0.43	0.33
130.0	--	1.26	0.91	0.89	1.04	0.70	0.60	0.67	0.62
140.0	0.0	1.15	0.90	0.90	0.50	0.77	0.89	0.95	1.32
150.0	--	1.88	1.89	1.55	1.89	1.40	1.67	1.50	0.66
160.0	--	2.38	2.11	2.06	2.50	2.39	2.46	2.66	4.00
170.0	--	1.98	1.97	2.71	3.66	2.73	2.44	2.63	2.85
180.0	--	2.60	2.92	3.21	3.77	2.53	1.42	1.77	1.57



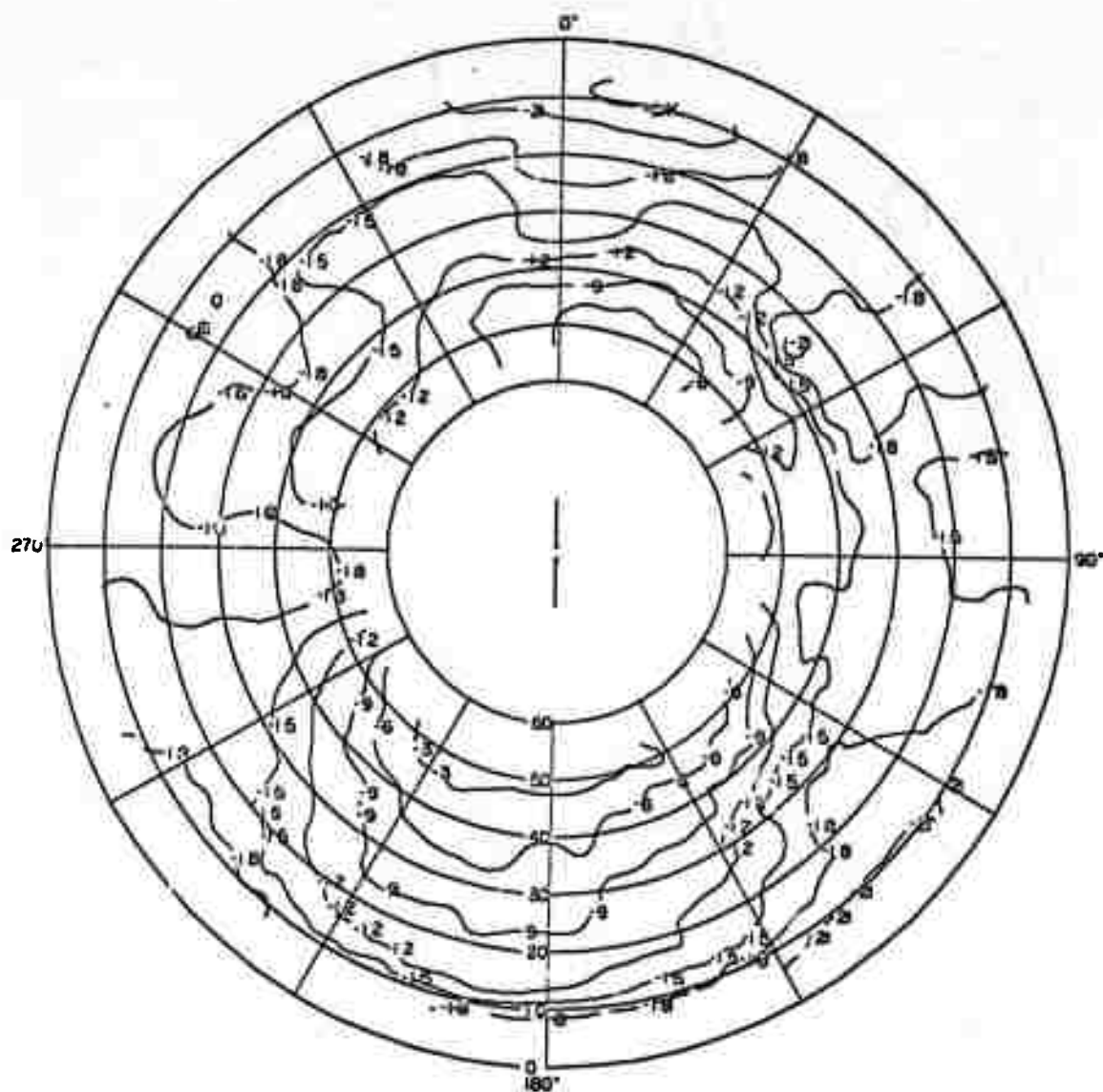
TA-8663-221

FIGURE B-2 CONTOUR PLOT OF THE MEDIAN RESPONSE OF THE HORIZONTAL UNBALANCED DIPOLE IN THE CLEARING— E_{ϕ} AT 50 MHz

Table B-3

STANDARD DEVIATIONS ABOUT THE MEDIAN FOR THE HORIZONTAL FOLDED DIPOLE
IN THE FOREST-- E_0 AT 50 MHz

Elevation Azimuth	10.0	15.0	20.0	25.0	30.0	35.0	40.0	45.0	50.0
-170.0	2.95	1.70	1.65	1.11	0.97	0.75	0.72	0.64	0.52
-160.0	3.02	2.08	1.93	1.34	1.21	0.79	0.67	0.50	0.43
-150.0	2.95	2.34	1.91	1.12	1.10	0.95	0.66	0.61	0.92
-140.0	3.22	2.47	2.15	1.12	1.03	0.94	0.87	0.69	0.92
-130.0	3.11	3.38	2.85	2.07	1.70	1.44	1.25	0.78	0.59
-120.0	3.93	3.95	3.40	2.53	2.08	1.86	1.56	1.33	1.31
-110.0	3.57	2.68	2.74	2.16	2.67	2.47	2.13	2.00	1.86
-100.0	3.22	2.41	3.01	3.73	2.85	2.66	2.90	2.98	2.14
-90.0	2.78	2.36	2.93	3.67	2.73	2.22	2.75	2.48	1.72
-80.0	3.47	3.22	2.43	1.84	2.57	2.60	2.24	1.96	1.61
-70.0	3.89	3.23	2.80	1.66	2.02	1.70	1.54	1.07	1.02
-60.0	4.01	3.36	3.58	3.44	2.72	2.16	1.72	1.32	1.47
-50.0	3.47	3.54	2.99	2.57	2.41	2.41	2.12	1.88	1.83
-40.0	2.75	2.28	2.64	2.43	1.72	1.44	2.23	2.89	2.20
-30.0	3.27	2.72	2.56	1.86	1.56	1.56	1.42	1.56	1.53
-20.0	3.27	3.03	2.53	1.47	1.52	1.31	1.60	1.85	1.40
-10.0	3.10	3.09	2.83	1.78	1.88	1.33	1.06	1.12	1.02
0.0	3.27	2.98	3.35	2.87	2.48	1.75	1.22	1.08	0.88
10.0	3.88	3.48	3.28	2.85	2.21	1.89	1.13	0.88	0.77
20.0	4.19	3.40	2.88	1.83	1.54	1.58	0.87	0.90	0.48
30.0	4.16	3.66	3.18	2.08	2.17	1.91	1.25	1.10	0.49
40.0	3.68	2.77	3.33	3.53	3.21	3.69	2.10	1.56	0.87
50.0	3.21	3.42	3.47	3.05	3.06	2.76	1.73	1.40	1.15
60.0	3.77	4.10	3.49	3.48	3.39	3.34	2.20	1.56	1.77
70.0	2.73	3.27	3.15	3.70	3.19	3.34	2.17	1.43	1.79
80.0	3.64	2.32	2.33	1.60	1.95	1.99	1.62	1.58	1.86
90.0	4.04	2.02	1.96	1.87	1.81	1.74	1.68	1.60	1.80
100.0	3.24	1.93	2.27	2.38	2.24	2.22	1.70	1.55	1.54
110.0	2.75	4.11	3.36	3.46	3.00	2.73	2.08	1.67	1.33
120.0	3.67	4.11	3.64	3.13	3.02	3.25	2.49	2.40	1.79
130.0	4.15	4.94	4.47	4.43	3.32	3.06	2.03	1.68	0.93
140.0	3.54	3.76	3.89	3.66	2.60	2.25	1.21	1.15	0.66
150.0	3.86	3.47	3.41	3.25	2.09	1.59	0.84	0.82	0.65
160.0	3.24	2.44	2.32	2.14	1.63	1.73	1.06	0.85	0.69
170.0	2.75	1.88	2.01	1.78	1.46	1.30	1.01	0.95	0.71
180.0	2.45	1.75	1.59	1.12	1.11	0.96	0.88	0.77	0.60



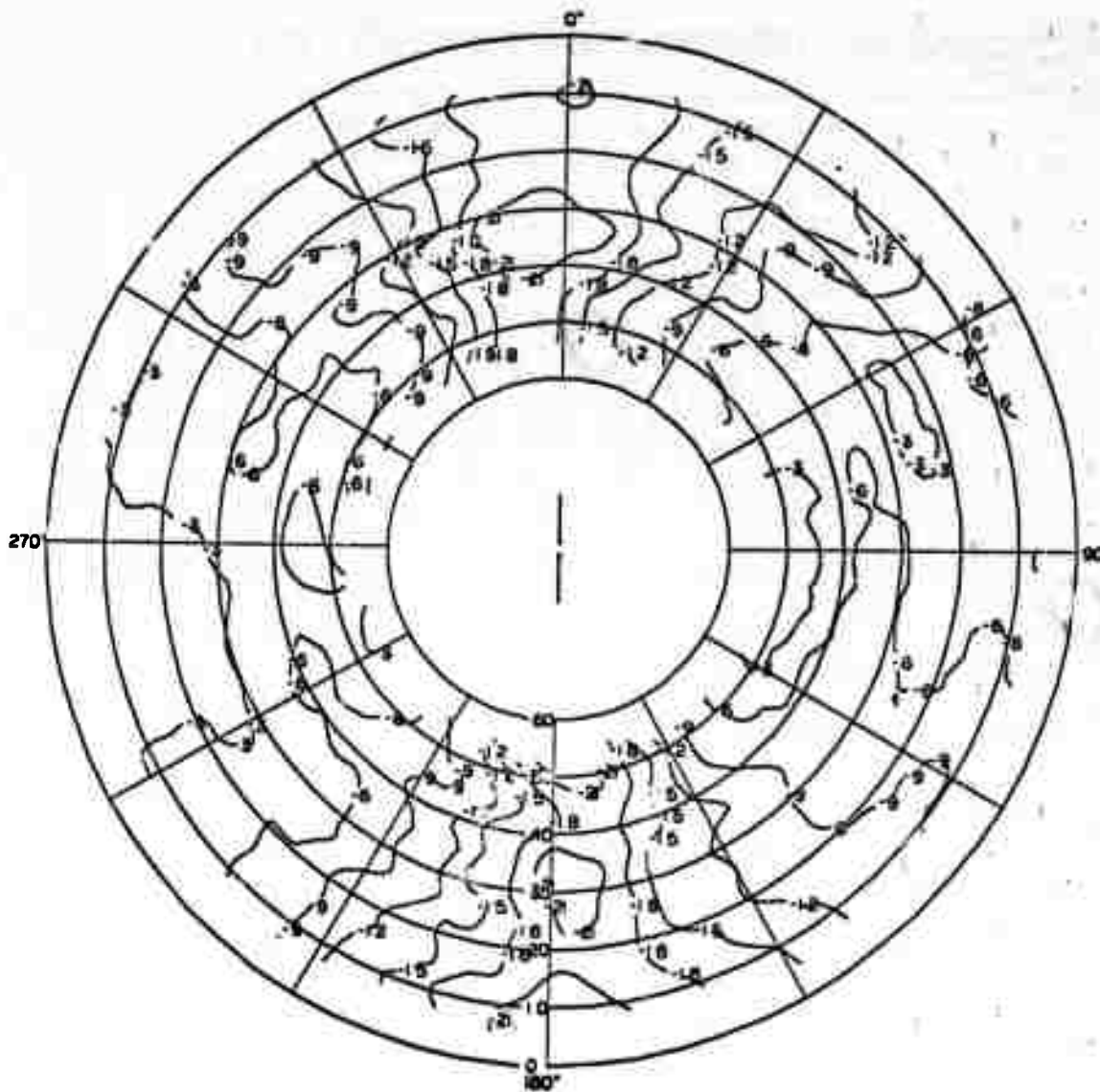
TA-8663-222

FIGURE B-3 CONTOUR PLOT OF THE MEDIAN RESPONSE OF THE HORIZONTAL FOLDED DIPOLE IN THE FOREST— E_θ AT 50 MHz

Table B-4

STANDARD DEVIATIONS ABOUT THE MEDIAN FOR THE HORIZONTAL FOLDED DIPOLE
IN THE FOREST-- E_c AT 50 MHz

Elevation Azimuth	5.0	10.0	15.0	20.0	25.0	30.0	35.0	40.0	45.0
-170.0	--	3.48	2.76	2.30	1.91	3.18	3.14	2.97	2.79
-160.0	0.0	2.91	1.96	1.93	1.55	1.89	1.90	1.95	1.64
-150.0	--	2.18	1.65	1.67	1.05	1.00	0.93	1.10	0.93
-140.0	--	1.66	1.00	1.04	0.57	0.67	0.53	0.92	1.37
-130.0	--	1.18	1.06	1.03	0.79	0.69	0.75	0.70	0.71
-120.0	0.0	1.26	1.26	0.97	0.57	0.52	0.62	0.89	0.83
-110.0	--	1.09	0.82	0.75	0.51	0.53	0.72	0.83	0.79
-100.0	--	0.90	0.52	0.55	0.41	0.55	0.78	0.93	0.57
-90.0	--	0.84	0.66	0.65	0.54	0.58	0.57	0.56	0.34
-80.0	--	1.26	1.19	0.99	0.65	0.83	0.76	0.62	0.89
-70.0	--	1.37	1.22	1.20	0.73	0.90	1.22	0.63	0.36
-60.0	--	1.53	1.67	1.25	0.69	0.77	0.68	0.72	0.52
-50.0	--	1.47	1.72	1.53	1.07	1.39	1.26	0.87	0.75
-40.0	--	2.02	1.61	1.63	1.62	1.09	0.75	0.82	0.91
-30.0	--	2.99	2.56	2.05	1.68	1.61	1.35	1.55	1.48
-20.0	--	2.14	2.17	2.35	2.45	2.70	2.61	2.42	2.50
-10.0	--	3.35	2.83	2.95	2.99	3.01	2.94	3.30	3.64
0.0	0.0	3.39	3.10	3.11	3.04	3.14	2.98	3.21	3.25
10.0	--	3.57	3.16	2.88	1.88	2.64	3.33	2.68	1.86
20.0	--	3.23	3.45	2.56	1.26	1.56	2.38	2.21	2.11
30.0	--	2.59	3.04	2.27	1.47	1.53	1.69	1.55	1.35
40.0	0.0	3.12	3.52	2.28	1.57	1.19	1.15	0.98	0.84
50.0	--	2.08	2.43	1.95	1.44	1.15	1.40	0.92	0.70
60.0	--	1.31	1.09	1.15	1.09	0.96	0.76	0.62	0.79
70.0	--	1.78	1.91	1.21	0.99	0.83	0.76	0.69	0.56
80.0	--	0.88	0.71	0.99	0.62	0.80	1.01	0.82	0.67
90.0	--	1.34	1.38	1.09	1.05	0.96	1.07	0.91	0.71
100.0	--	1.33	1.54	1.41	0.99	1.08	1.25	0.92	0.70
110.0	--	1.31	1.55	1.60	1.92	1.36	0.77	0.74	0.71
120.0	0.0	1.51	1.60	1.45	1.33	1.06	0.62	0.64	0.62
130.0	--	1.31	1.19	1.21	1.06	1.24	1.50	0.99	0.78
140.0	--	1.13	1.07	1.39	1.40	1.29	1.28	1.24	0.86
150.0	--	2.30	2.05	1.65	1.35	1.26	1.59	1.81	2.11
160.0	0.0	2.69	2.74	1.93	1.61	1.34	1.94	2.22	2.34
170.0	--	3.01	3.55	4.05	4.92	3.67	3.28	3.04	3.15
180.0	--	3.03	3.47	3.56	3.56	3.93	4.08	3.64	3.43



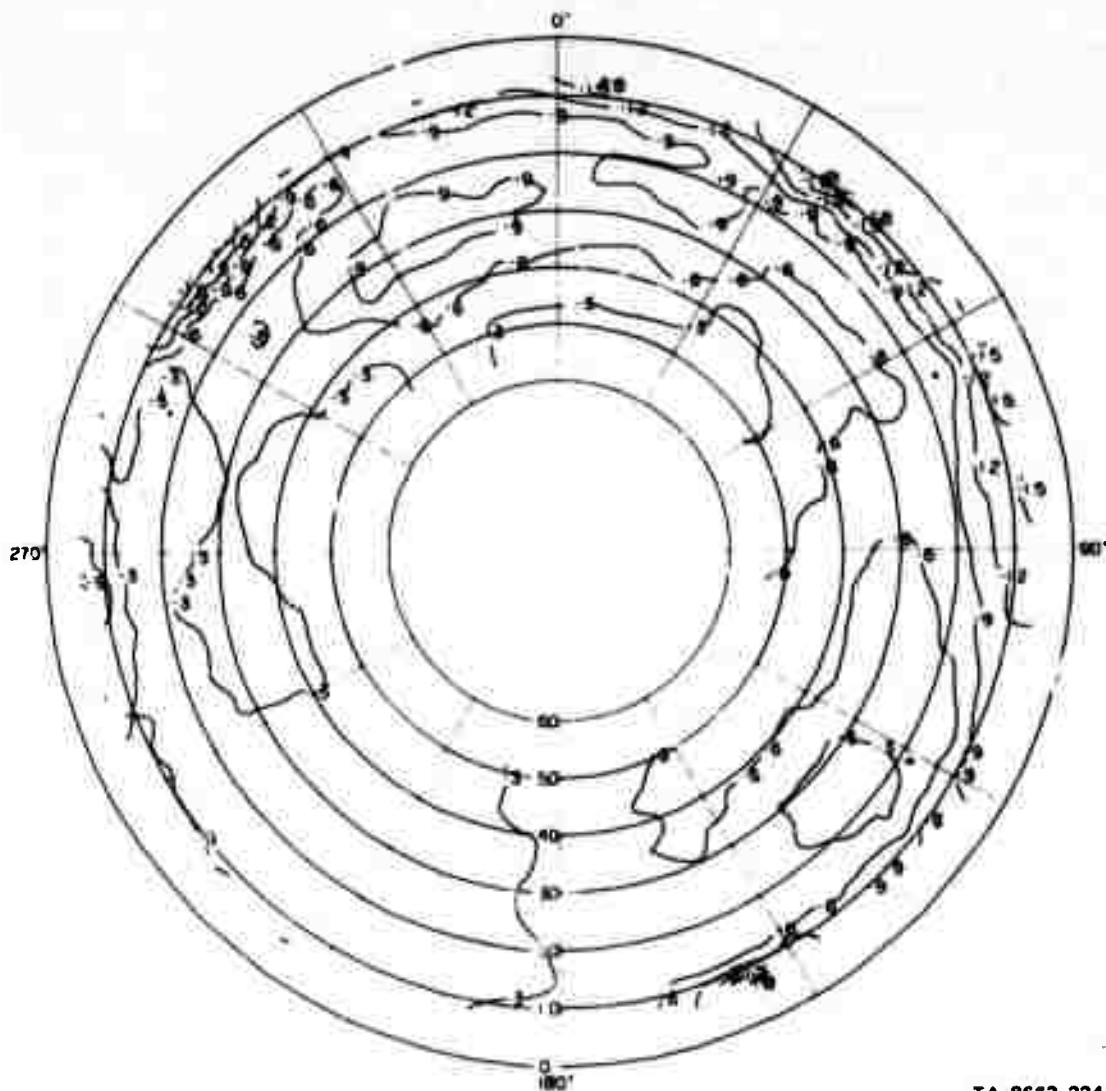
TA-8663-223

FIGURE B-4 CONTOUR PLOT OF THE MEDIAN RESPONSE OF THE HORIZONTAL FOLDED DIPOLE IN THE FOREST— E_{ϕ} AT 50 MHz

Table B-5

STANDARD DEVIATION ABOUT THE MEDIAN FOR THE VERTICAL SLEEVE DIPOLE
IN THE CLEARING-- E_0 AT 50 MHz

Elevation Azimuth	10.0	15.0	20.0	25.0	30.0	35.0	40.0	45.0	50.0
-170.0	1.56	1.06	1.02	1.03	1.06	1.06	1.06	0.97	0.82
-160.0	1.20	0.81	0.82	0.83	0.90	0.93	0.94	0.66	0.64
-150.0	1.63	0.99	1.10	1.25	1.01	0.95	0.88	0.54	0.56
-140.0	2.07	1.23	1.27	1.18	1.08	0.99	0.86	0.40	0.50
-130.0	1.96	0.95	0.93	0.90	1.13	1.36	1.16	0.66	0.62
-120.0	1.87	0.71	0.75	1.11	1.48	1.32	1.42	1.09	1.09
-110.0	1.23	0.72	0.78	2.43	1.91	1.23	1.11	0.94	1.28
-100.0	1.21	0.73	0.82	1.91	1.82	1.34	1.32	1.64	1.49
-90.0	1.51	1.01	0.94	0.78	1.13	1.01	1.20	1.70	1.73
-80.0	1.54	1.34	1.05	0.81	0.79	0.75	0.73	0.97	1.36
-70.0	1.31	1.20	1.35	1.28	1.31	0.94	0.76	0.78	0.73
-60.0	1.01	1.37	1.56	1.53	1.42	0.91	0.85	0.84	0.74
-50.0	1.08	1.89	1.65	1.54	1.53	0.68	0.85	0.78	0.87
-40.0	1.35	1.98	2.21	2.33	2.27	1.28	1.17	1.01	0.81
-30.0	1.64	2.34	2.71	2.79	2.38	1.34	1.32	1.23	0.94
-20.0	2.94	2.62	2.42	1.89	1.67	1.18	1.11	1.10	0.96
-10.0	2.36	2.19	1.94	1.55	1.46	1.28	0.93	1.03	0.59
0.0	2.30	1.63	1.81	1.72	1.93	2.12	1.41	1.02	0.45
10.0	2.45	2.26	2.40	2.03	1.93	1.96	1.30	1.19	0.86
20.0	3.92	2.75	2.64	1.94	1.80	1.41	0.88	0.95	0.99
30.0	2.84	2.71	2.30	1.60	1.55	1.52	0.98	0.91	0.75
40.0	1.94	1.96	2.11	1.49	1.55	1.66	1.16	1.11	0.99
50.0	2.97	2.33	2.52	1.55	1.58	1.60	1.28	1.27	1.24
60.0	3.88	3.28	2.86	1.61	1.53	1.46	1.16	1.15	1.21
70.0	3.09	2.75	2.76	1.51	1.46	1.31	1.09	1.14	1.09
80.0	2.45	2.12	2.29	1.37	1.35	1.35	1.15	1.21	0.90
90.0	2.68	1.87	1.85	1.09	1.19	1.33	1.11	1.05	0.69
100.0	2.55	1.62	1.49	0.70	0.82	0.85	0.82	0.80	0.72
110.0	2.25	1.50	1.24	0.57	0.56	0.57	0.70	0.79	0.87
120.0	1.90	0.85	1.00	0.63	0.69	0.75	0.89	0.92	0.99
130.0	2.22	1.10	0.93	0.70	0.75	0.78	0.79	0.76	0.85
140.0	2.15	1.71	1.50	1.26	1.18	0.95	1.10	1.11	1.03
150.0	1.32	1.91	1.96	2.08	1.67	1.17	1.25	1.67	1.15
160.0	1.14	1.63	1.78	1.91	1.91	1.45	1.27	--	0.96
170.0	1.80	1.36	1.43	1.67	1.75	1.25	1.16	--	0.94
180.0	1.95	1.38	1.34	1.57	1.58	1.45	1.25	--	0.94



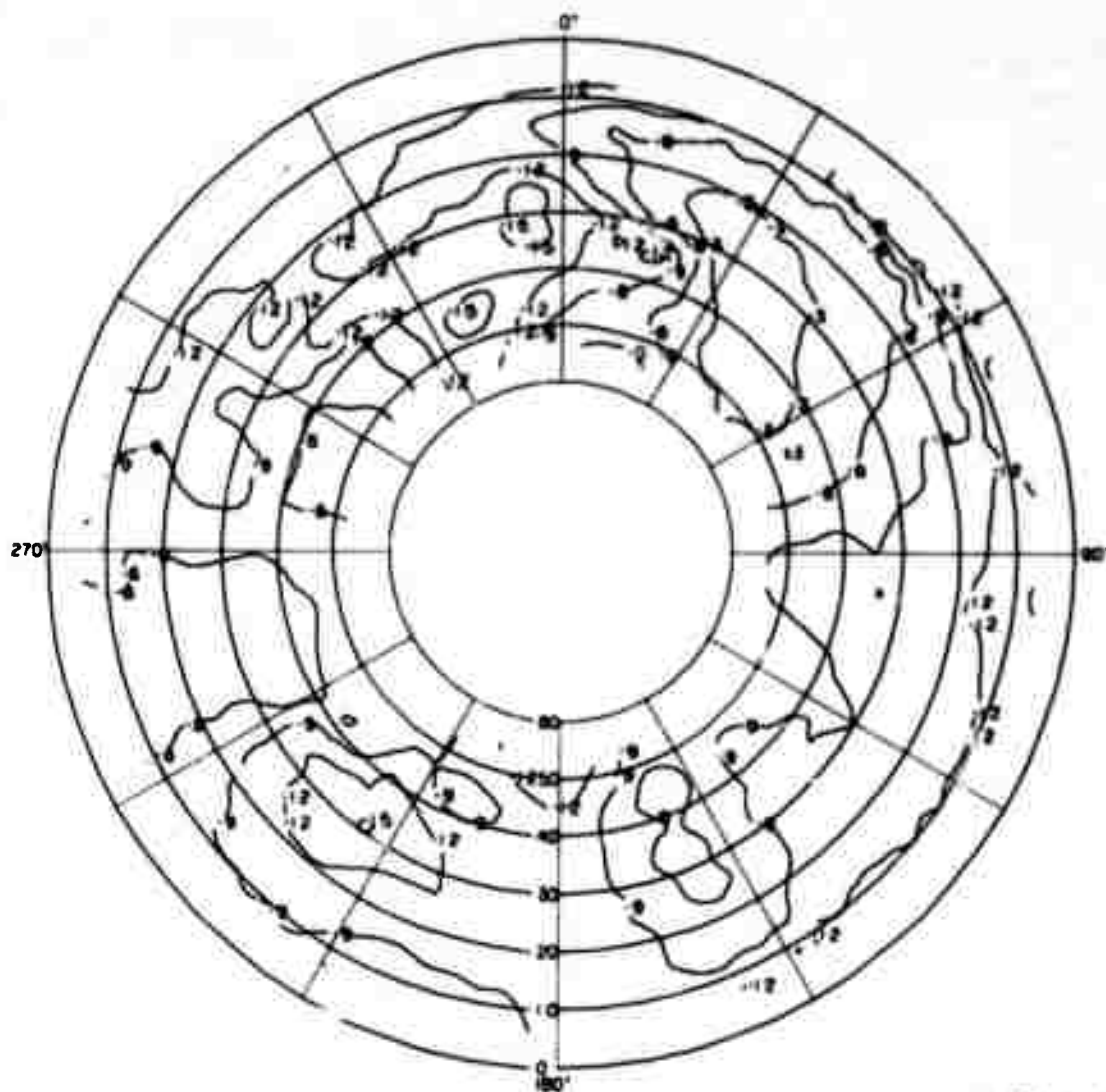
TA-8663-224

FIGURE B-5 CONTOUR PLOT OF THE MEDIAN RESPONSE OF THE VERTICAL SLEEVE DIPOLE IN THE CLEARING— E_{θ} AT 50 MHz

Table B-6

STANDARD DEVIATIONS ABOUT THE MEDIAN FOR THE VERTICAL SLEEVE DIPOLE
IN THE CLEARING--E₀ AT 50 MHz

Elevation Azimuth	5.0	10.0	15.0	20.0	25.0	30.0	35.0	40.0	45.0
-170.0	--	2.71	3.27	3.26	2.97	2.65	1.90	2.10	2.60
-160.0	0.0	2.41	2.55	2.47	2.09	2.18	1.44	1.24	1.44
-150.0	--	2.37	2.26	2.29	2.02	1.98	1.75	1.83	1.73
-140.0	0.0	2.39	2.68	2.76	2.77	2.40	2.40	2.65	2.91
-130.0	--	2.28	2.90	2.76	2.75	2.86	2.83	2.81	2.23
-120.0	--	1.94	2.42	2.41	2.30	2.53	2.55	2.42	1.95
-110.0	--	1.39	1.66	1.87	1.97	1.69	1.49	1.68	1.41
-100.0	--	1.65	2.08	1.78	1.63	1.13	1.24	1.20	1.00
-90.0	--	2.29	2.18	2.47	2.73	2.52	1.87	1.53	1.32
-80.0	--	3.12	3.18	3.15	3.34	3.17	2.00	1.60	1.49
-70.0	--	3.20	3.26	3.23	2.94	2.03	1.35	1.69	1.78
-60.0	--	2.94	2.94	2.82	2.72	2.15	1.70	1.70	1.90
-50.0	--	2.79	2.75	2.62	2.73	2.47	2.01	1.82	1.62
-40.0	--	2.77	2.39	2.41	2.23	1.75	1.69	1.88	1.92
-30.0	--	2.44	2.28	2.19	1.99	1.74	1.99	1.98	2.18
-20.0	--	2.21	2.32	2.39	2.09	2.26	2.29	2.22	1.99
-10.0	--	2.94	3.01	2.74	1.90	1.93	1.78	1.89	1.68
0.0	--	3.44	3.57	3.33	3.17	2.21	1.87	1.94	2.31
10.0	--	2.40	2.33	2.57	2.82	1.46	1.52	1.36	1.58
20.0	0.0	1.72	1.85	1.51	1.19	1.04	0.95	1.02	1.01
30.0	--	2.07	1.47	1.55	1.29	1.30	0.95	0.93	1.01
40.0	--	2.20	1.70	1.95	1.68	1.47	1.22	0.81	0.70
50.0	--	2.24	2.24	2.11	1.94	1.48	1.29	0.82	0.71
60.0	--	1.94	2.12	2.27	1.59	1.43	1.30	0.98	1.00
70.0	--	1.92	2.34	2.21	1.59	1.44	1.26	1.27	1.47
80.0	--	2.10	2.53	2.32	1.88	1.90	1.98	1.99	1.82
90.0	--	1.97	2.26	2.38	2.27	2.39	2.54	2.45	2.29
100.0	--	2.07	2.44	2.37	2.29	2.35	2.44	2.43	2.66
110.0	--	2.04	2.50	2.45	2.29	2.23	2.08	2.05	1.93
120.0	--	1.90	2.46	2.46	2.40	2.47	2.28	2.10	1.88
130.0	--	2.13	2.47	2.60	2.64	2.61	2.42	2.51	2.50
140.0	--	2.16	2.20	2.34	2.33	2.19	1.98	2.05	2.32
150.0	--	1.90	1.69	1.79	1.64	1.67	1.46	1.54	1.66
160.0	0.0	1.95	1.84	1.62	1.45	1.68	1.64	1.43	1.10
170.0	--	2.35	2.81	2.54	2.58	2.43	2.29	2.09	1.96
180.0	0.0	2.65	3.30	3.62	3.76	3.23	2.65	2.82	2.80



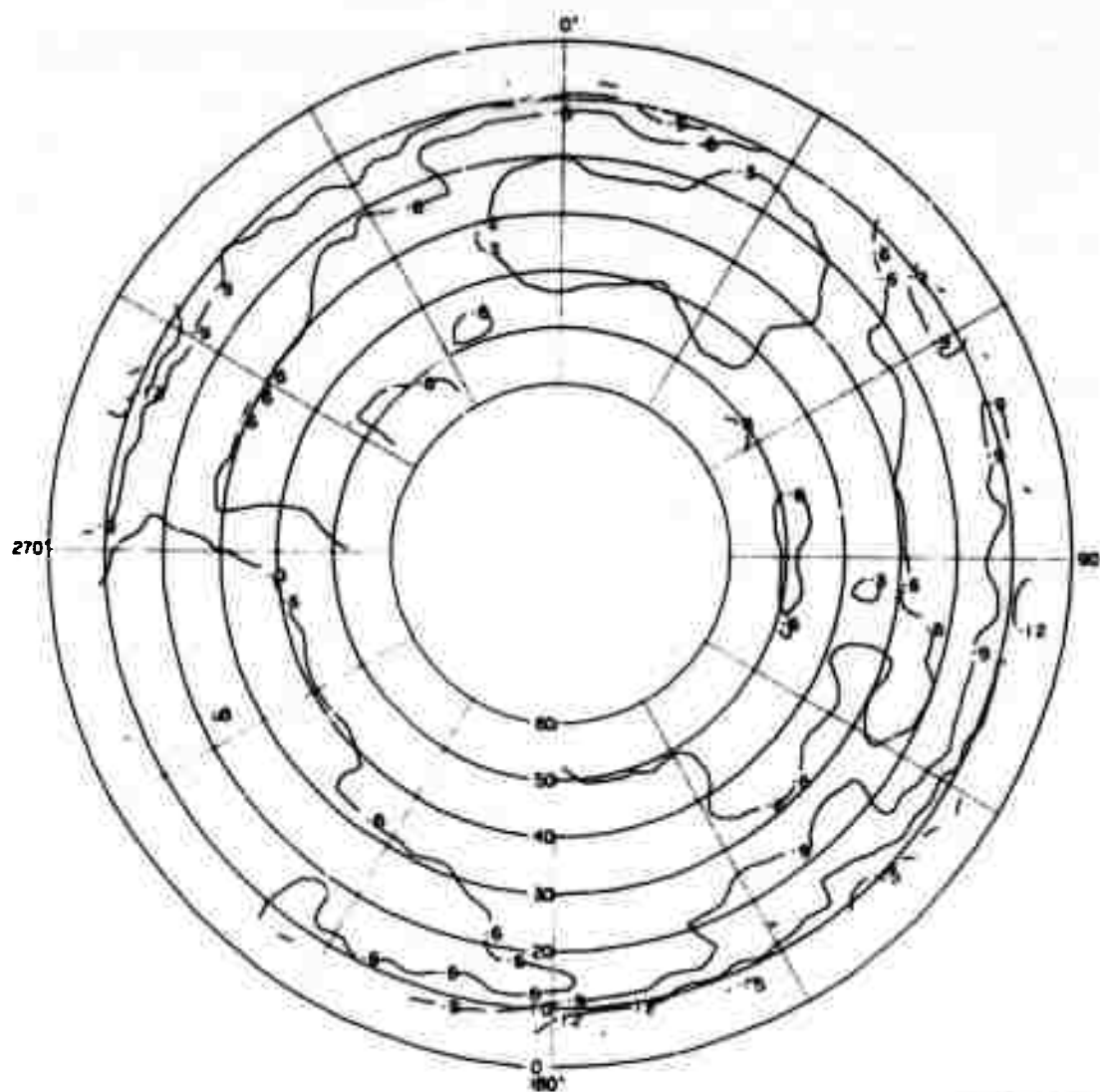
TA-8663-225

FIGURE B-6 CONTOUR PLOT OF THE MEDIAN RESPONSE OF THE VERTICAL SLEEVE DIPOLE IN THE CLEARING— E_{ϕ} AT 50 MHz

Table B-7

STANDARD DEVIATIONS ABOUT THE MEDIAN FOR THE VERTICAL FOLDED DIPOLE
IN THE FOREST-- E_{θ} AT 50 MHz

Elevation Azimuth	10.0	15.0	20.0	25.0	30.0	35.0	40.0	45.0	50.0
-170.0	3.50	2.35	1.99	1.22	1.07	0.96	0.92	0.95	1.23
-160.0	4.01	2.68	2.23	1.31	1.44	1.34	1.13	0.96	0.92
-150.0	2.47	2.27	2.53	2.36	1.73	1.52	1.36	1.11	0.95
-140.0	2.67	2.32	1.88	1.33	1.63	1.38	1.44	1.03	0.86
-130.0	1.98	1.48	1.81	1.18	1.25	1.00	0.93	0.72	0.85
-120.0	2.34	2.11	2.26	1.64	1.23	0.83	0.96	0.79	0.75
-110.0	2.86	2.67	2.13	1.25	1.41	1.20	1.35	0.83	0.72
-100.0	2.42	2.01	1.99	1.46	1.76	1.96	1.43	0.71	0.60
-90.0	2.53	1.90	1.81	1.26	1.49	1.39	1.29	0.74	0.88
-80.0	3.19	2.10	2.05	1.52	1.34	1.03	0.91	0.76	0.79
-70.0	3.87	2.39	2.68	1.56	1.61	0.93	0.81	0.57	0.54
-60.0	3.91	4.14	3.33	2.05	1.81	0.87	0.75	0.63	0.86
-50.0	3.80	3.38	3.49	2.40	1.94	0.99	0.80	0.62	0.68
-40.0	4.06	2.83	2.73	1.47	1.30	0.73	0.68	0.67	0.59
-30.0	4.89	3.62	2.44	0.77	0.88	0.54	0.73	1.00	0.75
-20.0	4.08	2.37	2.25	1.47	1.10	0.86	0.75	0.86	0.88
-10.0	4.03	1.33	1.46	1.28	1.18	0.98	0.98	0.01	0.87
0.0	4.55	2.52	1.93	1.14	1.14	1.16	0.99	0.82	0.68
10.0	4.67	3.19	2.34	1.52	1.08	0.90	0.77	0.74	0.51
20.0	3.97	1.90	1.79	0.96	1.03	1.22	0.93	0.76	0.59
30.0	2.09	1.27	1.23	1.22	1.06	1.01	0.86	0.80	0.64
40.0	2.06	1.37	1.31	1.17	1.00	1.14	0.83	0.78	0.99
50.0	2.56	1.47	1.60	1.76	1.32	1.24	0.87	0.78	1.31
60.0	3.60	1.96	1.90	2.12	1.41	1.19	0.73	0.86	1.10
70.0	3.05	2.37	2.47	2.23	1.44	1.62	0.91	0.85	0.77
80.0	3.64	3.24	3.08	2.90	1.86	1.82	1.09	0.86	0.50
90.0	3.82	3.38	3.26	3.25	2.20	1.82	0.91	0.99	0.64
100.0	3.99	2.62	3.17	3.28	2.27	1.98	1.19	1.18	0.83
110.0	4.03	2.78	2.41	2.43	1.75	2.00	1.09	0.94	0.64
120.0	3.85	2.75	2.92	2.46	1.52	1.29	0.78	0.80	0.52
130.0	5.27	4.79	3.86	3.52	2.28	1.75	0.86	0.69	0.69
140.0	4.51	4.05	3.88	3.18	1.88	1.39	1.00	1.06	1.00
150.0	3.70	2.46	2.60	1.58	1.35	1.18	1.14	1.36	1.19
160.0	3.90	2.77	2.46	1.41	1.22	0.94	1.15	--	0.90
170.0	3.04	2.04	2.12	1.82	1.50	0.98	1.05	--	0.93
180.0	2.65	1.40	1.43	0.99	1.27	1.38	1.37	--	1.27



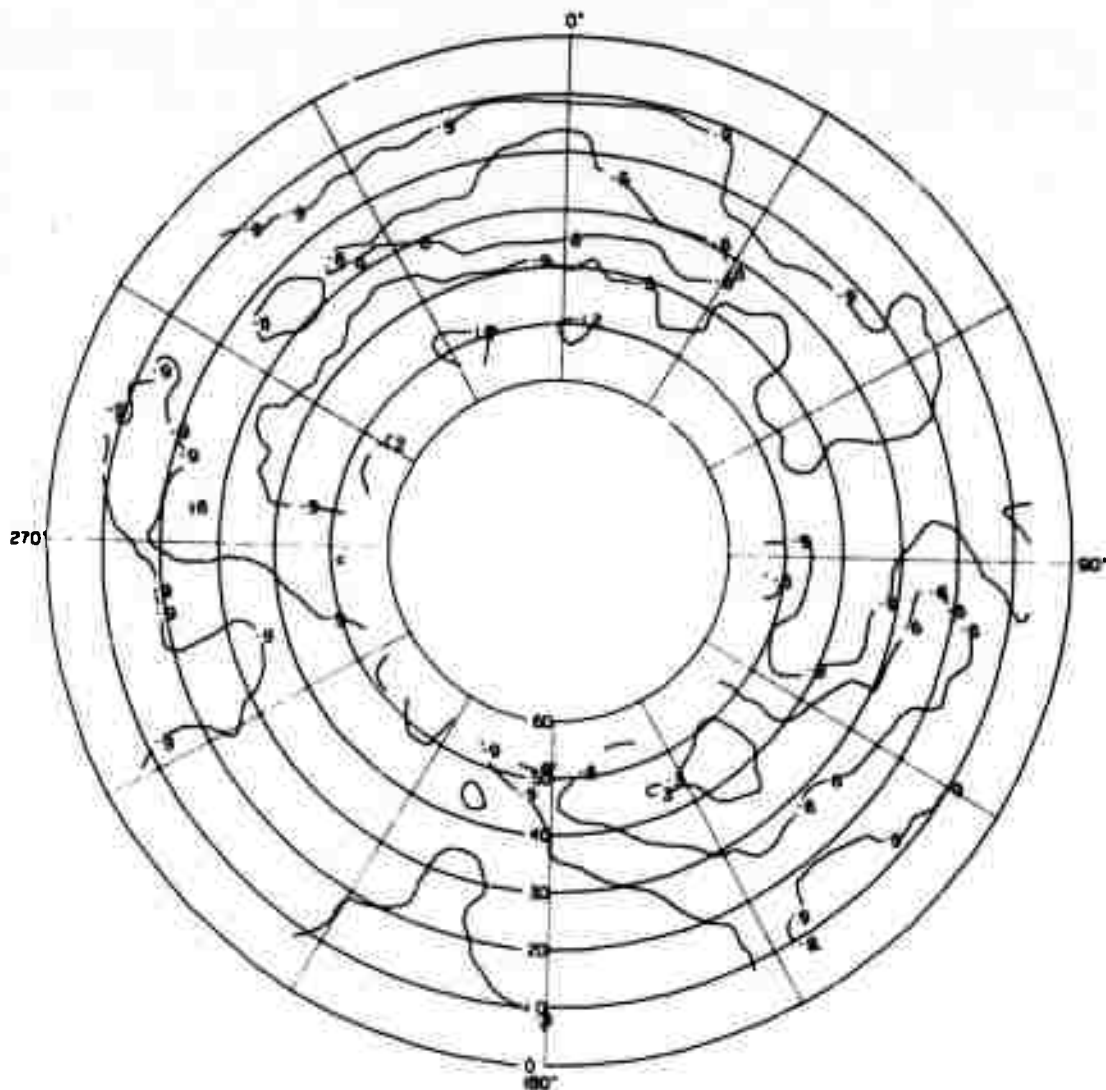
TA-8663-226

FIGURE B-7 CONTOUR PLOT OF THE MEDIAN RESPONSE OF THE VERTICAL FOLDED DIPOLE IN THE FOREST— E_θ AT 50 MHz

Table B-8

STANDARD DEVIATIONS ABOUT THE MEDIAN FOR THE VERTICAL FOLDED DIPOLE
IN THE FOREST-- E_{ϕ} AT 50 MHz

Elevation Azimuth	5.0	10.0	15.0	20.0	25.0	30.0	35.0	40.0	45.0
-170.0	--	3.04	2.49	2.16	1.77	1.85	2.23	2.38	2.55
-160.0	0.0	3.02	2.77	2.39	2.28	2.47	2.39	1.98	1.92
-150.0	--	3.03	3.07	3.11	2.88	2.48	2.11	2.02	1.82
-140.0	0.0	2.43	2.51	2.71	2.31	2.27	1.97	2.01	1.76
-130.0	--	2.84	2.48	2.31	1.86	1.89	1.86	1.96	1.44
-120.0	--	3.06	2.59	2.47	2.14	2.09	2.24	2.34	1.51
-110.0	--	2.60	2.49	2.52	2.20	2.21	2.44	2.50	1.89
-100.0	--	2.70	2.55	2.33	2.29	2.39	2.66	2.67	1.65
-90.0	--	2.51	2.44	2.65	3.07	2.95	2.92	2.98	1.90
-80.0	--	2.46	2.35	2.49	3.00	2.96	3.12	2.85	2.39
-70.0	--	2.26	2.25	2.18	2.34	2.64	2.79	2.30	2.34
-60.0	--	2.46	2.17	1.93	1.88	1.70	1.82	1.92	1.77
-50.0	--	2.78	2.14	1.84	1.60	1.37	1.76	1.96	2.22
-40.0	--	2.85	2.06	1.99	2.03	1.95	2.20	2.05	1.96
-30.0	--	3.03	2.33	2.29	2.15	2.22	2.27	2.09	1.71
-20.0	--	2.83	2.62	2.18	1.85	2.89	3.35	2.67	2.05
-10.0	--	2.33	1.92	2.03	1.51	1.88	2.05	1.95	1.67
0.0	--	2.56	2.28	2.08	1.70	1.15	1.25	1.57	1.53
10.0	--	3.40	3.29	2.59	2.20	1.69	1.64	1.43	1.44
20.0	--	2.93	2.39	2.35	2.30	2.06	1.94	1.63	1.70
30.0	--	2.35	2.24	2.57	2.62	2.62	2.65	2.18	2.23
40.0	--	2.67	2.93	2.78	2.61	2.59	2.38	2.05	2.24
50.0	--	2.71	2.90	2.84	2.84	3.04	3.19	2.78	2.70
60.0	--	2.51	2.50	2.54	2.52	3.10	3.46	3.07	2.81
70.0	--	2.72	2.53	2.43	2.32	2.35	2.85	2.64	2.16
80.0	--	2.18	2.28	2.66	2.97	2.77	2.22	2.29	2.58
90.0	--	2.32	2.35	2.67	3.23	3.11	2.43	2.49	2.91
100.0	--	3.38	3.03	2.32	1.96	2.39	2.92	2.61	2.32
110.0	--	2.70	2.71	2.55	2.05	2.22	2.54	2.82	2.29
120.0	--	2.40	2.78	2.91	2.92	2.63	2.31	2.44	2.79
130.0	--	2.24	2.75	2.85	2.69	2.25	1.58	1.64	1.99
140.0	0.0	2.48	2.38	2.48	2.15	1.54	0.89	0.95	0.82
150.0	--	2.97	2.69	2.21	1.61	1.90	1.66	1.40	1.07
160.0	--	2.60	2.30	2.35	2.32	2.31	2.41	1.85	1.60
170.0	--	2.76	2.05	2.10	1.97	2.17	2.10	2.01	1.59
180.0	0.0	3.19	2.55	2.16	1.85	2.15	2.45	2.13	1.78



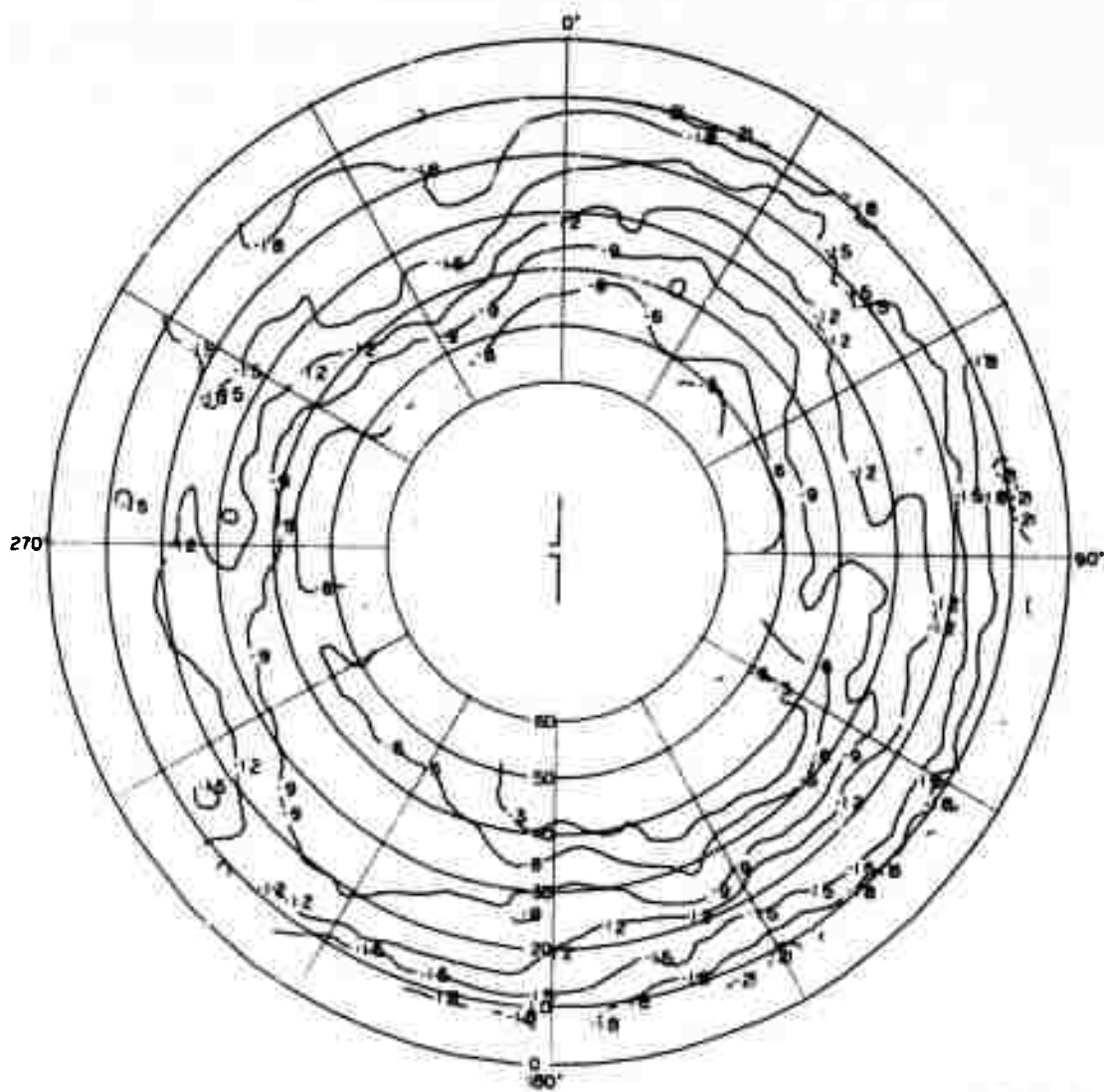
TA-8663-227

FIGURE B-8 CONTOUR PLOT OF THE MEDIAN RESPONSE OF THE VERTICAL FOLDED DIPOLE IN THE FOREST— E_ϕ AT 50 MHz

Table B-9

STANDARD DEVIATIONS ABOUT THE MEDIAN FOR THE HORIZONTAL UNBALANCED DIPOLE
IN THE FOREST-- E_{θ} AT 75 MHz

Elevation Azimuth	10.0	15.0	20.0	25.0	30.0	35.0	40.0	45.0	50.0
-170.0	3.02	4.10	4.16	4.20	4.15	3.90	3.21	2.42	1.68
-160.0	3.31	4.24	4.66	4.79	4.59	4.46	4.29	3.31	2.35
-150.0	3.62	4.11	4.45	4.99	4.59	4.30	4.29	3.21	2.50
-140.0	3.32	3.57	3.46	3.30	3.85	3.82	3.53	2.76	2.50
-130.0	3.39	3.96	3.96	3.71	3.75	3.72	3.61	3.48	3.48
-120.0	4.37	4.12	4.39	4.46	4.12	4.08	4.28	4.11	3.86
-110.0	4.19	3.71	3.99	3.62	3.79	3.83	3.73	3.79	3.79
-100.0	4.41	4.11	3.61	3.27	3.34	3.63	3.73	3.94	3.89
-90.0	3.63	3.85	3.69	3.45	3.53	3.56	3.72	4.38	4.40
-80.0	3.16	3.39	3.89	3.95	3.63	4.15	4.32	5.30	5.24
-70.0	3.81	3.56	3.56	3.59	3.68	4.17	4.77	6.09	5.87
-60.0	4.01	3.74	3.67	3.74	3.72	3.76	3.92	4.80	5.14
-50.0	3.75	3.71	3.80	3.88	3.85	3.96	3.88	4.16	3.97
-40.0	3.50	3.62	3.65	3.68	3.78	3.93	4.30	3.94	3.03
-30.0	3.56	3.90	3.77	4.15	4.19	4.29	3.88	2.63	2.09
-20.0	3.47	3.33	3.61	4.07	4.21	3.87	3.47	2.41	1.62
-10.0	3.44	3.57	3.40	3.93	3.86	3.67	3.52	3.41	2.13
0.0	3.30	3.18	3.43	3.71	3.62	3.28	3.36	3.63	2.93
10.0	2.22	2.98	3.34	4.19	3.85	4.11	3.52	2.91	2.46
20.0	2.33	2.98	2.85	3.07	3.35	3.60	3.51	3.69	2.57
30.0	2.43	3.32	3.24	3.52	3.32	3.09	3.12	3.07	2.32
40.0	2.94	3.37	3.46	3.59	2.95	2.46	2.94	3.27	2.61
50.0	2.79	2.94	3.16	3.16	2.46	2.34	2.83	3.26	3.08
60.0	3.18	3.45	3.42	3.48	3.37	3.69	3.75	3.71	3.28
70.0	3.37	3.72	3.66	3.80	4.09	4.25	4.43	4.80	4.96
80.0	2.76	3.46	3.81	3.98	4.34	4.20	4.05	4.35	5.17
90.0	3.03	3.50	3.78	4.06	4.15	4.19	3.96	3.31	4.33
100.0	3.31	3.93	3.76	3.61	3.43	3.51	3.60	3.56	4.61
110.0	3.07	4.08	3.75	3.41	2.74	2.96	3.43	4.24	4.85
120.0	2.65	3.90	3.97	3.89	2.88	2.80	2.58	3.04	3.41
130.0	3.13	4.38	4.11	4.24	2.79	2.34	1.58	1.56	1.65
140.0	3.13	4.25	3.91	3.94	2.83	2.72	1.98	1.78	1.73
150.0	2.47	3.46	3.87	3.74	3.47	2.50	2.10	1.98	1.63
160.0	3.14	4.49	4.40	4.50	4.16	2.69	2.14	1.59	1.26
170.0	3.15	4.20	4.31	3.99	3.85	2.68	2.38	--	1.78
180.0	3.36	4.34	4.42	4.74	4.15	2.68	2.27	--	2.12



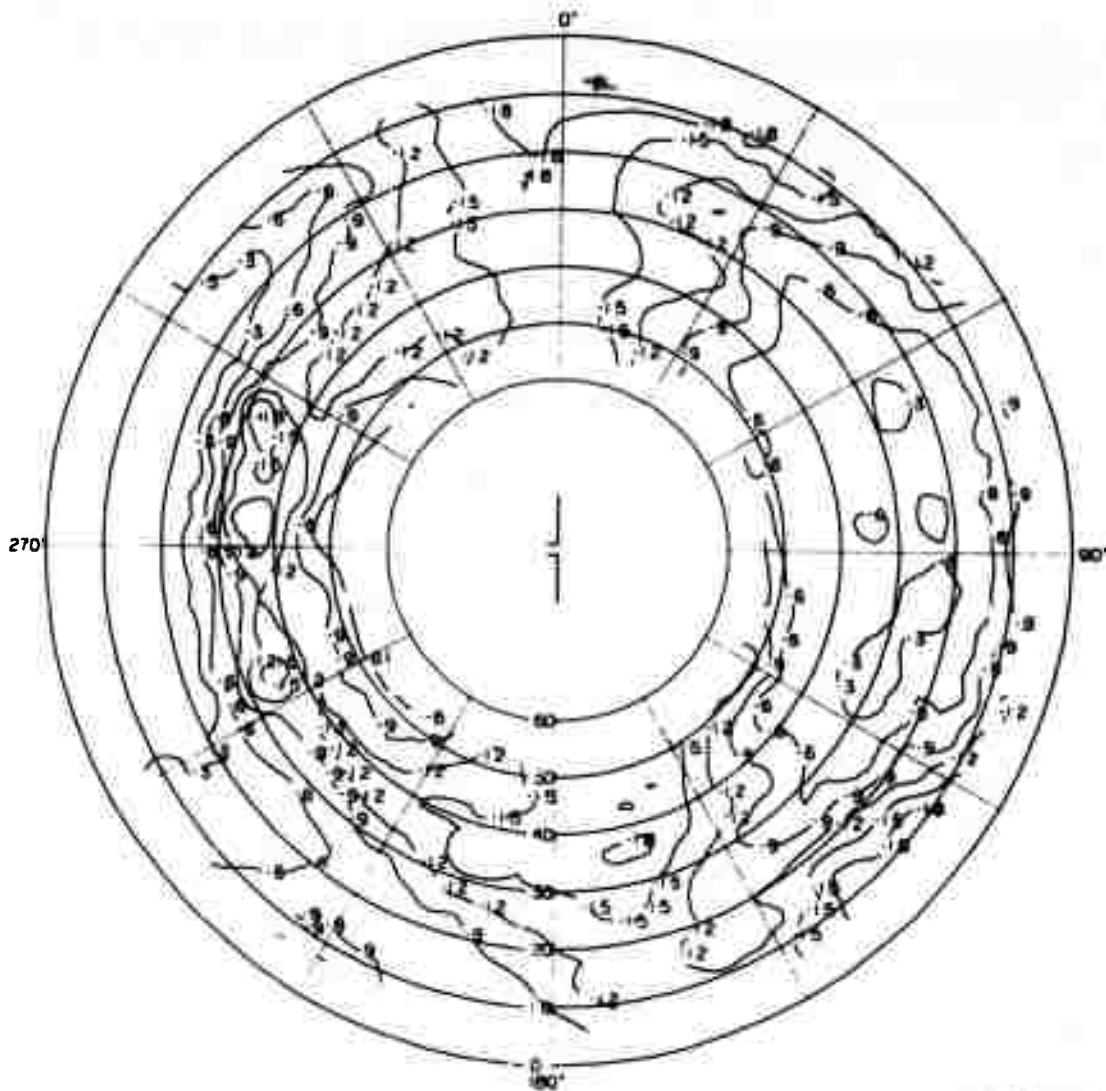
TA-8663-228

FIGURE B-9 CONTOUR PLOT OF THE MEDIAN RESPONSE OF THE HORIZONTAL UNBALANCED DIPOLE IN THE FOREST— E_0 AT 75 MHz

Table B-10

STANDARD DEVIATIONS ABOUT THE MEDIAN FOR THE HORIZONTAL UNBALANCED DIPOLE
IN THE FOREST--E_φ AT 75 MHz

Elevation Azimuth	5.0	10.0	15.0	20.0	25.0	30.0	35.0	40.0	45.0
-170.0	--	2.04	2.89	3.42	4.06	3.86	3.56	3.79	3.55
-160.0	0.0	2.42	2.87	3.32	4.07	3.30	2.66	3.55	4.43
-150.0	--	3.58	2.86	2.75	1.90	2.73	2.84	2.56	3.02
-140.0	--	4.64	3.50	3.28	2.17	2.15	2.20	2.33	2.48
-130.0	--	4.18	3.04	3.14	2.04	2.20	3.01	3.43	3.73
-120.0	0.0	3.98	2.95	2.93	2.29	2.11	2.52	2.94	3.55
-110.0	--	3.36	2.87	2.52	1.34	1.43	1.51	2.03	2.78
-100.0	--	2.12	1.71	2.00	1.31	1.29	1.81	2.15	2.76
-90.0	--	1.84	1.37	1.42	1.08	1.32	1.81	1.91	2.35
-80.0	--	1.36	1.27	1.27	0.99	0.81	1.25	1.81	2.32
-70.0	--	1.66	1.44	1.46	1.43	0.81	1.16	1.50	1.72
-60.0	--	2.04	1.53	1.53	1.48	1.09	1.44	1.57	1.57
-50.0	--	2.78	1.65	1.73	1.83	1.97	1.80	1.86	2.14
-40.0	--	3.05	1.67	1.78	2.02	2.23	1.79	1.79	1.41
-30.0	--	3.06	2.28	2.29	2.10	1.98	2.12	2.11	1.78
-20.0	--	3.71	3.47	3.13	3.37	3.29	3.44	3.03	3.21
-10.0	--	3.76	3.61	3.52	3.43	3.76	3.61	3.50	3.46
0.0	--	3.22	3.53	3.95	3.26	3.23	3.88	4.14	4.30
10.0	--	3.96	4.49	3.95	2.38	3.05	4.03	4.62	4.94
20.0	--	3.41	3.17	2.60	1.90	3.20	3.63	3.98	3.31
30.0	--	2.32	1.55	1.48	1.12	2.96	3.94	3.10	2.03
40.0	--	2.02	1.57	1.48	1.60	2.36	2.82	1.90	1.69
50.0	--	2.46	1.86	1.69	1.80	1.98	1.68	1.38	1.51
60.0	--	1.55	1.73	1.68	1.58	1.70	1.60	1.62	1.83
70.0	--	--	1.48	1.52	1.40	1.52	1.64	2.09	2.15
80.0	--	--	1.86	1.93	1.94	2.25	2.81	2.48	2.37
90.0	--	--	2.27	2.00	1.73	2.73	3.35	3.24	2.88
100.0	--	--	2.66	1.94	1.38	2.55	3.27	3.18	3.02
110.0	--	--	2.21	1.63	1.35	2.08	2.80	2.79	2.72
120.0	--	--	1.89	1.90	2.35	2.54	2.71	2.70	2.47
130.0	--	2.09	1.03	1.54	2.74	3.36	3.42	3.02	2.83
140.0	0.0	3.54	2.72	2.61	3.17	3.31	3.61	3.53	3.27
150.0	--	5.35	5.14	3.92	3.17	3.56	4.15	3.80	3.41
160.0	--	4.63	4.21	4.19	3.25	3.25	3.84	3.96	4.02
170.0	--	3.31	3.48	3.43	3.25	3.16	3.47	3.87	4.21
180.0	0.0	2.49	2.85	3.03	3.45	3.67	4.15	3.94	4.06



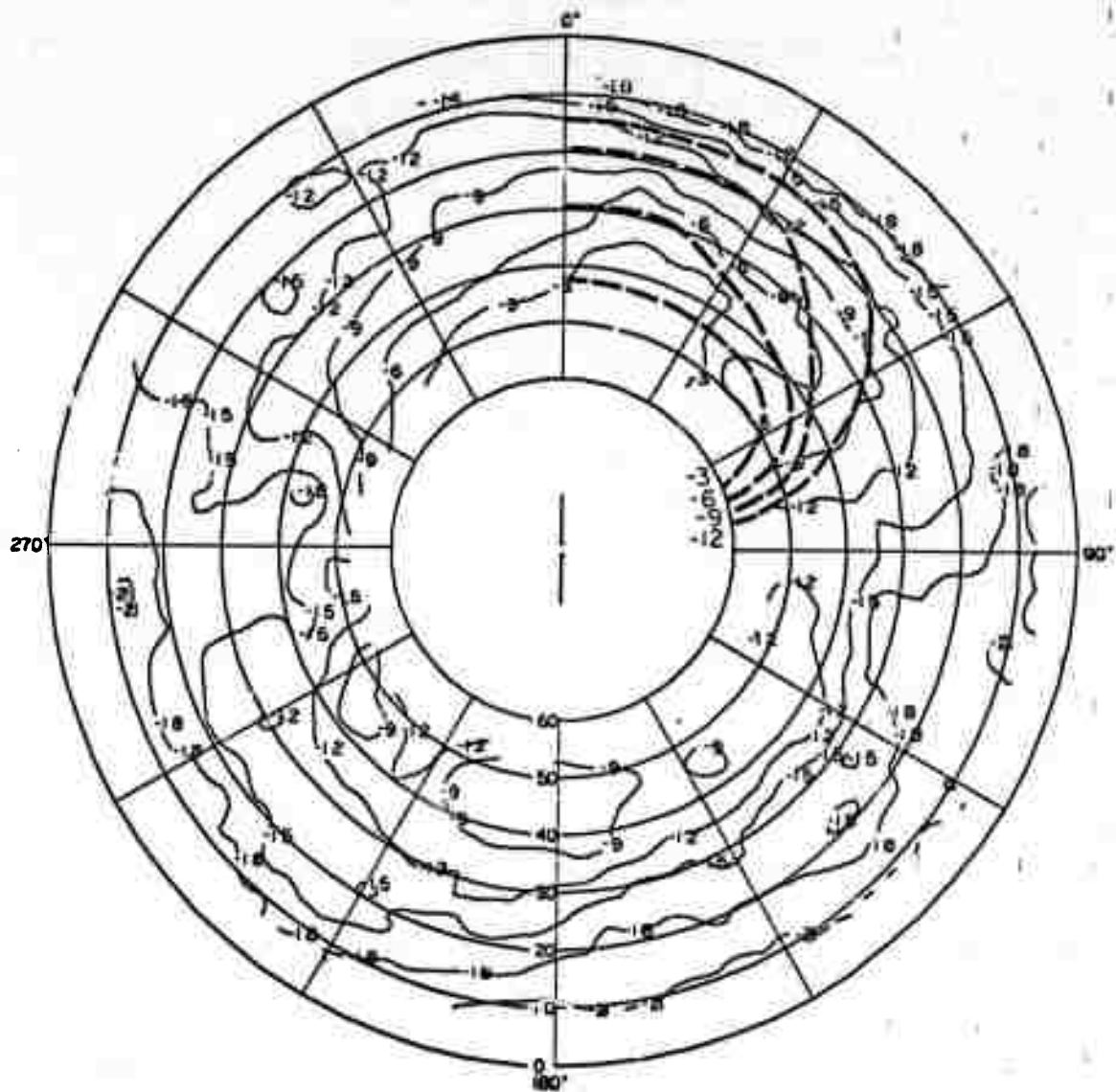
TA-8663-229

FIGURE B-10 CONTOUR PLOT OF THE MEDIAN RESPONSE OF THE HORIZONTAL UNBALANCED DIPOLE IN THE FOREST— E_{ϕ} AT 75 MHz

Table B-11

STANDARD DEVIATIONS ABOUT THE MEDIAN FOR THE HORIZONTAL DIPOLE WITH BALUN
IN THE FOREST-- E_{θ} AT 75 MHz

Elevation Azimuth	10.0	15.0	20.0	25.0	30.0	35.0	40.0	45.0	50.0
-170.0	2.22	2.65	2.74	2.41	2.35	2.08	1.91	1.41	0.84
-160.0	2.95	3.25	3.01	2.81	2.76	2.12	1.94	1.70	1.14
-150.0	3.21	3.38	3.52	3.54	3.19	2.95	2.23	1.83	1.61
-140.0	2.05	2.53	3.38	3.59	3.13	2.69	2.51	1.52	1.53
-130.0	2.95	3.17	3.08	2.59	2.53	2.38	2.06	1.21	1.33
-120.0	3.41	3.34	2.92	1.59	2.17	2.39	2.48	1.78	1.48
-110.0	3.19	2.80	2.72	1.89	2.11	2.38	2.85	2.37	1.84
-100.0	2.80	2.68	2.75	2.83	2.71	2.58	2.54	1.97	2.00
-90.0	2.88	3.05	3.23	2.78	2.89	2.86	2.46	1.91	1.88
-80.0	2.82	3.08	3.12	2.44	2.30	1.94	2.07	1.71	1.87
-70.0	3.53	3.17	3.15	2.60	2.06	1.94	2.20	2.29	1.52
-60.0	3.16	2.95	2.50	1.37	1.86	1.37	1.46	1.04	1.25
-50.0	3.30	3.03	3.02	2.56	2.13	1.47	0.89	0.49	0.72
-40.0	3.86	2.84	2.86	2.09	2.05	1.03	1.01	1.03	--
-30.0	3.46	3.05	3.03	3.04	2.00	0.70	1.02	1.05	--
-20.0	2.86	2.13	2.38	2.32	2.41	1.96	1.31	1.12	--
-10.0	1.85	1.46	2.04	2.36	1.89	1.06	1.30	0.99	0.74
0.0	2.37	2.08	1.85	1.57	1.71	1.55	1.19	0.90	0.58
10.0	2.71	2.20	2.13	1.81	1.72	1.33	1.14	1.01	0.85
20.0	2.83	3.01	2.56	2.05	1.92	1.99	1.43	1.25	0.87
30.0	3.28	3.96	3.15	2.03	2.10	2.39	1.74	1.26	0.80
40.0	3.24	3.49	3.13	1.69	1.70	1.28	1.41	1.54	0.99
50.0	3.43	3.29	3.28	1.67	1.44	1.27	1.13	1.20	1.05
60.0	4.10	4.35	3.72	2.22	1.68	1.52	1.14	0.91	0.90
70.0	4.51	3.87	3.50	2.60	2.05	1.63	1.23	1.48	1.75
80.0	3.44	3.14	3.03	2.49	2.38	2.85	1.99	1.71	1.61
90.0	3.44	3.18	2.91	2.88	2.74	2.96	2.28	1.68	1.34
100.0	2.82	2.39	2.53	2.45	2.79	2.47	2.01	2.35	1.57
110.0	2.81	2.52	2.51	2.35	2.94	3.53	2.60	2.37	1.30
120.0	3.26	2.93	2.64	2.44	2.89	2.95	2.22	1.99	0.90
130.0	2.81	3.18	3.14	2.79	2.78	2.86	1.96	1.90	0.87
140.0	2.49	3.06	3.04	2.76	2.50	2.51	1.74	1.58	1.04
150.0	3.15	4.15	3.40	2.86	2.47	2.21	1.47	1.56	1.23
160.0	2.84	3.68	3.52	3.35	3.02	2.93	2.02	1.52	1.02
170.0	2.45	3.29	3.39	2.74	2.82	2.57	1.81	1.52	0.83
180.0	2.22	2.94	2.92	2.48	2.48	2.32	1.78	1.58	0.89



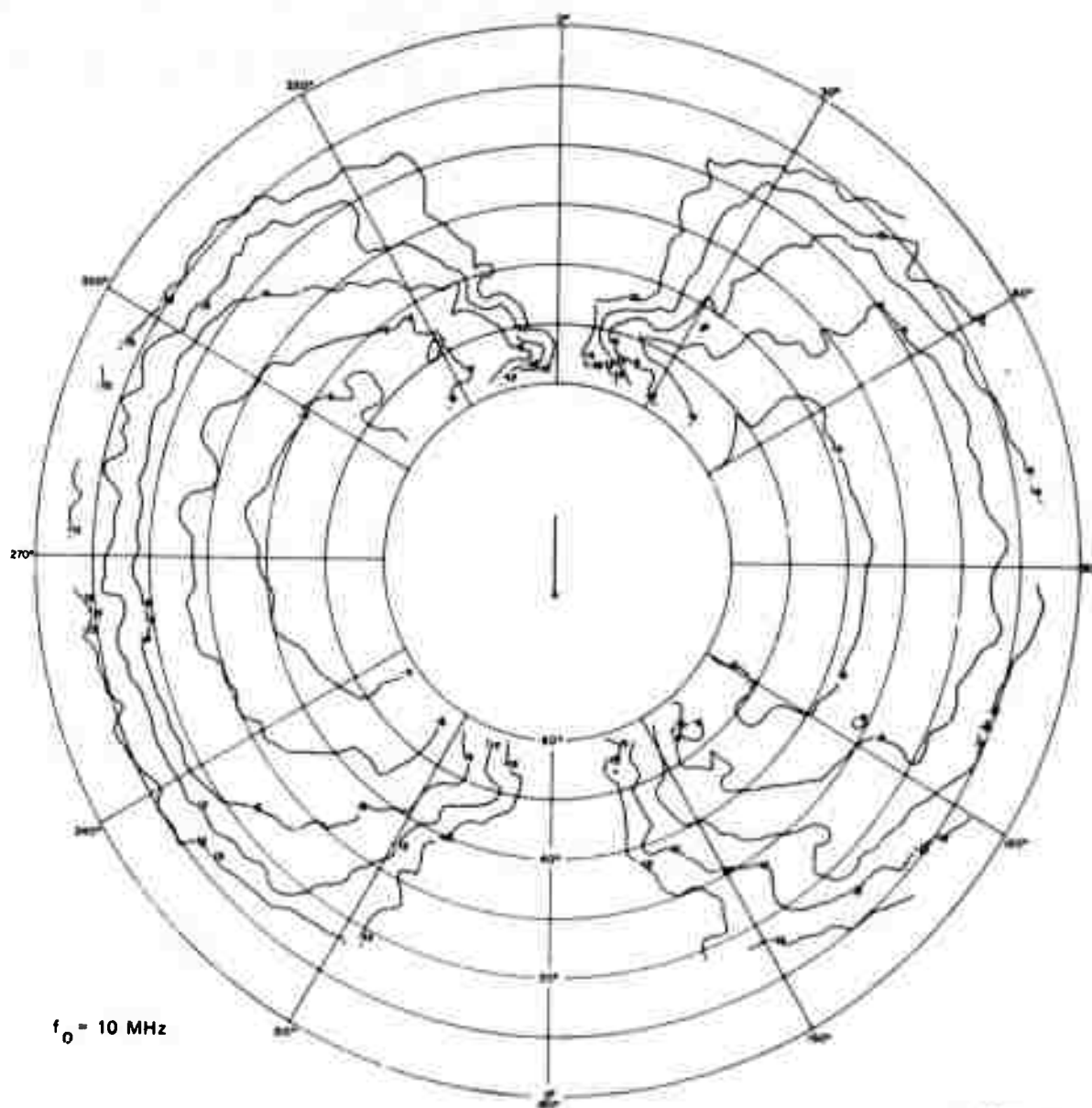
TA-8663-230

FIGURE B-11 CONTOUR PLOT OF THE MEDIAN RESPONSE OF THE HORIZONTAL DIPOLE WITH BALUN IN THE FOREST— E_θ AT 75 MHz

Table B-12

STANDARD DEVIATIONS ABOUT THE MEDIAN FOR THE HORIZONTAL DIPOLE WITH BALUN
IN THE FOREST--E_φ AT 75 MHz

Elevation Azimuth	5.0	10.0	15.0	20.0	25.0	30.0	35.0	40.0	45.0
-170.0	--	3.38	3.49	3.29	2.73	2.84	2.72	2.27	1.75
-160.0	0.0	2.94	2.45	2.54	1.88	2.39	2.64	2.65	2.51
-150.0	--	2.78	2.21	2.14	1.47	1.58	2.16	2.65	3.05
-140.0	0.0	2.41	1.53	1.46	0.93	0.94	1.48	1.95	2.37
-130.0	--	1.68	0.71	0.91	0.88	1.05	1.56	1.61	1.55
-120.0	--	1.43	0.81	0.79	1.02	1.12	1.53	1.45	1.29
-110.0	--	0.94	1.00	1.02	1.15	1.07	1.04	1.06	0.77
-100.0	--	0.67	0.83	0.92	0.89	0.81	0.79	0.67	0.55
-90.0	--	1.00	0.91	0.78	0.63	0.67	0.78	0.98	1.00
-80.0	0.0	0.84	0.72	0.74	0.56	0.78	0.99	0.89	0.69
-70.0	--	0.82	0.67	0.81	1.16	1.03	0.84	0.72	0.53
-60.0	--	0.97	0.61	0.87	0.79	0.98	1.00	0.83	0.87
-50.0	--	1.57	1.60	1.21	1.14	1.22	1.13	1.02	0.91
-40.0	--	1.43	1.30	1.33	1.22	1.41	1.45	1.43	1.11
-30.0	--	2.28	1.64	1.65	1.95	2.37	2.64	1.73	1.07
-20.0	0.0	1.93	1.41	2.02	2.39	3.41	3.35	2.86	2.66
-10.0	--	4.01	3.34	2.98	3.13	3.55	3.55	3.42	4.05
0.0	--	3.88	3.53	3.26	2.97	2.77	2.51	3.16	3.40
10.0	--	3.34	3.48	3.06	2.39	2.52	2.92	2.77	2.28
20.0	--	3.63	2.68	2.78	3.55	3.25	2.74	2.47	2.18
30.0	--	2.41	1.76	2.22	2.13	2.62	2.45	2.00	1.30
40.0	--	2.32	2.13	1.75	1.66	1.59	1.27	1.10	0.75
50.0	--	2.04	1.55	1.41	1.40	1.05	0.85	0.70	0.69
60.0	--	2.11	1.35	1.15	0.94	0.71	0.66	0.58	0.48
70.0	--	2.30	1.06	0.97	0.74	0.69	0.54	0.49	0.55
80.0	--	1.80	1.09	0.99	0.97	0.66	0.62	0.58	0.62
90.0	--	1.20	0.80	0.88	1.04	0.77	0.56	0.55	0.59
100.0	0.0	1.10	0.69	0.93	0.93	0.73	0.62	0.76	0.82
110.0	--	2.61	1.28	1.24	1.35	1.38	1.19	1.02	1.05
120.0	--	2.99	1.57	1.30	1.20	1.09	0.98	0.90	0.83
130.0	--	2.48	1.50	1.22	0.93	0.67	0.94	0.94	0.70
140.0	--	2.30	1.43	1.45	1.66	1.79	2.34	1.87	1.68
150.0	--	2.59	2.24	1.82	1.94	2.19	2.68	2.52	2.23
160.0	0.0	3.59	3.89	3.34	2.81	2.71	2.72	2.87	2.89
170.0	--	3.35	4.11	4.02	3.54	3.10	2.54	2.51	2.70
180.0	--	2.87	3.50	3.74	3.30	3.21	2.40	2.30	2.10



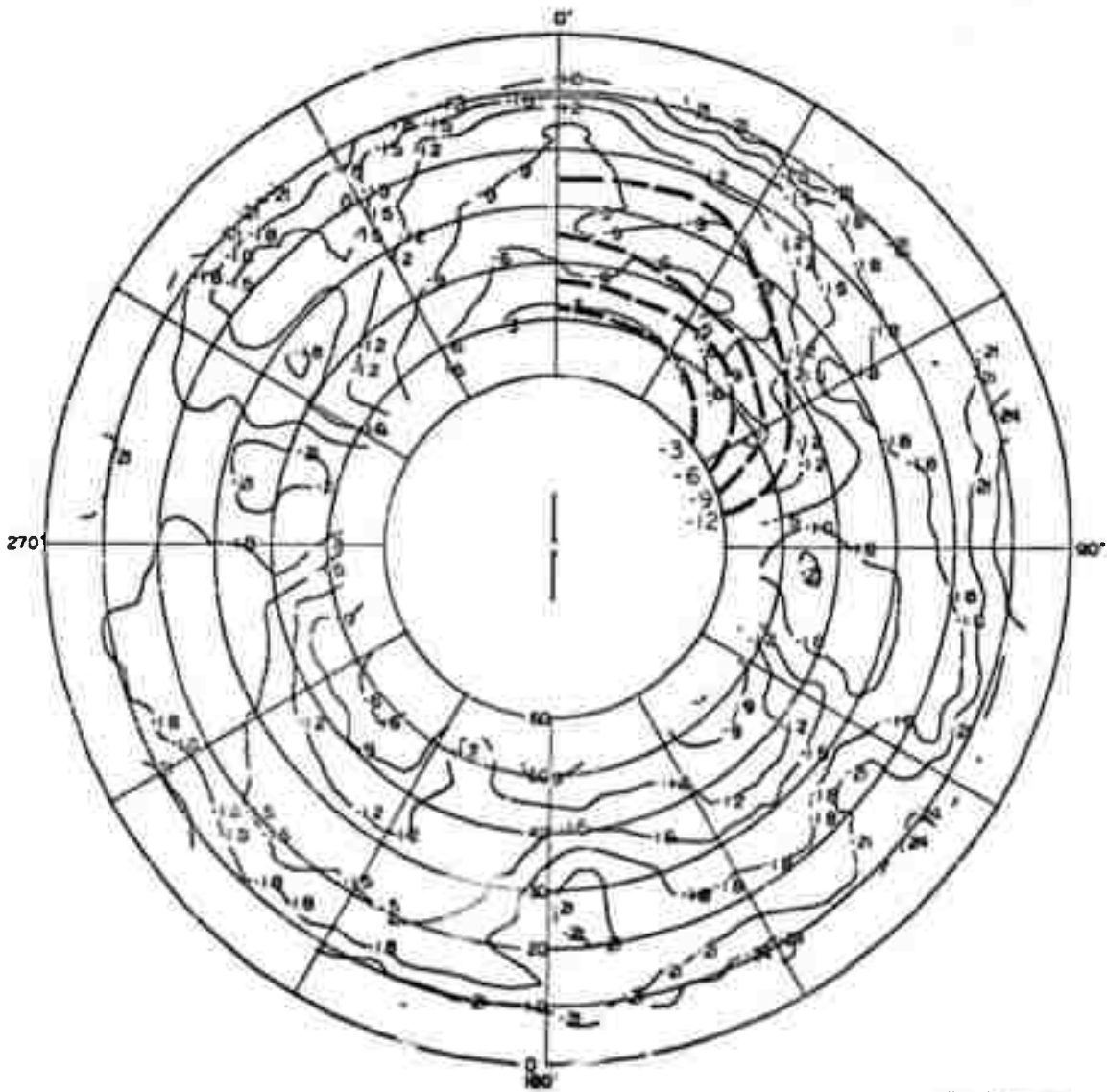
TA-8563-132

FIGURE A-38 MEASURED PATTERN OF 5:1 INVERTED-L ANTENNA IN FOREST
AT BAN MUN CHIT, E_ϕ AT 10 MHz

Table B-13

STANDARD DEVIATIONS ABOUT THE MEDIAN FOR THE HORIZONTAL BALANCED DIPOLE
IN THE FOREST--E_θ AT 75 MHz

Elevation Azimuth	10.0	15.0	20.0	25.0	30.0	35.0	40.0	45.0	50.0
-170.0	4.86	4.67	4.75	5.63	3.98	3.46	2.43	2.25	2.71
-160.0	4.01	3.90	3.48	2.77	2.89	2.68	2.66	1.78	2.90
-150.0	3.66	3.47	3.32	2.24	2.15	2.47	2.59	2.52	2.10
-140.0	4.02	4.13	3.34	2.33	2.00	2.01	1.84	0.97	1.43
-130.0	3.28	3.60	3.21	2.03	2.35	1.89	1.79	0.94	0.76
-120.0	4.68	4.42	3.73	2.45	2.83	2.24	2.12	1.12	1.14
-110.0	4.59	4.73	4.54	4.33	4.10	3.79	2.98	1.36	1.57
-100.0	3.69	3.30	3.99	4.75	4.31	3.64	3.72	2.91	2.18
-90.0	4.81	4.22	3.63	3.73	3.99	3.33	3.12	2.64	2.69
-80.0	4.72	4.65	5.01	4.22	3.62	2.56	2.47	2.13	1.95
-70.0	5.12	5.15	5.04	3.93	3.49	2.55	2.71	2.45	2.23
-60.0	5.19	4.58	4.41	3.18	3.17	2.72	2.76	2.20	2.19
-50.0	4.74	4.62	4.16	2.97	3.63	3.05	2.47	1.52	1.55
-40.0	4.94	5.52	5.16	4.34	4.41	2.78	2.26	1.37	1.47
-30.0	4.61	4.99	5.24	4.68	3.81	1.91	1.70	1.41	1.26
-20.0	3.90	4.03	4.24	4.12	3.30	1.79	1.50	1.49	1.34
-10.0	4.08	3.32	2.73	1.85	1.62	1.53	1.16	1.62	1.20
0.0	3.70	2.50	2.34	2.25	2.46	2.10	1.78	1.48	0.86
10.0	3.52	2.96	3.03	2.23	2.96	3.63	2.41	1.86	0.89
20.0	4.56	4.56	3.78	2.71	2.86	2.19	1.33	1.17	0.78
30.0	4.11	4.11	4.14	2.83	2.31	1.54	1.15	1.34	0.89
40.0	3.54	3.65	3.88	3.44	2.99	2.59	2.02	2.28	1.55
50.0	4.16	4.23	3.66	2.87	3.38	4.36	3.05	2.77	1.80
60.0	3.88	4.47	4.56	4.32	4.46	4.16	2.78	2.46	1.61
70.0	4.06	4.07	4.38	4.85	4.35	4.13	3.01	2.40	1.77
80.0	4.56	4.92	4.38	4.26	3.72	3.85	3.41	3.71	2.63
90.0	4.55	4.40	4.06	3.18	3.33	3.10	3.40	3.71	3.26
100.0	3.89	5.00	4.83	4.92	4.27	4.34	3.82	3.52	3.92
110.0	2.79	3.53	4.28	4.80	3.64	3.47	2.89	3.83	3.77
120.0	3.13	3.94	4.28	4.27	2.99	1.72	1.24	1.90	1.89
130.0	3.11	4.52	4.53	4.79	3.13	1.36	0.87	0.76	0.93
140.0	3.22	3.95	4.53	5.55	3.57	1.95	1.56	1.18	1.35
150.0	3.50	3.71	3.67	3.36	3.24	3.39	2.77	1.82	1.73
160.0	3.80	3.95	3.98	3.27	3.45	3.36	2.96	2.75	2.31
170.0	4.34	4.93	4.11	3.90	3.48	3.45	3.35	--	2.63
180.0	--	--	--	--	--	--	--	--	--



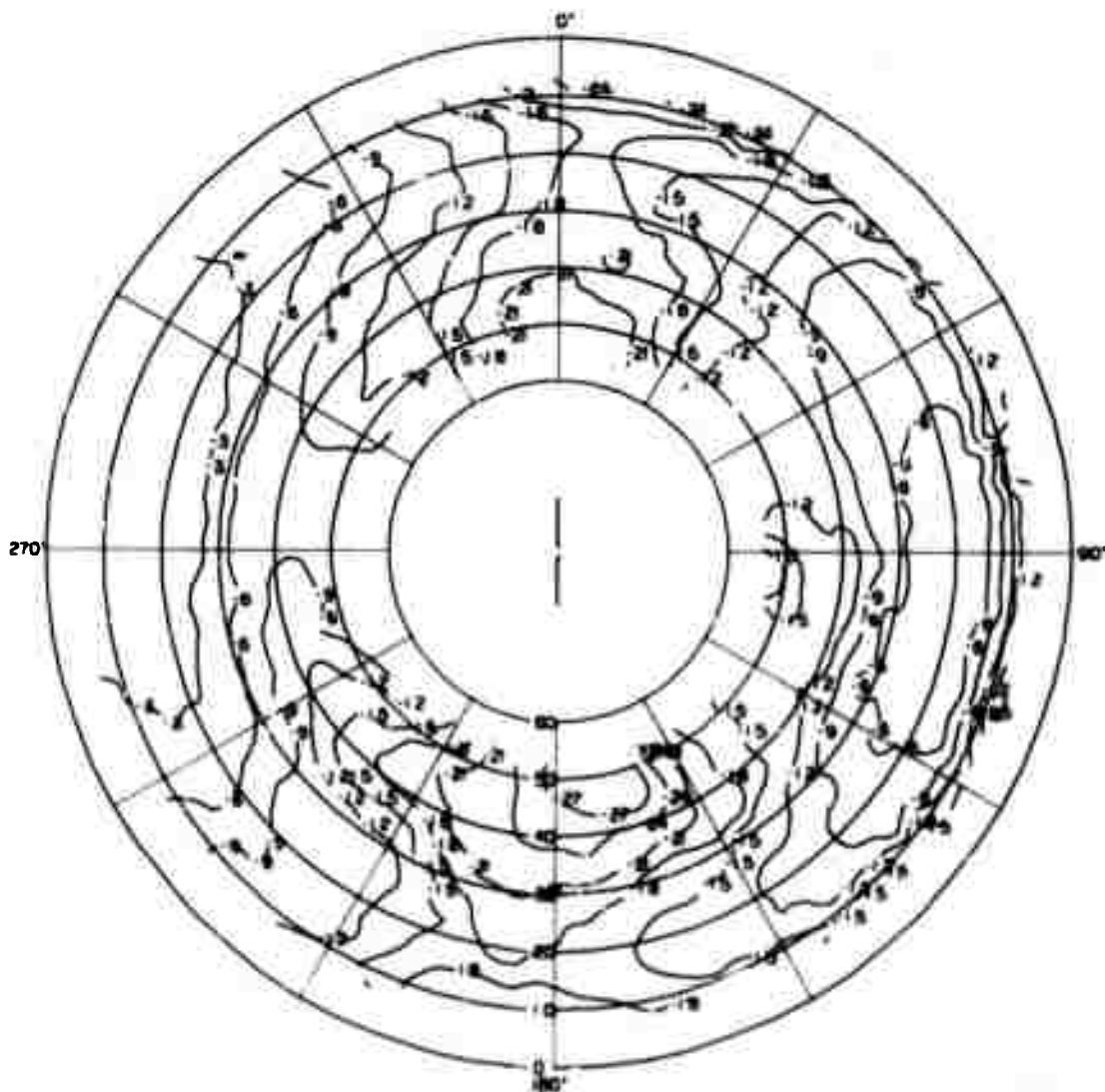
TA-8663-232

FIGURE B-13 CONTOUR PLOT OF THE MEDIAN RESPONSE OF THE HORIZONTAL BALANCED DIPOLE IN THE FOREST-- E_0 AT 75 MHz

Table B-14

STANDARD DEVIATIONS ABOUT THE MEDIAN FOR THE HORIZONTAL BALANCED DIPOLE
IN THE FOREST--E₀ AT 75 MHz

Elevation Azimuth	5.0	10.0	15.0	20.0	25.0	30.0	35.0	40.0	45.0
-170.0	--	3.85	2.66	3.31	3.48	4.30	4.07	3.95	5.26
-160.0	0.0	4.50	4.43	4.03	5.16	3.29	2.91	3.04	3.70
-150.0	--	2.75	1.07	1.86	1.40	1.74	1.32	1.94	2.10
-140.0	--	2.74	1.84	1.81	1.75	1.39	1.45	2.02	2.72
-130.0	--	1.81	1.82	1.83	2.05	1.50	1.48	1.58	1.76
-120.0	--	1.10	1.19	0.87	0.60	0.87	0.99	1.20	1.85
-110.0	--	1.13	0.67	0.73	0.61	0.74	1.04	0.99	1.89
-100.0	--	1.03	0.62	0.74	0.91	0.79	0.98	1.25	1.27
-90.0	--	0.81	0.71	0.65	0.63	0.76	1.00	0.83	0.63
-80.0	--	0.77	0.73	0.70	0.72	0.73	0.82	0.77	0.70
-70.0	--	0.84	0.72	0.74	0.74	0.59	0.73	0.80	0.89
-60.0	--	1.18	1.04	0.87	0.72	0.55	0.73	0.88	1.06
-50.0	--	1.01	0.75	0.88	1.08	0.86	0.77	0.93	1.03
-40.0	--	1.16	0.95	1.03	1.01	1.28	1.36	1.39	1.45
-30.0	--	1.64	1.24	1.09	1.09	1.55	1.76	1.64	1.62
-20.0	--	1.78	1.31	1.29	1.29	1.60	2.22	2.49	2.47
-10.0	--	3.08	1.46	1.98	1.66	2.61	3.38	3.93	4.60
0.0	--	4.49	2.99	2.87	3.18	3.90	4.02	3.87	3.52
10.0	--	3.71	2.90	2.64	2.67	3.54	3.68	3.06	2.39
20.0	--	3.10	2.04	2.03	1.67	2.04	2.10	1.67	1.72
30.0	--	3.19	2.37	2.22	1.62	1.66	1.69	1.84	1.77
40.0	--	3.00	2.34	1.99	1.63	1.36	1.34	1.60	1.57
50.0	--	2.13	1.48	1.51	1.18	1.11	1.25	1.38	1.25
60.0	--	2.29	1.23	1.15	1.07	0.88	1.00	0.96	1.01
70.0	--	2.73	1.29	1.03	0.93	0.68	0.45	0.52	0.58
80.0	0.0	1.94	0.83	0.89	0.97	0.75	0.64	0.64	0.59
90.0	--	2.74	0.74	0.84	0.81	0.66	0.75	0.70	0.60
100.0	--	3.76	1.20	1.09	0.55	0.57	0.67	0.61	0.54
110.0	--	3.90	1.78	1.20	0.77	0.65	0.70	0.64	0.56
120.0	--	2.59	1.55	1.27	0.83	0.77	0.65	0.78	0.77
130.0	--	2.72	1.20	1.43	1.20	1.68	1.45	1.45	1.34
140.0	--	2.86	1.53	1.82	2.87	2.26	2.65	1.95	1.62
150.0	--	2.87	1.32	1.46	1.15	1.69	1.64	2.09	1.83
160.0	--	2.88	2.13	2.03	1.95	2.33	2.71	2.63	1.97
170.0	--	3.78	3.76	3.16	2.43	3.37	4.15	3.49	3.76
180.0	--	3.41	2.88	4.48	--	--	--	--	--



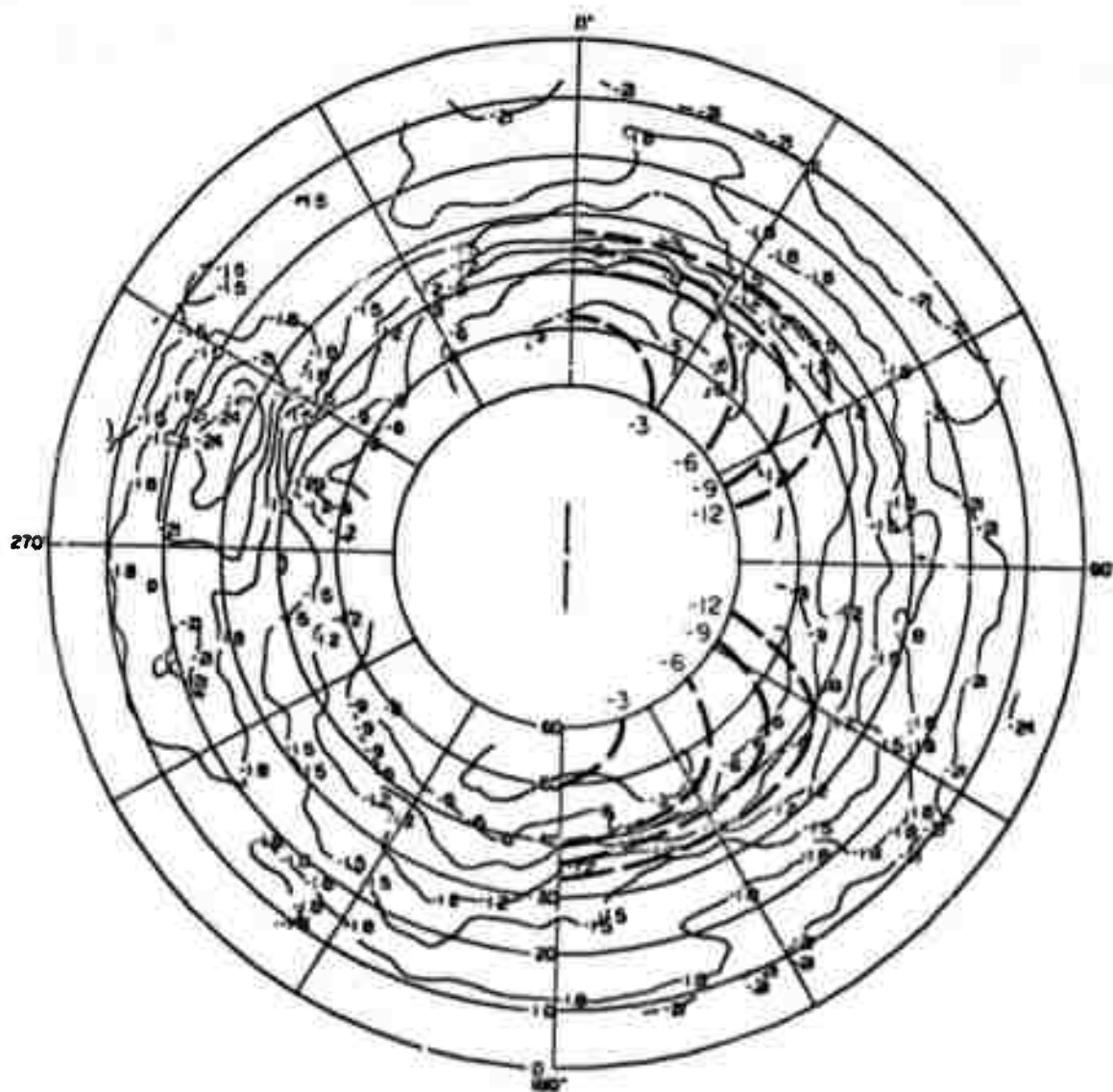
TA-R663-233

FIGURE B-14 CONTOUR PLOT OF THE MEDIAN RESPONSE OF THE HORIZONTAL BALANCED DIPOLE IN THE FOREST— E_{ϕ} AT 75 MHz

Table B-15

STANDARD DEVIATIONS ABOUT THE MEDIAN FOR THE HORIZONTAL BALANCED DIPOLE
IN THE FOREST-- E_{θ} AT 100 MHz

Elevation Azimuth	10.0	15.0	20.0	25.0	30.0	35.0	40.0	45.0	50.0
-170.0	2.25	2.02	2.41	2.41	2.23	2.44	2.53	2.13	1.30
-160.0	2.96	2.05	2.72	2.12	2.48	2.65	3.00	3.33	1.82
-150.0	3.79	3.51	3.83	4.23	2.75	2.34	2.23	1.32	1.84
-140.0	4.37	4.50	3.72	2.94	2.84	2.47	1.80	0.77	1.44
-130.0	3.14	3.36	3.57	2.88	2.98	2.55	2.12	1.00	1.26
-120.0	3.39	4.36	4.15	3.87	3.76	3.09	3.03	1.74	1.44
-110.0	4.63	4.97	4.28	4.33	4.58	4.26	3.28	1.55	1.71
-100.0	3.69	4.01	3.86	4.07	4.27	3.96	3.57	2.08	2.13
-90.0	3.96	3.24	3.44	3.74	3.35	3.47	3.67	2.91	2.81
-80.0	4.42	2.60	2.63	2.06	2.15	2.65	3.01	2.46	2.00
-70.0	5.65	3.92	2.41	0.77	1.51	2.26	1.73	1.05	1.38
-60.0	3.30	2.39	2.75	1.54	1.96	2.00	1.90	1.24	1.25
-50.0	3.41	2.94	3.13	2.41	2.31	2.49	2.22	1.88	1.85
-40.0	3.03	3.88	3.36	2.39	2.36	1.62	1.76	2.03	1.81
-30.0	2.83	3.75	3.88	3.22	2.93	1.59	1.42	1.41	1.45
-20.0	2.75	3.05	3.75	3.46	2.90	1.46	1.23	1.23	1.29
-10.0	3.53	3.88	3.60	2.59	2.51	1.97	1.38	1.27	1.53
0.0	3.94	3.89	3.74	2.77	2.30	2.00	1.29	1.10	1.12
10.0	3.42	3.37	3.19	2.37	2.20	1.88	0.97	1.24	0.89
20.0	3.23	2.99	3.14	2.41	2.42	2.00	1.41	1.22	0.98
30.0	3.49	3.58	3.54	3.20	3.10	3.51	1.85	1.45	0.92
40.0	3.53	3.89	3.76	3.26	3.19	2.79	1.69	1.81	1.41
50.0	3.60	3.65	4.20	4.25	4.38	3.92	2.76	2.86	2.18
60.0	4.55	4.22	4.21	4.38	4.97	5.35	4.15	3.21	2.68
70.0	4.43	4.48	4.11	3.96	4.93	5.80	4.93	4.43	3.50
80.0	4.16	4.09	3.65	3.30	3.97	3.66	4.09	5.37	3.86
90.0	4.11	3.09	3.32	3.25	3.67	4.53	3.90	3.30	2.07
100.0	3.67	3.50	3.42	3.18	3.39	3.27	1.96	1.72	1.04
110.0	2.96	3.56	3.16	2.88	2.42	1.76	1.48	1.45	1.04
120.0	3.20	2.96	2.73	1.81	2.78	3.95	2.34	1.47	1.02
130.0	3.26	3.82	3.15	3.05	2.38	2.15	1.42	1.06	0.67
140.0	3.94	3.78	3.50	2.44	2.19	2.28	1.49	1.18	0.87
150.0	5.04	4.91	4.11	2.83	2.66	2.16	1.87	--	0.83
160.0	4.23	4.41	4.20	3.59	2.84	2.21	1.99	--	1.33
170.0	2.76	2.94	3.83	4.13	3.19	2.79	2.16	--	1.40
180.0	--	--	--	--	--	--	--	--	--



TA-8663-234

FIGURE B-15 CONTOUR PLOT OF THE MEDIAN RESPONSE OF THE HORIZONTAL
BALANCED DIPOLE IN THE FOREST — E_0 AT 100 MHz

Table B-16

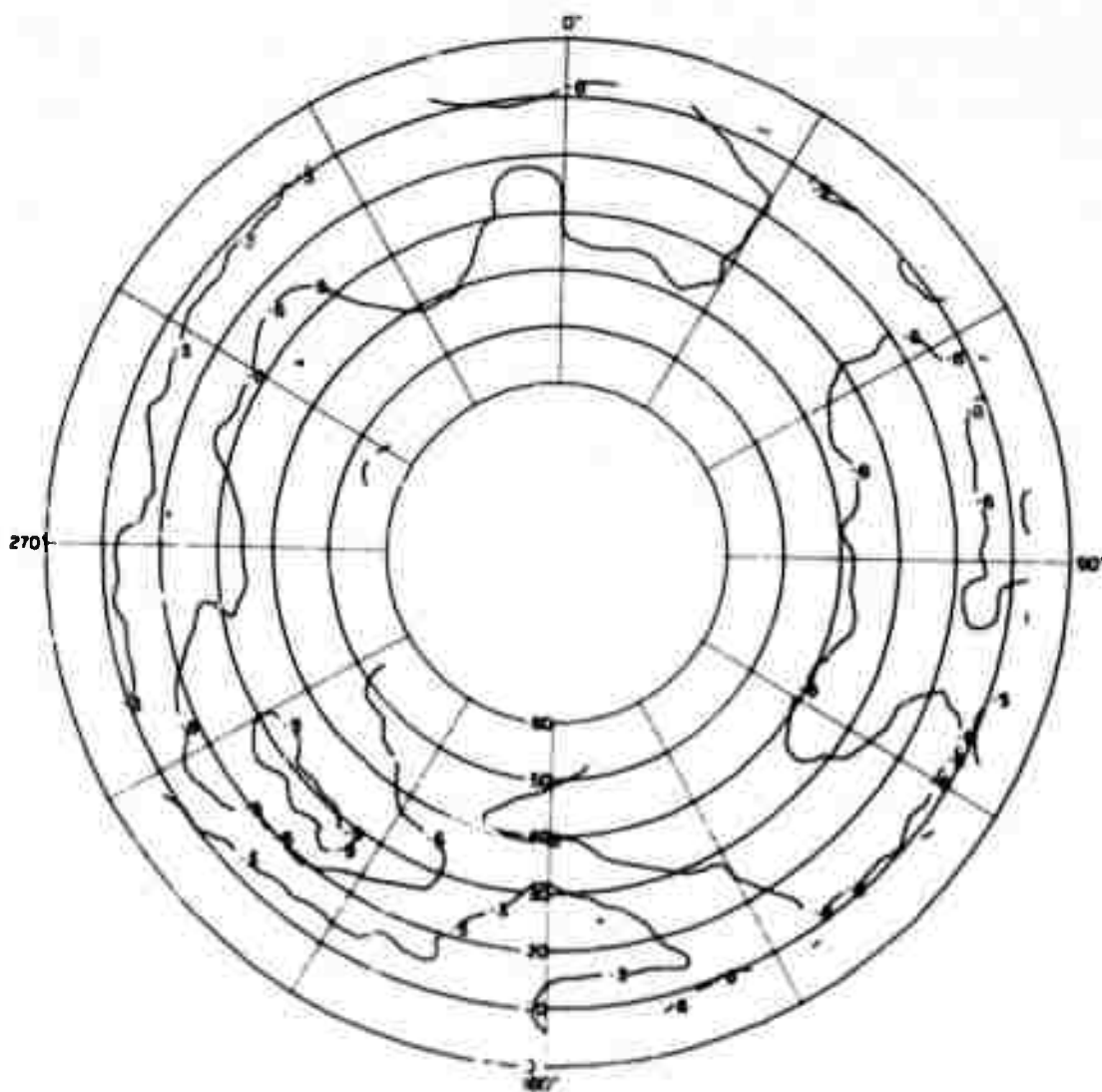
STANDARD DEVIATIONS ABOUT THE MEDIAN FOR THE HORIZONTAL BALANCED DIPOLE
IN THE FOREST-- E_{ϕ} AT 100 MHz

Elevation Azimuth	5.0	10.0	15.0	20.0	25.0	30.0	35.0	40.0	45.0
-170.0	--	3.28	3.39	3.85	5.25	3.31	2.48	1.94	1.84
-160.0	0.0	2.79	2.34	1.95	1.18	2.19	1.88	1.54	1.48
-150.0	--	2.27	1.86	1.79	2.85	1.13	0.73	1.02	0.74
-140.0	0.0	1.41	0.80	1.02	1.06	1.27	1.17	1.11	0.99
-130.0	--	1.13	1.09	0.90	1.17	1.26	1.13	1.06	0.47
-120.0	--	0.59	0.65	0.89	1.59	1.74	1.53	1.50	0.60
-110.0	--	0.69	0.68	0.76	1.43	2.20	2.82	1.61	0.35
-100.0	--	0.76	0.73	1.00	1.71	1.28	1.02	1.04	0.31
-90.0	--	0.87	0.81	0.99	1.22	0.90	0.62	0.62	0.39
-80.0	0.0	0.98	1.13	0.98	0.80	0.99	0.99	0.88	0.83
-70.0	--	1.07	1.12	1.07	0.99	2.35	2.25	1.80	1.55
-60.0	--	1.03	1.04	1.09	1.39	2.78	2.64	2.14	1.64
-50.0	--	1.24	1.07	1.46	.49	2.37	2.00	1.82	1.26
-40.0	--	1.76	1.53	1.84	2.50	3.17	2.24	1.92	1.64
-30.0	--	2.41	2.39	2.69	2.96	3.38	2.32	2.15	2.22
-20.0	--	3.12	1.91	2.63	3.57	3.12	1.77	2.01	2.19
-10.0	--	3.55	2.19	3.22	3.16	2.89	2.19	2.15	2.47
0.0	--	3.98	3.83	2.43	4.43	1.27	3.09	2.61	2.00
10.0	--	3.59	3.24	3.39	4.62	4.77	3.82	2.77	2.17
20.0	--	2.60	2.84	3.3	4.12	4.11	4.35	2.57	1.85
30.0	--	1.89	2.09	2.3	3.41	3.48	3.07	1.74	1.32
40.0	--	2.16	1.84	2.16	2.36	2.16	2.07	1.26	1.26
50.0	--	2.94	2.07	1.82	1.74	1.77	1.65	1.14	1.21
60.0	--	3.12	1.86	1.75	1.80	1.61	1.57	1.08	0.81
70.0	--	2.66	1.48	1.34	1.18	1.09	1.01	0.90	1.15
80.0	0.0	3.79	0.84	0.91	1.03	1.01	1.05	0.83	0.48
90.0	--	2.35	0.74	0.73	0.94	0.75	0.66	0.74	0.80
100.0	--	3.11	1.42	0.78	0.66	0.58	0.49	0.65	0.74
110.0	--	3.27	1.01	1.35	1.21	0.85	0.47	0.36	0.68
120.0	--	2.68	1.36	1.37	1.19	1.27	1.19	0.98	0.57
130.0	--	3.02	2.07	1.95	1.67	1.96	2.00	1.36	0.71
140.0	--	3.26	2.51	2.94	2.98	2.16	1.61	2.01	1.09
150.0	--	3.45	3.30	3.01	3.04	2.62	2.58	2.55	1.64
160.0	--	3.90	4.30	3.44	2.13	3.49	3.88	4.43	4.76
170.0	--	3.61	3.94	4.07	4.72	4.70	6.34	4.98	4.29
180.0	--	3.53	3.43	3.00	--	--	--	--	--

Table B-17

STANDARD DEVIATIONS ABOUT THE MEDIAN FOR THE VERTICAL SLEEVE DIPOLE
IN THE CLEARING--E_θ AT 100 MHz

Elevation Azimuth	10.0	15.0	20.0	25.0	30.0	35.0	40.0	45.0	50.0
-170.0	1.82	1.60	1.74	1.84	1.70	1.59	1.46	1.31	1.04
-160.0	1.54	1.33	1.10	0.79	1.23	1.27	1.34	1.28	1.24
-150.0	1.63	1.03	0.96	0.46	0.67	1.04	1.51	1.33	1.30
-140.0	1.56	1.12	0.74	0.38	0.59	0.92	1.12	1.21	1.22
-130.0	1.49	1.33	1.61	0.71	0.83	0.80	0.78	0.84	0.78
-120.0	1.91	2.07	2.06	1.18	1.28	0.87	0.82	0.37	0.37
-110.0	1.96	2.40	2.18	2.33	1.96	1.02	1.08	0.33	0.29
-100.0	1.92	2.23	2.40	2.49	2.54	1.55	1.35	0.40	0.33
-90.0	2.29	2.36	2.12	2.10	2.34	1.45	1.23	0.25	0.29
-80.0	1.84	1.86	2.05	2.15	1.95	1.14	1.18	0.34	0.25
-70.0	1.47	1.74	1.89	1.73	1.56	0.90	0.88	0.45	0.54
-60.0	2.14	2.24	1.90	1.47	1.63	1.25	0.96	0.52	0.74
-50.0	2.38	2.16	1.98	1.55	1.61	1.20	1.08	0.67	0.66
-40.0	1.93	1.72	1.81	1.54	1.46	0.97	1.12	0.75	0.63
-30.0	1.74	1.62	1.64	1.31	1.17	0.88	0.63	0.78	0.53
-20.0	2.25	1.83	1.98	1.99	1.72	1.73	1.16	0.97	0.47
-10.0	2.41	2.37	2.28	1.79	1.70	1.81	1.30	1.20	0.55
0.0	2.08	2.46	2.19	1.46	1.65	1.56	1.12	1.12	0.69
10.0	2.30	2.46	2.30	1.65	1.63	1.68	1.23	0.96	0.92
20.0	2.32	2.30	2.37	1.94	1.84	1.68	1.02	1.04	0.63
30.0	1.38	1.95	2.20	2.03	1.83	1.85	0.76	0.71	0.33
40.0	1.58	2.15	1.97	1.70	1.81	1.78	0.79	0.61	0.05
50.0	1.62	2.11	2.09	1.90	1.89	1.75	0.86	0.99	0.34
60.0	1.22	1.85	2.23	2.15	1.98	2.07	1.31	1.23	0.66
70.0	1.24	2.30	1.97	1.78	2.00	2.05	1.35	1.15	0.60
80.0	1.32	2.43	2.19	2.05	2.10	1.99	1.24	1.32	0.59
90.0	1.19	2.10	2.33	2.45	2.41	2.41	1.55	1.12	0.45
100.0	2.30	2.55	2.65	2.61	2.43	2.46	1.19	1.09	0.40
110.0	2.15	2.88	2.85	2.90	2.14	1.70	0.41	0.50	0.28
120.0	2.11	2.80	2.75	2.13	1.86	1.23	0.74	0.60	0.24
130.0	2.76	2.61	2.36	2.16	2.36	1.96	1.58	0.88	0.19
140.0	1.69	1.75	2.15	2.11	2.25	1.49	1.47	1.05	0.27
150.0	1.11	1.83	1.64	2.03	1.87	1.23	1.09	0.91	0.30
160.0	1.78	1.79	1.64	1.06	1.27	0.92	0.87	--	0.39
170.0	1.69	1.55	1.50	1.19	1.11	1.17	1.00	--	0.87
180.0	1.62	1.82	1.98	2.32	1.93	1.55	1.31	--	1.05



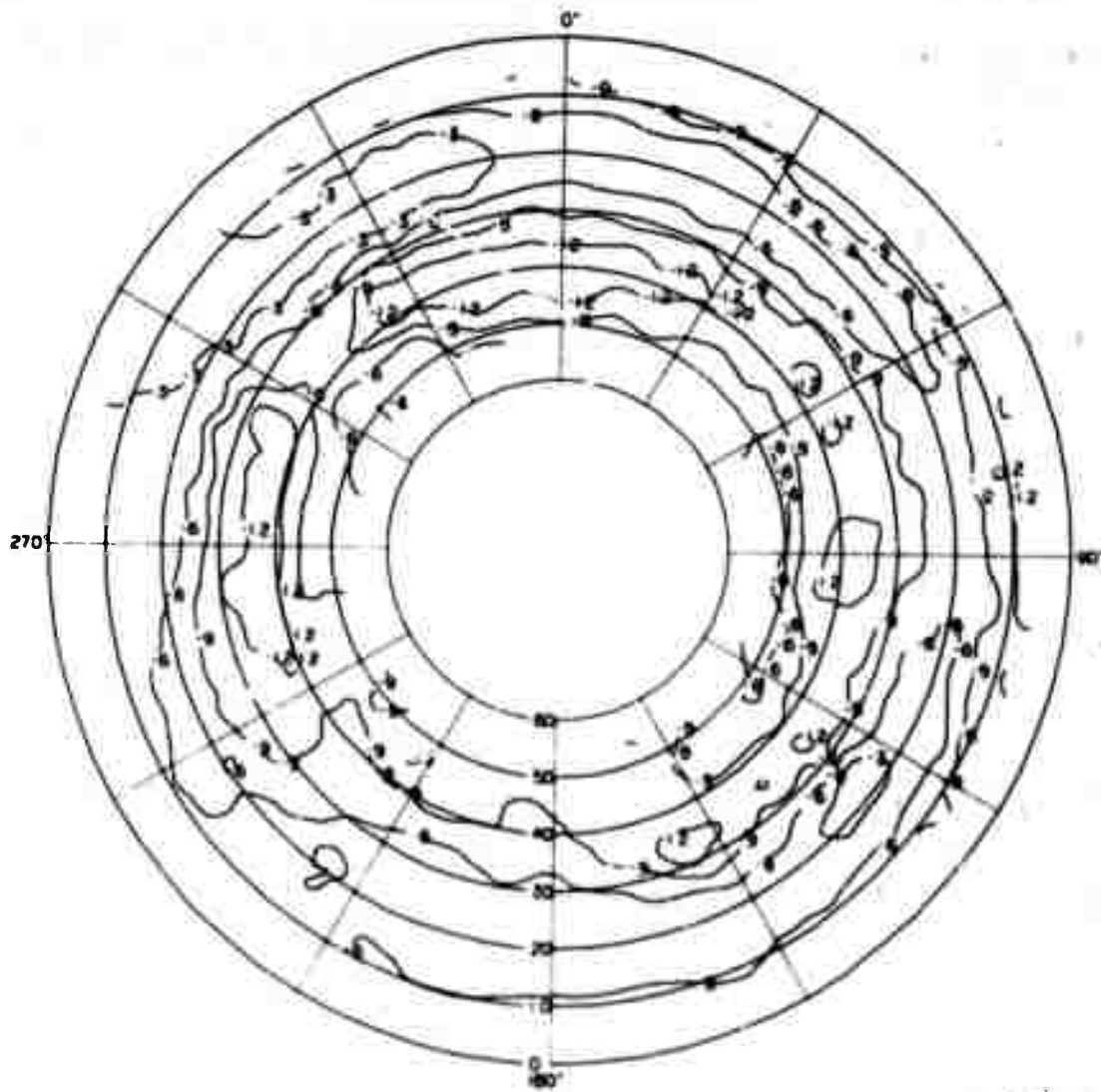
TA-8663-236

FIGURE B-17 CONTOUR PLOT OF THE MEDIAN RESPONSE OF THE VERTICAL SLEEVE DIPOLE IN THE CLEARING— E_0 AT 100 MHz

Table B-18

STANDARD DEVIATIONS ABOUT THE MEDIAN FOR THE VERTICAL SLEEVE DIPOLE
IN THE FOREST--E_θ AT 100 MHz

Elevation Azimuth	10.0	15.0	20.0	25.0	30.0	35.0	40.0	45.0	50.0
-170.0	3.58	3.48	3.36	2.16	2.17	2.25	2.42	2.39	2.03
-160.0	4.55	4.99	4.93	3.40	2.80	2.47	2.43	2.05	1.97
-150.0	4.97	4.33	3.78	3.17	2.89	2.59	2.40	1.78	1.73
-140.0	2.92	2.75	3.04	2.78	3.18	2.78	2.61	2.01	1.84
-130.0	3.67	3.89	3.86	3.84	3.55	3.19	3.18	2.33	2.10
-120.0	4.32	4.21	4.07	3.34	3.43	2.83	2.57	2.06	2.04
-110.0	3.92	3.50	3.47	2.83	2.66	2.09	2.36	2.11	2.04
-100.0	3.89	2.77	2.66	2.19	2.46	2.23	2.10	2.19	2.18
-90.0	3.59	2.51	2.81	2.06	2.19	1.86	1.83	1.92	2.01
-80.0	3.79	3.75	3.57	2.59	2.07	1.94	1.92	2.34	2.33
-70.0	3.89	3.52	3.09	1.93	1.92	2.08	2.66	3.06	2.48
-60.0	2.55	2.31	2.41	1.73	1.64	1.97	1.92	2.27	2.48
-50.0	2.18	1.99	2.38	2.37	2.00	1.89	1.64	1.95	2.03
-40.0	3.64	2.63	2.31	1.91	1.76	1.91	2.14	2.71	2.07
-30.0	3.23	2.16	2.08	1.37	1.26	1.53	1.79	2.24	2.06
-20.0	3.01	2.16	2.26	1.50	1.49	1.69	1.85	2.21	1.96
-10.0	3.54	2.78	2.50	1.76	2.14	2.24	2.15	2.12	2.14
0.0	3.68	3.06	3.13	2.67	2.13	1.84	1.66	1.53	1.82
10.0	3.38	2.40	2.55	1.93	1.91	1.69	1.85	2.23	2.40
20.0	3.30	2.43	2.37	2.04	1.64	1.69	1.77	1.86	2.10
30.0	3.07	2.88	3.24	2.80	1.98	1.90	1.72	1.76	1.92
40.0	3.25	4.01	4.05	3.45	2.47	2.09	1.85	2.17	2.20
50.0	3.38	3.64	3.77	3.83	2.28	1.96	1.84	2.04	2.31
60.0	3.15	3.12	3.38	3.26	1.81	1.90	1.84	2.15	2.36
70.0	3.10	3.34	3.32	3.28	1.93	2.05	1.80	1.83	2.08
80.0	3.10	3.36	3.38	3.46	2.28	1.98	1.91	1.58	1.70
90.0	2.84	3.55	3.10	2.70	1.60	1.63	1.87	2.25	2.20
100.0	3.16	3.07	2.86	2.62	1.20	1.72	1.92	2.14	2.15
110.0	3.34	3.78	3.84	3.47	2.50	1.99	1.65	1.83	1.92
120.0	3.28	3.24	3.97	4.46	3.08	2.35	1.89	2.22	2.23
130.0	3.52	3.78	3.68	3.13	2.34	2.37	1.66	1.62	1.40
140.0	4.12	3.95	3.43	2.54	1.94	2.18	2.27	2.47	2.06
150.0	3.56	3.37	2.85	1.61	1.35	1.41	2.15	3.23	2.16
160.0	3.12	2.50	3.12	1.99	1.77	1.65	1.80	--	1.15
170.0	3.97	3.76	3.45	2.78	2.41	1.99	2.15	--	2.02
180.0	3.82	3.56	2.96	1.32	1.86	2.37	2.73	--	2.22



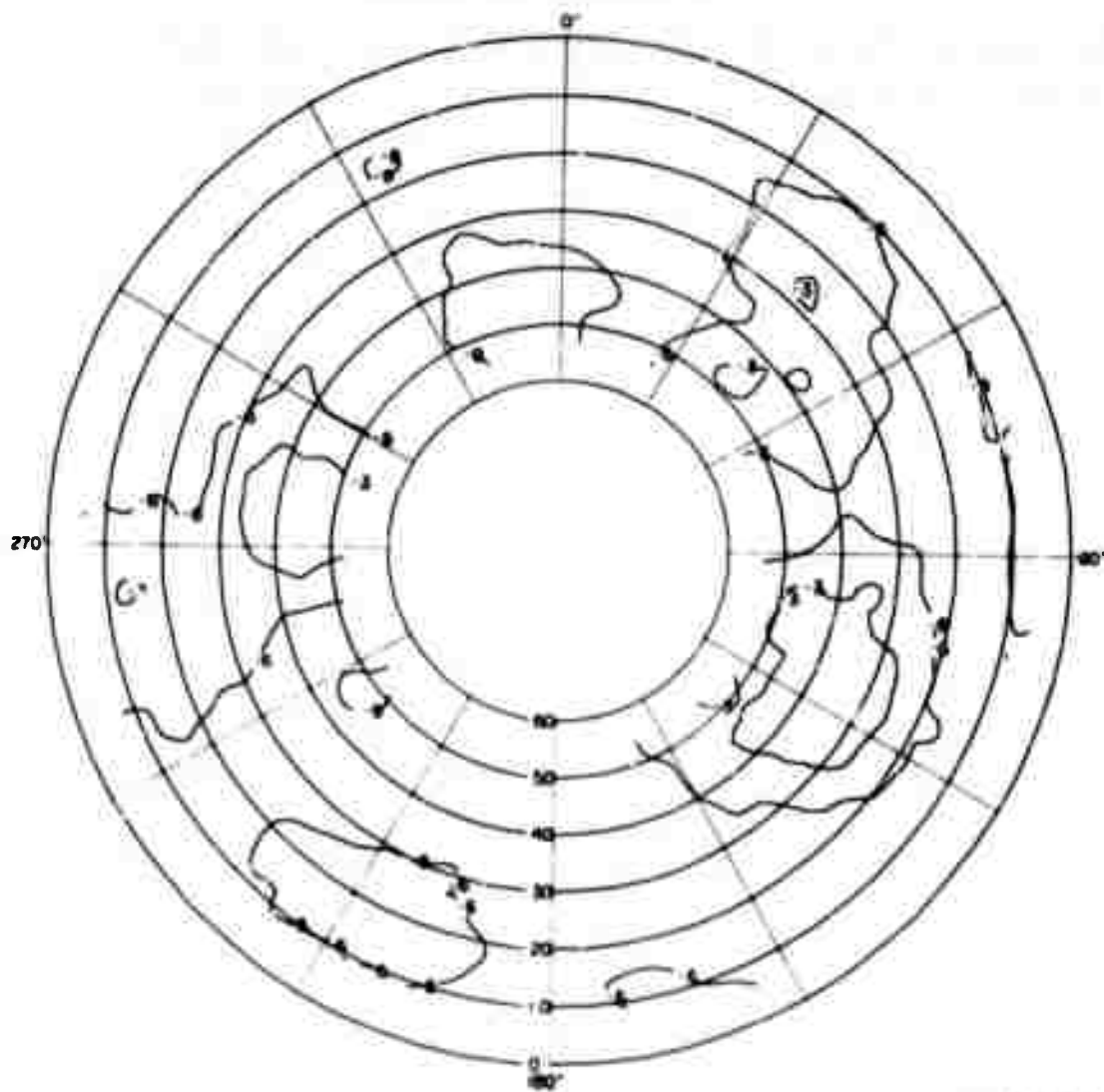
TA-8663-237

FIGURE B-18 CONTOUR PLOT OF THE MEDIAN RESPONSE OF THE VERTICAL SLEEVE DIPOLE IN THE FOREST— E_0 AT 100 MHz

Table B-19

STANDARD DEVIATIONS ABOUT THE MEDIAN FOR THE VERTICAL SLEEVE DIPOLE
IN THE FOREST--E₀ AT 100 MHz

Elevation Azimuth	5.0	10.0	15.0	20.0	25.0	30.0	35.0	40.0	45.0
-170.0	--	1.57	2.33	2.12	1.65	1.48	1.26	1.29	1.15
-160.0	0.0	1.66	2.33	2.22	1.94	1.94	1.80	1.49	1.18
-150.0	--	1.59	2.09	2.08	1.89	1.92	1.81	1.67	1.17
-140.0	0.0	1.56	1.88	1.92	1.73	1.71	1.72	1.76	1.45
-130.0	--	1.42	1.74	1.71	1.53	1.50	1.38	1.27	1.20
-120.0	--	1.40	1.86	1.82	1.64	1.63	1.33	1.14	1.01
-110.0	--	1.73	2.19	2.23	2.17	1.95	1.68	1.62	1.88
-100.0	--	2.06	2.24	2.29	2.31	2.08	1.73	1.70	1.97
-90.0	--	2.29	2.42	2.15	2.00	1.84	1.92	1.62	1.42
-80.0	--	2.03	2.04	2.07	1.93	1.67	1.68	1.64	1.72
-70.0	--	1.98	2.30	2.06	2.04	1.83	1.58	1.62	1.56
-60.0	--	1.74	1.91	1.73	1.54	1.61	1.66	1.55	1.36
-50.0	--	1.11	1.32	1.29	1.18	1.57	1.82	1.58	1.51
-40.0	--	1.19	1.52	1.54	1.71	1.59	1.34	1.37	1.32
-30.0	--	1.37	1.85	1.95	2.11	1.68	1.11	1.13	1.16
-20.0	--	1.42	2.05	1.96	1.73	1.09	0.62	0.76	0.83
-10.0	--	1.70	2.13	1.94	1.74	1.13	0.81	0.82	0.75
0.0	0.0	1.52	1.71	1.70	1.49	1.42	1.05	0.85	0.79
10.0	--	1.29	1.49	1.39	1.45	1.35	1.21	1.07	1.15
20.0	--	1.11	1.75	1.83	1.84	1.81	1.20	1.01	1.14
30.0	--	0.92	1.89	2.07	2.22	2.23	1.23	0.93	1.09
40.0	--	1.26	2.00	1.97	1.86	1.99	1.69	1.44	1.43
50.0	--	1.29	1.87	1.88	1.71	2.07	2.18	2.04	1.97
60.0	--	0.88	1.66	1.66	1.84	2.36	2.27	2.11	2.07
70.0	--	0.76	1.40	1.40	1.43	1.87	2.09	1.97	1.73
80.0	--	0.83	1.20	1.24	1.05	1.38	1.76	1.77	1.60
90.0	--	1.04	1.20	1.20	1.41	1.84	1.87	1.85	1.87
100.0	--	1.05	1.28	1.34	1.49	1.71	1.78	1.89	2.21
110.0	--	0.98	1.45	1.28	1.28	1.43	1.42	1.55	1.68
120.0	0.0	0.85	1.71	1.79	1.82	1.80	1.26	1.24	1.32
130.0	--	0.93	1.66	1.74	1.90	1.67	1.18	1.13	1.05
140.0	--	0.68	1.14	1.21	1.44	1.59	1.44	1.27	1.08
150.0	--	0.95	1.24	1.35	1.70	1.81	1.89	1.67	1.48
160.0	--	1.38	1.71	1.65	1.79	1.83	1.85	1.69	1.49
170.0	--	1.29	1.73	1.50	1.16	1.46	1.53	1.50	1.44
180.0	0.0	1.29	1.93	1.81	1.28	1.18	1.19	1.33	1.47



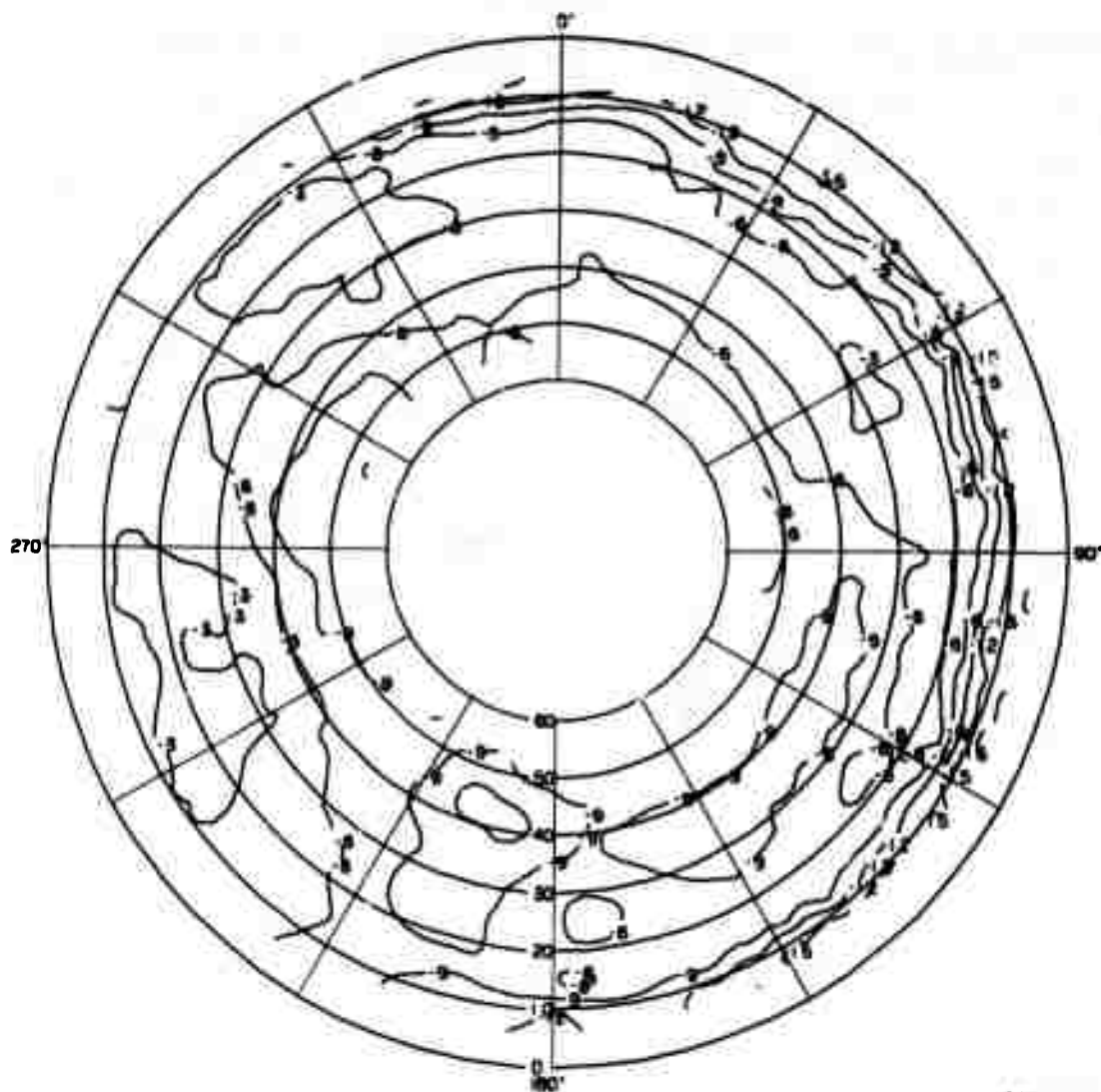
VA-8663-238

FIGURE B-19 CONTOUR PLOT OF THE MEDIAN RESPONSE OF THE VERTICAL SLEEVE DIPOLE IN THE FOREST— E_{ϕ} AT 100 MHz

Table B-20

STANDARD DEVIATIONS ABOUT THE MEDIAN FOR THE VERTICAL BALANCED DIPOLE
IN THE FOREST--E_θ AT 100 MHz

Elevation Azimuth	10.0	15.0	20.0	25.0	30.0	35.0	40.0	45.0	50.0
-170.0	4.27	3.77	3.77	2.79	2.47	2.40	2.40	1.89	1.77
-160.0	4.44	4.43	4.29	3.22	3.08	2.74	2.79	2.30	2.01
-150.0	3.34	3.08	3.13	3.15	2.68	2.45	2.07	1.51	1.94
-140.0	1.90	2.02	2.31	2.15	2.25	2.36	2.48	1.90	1.68
-130.0	2.36	1.80	1.71	1.61	1.89	2.09	2.02	1.81	1.78
-120.0	2.67	1.96	1.73	1.42	1.52	1.59	1.53	1.42	1.50
-110.0	2.67	1.93	2.11	1.68	1.53	1.39	1.52	1.50	1.26
-100.0	3.35	2.37	2.24	1.64	1.70	1.44	1.41	1.49	1.78
-90.0	3.35	2.43	2.31	1.93	1.83	1.95	2.18	2.27	1.82
-80.0	2.96	2.38	2.72	2.53	2.61	3.01	3.23	3.48	2.92
-70.0	3.50	3.01	3.21	2.96	2.75	2.84	2.96	3.02	2.75
-60.0	3.73	3.62	3.16	2.44	1.99	1.79	2.21	2.42	2.30
-50.0	2.57	2.43	2.29	1.74	1.95	2.14	1.87	1.84	1.71
-40.0	2.34	1.70	1.58	1.46	1.45	1.47	1.49	1.28	1.16
-30.0	3.23	1.64	2.02	1.41	1.81	1.62	1.32	1.30	1.01
-20.0	4.43	4.06	3.66	2.88	2.56	2.24	1.37	1.11	0.98
-10.0	4.53	3.67	3.68	2.88	2.31	1.54	1.21	1.22	1.22
0.0	3.65	2.06	1.89	1.66	1.53	1.45	1.14	1.11	1.35
10.0	3.35	2.11	2.01	1.23	1.18	1.12	1.20	1.24	1.36
20.0	4.50	2.48	2.46	1.20	1.11	1.01	1.13	1.29	1.43
30.0	4.72	3.31	2.93	1.29	1.12	1.19	1.37	1.47	1.63
40.0	3.76	3.27	2.94	1.88	1.51	1.54	1.58	1.60	1.82
50.0	4.02	2.65	2.43	1.97	1.72	1.85	1.53	1.38	1.66
60.0	3.72	1.94	2.23	2.27	1.79	1.64	1.19	1.18	1.19
70.0	3.12	1.59	1.79	1.88	1.57	1.48	1.44	1.37	1.16
80.0	3.14	1.45	1.67	1.29	1.27	1.52	1.79	1.87	1.63
90.0	3.40	2.28	2.06	1.27	1.22	1.23	1.64	1.89	1.59
100.0	3.51	2.71	2.28	1.25	1.32	1.26	1.37	1.30	0.89
110.0	2.83	1.80	1.84	1.21	1.47	1.67	1.67	1.48	0.99
120.0	3.50	2.17	1.96	1.25	1.52	1.70	1.65	1.69	1.25
130.0	4.12	3.30	2.21	1.22	1.51	1.58	1.45	1.40	1.19
140.0	3.82	2.68	2.83	1.86	1.94	1.56	1.20	0.96	0.88
150.0	4.65	3.98	3.58	2.56	2.03	1.42	1.25	1.11	0.84
160.0	4.55	3.79	3.51	2.43	2.25	1.70	1.70	--	1.33
170.0	4.20	2.86	3.03	1.75	1.83	1.46	1.57	--	1.42
180.0	4.44	3.60	2.83	1.69	1.75	1.64	1.49	--	1.30



TA-8663-240

FIGURE E-20 CONTOUR PLOT OF THE MEDIAN RESPONSE OF THE VERTICAL
BALANCED DIPOLE IN THE FOREST— E_{θ} AT 100 MHz

Table B-21

STANDARD DEVIATIONS ABOUT THE MEDIAN FOR THE VERTICAL BALANCED DIPOLE
IN THE FOREST-- E_0 AT 100 MHz

Elevation Azimuth	5.0	10.0	15.0	20.0	25.0	30.0	35.0	40.0	45.0
-170.0	--	2.43	2.82	2.74	3.45	3.14	3.70	3.67	3.72
-160.0	0.0	2.60	3.03	3.14	3.58	3.61	3.49	3.50	3.35
-150.0	--	2.96	3.21	3.17	3.56	3.43	3.22	3.07	3.01
-140.0	--	3.05	2.93	2.91	3.03	2.97	2.80	3.06	3.19
-130.0	--	3.09	2.63	2.88	2.92	2.96	2.84	2.95	3.13
-120.0	0.0	3.80	3.25	2.97	2.93	2.93	2.80	2.50	2.31
-110.0	--	3.41	2.93	2.89	2.72	3.00	2.80	2.81	2.06
-100.0	--	2.47	2.51	2.72	2.56	3.49	3.79	3.66	3.31
-90.0	--	2.35	2.63	2.75	3.00	3.94	4.26	4.27	4.23
-80.0	--	2.61	2.82	3.10	3.34	3.72	3.68	3.94	3.85
-70.0	--	3.08	3.24	3.31	3.29	3.43	3.60	3.70	3.65
-60.0	0.0	3.30	3.54	3.49	3.63	3.97	3.71	3.32	2.81
-50.0	--	3.22	3.42	3.58	3.65	3.59	2.98	2.86	2.69
-40.0	--	3.26	3.32	3.44	3.48	3.18	2.65	2.79	2.80
-30.0	--	3.21	3.19	3.15	3.10	3.16	3.00	2.92	2.91
-20.0	--	3.02	3.30	3.25	3.26	3.13	2.81	2.76	2.56
-10.0	--	2.66	3.20	3.29	3.61	3.17	2.62	2.75	2.79
0.0	--	2.39	3.08	3.17	3.33	2.87	2.54	2.54	2.62
10.0	--	2.29	2.95	2.92	2.72	2.38	2.27	2.54	2.74
20.0	--	2.69	3.21	3.03	2.88	2.28	2.26	2.83	3.19
30.0	--	2.89	3.26	3.22	3.25	3.18	2.86	2.99	3.09
40.0	0.0	2.66	3.54	3.82	3.92	4.01	3.72	3.02	2.88
50.0	--	2.93	3.78	3.90	4.12	4.04	3.76	3.09	2.99
60.0	--	2.69	3.64	3.71	3.63	3.73	3.75	3.23	3.25
70.0	--	2.27	3.45	3.45	3.40	3.64	3.36	3.20	2.95
80.0	--	2.40	3.38	3.32	3.30	3.50	3.03	2.88	2.46
90.0	--	2.27	3.15	3.22	3.37	3.79	3.45	3.24	2.96
100.0	--	1.93	2.86	3.08	3.27	3.94	3.99	3.85	3.77
110.0	--	1.90	2.96	2.86	3.12	3.32	3.28	3.47	3.45
120.0	--	1.96	3.03	3.11	3.02	3.07	2.73	2.91	3.11
130.0	--	1.99	2.69	2.99	3.35	2.85	2.48	2.59	2.86
140.0	--	2.28	2.47	2.44	2.72	2.90	2.72	2.70	2.56
150.0	--	2.60	3.19	3.12	3.53	3.54	3.66	3.19	2.91
160.0	--	2.67	3.41	3.51	3.81	3.72	3.71	3.66	3.51
170.0	--	2.37	2.74	2.72	3.29	3.60	3.82	3.61	3.52
180.0	0.0	2.05	2.06	2.48	3.08	3.25	3.52	3.60	3.47



179

Appendix C

EXAMPLE APPLICATIONS OF THE VHF ANTENNA PATTERN DATA

Appendix C

EXAMPLE APPLICATIONS OF THE VHF ANTENNA PATTERN DATA

This appendix provides example calculations employing the VHF antenna pattern data presented in this report. The purpose of this appendix is to make the interpretation and the use of the data more understandable to the reader. First, the calculation of the required transmitter power for a particular problem is provided and a comparison of four antenna/environment situations is given; then a description of the use of the standard deviation data is provided; and, finally, a brief discussion is presented on the effect of the antenna height on the antenna gain.

1. Problem Statement

For the calculations presented in this appendix, it will be assumed that a ground station in an environment similar to the Ban Mun Chit field site is to employ a low-power transceiver to communicate at 100 MHz with a similar unit in an aircraft flying at 8000 ft above the surface and at a ground range of 6 miles from the ground station. It will be assumed that the RF input to the receiver must be greater than $1.0 \mu\text{V}$ to obtain an adequate signal-to-noise ratio. It is necessary to determine the required transmitter power to obtain a 99-percent-reliable communication link for the following antenna/environment situations:

- (1) A horizontal dipole located 10 feet above the ground in a clearing
- (2) A horizontal dipole located 10 feet above the ground in a forest

(3) A vertical dipole located 10 feet above the ground in a clearing

(4) A vertical dipole located 10 feet above the ground in a forest.

For each of the above cases, it will be assumed that the primary polarization of the aircraft antenna is the same as the ground antenna.

2. Calculation of the Median Transmitter Power

To estimate the required transmitter power for 99-percent reliability will first require a determination of the median transmitter power (median power provides 50-percent reliability) as is determined by the path equation, which can be expressed in decibels:

$$P_t = P_a + L_{tl} + L_{tm} + L_{tr} - G_{ta} + L_{bm} - G_{ra} + L_{rr} + L_{rm} + L_{rl} \quad ,^* \quad (C-1)$$

where

P_t = the power output of the transmitter

P_a = the power available at the receiver input

L_{tl}, L_{rl} = the transmission-line losses for the transmitter and receiver, respectively

L_{tm}, L_{rm} = the matching network losses for the transmitter and receiver, respectively

* Note: P_a and P_t must be expressed in the same units, i.e., dBW or dBm.

L_{tr}, L_{rr} = any residual losses (e.g., losses due to an imperfect impedance match) between the transmitter and receiver and their respective antennas

G_{ta}, G_{ra} = the absolute gains of the transmitting and receiving antennas for the path geometry and polarization of interest

L_{bm} = the median basic transmission loss for the equivalent free-space path as computed from $20 \log_{10} (4\pi r/\lambda)$, where r is the slant range to the aircraft in the same units as the wavelength, λ .

Since the ground transceiver and the aircraft transceiver are assumed to be identical units for this example, the path equation is reciprocal. If this were not the case, it would be necessary to calculate the power for the aircraft transmitter and the ground transmitter as two separate operations. For the remainder of the calculations, it will be assumed that the transmitter is located in the aircraft and the receiver is located at the ground station.

If the input impedance of the receiver is assumed to be 50Ω (purely resistive), the power required at the receiver terminals can be expressed as

$$\begin{aligned} P_a &= (V_{min})^2 / R \\ &= (1.0 \times 10^{-6})^2 / 50 = 8 \times 10^{-14} \text{ W} = -137 \text{ dBW} \end{aligned} \quad (C-2)$$

The efficiency of the antenna tuning network (and consequently the antenna tuning network loss) for the receiving antenna, L_{rm} , can be estimated by employing the antenna impedance data provided in Tables 20 and 21, or other measurement data, and curves of matching network efficiency

as a function of antenna impedance similar to Figure 27-21 of Ref. 18. The loss caused by the transmitting antenna tuning network, L_{tm} , can be estimated similarly. The residual losses, L_{rr} and L_{tr} , can then be assumed to be less than 1 dB. For the case of a receiver with a fixed input impedance or a transmitter with a fixed output impedance, L_{rm} and L_{tm} can represent the mismatch loss between the set and the antenna. For this example, conservatively large values for these losses will be assumed:

$$L_{rl} + L_{rr} = 6 \text{ dB} \quad \text{and} \quad L_{tl} + L_{tm} + L_{tr} = 9 \text{ dB} .$$

Also, it will be assumed that the gain of the aircraft antenna, G_{ta} , is +3 dB. The ground range of 6 miles is equivalent to a slant range of 32,600 feet and an elevation angle of approximately 15 degrees (actually 14.2 degrees) for the 8000-foot altitude of the aircraft. From the calculated slant range, the median equivalent free-space basic transmission loss for the path, L_{bm} , can be calculated as 92 dB for 100 MHz.

Using the above calculated values, the path equation (C-1) becomes:

$$P_t = -137 + 9 - 3 + 92 - G_{ra} + 6 + L_{rm} = L_{rm} - G_{ra} - 33 \quad . \quad (C-3)$$

The value of G_{ra} can be derived theoretically using the slab model described in Section VIII or can be estimated from the data provided in this report.

The absolute gains of the antennas can be approximated by estimating the gain of the measured horizontal dipole antenna in the clearing. FitzGerrell¹⁹ has shown that the maximum observed absolute power gain for antenna heights greater than $\lambda/2$ should lie between +6 and +9 dB relative to an isotropic radiator. Since antenna construction and site

imperfections can cause minor reductions of gain, a more conservative estimate of +5 dB for the maximum gain of the horizontal dipole in the clearing will be used here.

Using Figure A-17 to represent the horizontal dipole antenna in a clearing, one can see that at 15 degrees elevation and in the direction away from the forest (270 degrees azimuth), the relative gain for the antenna is down 3 dB from the observed maximum. The absolute gain can be calculated as +2 dB (-3 dB + 5 dB) for this direction and polarization. The impedance of the antenna is $35 + j20 \Omega$ (Table 20). Again assuming a receiver input impedance of $50 + j0 \Omega$, this results in a VSWR of 1.8:1, and the matching loss (without the use of an antenna tuner) can be calculated as 0.4 dB using the relationship $(VSWR + 1)^2 / (4 \cdot VSWR)$. Thus, the required median input power to the transmitting antenna becomes

$$P_t = 0.4 - 2.0 - 33 = -34.6 \text{ dBW} \quad (C-4)$$

To estimate the absolute gain of the horizontal dipole in the forest, the data in Table 17 must be used in addition to Figure A-19. Table 17 indicates that the maximum E_ϕ gain of the horizontal unbalanced dipole in the forest is 6.6 dB below a similar antenna in the clearing, or 0 dB on Figure A-19 is 6.6 dB below the 0 dB point on Figure A-17. In the direction of the forest (90 degrees azimuth) and at 15 degrees elevation, the gain is 12.0 dB below the maximum observed value on Figure A-19; thus the absolute gain in this direction is -13.6 dB ($5.0 - 6.6 - 12.0$). The impedance of this antenna is $40 + j20$, and the mismatch loss (again without an antenna tuner) can be calculated as 0.3 dB. Thus, the required transmitter power is -19.1 dBW.

The pertinent results from these calculations and those for the other two cases are presented in Table C-1.

Table C-1

MEDIAN TRANSMITTER POWER CALCULATIONS

Parameter	Horizontal Dipole in Clearing	Horizontal Dipole in Forest	Vertical Dipole in Clearing	Vertical Dipole in Forest
Antenna Pattern Figure Number	A-17	A-19	A-20	A-22
Absolute Gain at Pattern Maximum, dB	+5.0	-1.6	-0.3	-4.7
Pattern Relative Gain at 15° Elevation, dB	-3.0	-12.0	-12.0	-12.0
Antenna Absolute Gain at 15° Elevation, dB	+2.0	-13.6	-12.3	-16.7
Antenna Impedance, Ω	35 + j20	40 + j20	30 + j90	140 + j150
Mismatch Loss, dB	+0.4	+0.3	+3.8	+3.2
Required Median Transmitter Power, dBW	-34.6	-19.1	-16.9	-13.1

The data in Table C-1 apparently show that the forest affected the absolute gain of the horizontal antennas for this geometry by approximately 15 dB, whereas the absolute gain of the vertical antenna was reduced by only 4 dB when it was situated in the forest. By comparing Figures A-17 and A-19, it is evident that this reduction in gain is caused by not only the attenuation of the forest, but a change in the antenna pattern factor due to the forest surrounding the antenna.

From the data derived in Table C-1, it appears that the horizontal dipole in the clearing would be the best choice of antennas (i.e., it requires the least power), but to acquire the required power for a 99-percent-reliable communication system, one must also consider the variation of the signal strength.

3. Designing for Reliable Communications

To determine the reliability of the antenna at the ground station, one must use the standard deviation values, $\hat{\sigma}'$, provided in the tables opposite each antenna contour plot. Although the actual distribution function of the antenna pattern data has not been determined, it is reasonable to assume a log-normal distribution to make probability statements about the antenna gains in a given direction. A table of areas of the normal curve can be employed to determine that 99 percent of the normal curve is to the right of the median value plus $2.33 \hat{\sigma}'$. Thus the standard deviation values (as provided in the tables opposite the contour plots) for the elevation and azimuth angle of interest can be multiplied by 2.33 to determine the amount that the median power must be incremented to provide the required system reliability (assuming a constant gain--a standard deviation of zero--for the aircraft transmitting antenna). These calculations are tabulated in Table C-2.

Table C-2

CALCULATION OF TRANSMITTER POWER FOR 99-PERCENT RELIABILITY

Table Number	Horizontal Dipole in Clearing	Horizontal Dipole in Forest	Vertical Dipole in Clearing	Vertical Dipole in Forest
Standard Deviation, $\hat{\sigma}'$, in Area of Interest, dB	A-17	A-19	A-20	A-22
2.33 $\hat{\sigma}'$, dB	1.0	2.7	1.4	2.5
Median Transmitter Power, $\hat{\mu}'$, dBW (from Table C-1)	+2.3	+6.3	+3.3	+5.8
Power for 99-Percent Reliability, dBW	-34.6	-19.1	-16.9	-13.1
Power for 99-Percent Reliability, mW	-32.3	-12.8	-13.6	-7.3
	0.6	52.5	43.5	187.0

The data in Table C-2 again indicate that the horizontal dipole in the clearing would ideally be the best choice of antennas. But, if one wanted omnidirectional coverage, the vertical dipole would be required and one would need to increase the transmitter power by 6.3 dB to use this antenna in the forest (as compared to operation in the clearing) and not by only 3.8 dB as is shown in Table C-1. Alternative solutions are to employ two crossed horizontal dipoles or a horizontal turnstile antenna; thus the gain will be about that of a single dipole but an omnidirectional coverage can be obtained.

4. Effects of Antenna Height Above Ground

The maximum gain and the elevation angle at which the maximum gain occurs is dependent on the height of the antenna above the ground and the reflection coefficient of the ground. The directivity patterns of horizontal and vertical antennas over a perfect earth are discussed by Terman.²⁰ For the case of actual ground and no forest, some insight into the manner in which the gain and directivity of vertical antenna change with antenna height above ground can be found in FitzGerrell's²¹ work, and the effects of height on horizontal antennas have been investigated by Taylor⁷ and FitzGerrell.¹⁹

The effects of trees on the antenna impedance (and antenna efficiency) of horizontal dipoles is negligible relative to the effects of the ground whereas the effects of the trees on vertical antennas can become more significant. Data presented in this report provide an indication of these forest effects. Measurements of antenna height-gain relationships were beyond the scope of the measurement program discussed in this report, but measurements performed elsewhere in Thailand, using horizontal dipoles similar to those measured at Ban Mun Chit, have shown that the efficiency of these antennas was reduced negligibly when the

antenna heights were reduced from 10 feet to 5 feet, but an efficiency reduction of approximately 10 dB was observed as the height was reduced to 1 foot. A further reduction of another 15 dB was observed when horizontal dipoles were lowered from 1 foot to ground level.

The methods referenced above can be used for rough approximations. For accurate prediction of the path loss for a particular antenna height, the pattern of the antenna should be measured at the antenna height of interest, or the model described in Section VIII could be used to predict the directivity gain, and then the standard deviation data presented with the antenna patterns could be used to determine the path reliability for a given power level.

REFERENCES

1. G. H. Hagn, G. E. Barker, H. W. Parker, J. D. Hice, and W. A. Ray, "Preliminary Results of Full-Scale Pattern Measurements of Simple VHF Antennas in a Eucalyptus Grove," Special Technical Report 19, Contract DA 36-039 AMC-00040(E), SRI Project 4240, Stanford Research Institute, Menlo Park, California (January 1966).
2. G. E. Barker and G. D. Koehrsen, "Full-Scale Pattern Measurements of Simple HF Field Antennas in a Tropical Forest in Thailand," Special Technical Report 35, Contract DA 36-039 AMC-00040(E), SRI Project 4240, Stanford Research Institute, Menlo Park, California (February 1968).
3. N. K. Shrauger and K. L. Taylor, "Initial VHF Propagation Results Using Xeledop Techniques and Low Antenna Heights," Special Technical Report 26, Contract DA 36-039 AMC-00040(E), SRI Project 4240, Stanford Research Institute, Menlo Park, California (December 1966).
4. Co Tan Ho and G. M. Ranvier, "Patrol Antenna for the AN/PRC 10 Radio Set," Combat and Development Test Center, Viet Nam (1963-64).
5. W. A. Ray, "Full-Scale Pattern Measurements of Simple HF Field Antennas," Special Technical Report 10, Contract DA 36-039 AMC-00040(E), SRI Project 4240, Stanford Research Institute, Menlo Park, California (May 1966).
6. W. A. Ray, G. E. Barker, and S. S. Martensen, "Full-Scale Pattern Measurements of Simple HF Field Antennas in a U.S. Conifer Forest," Special Technical Report 25, Contract DA 36-039 AMC-00040(E), SRI Project 4240, Stanford Research Institute, Menlo Park, California (February 1967).
7. J. Taylor, "A Note on the Computed Radiation Patterns of Dipole Antennas in Dense Vegetation," Special Technical Report 16, Contract DA 36-039 AMC-00040(E), SRI Project 4240, Stanford Research Institute, Menlo Park, California (February 1966).

8. H. W. Parker and Withan Makarabhiromya, "Electric Constants Measured in Vegetation and in Earth at Five Sites in Thailand," Special Technical Report 43, Contract DA 36-039 AMC-00040(E), SRI Project 4240, Stanford Research Institute, Menlo Park, California (February 1966).
9. N. K. Shrauger and E. M. Kreinberg, "Selected Examples of VHF Signal Propagation Records in Tropical Terrains," Special Technical Report 36, Contract DA 36-039 AMC-00040(E), SRI Project 4240, Stanford Research Institute, Menlo Park, California (November 1967).
10. G. H. Hagn, N. K. Shrauger, and G. E. Barker, "VHF Propagation Results Using Low Antenna Heights in Tropical Forests," Special Technical Report 46, Contract DA 36-039 AMC-00040(E), SRI Project 4240, Stanford Research Institute, Menlo Park, California (in preparation).
11. R. E. Leo, G. H. Hagn, and W. R. Vincent, "Research-Engineering and Support for Tropical Communications," Semiannual Report 4, Covering the Period 1 September 1964 through 31 March 1965, Contract DA 36-039 AMC-00040(E), SRI Project 4240, Stanford Research Institute, Menlo Park, California, p. 74 (October 1965).
12. G. E. Barker, J. Taylor, and G. H. Hagn, "Measurements and Modeling of the Radiation Patterns of Simple HF Field Antennas over Level, Mountainous, and Forested Terrains," Special Technical Report 45, Contract DA 36-039 AMC-00040(E), SRI Project 4240, Stanford Research Institute, Menlo Park, California (in preparation).
13. C. Barnes, "Transmitter Towed through Air Test Antenna's Radiation Pattern," Electronics, pp. 96-101 (18 October 1965).
14. C. Barnes, "Xeledop Antenna Pattern Measuring Equipment, 50 to 100 Mc/s," Stanford Research Institute, Menlo Park, California (April 1966).
15. E. L. Younker, G. H. Hagn, and H. W. Parker, "Research-Engineering and Support for Tropical Communications," Semiannual Report 7, Covering the Period 1 April through 30 September 1966, Contract DA 36-039 AMC-00040(E), SRI Project 4240, Stanford Research Institute, Menlo Park, California (September 1966).
16. E. C. Hayden, "Radiolocation Systems," in Electromagnetics and Antennas, P. E. Mayes, Project Director, pp. 444-483 (University of Illinois, Urbana, Illinois, 1967).

17. G. E. Barker and W. A. Hall, "Full-Scale Pattern Measurements of Simple VHF Antennas in Rough Terrain," Final Report--Task II, Volume II, Contract DAHCO7-67-C-0144, SRI Project 6571, Stanford Research Institute, Menlo Park, California (May 1968).
18. J. T. Belljahn and J. V. N. Granger, "Aircraft Antennas," in Antenna Engineering Handbook, H. Jasik, Editor, Chapter 27, pp. 17-19 (McGraw-Hill Publishing Company, New York, 1961).
19. R. G. FitzGerrell, "The Gain of a Half-Wave Dipole Over Ground," IEEE Trans. Antennas and Propagation, Vol. AP-15, No. 4, pp. 569-571 (July 1967).
20. F. E. Terman, Electronic and Radio Engineering, pp. 882-886, Fourth Edition (McGraw-Hill Book Company, Inc., New York, New York, 1955).
21. R. G. FitzGerrell, "Gain Measurements of Vertically Polarized Antennas Over Imperfect Ground," IEEE Trans. Antennas and Propagation, Vol. AP-15, No. 2, pp. 211-221 (March 1967).



STANFORD RESEARCH INSTITUTE
Menlo Park, California 94025 · U.S.A.

ERRATUM

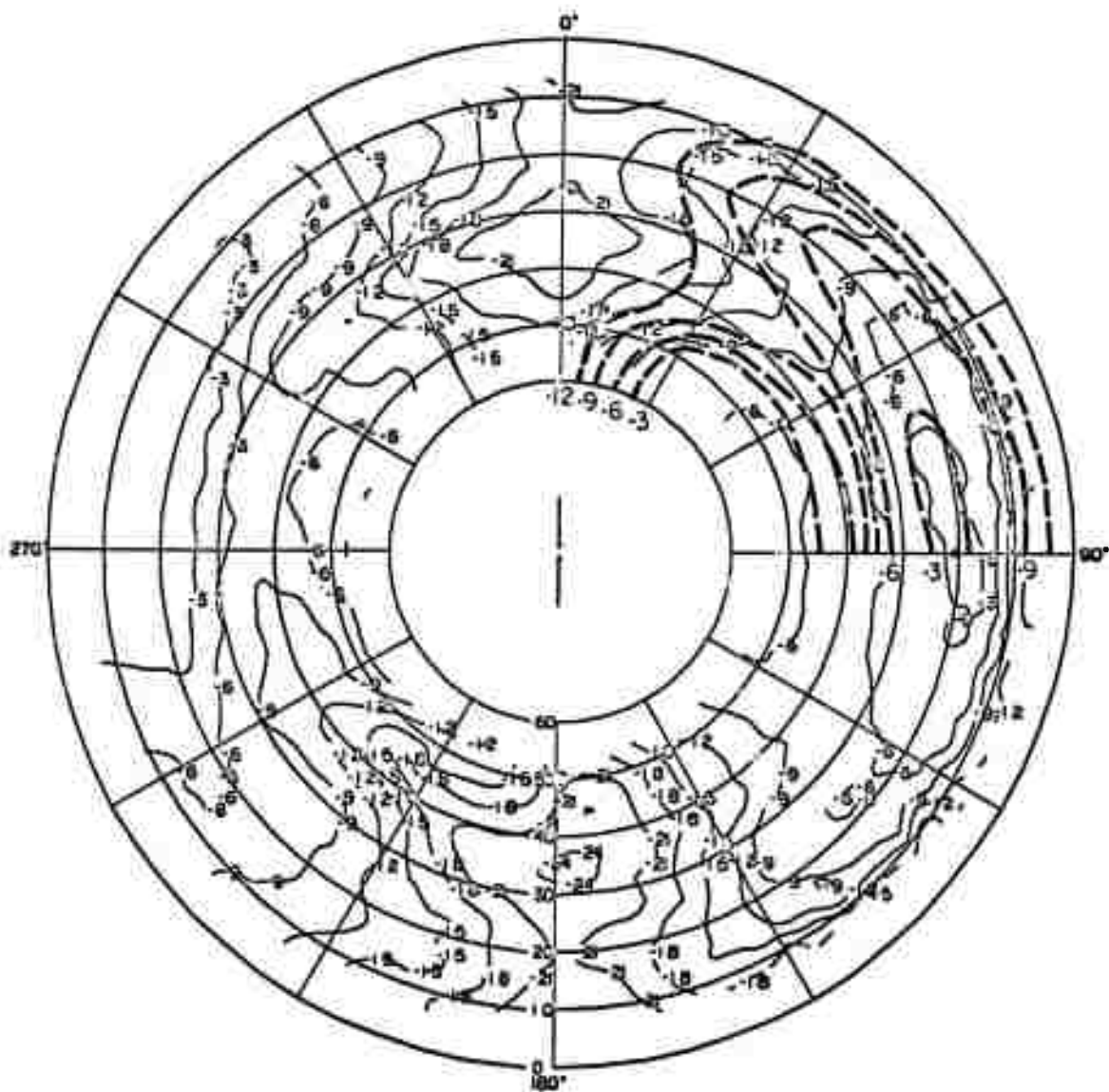
AD-738177

Reference is made to "Pattern Measurement and Modeling of Full-Scale VHF Antennas in a Thailand Tropical Forest," by G. E. Barker and W. A. Hall, Special Technical Report 39, Contract DAAB07-70-C-0220, Order No. 5284-PM-63-91, prepared by Stanford Research Institute (December 1971). Copies of this report were mailed to you on 2 March 1972.

An error resulted in the wrong illustration being printed at page 161 of the referenced report. The proper illustration (Figure B-12: Contour Plot of the Median Response of the Horizontal Dipole with Balun in the Forest-- E_0 at 75 MHz) has been printed on pressure-sensitive stock, and copies for your report are enclosed. Please place this plot over the incorrect illustration in your copies of this report.

Stanford Research Institute regrets any inconvenience caused by this inadvertence.

Reproduced by
NATIONAL TECHNICAL
INFORMATION SERVICE
Springfield, Va. 22151



TA-8663-231

FIGURE B-12 CONTOUR PLOT OF THE MEDIAN RESPONSE OF THE HORIZONTAL DIPOLE WITH BALOON IN THE FOREST— E_{ϕ} AT 75 MHz